VOLUME 102 NUMBER 1

THE ASTROPHYSICAL JOURNAL

AN INTERNATIONAL REVIEW OF SPECTROSCOPY AND ASTRONOMICAL PHYSICS

Founded in 1895 by GEORGE E. HALE *and* JAMES E. KEELER

Edited by

OTTO STRUVE
Managing Editor

S. CHANDRASEKHAR
Associate Managing Editor

Yerkes Observatory of the University of Chicago

PAUL W. MERRILL
Mount Wilson Observatory of the Carnegie Institution of Washington

HARLOW SHAPLEY
Harvard College Observatory
Cambridge, Massachusetts

J. H. MOORE
Lick Observatory
University of California

JULY 1945

THE UNIVERSITY OF CHICAGO PRESS
CHICAGO, ILLINOIS, U.S.A.

July 1945 Vol. 102, No. 1

THE ASTROPHYSICAL JOURNAL

AN INTERNATIONAL REVIEW OF SPECTROSCOPY AND ASTRONOMICAL PHYSICS

The Astrophysical Journal is published bimonthly by the University of Chicago at the University of Chicago Press, 5750 Ellis Avenue, Chicago, Illinois, during July, September, November, January, March, and May. ¶The subscription price is $10.00 a year; the price of single copies is $2.00. Orders for service of less than a full year will be charged at the single-copy rate. ¶Postage is prepaid by the publishers on all orders from the United States and its possessions, Argentina, Bolivia, Brazil, Chile, Colombia, Costa Rica, Cuba, Dominican Republic, Ecuador, Guatemala, Haiti, Republic of Honduras, Mexico, Morocco (Spanish Zone), Nicaragua, Panama, Paraguay, Peru, Rio de Oro, El Salvador, Spain (including Balearic Islands, Canary Islands, and the Spanish Offices in Northern Africa; Andorra), Spanish Guinea, Uruguay, and Venezuela. ¶Postage is charged extra as follows: for Canada and Newfoundland, 42 cents on annual subscriptions (total $10.42); on single copies, 7 cents (total $2.07); for all other countries in the Postal Union, 96 cents on annual subscriptions (total $10.96), on single copies 16 cents (total $2.16). ¶Patrons are requested to make all remittances payable to The University of Chicago Press, in United States currency or its equivalent by postal or express money orders or bank drafts.

The following are authorized agents:

For the British Empire, except North America, India, and Australasia: The Cambridge University Press, Bentley House, 200 Euston Road, London, N.W. 1, England. Prices of yearly subscriptions and of single copies may be had on application.

Claims for missing numbers should be made within the month following the regular month of publication. The publishers expect to supply missing numbers free only when losses have been sustained in transit, and when the reserve stock will permit.

Business correspondence should be addressed to The University of Chicago Press, Chicago 37, Illinois.

Communications for the editors and manuscripts should be addressed to: Otto Struve, Editor of THE ASTROPHYSICAL JOURNAL, Yerkes Observatory, Williams Bay, Wisconsin.

Line drawings and photographs should be made by the author, and all marginal notes such as co-ordinates, wave lengths, etc., should be included in the cuts. It will not be possible to set up such material in type.

One copy of the corrected galley proof should be returned as soon as possible to the editor, Yerkes Observatory, Williams Bay, Wisconsin. Authors should take notice that the manuscript will not be sent to them with the proof.

The cable address is "Observatory, Williamsbay, Wisconsin."

The articles in this journal are indexed in the *International Index to Periodicals*, New York, N.Y.

Applications for permission to quote from this journal should be addressed to The University of Chicago Press, and will be freely granted.

Entered as second-class matter, July 31, 1940, at the Post-Office at Chicago, Ill., under the act of March 3, 1879.
Acceptance for mailing at special rate of postage provided for in United States Postal Act of October 3, 1917, Section 1103, amended February 28, 1925.

[PRINTED IN U.S.A.]

THE ASTROPHYSICAL JOURNAL

AN INTERNATIONAL REVIEW OF SPECTROSCOPY AND ASTRONOMICAL PHYSICS

VOLUME 102 JULY 1945 NUMBER 1

INTERMEDIARY ELEMENTS FOR ECLIPSING BINARIES

HENRY NORRIS RUSSELL
Princeton University Observatory
Received May 14, 1945

ABSTRACT

In discussing an eclipsing binary, intermediary elements, based on a simplified model, should be derived, and later corrected, if the observations warrant, for refinements of the theory. The simplest generally useful model consists of two similar prolate ellipsoids. Limb-darkening, gravity-effect, and reflection must all be included in the first discussion of the variations outside eclipse. During eclipses the last two almost annul each other; and they may be ignored in the intermediary discussion of the "rectified" light.

The coefficients x_λ of limb-darkening and y_λ of gravity-effect depend on the effective temperature. The approximation $y_\lambda = 1.8\, x_\lambda$ is close enough for practical purposes.

When the radii, masses, and spectral types of the components are known, all these effects can be calculated theoretically. Unless complications not considered in the elementary theory are present, it should be possible to adjust the elements so that the observations are represented, and these relations satisfied, within reasonable limits. When the radii and masses are well known, this physical discussion may be used to find the darkening coefficient. An application to β Aurigae gave $x_\lambda = 0.57 \pm 0.17$. Many reliable determinations of x_λ may thus be obtained from published observations.

Only a physically satisfactory system of intermediary elements affords a safe starting-point for a definitive discussion which takes account of all refinements. This may be made by the method of "false position."

For the large majority of eclipsing variables the observations are not accurate enough to justify this heavy labor, and intermediary elements should suffice. When only photometric observations are available, the elements are often practically indeterminate over a considerable range. The computer should in this case give two (or more) sets of elements showing the extent of this range. Nomograms under construction by J. E. Merrill greatly expedite such calculations.

The most general laws of distribution of brightness over a triaxial ellipsoid, and of limb-darkening, which give light-curves capable of exact rectification (including eclipses) make the darkening-factor $\cos^n\gamma$ and the surface brightness const/H^n, where H is the perpendicular from the center to the tangent plane. Except for the familiar cases $n = 0$, $n = 1$, these solutions are irrelevant to the actual problem.

I. THE PROCESS OF APPROXIMATION

1. Eclipsing binaries present the most complicated problems of double-star astronomy. The number of parameters required for a complete specification of a system is large, and the relation between these and the observable light is intricate. The second difficulty may be met by the tabulation of special functions. The first demands that a complete solution shall be made by successive approximations—first determining intermediary elements, which take account of the main sources of variation, and then correcting these to allow for numerous refinements.

This process resembles the determination of the orbit of a comet or asteroid. A pre-

liminary orbit is derived from a theory which takes account of the sun's gravitation alone, usually by successive approximations, including more and more observations. With the positions given by this orbit, the perturbations which the attraction of the planets would produce on the observed co-ordinates of a body moving in it are then computed, and the observations are "corrected" by applying these in the opposite sense. The corrected normal places, when discussed as if only the sun's attraction were operative, lead to definitive elements.

It is essential that the intermediate orbit shall be good enough so that the perturbations calculated from it shall agree, without sensible error, with those derived from the final orbit. Otherwise the "corrections" would be inadequate, and a very laborious process of successive approximation would be required.

If the original observations are scanty or poor, the labor of computing perturbations and a definitive orbit is not worth while—at least for an asteroid, which may be better observed in future. Rough preliminary orbits, however, enable the selection of the interesting planets which will best repay observation. All these details have almost perfect analogues in the case of eclipsing variables.

2. The simplest model which can give a tolerable representation of the light-curves of the various types of eclipsing binaries consists of two similar prolate spheroids, revolving in a circular orbit. The methods which have been proposed for determining the elements of such a system have been thoroughly discussed by Dr. Kopal in a memoir now awaiting publication.[1]

Tables for their practical application have been published by various authors, and more extensive and precise ones, computed by Dr. J. E. Merrill, are also ready for publication. For the present purpose the solution of this problem may therefore be "taken as known." Darkening toward the limb, with a given coefficient, may be included in this.

The actual light of the system will differ from that computed from this model for many reasons. The figures of the components will differ from the assumed form, and usually from one another; and the distribution of brightness over the apparent disk will be modified by the gravity-effect and by "reflection." All these influences may be taken into account by means of the new functions developed by Kopal.[2] Numerical applications must await the computation and publication of tables of these, which is unavoidably delayed.

The differences between the light of the eclipsing system, computed with and without taking these refinements into account, play just the same part in the derivation of final elements for it as do the perturbations of an asteroid.

II. PHYSICAL RESTRICTIONS ON THE SOLUTION

3. One important detail, however, is different. In the refined theory the figures of the components and the values of gravity on their surfaces are determined by dynamical theory from the fundamental physical constants of the system—the masses, mean radii, and internal structure of the components—and the coefficients of the limb-darkening and gravity-effect may be derived from the effective temperatures of the stars and wave length of observation, while the reflection-effect is calculable from these and their radii.

The preliminary solution starts inevitably with assumed values of the darkening and gravity-coefficients and derives from the observations values of the principal parts of the effects of figure (ellipticity) and of reflection. It proceeds to find the radii and luminosities of the stars. If the masses are known, the ellipticity and reflection may then be calculated from physical theory. If the results disagree with those already obtained, the solution is physically unsatisfactory and does not afford a reliable base for further approximations.

[1] The writer is indebted to Dr. Kopal for the opportunity to become thoroughly acquainted with this work.

[2] *Proc. Amer. Phil. Soc.*, **85**, 399, 1942; **86**, 351, 1943.

A set of provisional elements which satisfies the physical relations is clearly to be preferred to one which does not, even though the latter should represent the observations more closely. There is no more reason to adopt it than there would be to adopt an apparent ellipse for a visual binary which did not satisfy the law of areas. It is therefore in order to examine these physical relations more closely. It will be assumed that the system is a "normal" one, free from such complications as intrinsic variability of the components or the presence of extensive envelopes or moving streams of gas. Orbital eccentricity will also be disregarded because, though it introduces considerable complication into the details of the discussion, it requires no modification of the general principles involved; because it is thoroughly discussed in Kopal's memoir; and because its effects are sensible only in a rather small proportion of actual cases.

4. The outward flux of energy from the surface of a tidally distorted star is proportional to the local gravity g.[3] For monochromatic radiation, the surface brightness is given by

$$J_\lambda = \text{const}\left(1 - y_\lambda + y_\lambda \frac{g}{g_0}\right). \tag{1}$$

For total radiation, $y = 1$. On gray-body assumptions and to the first order:[4]

$$y_\lambda = \frac{\dfrac{d \log J_\lambda}{dT}}{\dfrac{d \log J}{dT}} = \frac{\dfrac{C_2}{\lambda T}}{4\,(1 - e^{-C_2/\lambda T})}, \tag{1a}$$

or, numerically ($C_2 = 1.438$),

$C_2/\lambda T$	0.0	1.0	2.0	3.0	4.0	5.0	6.0	7.0	8.0	9.0
y_λ	0.25	0.39	0.58	0.79	1.02	1.26	1.50	1.75	2.00	2.25

The darkening-coefficient x should also be a function of λT. Gray-body theory, to the first order in dT/T, gives

$$x_\lambda = \frac{3 y_\lambda}{2 + 3 y_\lambda}. \tag{2}$$[5]

For total radiation, $x = 0.6$ to this approximation.

The change in T between center and limb is more than 20 per cent, so that second-order terms are not negligible, and the more detailed theory of limb-darkening is complicated. The observed values for the sun therefore afford a valuable guide. The data tabulated by Unsöld[6] give the values shown in the accompanying table. With $T = 5740°$, the

λ	3230	3860	4560	5340	6700	8660	12250	16550	20970
x_λ	0.88	0.85	0.77	0.66	0.53	0.43	0.34	0.26	0.22
Obs. x_λ/y_λ	0.46	0.53	0.56	0.55	0.56	0.56	0.59	0.54	0.53
Comp. x_λ/y_λ	0.38	0.43	0.49	0.54	0.61	0.70	0.80	0.87	0.91

observed darkening gives the values of x_λ/y_λ in the third line. The values given by equation (2) are in the next line. There is a serious systematic discrepancy, the darkening for large values of λT being much less than indicated by the elementary theory.

The more refined theory given by Unsöld (*loc. cit.*) agrees much better with the ob-

[3] Chandrasekhar, *M.N.*, **93**, 573, 1933.

[4] Kopal, *Ann. New York Acad. Sci.*, **41**, 19, 1941.

[5] Kopal, *ibid.*, p. 21.

[6] *Physik der Sternatmosphären*, p. 34, Table 3.

servations. For very high temperatures y approaches the limit 0.25. Numerical integration of the equations for the closest approximation given by Unsöld[7] gives, at the limit for infinite temperature, the following values:

$\cos\gamma$	1.0	0.9	0.8	0.6	0.4	0.2	0.0
Relative intensity	1000	989	968	942	905	860	790

Except at the very edge these are closely represented by $x = 0.17$. This makes $x_\lambda/y_\lambda = 0.68$ as against 1.09 given by equation (2).

For practical purposes, at present, it may suffice to adopt

$$x_\lambda = 0.55 y_\lambda , \tag{3}$$

which represents the solar data except for the shortest wave lengths.

5. To the first order in the ellipticity, the light of an uneclipsed ellipsoid is given by

$$I = I_0 (1 - C \sin^2 i \cos^2 \theta) , \tag{4}$$

where θ is the longitude in the orbit and the photometric ellipticity C is given by

$$C = \frac{15 + x}{15 - 5x} (1 + y + 2K - \tfrac{1}{2} K y) \epsilon . \tag{5}$$

Here ϵ is the geometrical ellipticity, and K depends on the internal constitution and is less than 0.02 in all well-determined cases.[8] Neglecting it,

$$\frac{C}{\epsilon} = \frac{(1 + y)\ (15 + x)}{15 - 5x} . \tag{6}$$

Setting $y = 1.8x$ we have the following values:

x	0.2	0.4	0.6	0.8
$(15 + x)/(15 - 5x)$	1.09	1.18	1.30	1.44
C/ϵ	1.48	2.04	2.71	3.50

If x is known or assumed and y neglected, the ellipticity deduced from the observations outside eclipse will be much too great.

According to dynamical theory, the ellipticities of the components are given, to the first approximation, by the equations

$$\epsilon_1 = \frac{a_1 - b_1}{r_1} = \frac{3}{2} \frac{m_2}{m_1} r_1^3 (1 + 2K) \tag{7}$$

and

$$\frac{b_1 - c_1}{r_1} = \frac{1}{2} \frac{m_1 + m_2}{m_1} r_1^3 (1 + 2K) . \tag{8}$$

Here m_1 is the mass of component 1; a_1, b_1, and c_1, the semi-axes (in terms of the orbital radius) of the ellipsoid which best fits its form; and r_1 the mean of these. Detailed expressions to the fifth order are given by Kopal.[9] The value of $b - c$ has a practically negligible influence on the variation outside eclipse (§16).

6. The reflection-effect presents the most complicated part of the theory of eclipsing variables and has been evaluated only for spherical stars, under simplifying assumptions.[10]

[7] *Ibid.*, pp. 104–6.

[8] Russell, *Ap. J.*, **90**, 641, 1939 (also pp. 652, 658).

[9] *Proc. Amer. Phil. Soc.*, **85**, 399, 1942; also p. 401. Our $2K$ is $1 - \Delta_2$ in his notation.

[10] Milne, *M.N.*, **87**, 43, 1926.

If a is the phase angle ($\cos a = \sin i \cos \theta$) and L_1, L_2, the luminosities of the sides of the components which face one another, the total radiation from a pair, if there is no eclipse, is given[11] by

$$\frac{I}{I_0} = 1 + 0.347\,(L_1 r_2^2 - L_2 r_1^2)\cos a + 0.073\,(L_1 r_2^2 + L_2 r_1^2)\cos 2a\,. \qquad (9)$$

Higher terms are negligible. For monochromatic light, if E_1, E_2 are the luminous efficiencies of the radiation from these sides, we have, with a slightly changed definition of I_0,

$$\left.\begin{aligned}\frac{I_\lambda}{I_0} = 1 + 0.347\left(\frac{E_2 L_1}{E_1}\,r_2^2 - \frac{E_1 L_2}{E_2}\,r_2^2\right)\sin i\cos\theta \\ + 0.073\left(\frac{E_2 L_1}{E_1}\,r_2^2 + \frac{E_1 L_2}{E_2}\,r_1^2\right)\sin^2 i\cos 2\theta\end{aligned}\right\} \qquad (10)$$

(neglecting the square of the last term).

For a black or gray body the relative values of E are as follows:

$C_2/\lambda T$	1	2	3	4	5	6	7	8	9	10
E	0.21	0.53	0.89	1.00	0.89	0.67	0.46	0.29	0.17	0.10

The value of E is a maximum when $C_2/\lambda T = 4$, or at about 6800° for visual, and 8400° for photographic, observations.

7. With Kuiper's temperatures[12] and assumed wave lengths of λ 5290 and λ 4250 for visual and photographic observations, the values of the parameters depending on the spectral type are as given in Table 1.

TABLE 1

Sp	T	Visual				Photographic			
		y	x	c/ϵ	E	y	x	C/ϵ	E
B0	25,000°	0.41	0.22	1.55	0.15	0.46	0.25	1.62	0.25
B5	15,500	0.53	.29	1.73	0.41	0.61	.34	1.86	0.60
A0	10,700	0.69	.38	1.98	0.75	0.83	.45	2.21	0.92
A5	8,500	0.83	.46	2.22	0.93	1.02	.56	2.57	1.00
F0	7,500	0.93	.52	2.42	0.99	1.14	.63	2.82	0.96
F5	6,500	1.06	.58	2.66	1.00	1.31	.72	3.18	0.84
G0	6,000	1.15	.63	2.84	0.96	1.41	.78	3.43	0.75
dG5	5,400	1.27	.70	3.08	0.88	1.57	.85	3.79	0.62
dK0	4,900	1.39	.76	3.36	0.77	1.73	.88	4.1:	0.49
dM0	3,600	1.9:	0.8:	4.1:	0.36:	2.3:	0.9:	5.1:	0.14:

The values of y are given by equation (1a) and those of x by equation (3), except for classes K and M, where they are estimates based on the observed solar values for the same λT. Those of C/ϵ are given by equation (6) and of E by black-body theory.

The values given for class M are rough estimates. The tabular values may be greatly affected by the limitations of the elementary theory from which they are derived. For example, these conclusions hold good if the monochromatic absorption coefficient is equal to the Rosseland mean for total radiation. The gravity-effect, which depends on conditions deep within the star, will be little altered by either the general or the monochromatic opacity of the surface layers. With a high value of the latter, the observable radiation

[11] Russell, *op. cit.*, 658. Star 1 is in front when $\theta = 0$.

[12] *Ap. J.*, **88**, 429, 1938.

will come from a thin surface layer, and the darkening will be small. This might be expected in A stars for wave lengths beyond the Balmer limit, but not at λ 4500.

The only observed data at present available to test them come from the few stars in which x has been directly determined by precise observations of annular eclipses. Kopal[13] gives for λ 4500 the values shown in the accompanying tabulation.

Star	Sp	x	Table 1
AR Cas A.....	B3	0.00±0.04	0.29
α CrB A.....	A0	.51± .24	.43
YZ Cas A.....	A3	.49± .04	.49
Sun.....	G2	0.74±0.02	0.76

The agreement is good except in the first case, where the observations are not reconcilable with any physical theory. Determinations of limb-darkening for other B stars are badly needed.

8. In the preliminary solution the light outside eclipses is first compared with the formula

$$I = I_0 (1 + A_1 \cos\theta + A_2 \cos 2\theta) , \tag{11}$$

the constants deduced (by least squares, if the observations warrant it), and the observed intensities "rectified" by dividing them by the computed values of I.

The rectified curve is then discussed by standard methods, obtaining values of L_1, L_2, r_1, r_2, and i. We should then have

$$A_1 = 0.347 \left(\frac{E_2 L_1}{E_1} r_2^2 - \frac{E_1 L_2}{E_2} r_1^2 \right) \sin i , \tag{12}$$

$$A_2 = \left\{ 0.073 \left(\frac{E_2 L_1}{E_1} r_2^2 + \frac{E_1 L_2}{E_2} r_1^2 \right) - \tfrac{1}{2} (C_1 L_1 + C_2 L_2) \right\} \sin^2 i , \tag{13}$$

when C_1, C_2, are given by equations (6) and (7).

It is practically necessary to adopt one of the values of x for which tables of the functions required have been computed; and the solution itself involves the constant $z = 2\epsilon \sin^2 i$.

If in equation (13) we set

$$L_1 C_1 + L_2 C_2 = C , \qquad L_1 r_2^2 + L_2 r_1^2 = \overline{r^2} , \qquad E_1 = E_2 ,$$

we have

$$C \sin^2 i = 2A_2 + 0.073 \overline{r^2} \sin^2 i .$$

Setting $\overline{r^2} = 0.08$ as a mean value in the small term, we have, closely enough,

$$z = \frac{4\epsilon}{C} (A_2 + 0.003) .$$

The values of x for which tables have been computed, the corresponding values of $4\epsilon/C$, and the limits of spectral type according to Table 1, for which the actual value of x differs from the tabular by less than 0.1, are given in Table 2.

If the spectral type of the combined light is known, the assumed value of x can be taken from this table. If it is not, x may be taken as 0.4 in most cases, and 0.6 or 0.8 for systems of high or very high density.

[13] *Proc. Amer. Phil. Soc.*, **86**, 350, 1943.

The preliminary solution for the elements may be greatly shortened by the construction of suitable nomograms—which are in preparation by Dr. J. E. Merrill.

9. The photometric solution is physically unacceptable unless relations (12) and (13) are satisfied within reasonable tolerances.

Calculation of A_1 demands knowledge of E_1 and E_2 and therefore of the temperatures of the components. The observed spectrum of the hotter component may safely be used to get E from Table 1. If there is much difference in temperature, the atmosphere of the cooler star is abnormally ionized by the dilute radiation of the other.[14] The relative surface brightness of the facing sides of the components should be used to find T and E for it.

If the observed and calculated values of A_1 disagree, the discrepancy may be reduced by changing the assumed elements. The nomograms are useful here in showing what correlated changes may be made without undue violence to the light-curve.

Outstanding discordances may arise from circumstances not considered in the present theory. Many well-observed light-curves—especially when the components are large compared with their separation[15]—show asymmetries, which can be partially represented by introducing terms $B_1 \sin \theta$, $B_2 \sin 2\theta$, in equation (11). In such cases the best policy is

TABLE 2

x	$4\epsilon/C$	Spectral Limits	
		Visual	Photographic
0.2	2.7	0–B5	0–B2
.4	2.0	B6–A8	B3–A2
.6	1.5	A9–G5	A3–F4
0.8	1.1	G6–M	F5–M

probably to include the sine-terms in equation (11), rectify by dividing by the computed value, and proceed as usual. The same may be done if the cosine terms disagree with physical theory. But this is making the best of a bad business, and not much confidence should be placed in the results.

It might also happen that the black-body assumptions were inadequate or that the observations were not so good as they were supposed to be. The discussion of such problems must be left to the intelligence of the investigator. The technique of testing observations for homogeneity and systematic errors is well known, though not always practiced. But, in a problem which is inherently as complicated as this and where the percentage errors of observation are as great as they are in all but the very best photometric work, it is not reasonable to hope for a method of solution which will lead automatically, though laboriously, to the goal; and there is no substitute for thorough knowledge and good judgment on the computer's part.

10. When the reflection-effect has been allowed for, equation (13) gives the photometric ellipticity $C = L_1C_1 + L_2C_2$. With the effective temperatures already adopted, C_1/ϵ_1 and C_2/ϵ_2 are given by equations (1a), (3), and (6). If the mass-ratio is known, equation (7) gives ϵ_1, ϵ_2, and C is determined.

The computed values of ϵ are sensitive to the adopted radii, and adjustments diminishing a discordance with observation may be possible. This is likeliest for systems of the W Ursae Majoris type, with components close together, high ellipticity, and long and shallow eclipses. In such cases a change in the assumed ellipticity may considerably alter the rectified depths and durations of the eclipses. Two or three exploratory solutions with

[14] Eddington, *M.N.*, **86**, 325, 1926.

[15] P. H. Taylor, *Ap. J.*, **94**, 46, 1941.

different assumed values of the photometric ellipticity should reveal the best adjustment. The nomograms will be useful.

If the components differ considerably in size and mass, their theoretical ellipticities may differ greatly. The best that can be done in the preliminary solution is to assume a mean ellipticity, the same for both components, which will reproduce the photometric ellipticity. Good judgment is again essential.

When the components are well separated, the ellipticities are moderate, the eclipse sharply defined, and the range of adjustment of the elements is limited. In view of the present uncertainty of the estimates of x and y from spectral type (§7), the best policy appears to be to adopt the dynamical values of ϵ, and find x from C/ϵ by equation (6) or the tabulation following it. A number of good determinations of x could thus be made from existing material.

For an extreme case, take β Aurigae. Stebbins' observations with the selenium photometer[16] give the variation between eclipses as $0^m011 \pm 0^m003$, corresponding to $A_2 = -0.0054 \pm 0.0016$. The components are equal, so that equations (7) and (13) become

$$\epsilon = \tfrac{8}{2} r^3 \qquad \text{and} \qquad C = 0.146 r^2 - 2A_2 .$$

Shapley[17] gives for $x = 0$, $r = 0.147$, whence $C/\epsilon = 2.94 \pm 0.67$, corresponding to $x = 0.67 \pm 0.18$, while for $x = 1$, $r = 0.159$, $C/\epsilon = 2.40 \pm 0.53$, $x = 0.51 \pm 0.16$. The consistent solution is $x = 0.57 \pm 0.17$. This value has small weight; but it is remarkable that the darkening can be derived at all from such a small variation with shallow partial eclipses.

When the mass-ratio is unknown, it is fairly safe to assume that $m_1 = m_2$ if $L_1 = L_2$. But with components of different brightness, it is unsafe to apply the mass-luminosity relation on account of observational selection.[18] To apply the empirical correction suggested for this should improve the representation on the average, but not always.

When more is known regarding the relation of limb-darkening to spectral type, it may be possible to revise the calculation, assuming x_1, x_2 and deriving a value of m_1/m_2; but it is not yet known how accurate the results would be.

III. CHOICE OF AN INTERMEDIARY MODEL

11. The model upon which the intermediary solution is based must satisfy these conditions: (*A*) it must be precisely specified in terms of physical elements similar to those which define the actual system; (*B*) with suitable values of these, it must be capable of giving a light-curve which differs but little from any actual light-curve of a normal eclipsing system; and (*C*) the calculation of the light-curve from the elements and the derivation of these from the curve must be as simple and rapid as possible.

Since successive approximations will usually be required to secure elements which satisfy the physical conditions discussed above, condition *C* is important. The computer, of course, is always concerned with the representation of the *observations* and not of a free-hand curve drawn to represent them; but the solution for the elements from regularly spaced points on such a curve saves a great deal of time. The light-curve resulting from these elements should always be plotted directly against the observations. Any discordances show how it may be improved. Here again the intelligence and experience of the computer are better guides than any formal rules.

It has long been customary to take account, throughout the variation, of ellipticity and limb-darkening (with an estimated value) and of reflection, also, between eclipses;

[16] *Ap. J.*, **34**, 112, 1911.

[17] *Princeton Contr.*, **3**, 82, 1915.

[18] Russell and Moore, *The Masses of the Stars*, Chicago, 1940, p. 106.

but the gravity-effect has been neglected. It is shown in §§ 4–6 that it is necessary and very easy to take this into account between eclipses. During eclipses, fortunately, this is not necessary.

The assumption that the isophotes on "darkened" elliptical disks are similar to and concentric with the limb[19] corresponds to $y = \frac{1}{4}$ when $x = 1$.[20] In general, the outstanding gravity-effect will be $y - \frac{1}{4}x$, or, by equation (3), $0.86y$.

For a prolate spheroid, seen end on, this will brighten the limb—the first-order effect for star 1 being[21]

$$J = J_0\left(1 - 5.2y\,\frac{m_2}{m}\,r_1^3\cos^2\gamma\right). \tag{14}$$

Reflection darkens the limb, giving[22]

$$J = J_0\left\{1 + \frac{1}{8}\,\frac{L_2}{L_1}\,r_1^2(1 + 2\cos\gamma)^2\right\}. \tag{15}$$

These are superposed on the normal limb-darkening. The mean change in brightness of the disk, with the center as standard, is one-half that at the limb for equation (14) and five-twelfths for equation (15). The ratio of these is $-6.2y(L_1m_2/L_2m_1)r_1$.

For equal components, these annul one another if $r_1 = 0.16/y$, or about 0.23 for spectrum A. If m_2/m_1 is large, L_2/L_1 will be larger, and the two effects will cancel for larger values of r_1. The net influence in the surface brightness will almost always be very small and may be neglected in the intermediary approximation. The neglected effects do not follow the standard law of darkening, nor are they symmetrical about the center of the disk, except at central eclipse.

12. The intermediary model here advocated differs from the actual physical system in several respects: (*a*) the components are supposed to be similar coaxial prolate spheroids; (*b*) the effects of gravity-darkening and reflection upon the distribution of brightness over the eclipsed portions of the disks are neglected (except that a fraction of the former is allowed for by the assumption that the isophotes are similar concentric ellipses); (*c*) all terms of the second order in the ellipticity are neglected; and (*d*) Milne's approximation for the reflection-effect is adopted.

Kopal's analysis takes account fully of the effects of geometrical figure and gravity and approximately of reflection, up to terms of the order of r^5, or $\epsilon^{5/3}$ (eq. [7]). He stopped here because the higher terms in the general theory are very complicated—the size and figure of each component influencing that of the other. When the mass is greatly concentrated toward the center, the constant K in equation (7) is very small, and this difficulty practically disappears. Calculations based on the Roche model ($K = 0$) should give close approximations to the higher terms and should determine whether any of them are sensible. With this extension, the theory should include everything but the finer details of the reflection-effect, which are discouragingly intricate.

13. The determination of the "perturbations" which are required for the derivation of precise elements may be made as follows: The observations are discussed as in §§ 9 and 10, until, perhaps after two or three approximations, a set of intermediary elements X are found which satisfy the physical conditions specified in §§ 4–8, while the light-curve A, deduced from them by strict application of the intermediary equations, gives a satisfactory representation of the observations. From the same elements, a second light-curve, B, is computed, applying all the refinements of the advanced theory. The difference

[19] Russell and Shapley, *Ap. J.*, **36**, 400, 1912.

[20] Russell, *Ap. J.*, **95**, 355, 1942.

[21] Russell, *Ap. J.*, **90**, 661, 1939.

[22] Milne, *op. cit.*, p. 50; Russell, *Ap. J.*, **90**, 661, 1939.

$B - A$ of the readings of the two curves at any phase is the perturbation at that phase. If O is the observed intensity at this phase, let $O' = O + A - B$. The "unperturbed" intensities O' are then discussed by means of the intermediary theory, obtaining new elements X', from which a new light-curve, A', is computed by the intermediary equations.

If the differences $X' - X$ are small, it may be assumed that a repetition of the exact calculation would give a light-curve, B', such that $B' - A'$ and $B - A$ were sensibly equal. The elements X' may then be finally improved by a least-squares solution (provided that the data are good enough to justify the labor), using the intermediary equations and the quantities $O' - A'$ as the residuals to be improved.

It is not necessary that the calculation of the light-curve B should be made as an improvement of curve A by the addition of correction terms. Any precise method which starts from the fundamental physical elements L_1, L_2, m_1, m_2, r_1, r_2, i, T_1, T_2, and λ serves equally well. When numerical values of Kopal's functions are available, the simplest methods for computation with the required accuracy can be investigated.

If X and X' differ considerably, it may be necessary to compute an accurate light-curve, B', by the exact formulae and continue the approximation.

If adequate care is used in deriving the elements X, this should not happen unless (1) the solution for the elements is nearly indeterminate or (2) the observations are too poor to give a reliable solution or (3) physical complications not considered in the present theory are present. The last two of these can usually be detected, or strongly suspected, upon inspection of the plotted normals, while the first will reveal itself during the solution for the intermediate elements. Systems with components almost in contact present the most difficult cases.

14. The computer should take advantage of any opportunity of determining the unknowns from other data. For example, the limb- and gravity-darkening should be estimated from the spectral type (§ 7) or from the variation outside eclipse (§ 10).

In a few very favorable cases the limb-darkening can be determined directly as an independent unknown. Unless the observed light during eclipse is corrected for the effects of reflection and gravity-darkening, which follow other laws, the results will not be exact. A summary calculation should show if the alteration is sensible.

When the eclipses are partial and nearly equal in depth, the photometric solution is inherently indeterminate, unless the ratio of the luminosities L_1 and L_2 is known. This should often be obtainable from spectrograms—though special care is necessary in their interpretation. Unless both spectra have been observed, the ratios of the masses and luminosities are uncertain, and the adjustment to physical conditions (§ 9) is impracticable.

In such cases, when the observations are precise, it is desirable to make intermediary solutions for various assumed values of the uncertain quantity (i.e., L_1/L_2) and find what range of values permits a satisfactory representation of the observations. Sets of elements for the extreme values and one near the middle of the range will then exhibit the available knowledge of the system. To go beyond a good intermediary solution is not likely to be worth while.

How wide a range of representation may be deemed satisfactory is a matter of judgment. A diagram showing the observations and the computed light-curves corresponding to the various sets of elements enables the reader to form his own opinion. If this is on an adequate scale *and provided with a co-ordinate grid*,[23] permitting easy and accurate readings, it is almost as good as a table of normals and residuals for the critical student, and much better for the general reader.

Limiting values of the elements convey reliable information, which may be of theoretical value. Elements derived from a single assumed value of the uncertain quantity

[23] In the writer's opinion, such a grid should be *required* editorially, unless the material is also given in tabular form.

may be actually misleading, especially if this value has been derived from some statistical relation. If carelessly quoted, they may be taken as evidence in its favor.

Unless the observations are of high precision, it will seldom, if ever, be worth while to go beyond a good intermediary solution; but this solution should be made by a sound method.

Far too often, even today, solutions are based mainly on the estimated times of beginning and end of eclipse—that is, on the most inaccurate points on a freehand light-curve. If the computer had taken the trouble to compute a light-curve from the resulting elements and plot it along with the observations, the need and possibility of improvement would sometimes have been obvious.

When the observations are poor, it may, nevertheless, be worth while to compute rough elements. Three principles may be urged in such cases.

1. The light-curve should always be computed and inserted on the published plot of the observations. The worse they are, the more important this is.

2. Any assumptions which have been made in deriving the elements should be not merely stated but emphasized.

3. Unless the observations are good enough to permit a definite estimate of the range of uncertainty of the elements derived from them, the latter are not competent evidence in the discussion of refined astrophysical problems—such as differences in the elements for light of different wave lengths. They may be very useful, however, in selecting interesting systems for precise observation.

Still rougher observations—for example, estimates on a scale of uncertain photometric significance—are of value in finding periods. No formal rules can separate these classes. There is no substitute for common sense.

IV. THEORETICAL NOTES

15. Exact expressions for the laws of surface brightness on an ellipsoid and of limb-darkening, which together make the isophotes on the apparent disk similar to and concentric with its boundary, may be derived as follows.[24] Let the ellipsoid E be

$$\frac{x^2}{A^2}+\frac{y^2}{B^2}+\frac{z^2}{C^2}=R^2 .$$

The transformation $x = Ax'$, $y = By'$, $z = Cz'$ changes this into the sphere S', $(x'^2 + y'^2 + z'^2 = R^2)$; a line T with direction cosines l, m, n, goes into T', for which $l = hAl'$, $m = hBm'$, $n = hCn'$, where

$$h^2=\frac{l^2}{A^2}+\frac{m^2}{B^2}+\frac{n^2}{C^2}. \tag{16}$$

The plane U, $(Lx + My + Nz = P)$, becomes U', $(L'x' + M'y' + N'z' = P')$. If L, L', etc., are direction cosines,

$$L=\frac{HL'}{A}, \qquad M=\frac{HM'}{B}, \qquad N=\frac{HN'}{C}, \qquad P=HP',$$

where

$$H^2=L^2A^2+M^2B^2+N^2C^2 . \tag{17}$$

The radius of E in the direction l, m, n, is $r = R/h$ and, if U touches E, $P = HR$. The angle γ between T and the normal to U transforms to γ', where

$$\cos\gamma = hH\cos\gamma' . \tag{18}$$

[24] Cf. Russell, *Ap. J.*, **95**, 352, 1942 (correcting misprints).

An element $d\sigma$ on U goes into $d\sigma'$ on U' such that $Hd\sigma = ABCd\sigma'$ and

$$\cos\gamma d\sigma = ABCh\cos\gamma' d\sigma' . \tag{19}$$

Now let the apparent surface brightness of any element $d\sigma$ on E, as seen by an observer O at a great distance D in the direction l, m, n, be J_a. The radiation received from this element at O will be $dI = (J_a d\sigma\cos\gamma)/D^2$. An observer O', at the same distance D from S', in the direction l', m', n', will receive the radiation $dI' = (J'_a\, d\sigma'\cos\gamma')/D^2$. Then $dI = dI'$ if

$$J'_a = ABChJ_a . \tag{20}$$

Now h is independent of position on E or S'. Hence, if equation (20) is satisfied, $dI = dI'$ for all corresponding elements, and $I = I'$. The apparent surface intensities of all elements of E, as seen from O, and of S', seen from O', are then in a fixed ratio.

If the isophotes on E are similar concentric ellipses, those on S' will be concentric circles, which, in general, demands that $J'_a = f(h, \cos\gamma')$. Upon E, physical plausibility demands that the darkening-function (for total radiation) should depend only on the angle of emission, whence

$$J_a = F_1(L, M\ \ N)\, F_2(\cos\gamma) .$$

We then have

$$J'_a = ABChF_1(L, M, N)\, F_2(\cos\gamma) = f\left(h, \frac{\cos\gamma}{hH}\right).$$

Since L, M, N appear in the second member only through H,

$$F_1(L, M, N) = F_1(H) \qquad \text{and} \qquad ABChF_1(H)\, F_2(\cos\gamma) = f_h\left(\frac{\cos\gamma}{H}\right),$$

where f_h is the expression of the second member for any particular value of h. The general solution of this equation is

$$F_1(H) = \alpha H^{-n}; \qquad F_2(\cos\gamma) = \beta\cos^n\gamma; \qquad f_h\left(\frac{\cos\gamma}{H}\right) = ABCh\alpha\beta\left(\frac{\cos\gamma}{H}\right)^n .$$

Since F_1 and F_2 must be independent of h, α and β are constants. Setting

$$\alpha\beta = J_n \qquad ABC\alpha\beta = J'_n$$

we have, by equation (18),

$$J_a = J_n\left(\frac{\cos\gamma}{H}\right)^n; \qquad J'_a = J'_n h^{n+1}\cos^n\gamma' . \tag{21}$$

The intrinsic brightness of E varies as H^{-n}—that is, inversely as the nth power of the distance from the center to the tangent plane at a given point, and the darkening-function is $\cos^n\gamma$, both on the ellipsoid and on the transformed sphere. The total radiation of E toward O, or of S toward O', is

$$I = \frac{2\pi R^2}{2+n}\, ABCJ_n h^{n+1} .$$

The direction cosines of O with respect to the axis of E are

$$l = \sin i\cos\theta , \qquad m = \sin i\sin\theta \qquad n = \cos i .$$

Without loss of generality, we may set $A^2 = 1$, $B^2 = 1 - e^2$, $C^2 = 1 - f^2$. Then, substituting in equation (16) and setting

$$h_0^2 = \frac{\cos^2 i}{1 - f^2} + \frac{\sin^2 i}{1 - e^2}, \qquad (1 - f^2)\tan^2 i = (1 - e^2)\tan^2 j, \qquad z = e^2 \sin^2 j, \quad (22)$$

we find

$$h^2 = h_0^2 (1 - z \cos^2 \theta), \qquad I = \text{const}\,(1 - z \cos^2 \theta)^{n+1/2}. \qquad (23)$$

Equations (21)–(23) are exact and represent a singly infinite series of physically reasonable distributions of radiation from E, which give isophotes of the desired type. It is easy to show that, for any pair of similar and similarly situated ellipsoids with the same value of n, the rectification of the light-curve by dividing by I as given in equation (23) is exact, and an exact solution for the elements could be obtained by familiar methods, providing that tables were available of the corresponding functions for the darkening-law, $\cos^n\gamma$.

It would, however, be useless to compute such tables, for the darkening-function, $1 - x + x \cos \gamma$ (which is well established both by observation and by theory as a good approximation), coincides with $\cos^n\gamma$ only when $x = 0$ and $x = 1$—the two previously known exact solutions of the problem. In practice, x will almost always lie between 0.2 and 0.8, and the isophotes will not be similar concentric ellipses. The corresponding corrections are included, with many others, in the final approximation described in § 13.

16. For all the exact solutions it is always possible to find a pair of similar prolate spheroids which will give identically the same light-curve outside and inside eclipse, as any pair of similar triaxial ellipsoids—the condition being that the inclinations i and j for the two shall be related as in equation (22). This has long been known for uniform disks.[25]

For other laws of darkening, the light-curves for prolate and triaxial systems will not be identical, nor will the rectification of the curve in the manner described above be exact.[26] There would be no advantage in applying special corrections for this, since all corrections are determined together in the final solution. An approximate correction for the ratio of the polar to the shorter equatorial axis, based on dynamical considerations,[27] was given in 1912. The new formulae will give a better one.

In conclusion, it appears that the advent of a new era of precision in the treatment of eclipsing variables awaits only the publication of tables of the associated alpha functions. Once more the analogy to planetary perturbations is close. These functions, being required all through the period, are comparable with general perturbations. As with them, the practical computer will be concerned with the numerical order of magnitude of the terms rather than with their order in powers of the small quantities required in the expansions.

The way will then be clear for a great expansion of precise observation and discussion. After forty years of activity, this field is more promising than at the start.

[25] A. Roberts, *M.N.*, **63**, 528, 1903; Russell, *Ap. J.*, **36**, 61, 1912.

[26] Kopal, *Proc. Amer. Phil. Soc.*, **85**, 428, 1942.

[27] Russell, *Ap. J.*, **36**, 62, 1912.

THE CO-ALBEDO OF THE MOON*

EDISON PETTIT
Mount Wilson Observatory
Received March 29, 1945

ABSTRACT

The co-albedo of the moon is defined as the ratio of the solar radiation received by the moon to the whole planetary heat emitted by it. The co-albedo is equivalent to $1 - A$, where A is the albedo determined radiometrically.

The magnitude of the full moon in planetary heat outside the atmosphere at mean distance, computed from the albedo formula, the solar constant, and the reflected radiation from the subsolar point on the moon, is used to calibrate the phase-radiation curve of the moon given in an earlier paper. This new calibration adds 0.4 mag. to the magnitudes read from the scale on the older curves. Of this discrepancy, 0.26 mag. can be accounted for by a rediscussion of the calibrations and reductions to no atmosphere.

The albedo A of a planet has been defined as the ratio of the whole amount of reflected light to the whole amount of incident light.[1] While the term "albedo" applies only to reflected radiation, a similar definition may be applied to the planetary heat reradiated by the warmed surface. The new quantity would be the ratio of the energy in the whole planetary heat radiated to the whole incident radiation from the sun. If the measurements include the whole spectrum, the ratio of the planetary heat to the incident solar radiation is $1 - A$. We shall, therefore, call this function the "co-albedo."

In evaluating the co-albedo we may (1) measure the albedo with a total-radiation device or (2) measure the planetary heat. In the second method it will be necessary to evaluate the radiation measures on both illuminated and unilluminated sides. This method is particularly applicable to Venus, whose dark side emits considerable radiation.[2] In the case of the moon, where there is no sensible radiation on the dark side, only the planetary heat over the illuminated portion need be evaluated. Venus and the moon are the only members of our planetary system for which the radiation characteristics of the dark side are known. It is difficult to study the dark side of Mercury, whose small image must be observed in daytime (with very poor seeing), and still more difficult is the case of Mars, for which the angular width of defective illumination does not exceed 2″. For all the other planets, the impossibility of studying the dark side prohibits the use of the second method.

About ten years ago the writer completed a series of measures of lunar radiation[3] with the thermocouple, comprising measures of the planetary heat plus all the reflected radiation. The reflected radiation was then isolated by a microscope cover glass $\frac{1}{8}$ mm thick. Since the $2\frac{1}{2}$-inch mirror used to form the image was far too small to give deflections on standard stars, calibration to radiometric magnitude was made by an electric light which had been tested through an intermediate standard against a Hefner lamp.

H. N. Russell has called the writer's attention to the fact that the lunar co-albedo computed from the resulting phase-radiation curves exceeds unity and that the calibration must be in error. A thorough recheck of the original measures and calculations shows (1) that, according to laboratory tests, wind blowing over the lamp bulb might reduce its radiation 8.6 per cent and (2) that the reduction of observed lunar planetary heat to no atmosphere (correction for atmospheric absorption) should be calculated from the mean

* *Contributions from the Mount Wilson Observatory, Carnegie Institution of Washington*, No. 705.

[1] Bond's definition. See H. N. Russell, *Ap. J.*, **43**, 175, 1916.

[2] Pettit and Nicholson, *Pub. A.S.P.*, **36**, 227, 1924; *Pop. Astr.*, **32**, 614, 1924; *Pub. A.A.S.*, **5**, 184, 1924.

[3] *Mt. W. Contr.*, No. 504; *Ap. J.*, **81**, 17, 1933.

values for different temperature zones on the moon, instead of from a reduction based on the temperature corresponding to mean radiation over the illuminated disk.

The lunar surface was, therefore, divided into ten temperature zones which were projected upon the celestial sphere for various phases, as described in a former paper.[4] It was assumed that the subsolar temperature is 374° K and that planetary heat is distributed proportionally to $\cos^{2/3}\theta$, where θ is the angular distance from the subsolar point.[5,4] The factor required to transfer observed planetary heat from the whole moon to no atmosphere is then 2.83, 2.81, 2.81, and 2.83 for phase angles (elongation of the earth from the sun as seen from the moon) 0°, 60°, 90°, and 120°, respectively.

We may, therefore, use 2.82 (or −1.13 mag.) as the factor for any phase angle, the form of the phase-energy curve outside our atmosphere being the same as that observed. Correcting the bulb of the calibrating light for wind cooling and revising the atmospheric corrections add to the magnitude of the moon's planetary heat outside the atmosphere at full phase 0.26 mag. and lead to a co-albedo of 0.926, which is still somewhat too high.

Russell[6] has proposed (1) to express the albedo as the product of two factors, $A = pq$, in which p contains all the geometrical quantities and q contains the law of distribution of radiation. It is shown[6] that

$$\log p = 0.4\,(G - g) - 2\log \sigma_1 + 10.63\,,$$

where σ_1 is the semidiameter of the planet in seconds of arc at unit distance from the earth, g its magnitude at unit distance from both sun and earth, and G the magnitude of the sun at unit distance from the earth. The factor q is defined by the equation

$$q = \int_{-\pi}^{+\pi} f(i) \sin i \, di\,.$$

For lunar radiation the phase-energy curve furnishes the function of (i), if the energy at phase angle $i = 0$ is taken as unity and the phase angles are in radians. The integral can be evaluated by mechanical quadratures. The resulting value of q is 1.14, both for planetary heat outside our atmosphere and for that observed at the telescope.

We may, therefore, so calibrate the measures that the magnitude of the planetary heat outside the atmosphere, m_b, will give the correct co-albedo. Since radiation is reflected from the moon[5] at the rate of 0.24 cal/cm²/min and the loss by conduction is negligible, the co-albedo is 0.88, which is the ratio of (1.95 − 0.24) cal/cm²/min, the radiation emitted by the moon, to 1.95 cal/cm²/min, the radiation received by it. Since $q = 1.14$, then $p = 0.772$, and we may determine g from the relation

$$g = 2.5\,(0.4G - \log p - 2\log \sigma_1 + 10.63)\,.$$

Here the radiometric value of G outside the atmosphere, G_a, must be used. If m_r is the radiometric magnitude of the sun and Δm_r is the reduction to no atmosphere,[7] we have

$$G_a = m_r + \Delta m_r = -27.18 - 0.45 = -27.63\,.$$

The value of σ_1 is 2″.40. Hence we find that $g = -2.68$ mag. Since the correction to reduce lunar radiation from unit to mean distance is −12.95 mag., the magnitude of lunar planetary heat at full moon outside the atmosphere and at mean distance, m_{b_0}, is −15.63. This value was used to establish the calibration scale on the phase-energy curves.

Figure 1 shows in full-line graphs the phase-energy curves of (1) lunar planetary heat outside the atmosphere, (2) lunar planetary heat observed, and (3) reflected light as observed with the thermocouple,[8] all with a scale of magnitudes based on the foregoing re-

[4] Pettit and Nicholson, *Mt. W. Contr.*, No. 533; *Ap. J.*, **83**, 84, 1936.

[5] Pettit and Nicholson, *Mt. W. Contr.*, No. 392; *Ap. J.*, **71**, 102, 1930. [6] *Op. cit.*, p. 190.

[7] Pettit and Nicholson, *Mt. W. Contr.*, No. 369; *Ap. J.*, **68**, 279, Table III, 1928.

[8] Pettit, *op. cit.*, Fig. 3.

sults and a scale of phase angle in degrees below and radians above. The radiometric magnitude of the full moon in planetary heat is -14.50 and in reflected radiation, -13.10. Moreover, when we use the radiometric value of G, we obtain $p = 0.115$; and since the value of q is 0.87 for reflected radiation determined in the same manner as that described for planetary heat, we have $A = 0.100$ for the albedo of the moon in reflected radiation determined with the thermocouple and 0.90, for the co-albedo, nearly the value given by the direct radiometric observations.

Figure 1 also shows the theoretical phase-radiation curve (dashed line) for a slowly

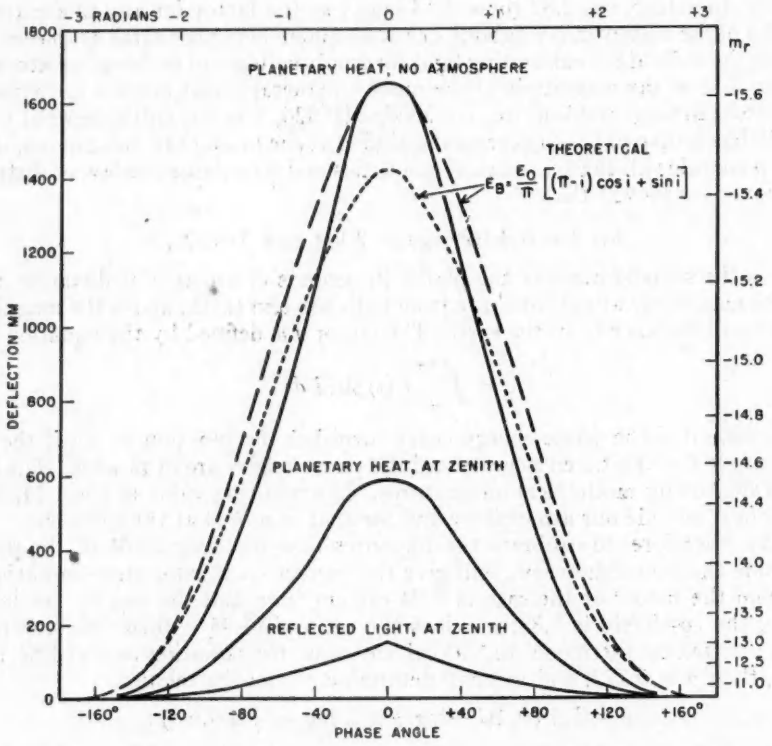

FIG. 1.—Total radiation from the moon at various phase angles. A deflection of 303 mm is equivalent to 10^{-5} cal/cm²/min.

rotating, nonconducting, smooth black sphere for which the planetary heat emitted, ϵ_B, can be computed from the radiation at zero phase angle, ϵ_0, by the formula

$$\epsilon_B = \frac{\epsilon_0}{\pi}[(\pi - i)\cos i + \sin i] .$$

At all phases except 0°, this curve is higher than the observed curve. If we assume that A is constant and that the total emission of the moon is the same as that for the theoretical smooth sphere, the area of the dashed line should be the same as that for the observed curve (full line, no atmosphere). This condition is met by the dotted line. From this curve we see that, if the moon were smooth, the emitted radiation at phase angle 0° would be 0.2 mag. fainter than that observed but that at phase angle 40° it would be the same.

THE GLOBULAR CLUSTERS NGC 5634 AND NGC 6229*

W. BAADE
Mount Wilson Observatory
Received April 18, 1945

ABSTRACT

Improved distance moduli for the two globular clusters NGC 5634 and NGC 6229 are derived from a photometric investigation of their cluster-type variables. The resulting values are $m - M = 16.91 \pm 0.04$ for NGC 5634 and $m - M = 17.53 \pm 0.02$ for NGC 6229. Both globular clusters are of less than average luminosity.

NGC 5634

NGC 5634 (1900.0 $14^h24^m.4$, $-5°32'$; $l = 310°.8$, $b = +48°.1$) is a well-concentrated, moderately rich globular cluster. Its photographic magnitude, according to Stebbins and Whitford,[1] is $m_{pg} = 10.48$. Although this value refers only to the central area, 64 seconds of arc in diameter, it should be closely identical with the total magnitude of the cluster, since the stars outside the central area probably contribute less than 0.2 mag. From densitometer tracings Shapley and Sayer[2] obtained $d = 6'.8$ for the apparent diameter of NGC 5634. Long exposures at the 100-inch reflector indicate a somewhat smaller value. By tracing the cluster stars to where they merge with the foreground the writer obtained $d = 5'.9$. In view of the relatively high galactic latitude of NGC 5634, obscuration effects should be negligible. This is confirmed by the color of NGC 5634, which appears normal,[1] and by the nebular density in the surrounding field, which is the same as that found in the galactic caps.[3]

The only previous determination of the distance modulus of NGC 5634 is the provisional value $m - M = 17.49$, derived by Shapley.[4] It is of low weight because it is based only on the integrated magnitude and the angular diameter of the cluster.

The present investigation of NGC 5634 is based on 42 plates obtained with the Mount Wilson reflectors between 1932 and 1936. Intercomparison of 15 pairs of plates with the blink-comparator led to the discovery of 7 variables. Their co-ordinates, referred to the center of the cluster, are given in Table 1. (See also Pl. I.)

The search for variables should be rather complete in the outer parts of the cluster. No attempt was made to cover the central area, some 45 seconds of arc in diameter, because it is insufficiently resolved on most of the plates.

For the establishment of sequences in NGC 5634 two intercomparisons with S. A. 108 at the 100-inch reflector (diaphragmed down to 84 inches in order to eliminate coma effects) were available. The comparison stars are listed in Table 2 and marked on Plate I.

The estimated magnitudes of the variables are collected in Table 3. Variable No. 7 has been omitted because it is located in the central area, which, as already mentioned, is poorly resolved on the majority of the plates.

The character of the observed light-variations leaves no doubt that all the variables are of the cluster type. Since the present material is insufficient to derive light-curves,

* *Contribution from the Mount Wilson Observatory, Carnegie Institution of Washington*, No. 706.

[1] *Mt. W. Contr.* No. 547; *Ap. J.*, **84**, 132, 1936. NGC 5634 does not occur in W. H. Christie's list (*Mt. W. Contr.* No. 620; *Ap. J.*, **91**, 49, 1940) because the image of a near-by bright star overlapped the cluster on the schraffierkassette plates.

[2] *Proc. Nat. Acad. Sci.*, **21**, 593, 1935.

[3] H. Shapley, *Proc. Nat. Acad. Sci.*, **30**, 61, 1944.

[4] *Star Clusters* (Harvard Obs. Mono., No. 2), p. 225, 1930.

maximum and minimum magnitudes of the variables were read off from the data in Table 3. This procedure needs a few comments. There is usually no difficulty in obtaining correct values of the maximum brightness, since incomplete coverage of this phase is easily recognized. It is, however, more difficult to avoid systematic errors in the minimum brightness. Since, for various reasons, exposure times are usually chosen in such a manner that at minimum the variables are close to the plate limit, the observational errors

TABLE 1

CO-ORDINATES OF VARIABLE STARS IN NGC 5634

Var. No.	X	Y
1	−56".5	− 19".5
2*	−25.4	+ 83.1
3	−45.1	+ 41.9
4†	+54.2	− 65.2
5	−11.6	−162.9
6	+43.4	− 52.6
7‡	− 0.4	− 4.0

* S. preceding component of close double star.
† S. following component of double star.
‡ Following component of very close double star.

TABLE 2

MAGNITUDES OF COMPARISON STARS IN NGC 5634

STAR	m_{pg}	RESIDUALS	
		H647	H648
A	16.15	+ 1	− 1
B	15.98	− 4	+ 3
C	16.23	− 3	+ 4
D	16.16	− 4	+ 3
E	16.27	− 2	+ 1
a	16.41	+ 3	− 3
b	16.77	+ 8	− 8
c	16.90	0	+ 1
d	16.99	− 1	+ 1
e	17.27	−12	+12
f	17.57	− 8	+ 8

in the estimated magnitudes are not negligible. Hence the minimum brightness of a variable derived from the five or six faintest observed magnitudes will be, in general, systematically smaller than the true minimum brightness. In deriving the minimum magnitudes for the present variables efforts have been made to avoid this systematic error by taking advantage of those nights on which several plates were obtained in succession. The resulting photometric data for the variables are in Table 4. The small dispersion in the median magnitudes supports our former assumption that all the variables are of the cluster type.

PLATE I

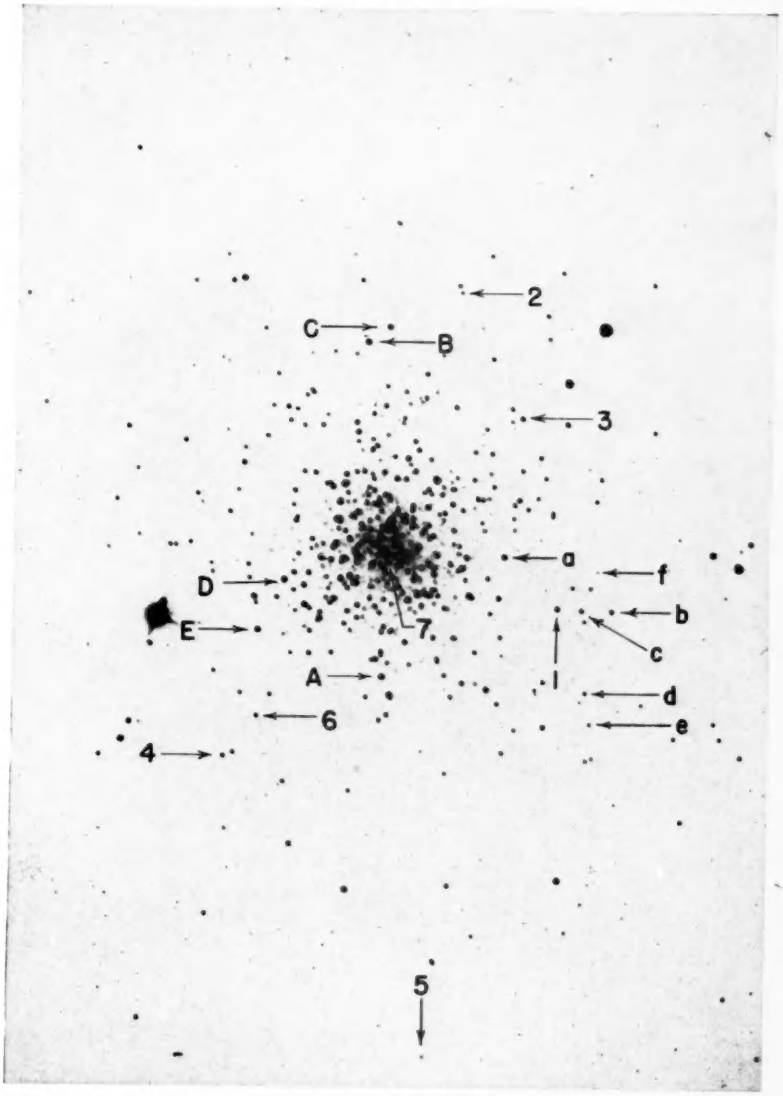

NGC 5634
Scale, 1 mm = 2″.46

PLATE II

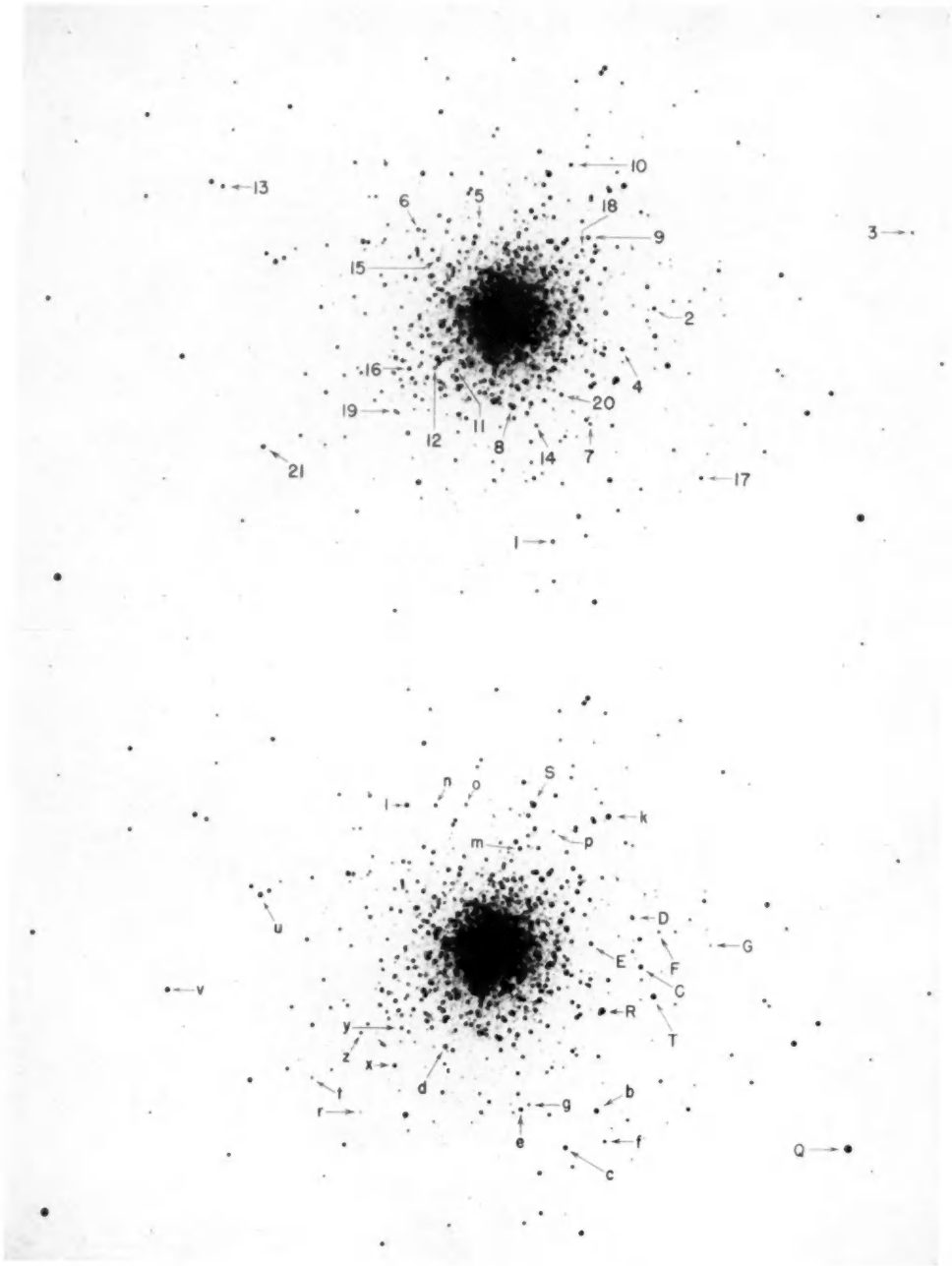

NGC 6229

Above, VARIABLE STARS; *below*, COMPARISON STARS

Scale, 1 mm = 3″.57

TABLE 3

PHOTOGRAPHIC MAGNITUDES OF VARIABLES IN NGC 5634

Helioc. G.M.T.	Plate*	1	2	3	4	5	6
2426828.932.....	S 37	17.16	17.08	17.50	17.35	17.28	16.76
27163.961.....	H205	16.52	.....	17.30	.....	17.15	16.75
27193.752.....	S158	16.87	17.32	17.52	17.45	16.94	17.04
.780.....	159	16.95	17.27	17.48	17.42	16.95	16.95
.808.....	160	16.96	17.34	17.47	17.15	16.96	16.90
.838.....	161	16.98	17.17	17.44	16.95	16.93	16.70
.911.....	162	17.20	16.96	17.46	16.87	16.97	16.90
27209.675.....	S165	16.98	17.42	16.95	16.89	16.93	16.71
27210.761.....	S175	16.50	17.48	17.49	17.20	16.99	16.82:
27211.712.....	S184	17.32	16.95	16.95	16.54	16.88	16.71
27215.685.....	H217	17.27	17.40	16.83	17.21	16.93	16.97
27243.696.....	S195	16.53	16.45	17.44	16.96	16.98	16.96
27505.964.....	S312	16.93	17.25	17.24	16.87	16.96	16.98
506.012.....	313	16.96	16.90	17.41	16.90	16.92	16.99
27539.919.....	S316	17.35	16.73	16.86	17.12	17.17	16.80
.942.....	317	17.39	16.63	16.48	16.96	17.20	16.96
27568.821.....	S319	17.24	17.42	16.65	17.05	17.25	16.95
27630.693.....	S343	17.34	16.91	16.96	17.39	17.05	16.95
27631.703.....	S348	16.70	17.33	17.48	16.95	16.97	16.95
27892.797.....	S405	17.27	16.91:	17.48	16.85	16.95	16.73
.906.....	407	17.41	17.27:	17.46	17.38	17.32	16.92
28284.745.....	S436	17.41	.....	17.43	17.36	16.95	16.95
.835.....	440	17.38	>17.0	17.44	.....	16.92	16.62
.927.....	442	17.29	>17.0	17.44	16.70	16.89	16.81
.961.....	443	17.41	>17.0	17.51	16.57	16.70	.....
28285.741.....	S445	16.95	16.21	16.67	16.92	16.95	17.19
.836.....	449	16.69	16.68	17.06	16.95	16.97	16.73
.921.....	451	16.92	16.84	17.22	17.36	17.24	16.68
28310.794.....	H628	16.54	17.06	17.40	16.55	17.20	16.95
28311.783.....	H636	17.41	16.48	17.39	17.30	16.89	16.81
28312.765.....	H646	16.62	17.13	16.57	16.81	.....	16.70
.791.....	647	16.41	17.22	16.66	16.86	17.21	16.81
.799.....	648	16.41	17.18	16.72	16.97	17.15	16.81
28313.821.....	S456	17.42	17.21	17.48	16.84	16.75	16.89
.857.....	457	17.49	16.95	17.51	16.84	16.92	16.92
28314.782.....	S463	16.63	16.17	17.28	17.10	16.99	16.68
.812.....	464	16.66	16.30	17.33	17.05	17.12	16.71
.844.....	465	16.72	16 41	17.39	17.18	17.07	16.68
28334.774.....	H652	17.21	16.87	17.45	16.82	.....	16.61
28335.703.....	H659	17.40	16.94:	16.99	17.27	.....	16.94
.776.....	662	17.24	16.90	17.16	16.90	.....	16.66
28336.794.....	H671	17.12	.....	16.62	17.24	.....	16.73

*"H" and "S" indicate plates taken with the 100-inch and 60-inch reflector, respectively.

Excluding variables Nos. 5 and 6, for which, respectively, the maximum and the minimum brightness are uncertain, we obtain for the distance modulus of NGC 5634, $m-M=16.91 \pm 0.04$, corresponding to a distance of $R = 24.1$ kpc.

TABLE 4

PHOTOMETRIC DATA FOR VARIABLES IN NGC 5634

Var. No.	Max.	Min.	Ampl.	Med. m
1*	16.41	17.39	0.98	16.90
2	16.19	17.38	1.19	16.79
3	16.48	17.47	0.99	16.98
4	16.55	17.39	0.84	16.97
5	16.72:	17.19	0.47:	16.96:
6	16.69	17.05:	0.36:	16.87:

* Period probably 0.65872 day.

In order to obtain information about the upper limit of luminosity of the stars in NGC 5634, the magnitudes of some 50 of the brightest stars were measured on a 100-inch plate of short exposure. The resulting data for the brightest stars are, in Shapley's notation:

$$m_6 = 15.97 \qquad M_6 = -0.94$$
$$m_{30} = 16.58 \qquad M_{30} = -0.33$$
$$m_{25} = 16.32 \qquad M_{25} = -0.59$$

NGC 6229

NGC 6229 (1900.0 $16^h44^m.2$, $+47°42'$; $l = 40°.3$, $b = +39°.4$) is in many respects similar to NGC 5634 but is considerably richer in stars. Its angular diameter, as inferred from the most distant cluster members on a 100-inch plate of one-hour exposure, is $d = 5'.9$. Nearly the same value, $d = 5'.3$, was obtained by Shapley and Sayer[2] from densitometer tracings on Harvard plates. Photometric measures of the apparent magnitude of NGC 6229 have been made by Christie[5] and by Stebbins and Whitford.[1] Their respective values, $m_{pg} = 10.26$ and $m_{pg} = 10.17$, are practically identical, although Stebbins and Whitford measured only the central area of the cluster, 64 seconds of arc in diameter. Obviously, the contribution of the outer fringe of the cluster is quite small. With a latitude $b = +39°$, NGC 6229 is well outside the zone of obscuration. Indeed, neither the color of the cluster[1] nor the nebular density in the surrounding field[3] gives any indication of detectable absorption effects.

Shapley's distance modulus for NGC 6229, $m-M = 17.36$, is based on the magnitudes of the brightest stars, total magnitude, and angular diameter.[4] It agrees closely, as we shall see later, with the value derived from the cluster variables.

The present investigation of the variables in NGC 6229 is based on 46 plates obtained in the years 1932–1935. Intercomparison of 11 pairs of plates with the blink-comparator resulted in the discovery of the 21 variables listed in Table 5. (See also Pl. II.) They are new, with the exception of variable No. 8, which had previously been announced by Miss H. Davis.[6]

Sequences of comparison stars were established through intercomparisons with S.A. 37. The stars are marked on Plate II; their magnitudes are in Table 6. Somewhat provisional are the values for the sequence Q, R, S, T since these stars are a little too bright on the present plates for accurate photometric measurement. The magnitudes of the variables are collected in Table 7.

[5] *Op. cit.* [6] *Pub. A.S.P.*, **29**, 260, 1917.

TABLE 5

CO-ORDINATES OF VARIABLE STARS IN NGC 6229

No.	X	Y	No.	X	Y
1	− 24".6	−105".5	11	+ 23".9	− 25".0
2	− 71.9	+ 4.9	12	+ 34.2	− 23.6
3	−195.7	+ 41.3	13	+140.2	+ 61.3
4	− 56.8	− 14.3	14	− 15.5	− 50.7
5	+ 14.5	+ 44.1	15	+ 34.2	+ 27.5
6	+ 44.1	+ 41.5	16	+ 47.0	− 24.2
7	− 41.7	− 49.9	17	− 96.3	− 75.0
8*	− 4.1	− 42.1	18	− 36.1	+ 32.2
9	− 38.9	+ 38.3	19†	+ 53.4	− 44.4
10	− 29.5	+ 72.7	20	− 27.5	− 36.1
			21	+117.3	− 61.6

* S. preceding component of double star. † N. following component of double star.

TABLE 6

MAGNITUDES OF COMPARISON STARS IN NGC 6229

STAR	m_{pg}	RESIDUALS		
		H510	H511	H516
b	16.65	+ 1	−19	+18
c	16.99	+ 7	− 5	− 2
d	17.23	+ 1	− 4	+ 4
e	17.46	− 2	− 7	+ 8
f	17.77	− 1	− 8	+ 8
g	18.11	+ 7	− 7	− 1
k	16.50	+ 7	− 8	0
l	16.99	+ 6	−13	+ 8
m	17.48	− 2	− 2	+ 3
n	17.65	− 1	+ 4	− 2
o	17.87	− 2	+ 2	− 1
p	18.10	+ 1	− 3	+ 1
u	16.72	+11	−22	+10
v	16.86	+ 6	− 6	0
x	17.51	− 4	− 5	+ 8
y	17.86	−12	+15	− 3
z	18.03	− 5	+ 5	0
r	18.21	− 3	+ 8	− 6
t	18.28	+ 2	−10	+ 8
C	16.88	+ 2	− 5	+ 2
D	17.47	− 1	−10	+12
E	17.58	−15	− 7	+23
F	17.85	− 3	+ 2	+ 1
G	18.12	0	+ 6	− 5
Q	15.16	+ 6	−16	+ 9
R	15.35	+ 1	−13	+11
S	15.93	− 3	− 5	+ 8
T	16.23	− 5	+ 3	+ 1

TABLE 7

PHOTOGRAPHIC MAGNITUDES OF VARIABLES IN NGC 6229

Helioc. G.M.T.	Plate	1	2	3*	4	5	6	7	8	9	10	11	12	13	14	15	16	17*	18	19	20	21
2426858^{d}910	S 48	17.72	17.73	17.78	17.78	17.60	17.73	17.39	15.71	17.62	18.00	17.85	17.58	17.52	17.48	17.62	17.83	17.71	18.04	17.92	18.08	17.48
.948	49	17.77	17.79	17.72	17.84	17.21	17.84	17.11	15.68	17.60	18.04	17.89	17.88	17.55	17.68	17.41	17.83	17.37	18.03	17.94	18.09	17.50
.978	50	17.92	17.84	17.72	17.96	17.38	18.00	17.25	15.62	17.98	18.03	18.00	17.89	17.58	17.63	17.43	17.51	17.16	18.06	17.83	18.08	17.86
26859.857	S 52	17.03	17.50	17.50	17.56	17.80	17.38	>17.8	15.50	17.50	17.92	18.07	17.53	17.98	17.44	17.62	17.96	17.61	17.83	17.96	18.08	18.02
.884	53	17.09	17.23	17.44	17.58	17.85	17.43	>17.7	15.42	17.62	17.89	17.88	17.34	17.86	17.44	17.75	17.93	17.68	17.76	18.00	17.98	17.89
.903	54	17.35	17.28	17.51	17.63	17.93	17.53	17.34	15.39	17.61	18.04	.....	.....	17.33	17.46	17.74	17.83	17.66	18.08	.....	18.03	17.64
.933	55	17.39	17.38	17.56	17.66	17.96	17.65	16.92	15.36	17.75	17.92	17.67	17.76	17.14	17.73	17.91	17.86	17.60:	17.93	17.64	18.02	17.48
27209.712	S166	17.73	17.32	17.53	17.61	17.75	17.94	17.40	16.51	17.86	17.43	17.64	18.01	17.50	17.01	17.93	17.99	17.65	17.95	17.92	17.96	17.94
.738	167	17.80	17.53	17.61	17.50	17.85	17.90	17.21	16.20	17.73	17.30	17.87	18.00	17.28	17.24	17.62:	17.88	17.64	17.98	17.94	18.04	17.96
.763	168	17.72	17.59	17.58	17.53	17.97	17.99	17.31	16.47	17.87	17.40	17.91	17.89	17.51	17.40	17.92	17.79	17.47	18.04	17.58	18.04	17.92
.974	172	17.70	17.86	17.80	17.86	17.92	17.48	17.74	16.51	17.43	17.92	18.02	17.85	18.08	17.76	17.81	18.02	17.46	17.51	17.86	17.17	17.72
27210.732	S174	17.30	17.84	17.75	17.88	17.79	17.98	17.34	16.62	17.76	17.97	17.97	17.93	17.60	17.67	17.57	17.79	17.61	17.86	17.01	18.11	17.88
27211.684	S183	18.00	17.94	17.82	17.78	17.26	17.62	17.97	16.12	17.75	17.96	17.96	17.95	18.00	17.67	17.92	17.86	17.60	17.68	16.97	18.06	17.53
.746	185	17.44	17.89	17.82	17.85	17.62	17.65	17.18	16.18	17.84	18.04	18.07	17.16	17.90	17.91	17.51	17.44	17.67	17.48	17.26	18.03	17.72
27244.704	S207	17.25	17.44	17.54	17.88	17.84	17.43	17.42	15.22	17.16	17.30	17.87	17.86	17.12	17.46	17.86	17.76	17.41	17.49	17.86	18.08	17.86
27599.899	S329	17.89	17.85	17.75	17.59	17.93	17.56	17.89	15.45	17.87	17.92	>18.0	17.96	17.40	17.89	17.58	17.88	17.74	18.02	17.95	18.03	17.10
.924	330	17.86	17.85	17.75	17.61	17.98	17.60	18.04	15.56	17.89	17.92	18.01:	17.98	17.17	17.96	17.63	18.07	17.80	18.03	18.05	18.06	17.33
.949	331	17.91	17.83	17.76	17.69	17.91	17.63	18.06	15.57	17.95	18.01	18.02	18.01	17.31	17.89	17.74	18.02	17.74	17.91	18.00	18.04	17.44
27600.908	S340	17.70	17.88	17.61	17.96	17.93	17.61	17.74	15.25	17.58	17.78	18.00	17.93	18.05	17.74	17.45	17.89	17.67	17.61	18.02	17.95	17.96
.929	341	17.78	17.90	17.63	17.75	17.91	17.60	17.70	15.36	17.67	17.64	17.90	17.51	18.06	17.84	17.52	17.85	17.64	17.62	17.81	17.24	17.95
.952	342	17.74	17.96	17.71	17.67	17.93	17.50	17.82	15.30	17.58	17.72	17.89	17.16	18.10	17.82	17.51	17.90	17.34	17.55	17.87	16.93	17.94

* Difficult to measure, since star is far from sequence.

TABLE 7—*Continued*

Helioc. G.M.T.	Plate	1	2	3*	4	5	6	7	8	9	10	11	12	13	14	15	16	17*	18	19	20	21
2427925.931	S414	17.19	17.15	17.44	17.78	17.98	17.44	18.01	15.78	17.09	17.25	18.08	17.18	18.01	17.57	17.95	17.76	17.11	18.03	.....	18.04	17.40
27927.985	H471	17.87	17.85	17.76	17.88	17.91	17.90	17.91	15.42	17.74	18.02	17.93	17.72	17.80	17.78	17.58	17.85	17.65	17.38	17.69	18.11	17.60
27953.802	S416	17.91	17.49	17.69	17.64	.....	.....	.....	16.19	.....	18.09	.....	.....	.....	17.29	.....	.....	.....	.....	.....	.....	.....
.916	418	16.86	17.75	17.83	17.85	17.26	17.28	>17.8	16.12	17.92	17.97	18.02	17.19	18.01	17.41	17.81	17.57	17.18	17.94	.....	18.04	17.34
.944	419	17.05	17.83	17.83	17.86	17.28	17.28	17.39	16.12	17.87	17.96	>18.1	17.23	18.01	17.68	17.21	17.58	17.36	18.05	17.86	18.11	17.53
27977.759	H503	17.81	17.78	17.66	17.84	17.93	17.95	17.89	15.79	17.80	17.94	18.08	18.01	17.75	17.84	17.97	17.78	17.55	17.38	17.87	18.08	17.89
.780	504	17.88	17.80	17.64	17.85	17.95	17.94	17.43	15.77	17.81	17.95	.....	18.01	17.78	17.80	17.76	17.62	17.51	17.33	17.97	17.98	17.89
.806	505	17.92	17.83	17.70	17.89	17.96	17.95	16.81	15.81	17.91	17.93	>18.0	17.94	17.82	17.87	17.64	17.60	17.37	17.35	17.97	18.05	17.88
.828	506	17.58	17.84	17.67	17.86	18.01	17.93	16.90	15.78	17.93	17.97	>18.0	18.03	17.93	17.91	17.52	17.51	17.14	17.57	17.89	18.02	17.86
.898	507	16.80	17.88	17.74	17.88	17.62	17.86	17.30	15.75	17.91	17.92	17.85	17.53	17.96	17.81	17.61	17.81	17.07	17.61	17.96	17.40	17.85
.927	508	16.85	17.96	17.84	17.94	17.17	17.65	17.48	15.79	17.79	17.98	17.44	17.16	17.92	17.66	17.69	17.83	17.13	17.94	17.94	16.87	17.87
27978.768	H510	17.65	17.54	17.71	17.75	17.95	17.79	17.84	16.23	17.52	17.82	18.03	18.07	17.54	17.97	17.83	17.47	17.48	17.94	18.01	18.03	17.58
.842	511	17.95	17.72	17.32	17.83	17.78	17.74	16.80	16.30	17.66	17.89	17.99	18.00	17.67	18.04	17.75	17.32	17.14	18.02	18.01	16.91	17.85
.910	512	17.91	17.82	17.46	17.84	18.04	17.87	17.31	16.18	17.66	17.92	18.01	17.14	17.74	16.94	17.51	17.86	17.25	17.48	17.90	17.35	17.89
.929	513	17.87	17.82	17.66	17.84	17.95	17.98	17.41	16.16	17.75	17.92	18.07	17.18	17.86	16.96	17.41	17.86	17.39	17.38	17.05	17.45	17.88
.951	514	17.88	17.85	17.69	17.84	17.77	18.04	17.57	16.07	17.84	17.95	>18.0	17.19	17.95	17.18	17.43	17.88	17.37	17.35	16.97	17.59	17.86
27979.759	H516	17.32	17.53	17.77	17.35	17.87	17.63	18.01	16.69	17.47	17.40	17.98	18.10	17.46	18.02	17.41	17.32	17.49	17.92	18.04	17.67	17.14
.807	517	17.49	17.15	17.80	17.38	17.84	17.74	17.63	16.51	17.51	17.61	17.96	17.99	17.19	17.14	17.51	17.30	17.39	17.92	18.01	16.88	17.44
.821	518	17.55	17.25	17.83	17.62	17.94	17.72	17.24	16.65	17.56	17.54	18.07	17.99	17.23	16.74	17.83	17.43	17.04	17.89	18.01	16.96	17.42
.863	519	17.66	17.49	17.76	17.64	17.93	17.92	16.90	16.67	17.67	17.80	17.99	17.71	17.62	17.13	17.86	17.86	17.11	17.92	17.90	17.42	17.60
.926	520	17.75	17.74	17.38	17.75	17.90	17.85	17.35	16.64	17.72	17.82	17.99	17.08	17.70	17.39	17.81	17.89	17.32	17.84	16.95	17.72	17.89
.943	521	17.79	17.78	17.23	17.78	18.02	17.92	17.60	16.73	17.84	17.88	18.05	17.14	17.75	17.62	17.89	17.86	17.44	17.93	17.07	17.85	17.81
.958	522	17.80	17.78	17.09	17.78	18.10	17.92	17.53	16.65	17.88	17.87	18.03	17.43	17.70	17.71	17.80	17.97	17.57	17.96	17.41	17.95	17.78
28015.786	S422	17.78	18.07	17.70	17.92	17.43	18.07	17.65	15.70	17.91	17.41	17.99	17.57	17.93	17.35	17.73	17.85	17.60	18.03	17.89	17.75	17.98
.816	423	17.86	17.99	17.72	17.94	17.35	18.01	17.13	15.71	17.92	17.46	18.01	17.78	18.03	17.52	17.61	17.87	17.56	17.97	18.00	17.95	17.92

In deriving the maximum and minimum brightness of the variables the procedure mentioned previously in connection with NGC 5634 has been followed. The resulting photometric data are given in Table 8.

TABLE 8

PHOTOMETRIC DATA FOR VARIABLES IN NGC 6229

Var. No.	Max.	Min.	Ampl.	Med. m
1	16.84	17.90	1.06	17.37
2	17.18	17.93	0.75	17.55
3	17.21	17.82	0.61	17.51
4	17.36:	17.89	0.53:	17.62:
5	17.21	17.95	0.74	17.58
6	17.28:	17.96	0.68:	17.62:
7	16.84	18.01	1.17	17.42
8	15.30	16.64	1.34	15.97
9	17.12:	17.91	0.79:	17.51:
10	17.28	17.99	0.71	17.63
11	<17.44	18.01	>0.57	.....
12	17.12	18.02	0.90	17.57
13	17.15	18.01	0.86	17.58
14	16.88	17.95	1.07	17.41
15	17.39	17.92	0.53	17.65
16	17.31	17.94	0.63	17.62
17	17.08	17.72	0.64	17.40
18	17.34	18.00	0.66	17.67
19	16.96	18.00	1.04	17.48
20	16.91	18.05	1.14	17.48
21	17.12	17.94	0.82	17.53

TABLE 9

SUMMARY OF RESULTS

	NGC 5634	NGC 6229
Galactic longitude (Lund tables)	310°.8	40°.3
Galactic latitude (Lund tables)	+ 48°.1	+39°.4
Modulus $(m-M)$	16.91	17.53
Distance from sun	24.1 kpc	32.1 kpc
Distance from center of galaxy ($R\odot = 8.0$ kpc)	19.9 kpc	31.2 kpc
Distance from galactic plane (Z-component)	+ 17.9 kpc	+20.4 kpc
Apparent diameter	5'.9	5'.9
Linear diameter	41 parsecs	55 parsecs
Apparent total brightness (phot.)	10.4 mag.	10.2 mag.
Absolute total brightness	− 6.5 mag.	− 7.3 mag.
Upper limit of luminosity for stars (M_6)	− 0.9 mag.	− 1.5 mag.

Obviously, the variables are of the cluster type, with the exception of the bright variable No. 8, which appears to be a long-period cepheid of $M_{\text{med}} = -1.6$. Excluding the incompletely observed variables Nos. 4, 6, 9, and 11, we obtain for the distance modulus of NGC 6229 $m-M = 17.53 \pm 0.02$. The corresponding distance is $R = 32.1$ kpc.

As mentioned previously, the magnitudes of the brightest stars in NGC 6229 have already been determined by Shapley. They can be used here without further adjustment, since they are, like the magnitudes of the present paper, on the International System. Shapley's apparent magnitudes, together with the absolute magnitudes based on the distance modulus $m-M = 17.53$, are as follows:

$$\begin{array}{ll} m_6 = 15.90 & M_6 = -1.63 \\ m_{30} = 16.37 & M_{30} = -1.16 \\ m_{25} = 16.18 & M_{25} = -1.35 \end{array}$$

The essential data for NGC 5634 and NGC 6229 are summarized in Table 9. Both clusters are of less than average luminosity. Their moderate stellar content is reflected in their linear diameters, which are about half as large as those of rich globular clusters like Messier 3 or Messier 13.

The writer is greatly obliged to Dr. Harold F. Weaver, who estimated the magnitudes for more than half of the variables in NGC 6229.

INVESTIGATIONS ON PROPER MOTION. XXIV. FURTHER MEASURES IN THE PLEIADES CLUSTER*

ADRIAAN VAN MAANEN
Mount Wilson Observatory
Received May 3, 1945

ABSTRACT

Five pairs of plates with intervals of about 25 years, taken at the 80-foot focus of the 60-inch telescope in the region of the Pleiades and covering about 0.80 of a square degree, were measured for proper motion. They contain 409 stars down to photographic magnitude 15.9. Including the measures given in *Mt. W. Contr.* No. 653, we have measured 452 stars. Of these, 71 are found to be probable members of the Pleiades, while 9 others have motions which are of about the same order. One star may be a member of the Hyades.

In 1941 I published an investigation on "Faint Members of the Pleiades Cluster,"[1] based on two pairs of plates taken at the Newtonian focus of the 100-inch reflector with exposures of from 30 to 60 minutes. The field covered a region 40′ by 32′ around Alcyone, and the limiting photographic magnitude was about 17.5. Since the accuracy of measures on these plates decreases rapidly beyond 10 minutes of arc from the center and since the purpose of the investigation was primarily to identify faint members of the Pleiades, it was decided to measure not all the 800 stars on the plates but only those stars which had been shown, by blinking, to have either group-motion or some other interesting motion. A number of comparison stars were, of course, included. Of the 70 stars selected for their motion, 56 were found to be possible members of the cluster; half of these had not been published before.

As long ago as 1918, I took several 30-minute exposures at the 80-foot focus of the 60-inch reflector in the region of the Pleiades. Several of these fields were reobserved in 1943, after an interval of 25 years. The plates, while partly overlapping, cover a field of 0.80 of a square degree; on most of the plates the limiting photographic magnitude is about 15.9, but in 0.08 of a square degree it is only 15.5. The scale of the plates at this focus varies so much that mere blinking of the plates does not show the group-motions with sufficient accuracy. On the other hand, the motion of a member of the Pleiades is, during the interval between the old and new plates, over 1 second of arc, or more than 0.1 mm. Hence, both the measures and the reductions can be simplified considerably and still enable us to obtain the necessary accuracy to distinguish between members and non-members of the group. On the 60-inch plates, 409 stars were measured on one or more of the five pairs of plates; adding 43 stars which were measured only on the 100-inch plates, we have 452 stars measured on from one to six sets of plates. Among these stars, 80 were found whose motions are within 0″.020 of the mean motion of the Pleiades, the limit taken at first as defining the membership of the cluster. Data for these stars are in Table 1. The succeeding columns give the current number; the number in Hertzsprung's list;[2] the right ascension and declination for 1900; the photographic magnitude and color index, when available, as given in Hertzsprung's memoir; the absolute proper motion in α and δ; the number of determinations; and, finally, some remarks.

Under "Number of Determinations" the results from the two pairs of plates, discussed in *Mount Wilson Contribution* No. 653, are counted as one determination because the

* *Contributions from the Mount Wilson Observatory, Carnegie Institution of Washington*, No. 707.

[1] *Mt. W. Contr.*, No. 653; *Ap. J.*, **94**, 399, 1941.

[2] "Effective Wave Lengths of Stars in the Pleiades," *K. Danske Vidensk. Selsk. Skrifter, Naturv. og Math. Afd.*, Ser. 8, **4**, 347, 1923.

TABLE 1

PROBABLE AND POSSIBLE MEMBERS OF THE PLEIADES

No.	He	α (1900) 3^h	δ (1900)	m_{ph}	I_λ	μ_α	μ_δ	No. of Det.	Remarks
1.....	265	$40^m\ 5^s$	24° 13′	6.7	−0.11	+0″.018	−0″.040	1	H II
2.....	300	16	23 45	15.8	.....	.034	.046	1	H III
3.....	313	19	23 53	8.4	+0.14	.028	.052	3	H II
4.....	323	23	23 38	4.2	−0.19	.040	.042	2	H IV
5.....	332	27	24 3	13.6	+0.93	.015	.038	2	H II
6.....	.....	28	23 51	16.7	.....	.030	.051	1	III
7.....	341	30	23 57	7.6	+0.08	.025	.049	3	H II
8.....	343	31	24 7	11.8	+0.49	.017	.037	1	H II
9.....	356	35	23 48	15.3	.....	.023	.046	3	H I
10.....	373	40	23 39	15.5	+0.74	.018	.042	2	H I
11.....	378	40	24 2	13.3	+0.99	.019	.042	2	H I
12.....	380	41	24 13	14.6	+1.19	.013	.037	1	H III
13.....	388	43	23 48	9.6	+0.21	.027	.047	3	H II
14.....	390	43	23 43	13.1	+0.84	.018	.047	2	H I
15.....	.....	47	23 41	>17	.....	.028	.043	1	II
16.....	.....	56	23 59	>17	.....	.030	.047	1	II
17.....	.....	57	23 54	>17	.....	.019	.043	1	I
18.....	436	41 2	24 13	7.0	−0.05	.018	.051	1	H II
19.....	454	7	23 51	15.1	.....	.022	.044	2	H I
20.....	457	8	23 41	8.6	+0.15	.023	.044	2	H I
21.....	.....	13	23 45	>17	.....	.021	.044	1	I
22.....	468	13	23 58	9.6	+0.17	.026	.045	3	H I
23.....	484	20	23 49	9.1	+0.23	.023	.041	3	H I
24.....	487	21	24 5	14.0	+1.26	.025	.045	1	H I
25.....	493	22	23 44	15.2	+0.73	.016	.047	2	H II
26.....	501	23	23 50	8.5	+0.14	.024	.043	3	H I
27.....	508	24	23 48	6.4	−0.02	.024	.045	3	H I
28.....	518	28	23 36	10.6	+0.37	.022	.047	2	I
29.....	520	28	23 36	7.6	−0.01	.028	.044	2	H II
30.....	.....	29	23 44	16.8	.....	.024	.047	1	I
31.....	540	32	23 59	7.0	+0.01	.018	.049	3	H II
32.....	542	32	23 48	2.9	−0.18	.018	.041	2	H I
33.....	577	43	24 3	11.1	+0.38	.016	.033	2	H III
34.....	578	43	24 0	14.9	.....	.027	.042	2	H II
35.....	588	45	23 40	14.6	+1.17	.026	.047	2	H I
36.....	.....	50	23 44	16.4	.....	.028	.046	1	II
37.....	620	56	23 38	10.2	+0.26	.020	.045	2	H I
38.....	.....	42 8	23 45	16.5	.....	.030	.044	1	II
39.....	681	10	23 50	9.9	+0.27	.027	.043	5	H I
40.....	693	16	24 1	8.7	+0.17	.020	.044	3	H I
41.....	.....	20	24 12	15.5	.....	.020	.048	1	H I
42.....	706	21	23 35	10.8	+0.35	.019	.046	3	H I
43.....	.....	22	23 35	15.9	.....	.019	.047	3	H I
44.....	736	30	23 44	10.4	+0.28	.027	.047	3	H II
45.....	742	33	24 2	7.2	+0.06	.016	.038	2	H II
46.....	.....	34	23 58	17.0	.....	.026	.041	1	I
47.....	757	38	23 52	9.5	+0.23	.020	.045	3	H I
48.....	807	52	23 58	11.6	+0.65	.020	.046	3	H I
49.....	809	53	23 40	13.9	+0.93	.023	.041	3	H I
50.....	.....	43 0	24 1	>17	.....	+0.020	−0.053	1	II

TABLE 1—*Continued*

No.	He	α (1900) 3^h	δ (1900)	m_{ph}	I_λ	μ_α	μ_δ	No. of Det.	Remarks
51.....	862	43 m10s	23°29′	11.4	+0.60	+0″.020	−0″.043	1	H I
52.....	870	13	23 45	3.6	−0.22	.028	.034	2	H III
53.....	878	14	23 50	4.9	−0.19	.026	.052	2	H II
54.....	885	16	23 35	8.2	+0.11	.016	.046	2	H II
55.....	891	19	24 5	7.6	+0.06	.015	.038	1	H II
56.....	910	24	24 5	6.6	−0.09	.017	.042	1	H II
57.....	922	28	23 32	11.8	+0.61	.018	.050	1	H II
58.....	924	29	23 57	8.1	+0.08	.024	.048	2	H I
59.....	936	33	23 24	12.1	+0.62	.023	.046	1	H I
60.....	946	37	23 29	11.4	+0.45	.018	.045	1	H I
61.....	956	39	23 59	12.3	+0.74	.018	.045	2	H I
62.....	972	44	24 9	13.3	+0.97	.016	.046	1	H II
63.....	977	47	23 24	6.0	−0.12	.016	.055	1	H III
64.....	986	54	23 24	12.3	+0.65	.018	.044	1	H I
65.....	996	59	24 3	7.4	+0.02	.019	.040	1	H I
66.....	1001	44 1	23 33	10.9	+0.30	.019	.044	1	H I
67*....	1002	1	23 33	10.9	.....	.011	.050	1	H III
68*....	1003	1	23 33	6.8	−0.03			1	H III
69.....	.....	8	23 49	15.1	.....	.018	.046	1	H I
70.....	1030	14	24 14	15.0	+0.99	.006	.046	1	H IV
71.....	1049	23	24 10	11.5	+0.47	+0.028	−0.044	1	H II
72.....	.....	40m25s	23°40′	16.5	.....	+0″.008	−0″.039	1	III
73.....	.....	53	23 37	15.9	.....	.012	.039	1	H III
74.....	426	58	23 48	15.3	+1.77	.035	.030	2	IV
75.....	.....	41 11	24 0	>17	.....	.036	.050	1	IV
76.....	490	21	23 47	15.2	+1.12	.036	.038	1	IV
77.....	.....	44	23 38	>17	.....	.015	.033	1	III
78.....	622	57	23 41	14.5	+0.50	.018	.042	2	H I
79.....	798	42 50	23 54	15.3	+0.06	.037	.043	3	IV
80.....	879	43 15	23 56	12.6	+0.55	+0.018	−0.031	2	III

* Nos. 67 and 68 were measured as one star.

probable error of this mean about equals the probable error of a single set of measures on a pair of the 60-inch plates.

Under "Remarks" we find the letter "H" and the Roman numerals I–IV. In *Mt. W. Contr.* No. 653, the letter "H" was used when the star was one of the 187 published by Hertzsprung[3] as probable members of the Pleiades. After *Mt. W. Contr.* No. 653 was printed, I received a letter from Hertzsprung, giving a more complete list of 256 stars in the Pleiades, "more or less suspected of membership," and also his results for the proper motions relative to Alcyone. In the present article I have used the letter "H" when the star appears in this improved list.

I have reduced all six sets of motions to one system, determined by the weighted mean motion of 25 stars selected by R. E. Wilson as giving the best motion of the cluster: $\mu_\alpha = +0''.022$, $\mu_\delta = -0''.044$. For this purpose, on each set of plates the mean motion of the probable members of the group was made equal to this weighted mean motion; for the six sets of plates the numbers of stars available for this purpose were 35, 13, 23, 20, 16, and 14, respectively.

[3] *M.N.*, 89, 660, 1929.

In *Mt. W. Contr.* No. 653[1] the stars with motions deviating less than 0".012 from the cluster-motion were designated "almost certain" members of the cluster; those with deviations of from 0".012 to 0".018, "probable"; and those with deviations of from 0".018 to 0".024, "possible" members of the cluster. From recent experience I find that these limits were rather too liberal, and I should now prefer that those stars whose motion deviates from the group-motion less than 0".010 and whose color index is not contradictory to membership should be designated "almost certain" group members; "probable" when the motion deviates not more than 0".015; and "possible" when the motion deviates 0".015 to 0".020.

The numeral "I" has been assigned to a star whose motion deviates not more than 0".005 from the mean motion of the cluster, while "II," "III," and "IV" are used when the motion deviates from 0".005 to 0".010, from 0".010 to 0".015, and from 0".015 to 0".020, respectively.

Table 1 is divided into two parts, the first 71 stars being, in my opinion, almost certain or probable members of the Pleiades, while the last nine, although their motions make their membership possible, are not likely to be members of the group.

In the first group are included two stars, Nos. 4 and 70, marked "IV" in the last column; No. 4, although undoubtedly a Pleiades star, is so bright that my measures are uncertain; No. 70 was measured with a fairly large deviation on only one pair of plates, but Hertzsprung's motion, with a small probable error, is so close to the cluster-motion that the star probably should be included as a member.

On the other hand, there are a number of reasons why the nine stars in the second part of Table 1 are probably not members of the cluster, although their motions deviate less than 0".020 from the motion of the cluster. For Nos. 72, 75, and 77 the only determinations are those of *Mt. W. Contr.* No. 653,[1] where the stars are more than 10 minutes of arc from the center of the 100-inch plate. For No. 73 (according to Hertzsprung's letter, "more or less suspected of membership") Hertzsprung's deviations are of the same order as those which I found, and rather point to nonmembership. The fact that Nos. 74, 76, 79, and 80 are not listed in his letter indicates that the deviations are too large for these stars to be included in the group. For Nos. 74 and 79 my new motions, moreover, confirm the larger deviations from the mean; while, finally, their color indices are incompatible with the magnitude if they are Pleiades stars.

Although No. 78 was included by Hertzsprung as a probable member, my later determination, rather confirmed by Hertzsprung's measures, would make its membership doubtful; moreover, the color index of 0.50 is also incompatible with the magnitude, if the star belongs to the cluster. Therefore, while the last nine stars in Table 1 have motions which do not definitely exclude them from the group, I prefer to include only the first group of 71 stars as probable Pleiades stars.

When we plot the number of all the stars according to their total motion, we find a curve which is built up of a skew frequency-curve on which a fairly symmetrical probability-curve is superposed with a maximum at 0".050. This excess is, of course, due to the cluster stars; it contains 70.2 stars, which is in excellent agreement with the number 71, given as the number of probable cluster stars.

While *Mt. W. Contr.* No. 653 included as possible members of the group several stars which are listed in the second part of Table 1 of the present paper, five more stars given as possible cluster stars in *Mt. W. Contr.* No. 653 (Nos. 27, 29, 70, 73, and 133) now fall outside our limits. New measures on the 60-inch plates have shown the motions of three of these stars—Nos. 27, 29, and 70—to be inconsistent with the cluster-motion. Hertzsprung also published a note[4] indicating that their motion deviated too much from that of the cluster.

It is interesting that in an earlier paper by the writer,[5] on two pairs of plates around

[4] *B.A.N.*, 9, 314, 1942.

[5] *Mt. W. Contr.*, No. 167, 1919.

Atlas and Pleione taken at the 80-foot focus of the 60-inch reflector with an interval of only five years, five stars were found whose motions indicate that they are members of the group, while the motions of eight other stars show possibility of membership. Of these eight, five are now included in Table 1: viz., Nos. 39, 47, 48, 79, and 80. Five other stars on the edge of these plates (Nos. 42, 43, 54, 61, and 69), which had not been measured before, are now also included.

TABLE 2

DISTRIBUTION OF PLEIADES STARS IN OBSERVED AREAS ACCORDING TO MAGNITUDES

M_{ph}	Mean m_{ph}	N	Mean I_λ	N'	Area (in Square Degrees)
≦6.....	3.9	4	−0.19	4	0.80
6.0– 6.9.....	6.5	5	−0.07	5	.80
7.0– 7.9.....	7.3	7	+0.02	7	.80
8.0– 8.9.....	8.4	6	+0.13	6	.80
9.0– 9.9.....	9.5	5	+0.22	5	.80
10.0–10.9.....	10.6	6	+0.31	5	.80
11.0–11.9.....	11.6	7	+0.52	7	.80
12.0–12.9.....	12.2	3	+0.67	3	.80
13.0–13.9.....	13.4	5	+0.93	5	.80
14.0–14.9.....	14.5	4	+1.21	3	.80
15.0–15.5.....	15.2	7	(+0.82)	3	.80
15.5–15.9.....	15.8	2	.....	.....	.72
16.0–16.9.....	16.6	4	.....	.....	.35
17.0–17.5.....	>17	6	.....	.....	0.35

TABLE 3

STARS WITH $\mu \geqq 0''.050$

No.	He	α (1900)	δ (1900)	m_{ph}	I_λ	μ_α	μ_δ	μ	No. of Det.
1....	292	$3^h40^m13^s$	+23° 46′	15.2	+1.51	−0″.002	−0″.086	0″.086	2
2....	.....	27	39	>17	.....	+ .086	− .048	.098	1
3....	.....	33	46	>17	.....	+ .058	− .041	.071	1
4....	.....	33	46	>17	.....	+ .055	− .041	.069	1
5....	360	36	40	14.7	+1.10	+ .040	− .060	.072	2
6....	365	37	50	12.7	+0.56	+ .049	− .041	.064	3
7....	545	41 33	39	14.1	+0.87	+ .088	+ .016	.089	1
8....	.....	48	38	15.6	.....	+ .156	− .016	.157	2
9....	667	42 7	26	15.7	.....	+ .041	− .119	.126	1
10....	836	43 1	33	7.1	+0.20	+ .038	− .062	.073	2
11....	984	50	26	11.8	+0.46	+ .046	− .042	.062	1
12....	1053	44 24	39	13.1	+1.21	− .040	− .060	.072	2
13....	.....	26	39	15.5	.....	−0.033	−0.059	0.068	1

Table 2 gives the distribution of the 71 probable cluster stars according to their photographic magnitudes. It is curious to see the low color index for the group of magnitude 15.0–15.5. Including all the 12 stars of this magnitude in Hertzsprung's list of

256, we would find a mean I_λ of +1.15; the weight of the color index for these fainter stars is so low that the value +0.82 for three stars is probably not significant.

In an area of 1 square degree in the central part of the cluster we should find about 105 cluster stars down to the magnitude of 17.5. If we keep in mind that the area observed for the fainter magnitudes is much smaller, we come to the same conclusion as in *Mt. W. Contr.* No. 653, that the maximum frequency has not yet been passed at this limiting magnitude.

In Table 3, thirteen stars are listed whose motions surpass 0".050 (the limit used by Oosterhoff and myself for our lists of faint stars with large proper motions) and which are not already in Table 1, which naturally includes a great number of stars with μ exceeding this limit because the cluster has a motion of 0".0492.

The most interesting star included in Table 3 is No. 8, with $\mu = 0''.157$ in $p = 96°$. As the motion of the Hyades at this point is about the same in $p = 107°$, it is not impossible that this faint star is a member of the Hyades. It may be recalled that Hertzsprung[6] called attention to a star in the Pleiades of magnitude 11.6 which possibly belongs to the Hyades, while I found near T Tauri a still fainter star of magnitude 16.5,[7] which has a motion indicating that it also is probably a member of the Hyades group.

[6] *B.A.N.*, **3**, 108, 1926.

[7] *Pub. A.S.P.*, **54**, 109, 1942.

DENSITY GRADIENTS IN THE ANTICENTER REGION OF THE MILKY WAY

S. W. McCuskey
Warner and Swasey Observatory, Case School of Applied Science
Received April 27, 1945

ABSTRACT

Star counts to $m = 17$ in thirteen selected regions of the Milky Way between $l = 142°$ and $l = 184°$ at galactic latitude 0° have been used to obtain the space-density distribution of the stars in this anticenter portion of the galaxy. The number of stars involved is 42,000. The interstellar absorption has been evaluated from the color-excess data for the B stars published by Stebbins, Huffer, and Whitford. In all areas an upper limit to the photographic absorption of 1.5–2.0 mag. is indicated. Over most of the region the absorption appears to set in abruptly at about 300–500 parsecs from the sun. In one longitude range, 160°–173°, however, the space is relatively clear by contrast. Here the absorption appears to set in at about 300 parsecs and increases at a rate of 0.4 mag/kpc outward from the sun.

The density functions resulting from a numerical solution based on the standard van Rhijn luminosity function, modified by Luyten's proper-motion results, are indicated in Table 7. The striking features of the galactic structure in this region are: (*a*) a definite excess of absolutely bright stars at distances of less than 500 parsecs in $l = 145°$ to 165°; (*b*) a high negative gradient in most of the area which reduces the density at 2500 parsecs to about 0.2 of that near the sun; and (*c*) an extensive region of relatively high density, 0.5–0.8, extending to 3000 parsecs in $l = 175°$ to 185°.

INTRODUCTION

The section of the Milky Way between galactic longitudes 140° and 190° embraces some of the smoothest and some of the most irregular stellar patterns of the entire galactic circle. To the north, in Orion, Taurus, and Auriga, masses of obscuring clouds produce a considerable variation in the apparent surface distribution of the stars. Farther south, however, in Monoceros, the stellar background is remarkably smooth and regular. An analysis of the Milky Way structure in this entire area is, therefore, difficult. In the present paper an attempt has been made to select for analysis small areas in which the obscuration appears to be at a minimum. On the basis of star counts in these areas a first approximation to the space-density distribution in the anticenter region may be obtained.

OBSERVATIONAL MATERIAL

Counts of stars in the magnitude range 11–17 have been made on photographic plates taken with the Burrell telescope[1] of the Warner and Swasey Observatory. This instrument is a 24–36-inch Schmidt-type reflector which photographs a region of the sky 5° in diameter on 8-inch circular plates.

For the star counts described herein, Eastman 103a-O plates of 10–15 minutes' exposure time were used. Longer exposures were prohibited by the resulting rapid increase in sky fog. Plates were taken in series of six, with four area plates and two Selected Area plates comprising a series. Care was taken to see that all plates of a series were from the same box and were developed together. The limiting magnitude of this series of plates obtained with the specified exposure times was about 17.1. It is to be emphasized, however, that more recent plates of the same type consistently reach stars 1 mag. fainter with the same exposure time. The plates used for this anticenter program were found to be considerably less sensitive than subsequent emulsions of the same type.

Plate centers were selected so that the observational material would cover a strip of the Milky Way 4° wide, centered on the galactic equator. Considerable overlap from

[1] For a description of the telescope see Nassau, *Ap. J.*, **101**, 275, 1945.

plate to plate was thus provided for the longitude range $l = 140°$ to $186°$. Three Selected Areas lie within this region and were included in the series of sixteen centers.

Within this belt of the Milky Way thirteen regions which appear to be relatively free of absorbing material have been selected for a preliminary analysis. Their centers are listed in Table 1, together with the area covered and the total number of stars counted in each. The galactic co-ordinates are based on the Harvard pole: R.A. (1900) = 12^h40^m; Dec. $+28°$. The countable limiting magnitude for each region is given in the last column of the table.

For the stars with $m = 8$ to 13, counts were made on Cramer Hi-Speed Special plates taken with the 4-inch Ross-Lundin camera at the Oak Ridge Station of the Harvard Observatory. These plates are a part of the observational material for an extensive star-counting program covering the Orion-Monoceros region; their limiting magnitude is 14.5. Uniformity of exposure time (60 minutes) and of sky conditions was made a requisite for the entire series of plates.

TABLE 1

REGIONS SELECTED FOR ANALYSIS

Region	R.A. 1900	Dec. 1900	l	b	Area (Square Degrees)	No. of Stars	Plate Limit (Mag.)
1	5^h21^m6	+32° 59′.7	142°.2	+0°.4	0.91	4730	16.67
2	5 36.8	+28 01.7	148.2	+0.5	.87	1805	16.94
3	5 39.0	+25 40.6	150.1	−0.6	.82	1901	16.78
4	5 45.2	+24 31.2	152.1	+0.2	.82	3185	16.97
5	5 57.6	+19 48.3	157.7	+0.4	.82	2094	17.17
6	6 06.9	+14 44.7	163.1	−0.2	.82	4707	17.56
7	6 11.0	+13 05.4	165.2	−0.2	.73	3282	17.35
8	6 17.1	+10 26.0	168.1	−0.1	.82	5267	17.27
9	6 23.8	+ 8 22.6	170.7	+0.4	.73	3133	16.95
10	6 32.9	+ 5 16.0	174.5	+1.0	.73	3305	17.00
11	6 40.0	+ 0 57.6	179.1	+0.5	.73	3324	16.93
12	6 43.9	− 1 38.7	181.5	0.0	.73	2613	17.10
13	6 47.9	− 3 57.0	184.0	−0.2	0.73	2470	17.18

Supplementary data for the brighter stars ($m < 10$) have been taken from the *Henry Draper Extension*[2] and from Seydl's counts based upon the *Henry Draper Catalogue*.[3]

THE MAGNITUDE SYSTEM

At the center of each of the sixteen areas photographed with the Burrell telescope a sequence of stars with $m = 10$ to 17 was selected for the calibration of the faint star counts. Magnitudes were determined for these stars in two ways: (1) by using the stars of the Selected Area plates in each series of six to provide calibration of the field plates in the same series and (2) by direct calibration from the Selected Area stars to the adjoining sequences on the same plates. The considerable overlap of fields adjacent to the Selected Areas permitted the latter procedure. In some instances, however, the overlap method was not applicable. The magnitudes published in the *Mount Wilson Catalogue of Selected Areas 1–139* were used for calibration.

Measurements of the plates were made with a graduated scale of stellar images. The final magnitudes in each sequence depend on six or more independent measures which yield ± 0.07 mag. for the maximum probable error of a single determination. A majority of the magnitudes, however, have probable errors of ± 0.05 mag.

[2] *Harvard Ann.*, Vol. **100**, 1925–1936.

[3] *Pub. Prague*, No. 6, 1929.

An estimate of the over-all consistency of the magnitude system determined for the faint stars is provided by the counts themselves. This will be discussed in a later paragraph.

Magnitudes between $m = 8$ and $m = 13$, necessary for calibration of the counts on the RL plates taken at Harvard, are somewhat uncertain. The sequences were established by a transfer process through overlapping plates, starting with Selected Areas 74, 75, 73, and 98 and Harvard Standard Regions C3 and C4 as primary bases. Calibration curves were established from the magnitudes of C Region stars[4] and of the *Mount Wilson Catalogue of Selected Areas*. Transfer from plate to plate was made through intermediate sequences, so that in the end three or four of the latter were available in the countable area of each RL plate. On the average, the adopted magnitudes of a sequence depend upon independent measures of two plates. A graduated scale of stellar images was used for the measurement.

Errors due to measurement, image quality, etc., have been estimated from magnitude determinations made on two or more plates of the same area. In each case the calibrating sequences have been the same. The average probable error of a single determination for stars in the range $m = 8$ to 13 is ± 0.14 mag. Ten sequences, averaging 16 stars in each, provided data for this estimate. A measure of the internal homogeneity of the magnitude system of the brighter stars as a whole may be gained by comparing the magnitudes derived for stars of the same sequence by approaches from different starting-points through completely different chains of overlapping plates. Three such sequences, averaging 20 stars in each, yield an average systematic closure difference of 0.32 mag. Expressed as a probable error, this would amount to ± 0.19 mag. Further discussion of the link between the magnitude systems for the bright and the faint stars will be given under the paragraph describing the counts themselves.

ACCURACY OF THE STAR COUNTS

The star counts have been made from both series of plates with a graduated scale of stellar images constantly in the field of view of the binocular microscope. Images of doubtful or borderline size could be referred instantly to this scale, so that any systematic tendency toward putting such images predominantly in the wrong magnitude group was largely eliminated. Counts were made of all images brighter than a given scale image over the entire area; then the process was repeated for the next image, etc. Finally, calibration of the graduated scale was obtained by estimating, in terms of the scale images, the sequence stars for the plate concerned. A graphical reduction yielded values of log $N(m)$, where $N(m)$ is the number of stars per square degree brighter than or equal to magnitude m.

As indicated in Table 1, the areas selected for counts in the range $m = 11$ to 17 are approximately three-quarters of a square degree in extent. For the brighter stars, counts on the RL plates were made in areas covering 3.2 square degrees. In each case the areas were selected so that statistical strength could be obtained without encroaching excessively on regions obscured by interstellar material. This selection was based on an examination of the star fields themselves and on the over-all appearance of the area in the *Atlas of the Milky Way* by Ross and Calvert.

In addition to the principal areas listed in Table 1, eleven secondary areas, 0.16 square degrees in extent, were selected in such a way that one of them appeared in each of an adjacent pair of plates taken with the Burrell telescope. Thus a continuous check was provided on the counts throughout the band of Milky Way studied. Counts in these wing areas were made concurrently with the counts of the principal area and were calibrated from the same sequence.

[4] *Harvard Ann.*, **71**, Nos. 3 and 4, 1917. These magnitudes were corrected according to *Harvard Bull.*, No. 781, 1923.

Differences in log $N(m)$ between the counts made for these common areas on adjacent plates serve to indicate the over-all consistency of the faint star counts. No dependence of size or sign of these residuals upon galactic longitude was found. The average systematic difference for the eleven areas, expressed in terms of the probable error of a single observation, is given in Table 2 as a function of magnitude. While there is evidence of some dependence of the probable error on the magnitude, it is not serious. These data include errors of counting and calibration, as well as errors in the magnitude system. The former have been found to be at least ± 0.03 in log $N(m)$, or about ± 0.1 in magnitude; and, hence, the internal consistency of the magnitude system appears to be satisfactory.

For the bright star counts made on RL plates, no overlapping areas were used. In general, three principal regions were counted on the same plate and calibrated from the

TABLE 2

PROBABLE ERRORS DERIVED FROM OVERLAPPING BT PLATES

	Magnitude						
	11	12	13	14	15	16	17
P.e. log $N(m)$.....	±0.10	0.07	0.05	0.04	0.03	0.03	0.02
P.e. (mag.).....	±0.30	0.20	0.15	0.12	0.10	0.10	0.06

TABLE 3

DIFFERENCES AT $m=11$ AND 12 BETWEEN COUNTS MADE ON TWO SERIES OF PLATES

(Δ log $N(m)$ = BT minus RL)

Region	Δ log $N(m)$	Region	Δ log $N(m)$	Region	Δ log $N(m)$	Region	Δ log $N(m)$
1.....	+0.13	5.....	+0.30	9.....	−0.24	13.....	−0.03
2.....	− .02	6.....	− .04	10.....	− .23		
3.....	+ .06	7.....	− .05	11.....	− .17		
4.....	+0.05	8.....	−0.22	12.....	−0.15		

same sequences. These counts were reduced independently of those made on the plate taken with the Burrell telescope. For $m = 11$ and 12, however, values of log $N(m)$ are available from each series. These have been used to tie the two magnitude systems together.

Differences in log $N(m)$, taken in the sense BT[5] minus RL, averaged for magnitudes 11 and 12, are shown in Table 3. Repetition of counts on a few of the RL plates indicates that these systematic residuals are not due to counting and calibration errors. They may be ascribed to uncertainties in one or both magnitude systems involved. There is the possibility that the magnitudes established with the Burrell telescope are influenced by a color equation due to the greater reach of the aluminized mirror into the ultraviolet region of the spectrum. An inspection of calibration curves of the North Polar Sequence, however, reveals no such systematic dependence upon color. As further discussion will show, the counts made on the BT plates agree well with counts made by van Rhijn and by Seares in the Selected Areas, both of which are based on the International scale of

[5] Herein "BT" refers to the plates taken with the Burrell 24–36-inch Schmidt-type telescope.

photographic magnitudes. Hence one may conclude that the magnitude system determined on the RL plates is probably at fault. The values of log $N(m)$ deduced from the latter have been corrected so as to agree with the BT plate data at $m = 11$ to 12, in accordance with the residuals given in Table 3.

Comparisons have been made between the values of log $N(m)$ obtained from the RL plates, corrected as above, and those derived from counts of stars in the *Henry Draper Extension*.[6] An area of 3.4 square degrees surrounding each of ten of the regions given in Table 1 was used for the comparison. Residuals in log $N(m)$, taken in the sense RL minus

TABLE 4

DIFFERENCES BETWEEN RL COUNTS AND COUNTS BASED ON THE *Henry Draper Extension*
(Δ log $N(m)$ = RL minus HDE)

MAG.	REGION										
	1	2	3	4	5	6	7	8	9	10	Mean
8.....	+0.11	+0.53	+0.15	+0.48	+0.29	+0.30	+0.12	−0.01	−0.10	−0.24	+0.16
9.....	+ .21	+ .09	− .02	+ .09	+ .26	+ .07	+ .03	+ .03	+ .01	− .31	+ .04
10.....	.00	+ .10	+ .07	− .02	+ .07	+ .07	.00	− .07	.00	− .24	− .01
11.....	+0.06	+0.06	+0.13	−0.13	−0.03	+0.07	−0.04	−0.17	−0.11	−0.17	−0.06

TABLE 5

COMPARISON WITH *Groningen Publications*, NO. 43, AND *Mt. Wilson Contribution* NO. 301

A: Δ log $N(m)$ = BT minus *Groningen Pub.*, Vol. **43**;
B: Δ log $N(m)$ = BT minus *Mt. Wilson Contr.* No. 301

m	S.A. 49 Δ LOG $N(m)$		S.A. 74 Δ LOG $N(m)$		S.A. 98 Δ LOG $N(m)$	
	A	B	A	B	A	B
11.....	−0.12	.....	+0.07	.....	−0.13	.....
12.....	− .02	.....	+ .24	.....	.00	.....
13.....	+ .08	−0.01	+ .09	+0.07	− .09	−0.12
14.....	+ .05	− .06	+ .11	+ .13	.00	+ .08
15.....	+ .12	− .01	+ .07	+ .10	+ .11	+ .13
16.....	+ .07	+ .04	− .01	.00	+ .07	+ .09
17.....	0.00	−0.01	−0.13	−0.12	−0.01	0.00

HDE, are exhibited in Table 4. For stars brighter than $m = 8$ the differences depend on very few stars, usually less than 5; hence the inclusion or exclusion of a single star creates a very large residual. The catalogue becomes incomplete between $m = 11$ and $m = 12$. With the exception of the values for Area 10, where there appears to be a considerable zero-point difference, the agreement is satisfactory.

For the counts in the magnitude range 11–17, three Selected Areas were included in the routine counting program. These were circular, 23′ in diameter, centered on the central star of the Selected Area. Counts and calibration were made in the same way as for all the other areas on the plate. Table 5 shows the differences between the present counts

[6] *Harvard Ann.*, Vol. **100**, 1925–1936.

and those obtained by van Rhijn[7] and by Seares, van Rhijn, Joyner, and Richmond[8] for Selected Areas 49, 74, and 98.

The agreement between the present counts and those previously published lends strength to the conclusion that the former are essentially on the International scale of photographic magnitudes.

ADOPTED VALUES OF LOG $A(m)$

The observed values of log $N(m)$ are plotted against the photographic magnitude in Figure 1. From the smooth curves drawn through these points, values of log $A(m)$, where $A(m)$ is the number of stars per square degree between $m-\frac{1}{2}$ and $m+\frac{1}{2}$, have been computed. Table 6 presents the values of log $A(m)$ for the thirteen regions.

In order to make the analysis complete for the stars brighter than $m = 7$, Seydl's counts,[9] based upon the *Henry Draper Catalogue*, have been used. The points for $m \leq 7$

TABLE 6

LOG $A(m)$ AS A FUNCTION OF APPARENT MAGNITUDE

(Thirteen Regions in Auriga, Taurus, Orion, and Monoceros)

m	REGION												
	1	2	3	4	5	6	7	8	9	10	11	12	13
8.....	0.25	0.34	0.30	0.25	0.33	0.39	0.52	0.30	0.27	0.23	0.19	0.29	0.33
9.....	0.73	0.69	0.72	0.60	0.74	0.86	0.83	0.71	0.71	0.69	0.60	0.68	0.79
10.....	1.20	1.02	1.17	0.98	1.15	1.24	1.13	1.16	1.16	1.12	1.01	1.10	1.23
11.....	1.59	1.36	1.51	1.38	1.50	1.53	1.53	1.50	1.50	1.60	1.46	1.50	1.56
12.....	1.92	1.69	1.84	1.73	1.81	1.82	1.81	1.84	1.83	1.86	1.82	1.88	1.86
13.....	2.23	1.99	2.16	2.07	2.06	2.13	2.16	2.21	2.19	2.24	2.23	2.29	2.22
14.....	2.58	2.30	2.48	2.41	2.31	2.46	2.48	2.54	2.53	2.62	2.65	2.66	2.52
15.....	2.90	2.63	2.78	2.80	2.59	2.77	2.81	2.91	2.91	2.97	3.03	3.03	2.86
16.....	3.24	2.95	3.08	3.17	2.86	3.08	3.15	3.26	3.25	3.34	3.36	3.21	3.11
17.....	3.58	3.27	3.39	3.53	3.13	3.41	3.48	3.61	3.60	3.69	3.67	3.48	3.36

in Figure 1 have been taken for the galactic latitude zone 0° to ±10° and for all longitudes. A check comparison with recounts made in the *Henry Draper Catalogue* for the immediate region concerned shows that the mean values deduced from a far greater number of stars represent satisfactorily this area of the Milky Way. In the case of the brighter stars, therefore, we take log $A(m) + 10$ equal to 8.32, 8.83, 9.32, and 9.82 for $m = 4$, 5, 6, and 7, respectively.

COLOR AND ABSORPTION DATA

The most extensive and homogeneous data on interstellar reddening and absorption in the anticenter region are provided by the photoelectric color excesses of B stars determined by Stebbins, Huffer, and Whitford.[10] Some 140 of these stars lie within galactic latitudes 0° to ±10° in longitudes 140°–190°. The color excesses E_1 for these stars were plotted against the star's position in galactic co-ordinates to obtain an over-all picture of the interstellar reddening in relation to the thirteen regions studied. From this array it was apparent that six subregions with $b = 0°$ to ±5° could be chosen in such a way

[7] *Groningen Pub.*, No. 43, Table 1, 1929.

[8] *Mt. W. Contr.*, No. 301; *Ap. J.*, **62**, 320, Table 1, 1925.

[9] *Op. cit.*

[10] *Ap. J.*, **91**, 20, 1940.

that the color excesses could be combined satisfactorily about one or more of the star-count areas.

Distances were computed for individual stars from the moduli given in the paper[10]

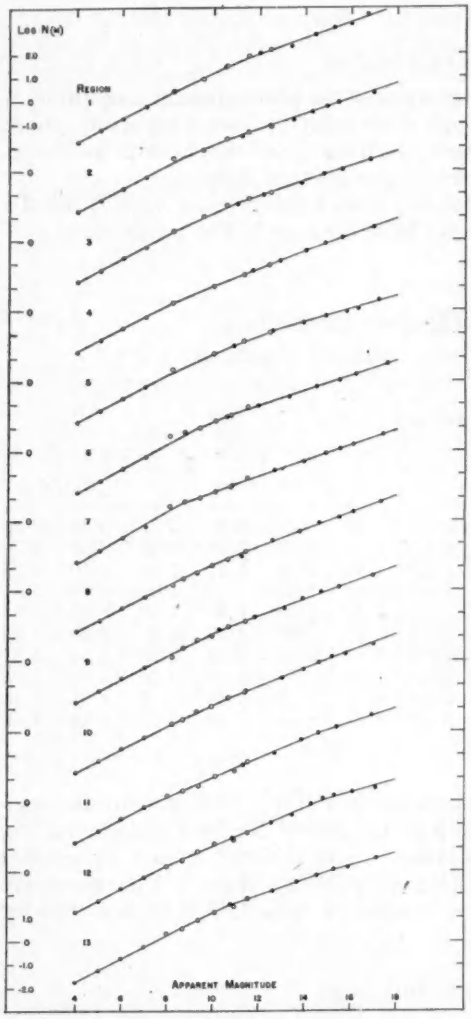

FIG. 1.—Observed values of log $N(m)$ as a function of apparent magnitude. Open circles are from Harvard RL plates; filled circles represent counts made on the plates taken with the Schmidt-type telescope. The first five circles on the left side of curve *1* and the first four circles of all the other curves are from Seydle's counts.

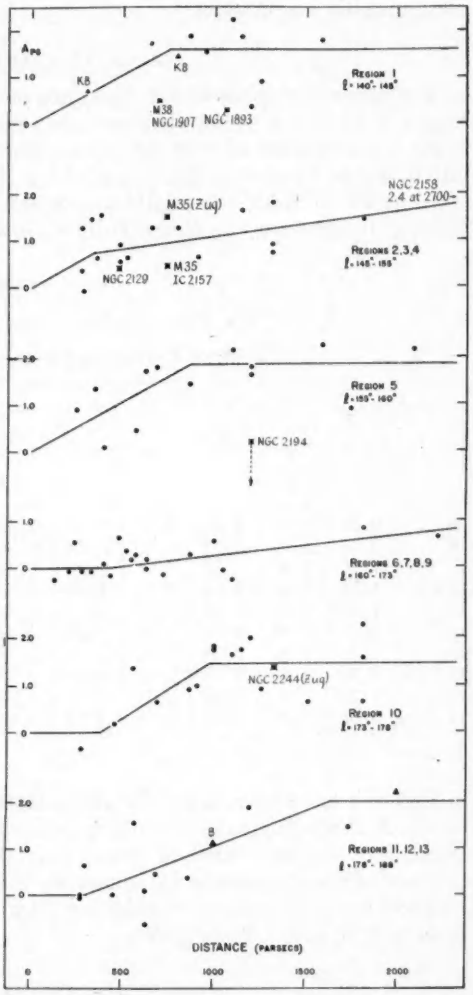

FIG. 2.—Photographic absorption as a function of the distance. The B-star data are represented by filled circles; Cuffey's data from clusters are indicated by M and NGC numbers. Letters *KB* in the diagram for Region 1 refer to the absorption data obtained by Kiefer and Baker; *B* in the diagram for Regions 11, 12, and 13 refers to the value given by Bok.

referred to above and were plotted against the photographic absorption, A_{pg}, for each subregion. The resulting trends of absorption with distance are shown by Figure 2. It was assumed in converting the color excesses E_1 into total photographic absorption that

$A_{pg}/E_1 = 9$. This is in accord with previously used estimates of the ratio,[11] although recent work by Stebbins on colors in the Andromeda nebula indicates that the value may be somewhat lower, perhaps 7 or 8. The longitude range encompassed by each group of stars and the counted areas within which the values of A_{pg} are assumed to be valid are indicated on the figure. The curves were drawn with due regard to average values of A_{pg} in the distance ranges 0–500, 500–1000 parsecs, etc.

The usual scatter in individual values is evident from these curves. The trends, however, appear to be satisfactory and, in the absence of more data, will be used in the succeeding analyses. In nearly all cases an upper limit of from 1.8 to 2.0 mag. is indicated for the absorption in the broad region. The notable exception is in the longitude range 160°–173°, a remarkably clear region relative to its neighbors. Stebbins, Huffer, and Whitford[12] have already pointed out the indicated upper limit to the color excesses in this anticenter region of the galaxy. The need for a great mass of color and spectral data immediately surrounding each computed area is apparent. It must be noted that a considerable dispersion in the absolute magnitudes of the B stars would tend to make quite uncertain the trend of the absorption curves beyond 1000 parsecs. The reality of the abrupt cutoff in absorption is therefore questionable.

A rather high absorption, setting in somewhat abruptly at 300 parsecs distance, is marked in the northerly half of the region. Farther north, in longitudes 115°–145°, Kiefer and Baker[13] have found the same indication of cloudlike structure in the absorbing medium. To the south there appears to be little absorption out to a distance of 500 parsecs.

A few avenues of comparison for the absorption values in this area are open. Bok[14] has investigated the absorption at $l = 180°$ by means of color excesses measured at Harvard. At $\bar{b} = 0°$ he finds a photographic absorption coefficient of 1.1 mag/kpc, while at $\bar{b} = +2.5°$ a value of 0.9 mag/kpc was found. These values have been used in the plots of Figure 2 to strengthen the B-star data at 1000 parsecs for the analysis of Regions 11, 12, and 13.

Cuffey[15] has determined red and blue magnitudes and corresponding color excesses for stars in galactic clusters M35, M38, NGC 2158, IC 2157, NGC 2129, NGC 1907, NGC 1893, and NGC 2194, which lie within 5° of the galactic plane in longitudes 140°–180°. These color excesses, converted into total photographic absorption by multiplication by a factor 3, may be compared with the B-star data at corresponding distances. Distances assigned to the clusters have been corrected for the absorption. Total absorption values thus derived are plotted in the appropriate parts of Figure 2.

It is evident that a considerable lack of agreement exists between the absorption values derived from clusters and those from the B-star data, particularly in the case of NGC 2194. An inspection of the latter region on long exposure plates (limit 17.0 mag.) and in the *Atlas of the Milky Way* by Ross and Calvert yielded little evidence for marked changes in the absorption over a considerable range in longitude. The presence of some twenty-two external galaxies[16] within 5° of the galactic plane indicates that the large absorption value demanded by the color excess of NGC 2194 is highly improbable.

The color excesses derived by Zug[17] for the galactic clusters M35 and NGC 2244 yield total absorptions of 1.5 mag at 800 parsecs and 1.4 mag at 1300 parsecs, respectively, in longitudes 154° and 165°. While the value for NGC 2244 agrees closely with the determination from the B-star data, that for M35 is three times the absorption derived

[11] Stebbins, Huffer, and Whitford, *Ap. J.*, **90**, 213, 1939; Henyey and Greenstein, *Ap. J.*, **93**, 327, 1941; Stebbins and Whitford, *Ap. J.*, **98**, 32, 1943; and Stebbins, *Science*, **99**, 271, 1944.

[12] *Ap. J.*, **90**, 225, 1939.

[13] *Ap. J.*, **94**, 487, 1941.

[14] *Ap. J.*, **90**, 257, 1939.

[15] *Harvard Ann.*, Vol. **105**, No. 21, 1937; Vol. **106**, No. 2, 1938; *Ap. J.*, **97**, 93, 1943.

[16] Hubble, *Ap. J.*, **79**, 18, 1934.

[17] *Lick Obs. Bull.*, No. 454, 1933.

from Cuffey's data for the same cluster and departs considerably from the curve defined by the B stars.

For $l = 140°$ to 145° Kiefer and Baker[13] have obtained from red-blue color indices total absorptions of 0.8 mag. at 300 parsecs and from 0.8 to 1.6 mag. at 800 parsecs. Region 1 of the present analysis lies near the transition zone from the lower to the higher absorption at 800 parsecs. The absorption assumed for Region 1 was 1.6 mag. at 800 parsecs and 0.7 mag. at 300 parsecs—values which compare favorably with those obtained by Kiefer and Baker. For comparison, these additional data are plotted on Figure 2.

DENSITY ANALYSES

From the values of log $A(m)$ and the absorption data given in the preceding sections the space-density functions may be readily derived. A standard (m, logπ) table published by Bok and MacRae[18] has been used for the analysis. This table is based upon the luminosity function derived by van Rhijn[19] and was modified for the fainter absolute magnitudes by the more recent results of Luyten.[20] The modified function is given by Bok and MacRae.[21] By the method of approximations the densities, expressed as fractions of that near the sun, have been chosen in such a way that the computed values of log $A(m)$ differ from the observed in general by no more than 0.05. The average systematic difference over the magnitude range 4–17 has been kept less than 0.015 in log $A(m)$ for each region. The resulting density functions for the thirteen regions are given in Table 7.

TABLE 7

DENSITY FUNCTIONS IN AURIGA, TAURUS, ORION, AND MONOCEROS

DISTANCE (PARSECS)	REGION												
	1	2	3	4	5	6	7	8	9	10	11	12	13
	$l=142°$ $b=+0.4$	148° +0.5	150° −0.6	152° +0.2	158° +0.4	163° −0.2	165° −0.2	168° −0.1	171° +0.4	175° +1.0	179° +0.5	182° 0.0	184° −0.2
40	1.0	1.0	1.0	1.0	1.0	1.0	1.0	1.0	1.0	1.0	1.0	1.0	1.0
63	1.0	1.0	1.0	1.0	1.0	1.0	1.0	1.0	1.0	1.0	1.0	1.0	1.0
100	1.8	1.8	1.8	1.8	2.0	1.0	1.0	1.0	1.0	1.0	1.0	1.0	1.0
158	1.8	2.0	2.0	2.5	2.5	1.5	1.4	1.0	1.0	1.0	0.8	1.0	1.0
251	1.8	2.0	2.0	1.8	2.5	1.5	1.4	1.0	1.0	1.0	0.7	1.0	1.0
400	1.8	1.0	1.5	1.0	1.8	1.0	1.0	0.7	0.7	0.7	0.5	0.6	1.0
630	1.2	0.5	1.0	0.5	1.2	0.6	0.8	0.5	0.5	0.5	0.5	0.5	1.0
1000	1.0	0.3	0.5	0.3	0.6	0.2	0.2	0.3	0.3	0.8	0.5	0.8	0.8
1580	0.5	0.2	0.2	0.2	0.1	0.15	0.1	0.1	0.1	0.8	1.0	1.0	0.4
2500	0.3	0.2	0.2	0.2	0.1	0.1	0.1	0.1	0.1	0.5	1.0	0.8	0.2
4000	0.05	0.2	0.3	0.5	0.09	0.1	0.1	0.3	0.3	0.2	0.2	0.05	0.2

Several conspicuous features of the space distribution of the stars in this part of the Milky Way are evident from this table. Over the longitude range from 145° to 165° there is a region of relatively high density, extending from about 100 parsecs to a distance of 500 parsecs. Thereafter the density decreases rapidly—to a value, at 2500 parsecs, approximating 0.2 of that near the sun.

[18] *Ann. New York Acad. Sci.*, **42**, 252, 1941.

[19] *Groningen Pub.*, No. 47, 1936.

[20] *Minnesota Pub.*, Vol. **2**, No. 7, 1939.

[21] *Op. cit.*, p. 223.

The excess in density at distances less than 500 parsecs from the sun, particularly in $l = 145°$ to 165°, is noteworthy. It can be removed only by the radical assumption that no interstellar absorption exists in the region. For example, in Region 5 the density values which would best fit the observed data if no absorption were present are:

r..... $\leq$	40	63	100	158	251	400	630	1000 parsecs
$D(r)$....	1.0	1.0	1.0	1.0	1.0	0.7	0.5	0.2

The large values of $D(r)$ for $r > 100$ parsecs (Table 7) appear to reflect a true excess of absolutely bright stars ($M < +3$) in this region, compared with the numbers in the solar neighborhood as given by the standard luminosity function. Between $l = 145°$ and $l = 155°$, in particular, the region of high density is pronounced to a distance of 500 parsecs.

The extensive work of Pannekoek[22] on the space distribution of the A and K stars, derived from the *Henry Draper Catalogue*, shows clearly a marked elongated condensation of the A stars in longitude 100°–180° at a distance of approximately 100 parsecs. Here the space density amounts to 1.5 times that of the A stars near the sun. A second

TABLE 8*

COMPARATIVE DENSITY FUNCTIONS IN THE ANTICENTER REGION OF THE GALAXY

Distance (Parsecs)	Kiefer-Baker $l = 130°$	van Rhijn 145°	McC$_1$ 148°	McC$_2$ 150°	Bok$_1$ 161°	McC$_3$ 164°	McC$_4$ 175°	Bok$_2$ 179°	van Rhijn 190°
0.....	1.00	1.00	1.00	1.00	1.00	1.00	1.00	1.00	1.00
100.....	1.00	0.93	1.00	1.82	1.00	1.00	1.00	1.00	0.95
250.....	0.95	0.76	1.10	2.00	1.00	1.45	0.94	0.70	0.75
400.....	0.90	0.68	1.10	1.42	0.60	1.00	0.64	0.70	0.70
1000.....	0.45	0.28	0.22	0.54	0.25	0.20	0.54	0.70	0.80
2500.....	0.10	0.55	0.05	0.20	0.15	0.10	0.50	0.50	0.60

* Absorption values used: Kiefer-Baker: 0.7 and 1.5 mag. at 300 parsecs; 2.1 mag. at 800 parsecs (*Ap. J.*, **94**, 491, 1941). McC$_1$: 0.5 mag/kpc (*Ap. J.*, **89**, 574, 1939). McC$_2$: see Fig. 2, Regions 1–5, inclusive. McC$_3$: see Fig. 2, Regions 6 and 7. McC$_4$: see Fig. 2, Regions 8–12, inclusive. Van Rhijn: 1.1 mag/kpc (*Groningen Pub.*, No. 47, 1936). Bok$_1$ and Bok$_2$: 0.5 mag/kpc (*Harvard Circ.*, No. 371, 1931).

condensation occurs in $l = 160°$ at a distance of 220 parsecs. This clustering tendency among the A stars tends to support the conclusion that the luminosity function for the solar neighborhood is not appropriate to this region of the galaxy. The high values of $D(r)$ within 400 parsecs of the sun simply reflect the fluctuation in $\varphi(M)$.

Another conspicuous feature of the space distribution is the long plateau-like region of moderately high density extending to a distance of nearly 3000 parsecs in $l = 175°$ to 180°. This is in marked contrast to the abrupt drop in density at 1000 parsecs in $l = 145°$ to 165°. The generally high negative density gradient characteristic of the anticenter region is present over a considerable range in longitude.

The results of several investigations of the galactic structure in the anticenter region are exhibited in Table 8. Values of the absorption used in the analyses are listed, together with references. Unfortunately, the observational data are somewhat heterogeneous. The broad features of the stellar structure are evident, however, and may be summarized as follows:

a) There exists over the longitude range from 145° to 165° a definite excess of absolutely bright stars at distances less than 500 parsecs, whose presence is reflected in the general star-count analyses by density factors of the order of 1.5–2.0. This excess does not appear for $l = 165°$ to 180°, nor for longitudes less than 145°.

[22] *Pub. Amsterdam*, No. 2, p. 16, 1929.

b) Beyond 500 parsecs a high negative gradient is evident, which reduces the relative density at 1000 parsecs to about 0.4 of that near the sun.

c) While in the great portion of this longitude range the density continues to decrease to a value 0.1 at 4000 parsecs, there is at $l = 175°$ to 185° an extensive region of relatively high density (0.5–1.0) extending to perhaps 3000 parsecs from the sun. This extension is evident also in the analysis of star counts in Selected Area 98 by Bok[23] and by van Rhijn.[24]

d) There appears to be little evidence from these star-count data to substantiate the high densities (1.5 at distances of 500–2000 parsecs) determined by Oort[25] for the anti-center region.

Neglecting the relatively high values of $D(r)$ at 100 parsecs in the present determinations, as compared with previous ones, the remaining differences may be ascribed primarily to the different values used for the interstellar absorption.

It is more and more apparent that the assumption of a "standard" luminosity function in analyzing general star counts serves only to give a rough first approximation to the density distribution in any given region. We must have complete spectral data for stars as faint as possible in order to obtain the true picture for the region concerned. A study of the fluctuations of the luminosity function in the galactic plane is one for which the Schmidt-type telescope, fitted with an objective prism, is admirably adapted. An investigation of this nature is now under way at the Warner and Swasey Observatory.

It is a pleasure to record my appreciation to Dr. Shapley and to Dr. Bok for obtaining and placing at my disposal the RL plates upon which a portion of the present work is based.

[23] *Harvard Circ.*, No. 371, 1931.

[24] *Groningen Pub.*, No. 47, 1936.

[25] *B.A.N.*, 8, 261, 1938.

CURVE OF GROWTH FOR α PERSEI

HELEN R. STEEL
Harvard College Observatory
Received March 15, 1945

ABSTRACT

Equivalent widths of 403 lines on McDonald coudé spectrograms of α Persei and Menzel and Goldberg's solar log X'_0 values provide data for a curve of growth of α Persei, an F5 supergiant. The excitation temperature derived for neutral iron is 4400°. The parameters of the theoretical curve, fitted to the observational curve of growth, are a velocity of 3.7 km/sec and a damping constant (Γ/ν) of 1.2×10^{-6}.

So far as observational and theoretical data permit, the numbers of the different types of atoms and ions in a centimeter-square column above the photosphere are determined. The electron pressure at the base of the reversing layer is derived from the product of the number of electrons in a centimeter-square column above the photosphere, the average mass of the atoms, and the surface gravity. For α Persei, this method, with assumptions about the degree of ionization and the abundances of some elements, gives an electron pressure of 4.7 dynes/cm². The electron pressure at the base of the solar reversing layer, by the same method, is 40 dynes/cm². The validity of the assumptions is investigated, and the sensitivity of the pressure to the temperature is shown.

The application of the observationally determined numbers of atoms in the Saha equation indicates that, in the atmosphere of α Persei, either the ionization or excitation temperature, or both, cannot be the same for silicon and titanium. A similar phenomenon has been found for the solar chromosphere.

The theory of curves of growth applied to the spectrum of α Persei, an F5 supergiant, provides information about the chemical composition and physical conditions in the atmosphere. The results so obtained make possible a comparison with similar work on the spectrum of the sun, a G0 dwarf.

The Yale catalogue of 1935 gives a value of $+0''.009 \pm 0''.004$ for the parallax of α Persei. Since the apparent magnitude is 1.90, the absolute magnitude is -3.3 for a parallax of $+0.009$. The range in absolute magnitude corresponding to the probable error is from -2.5 to -4.6.

A number of observers, including A. D. Thackeray,[1] O. Struve and C. T. Elvey,[2] T. Dunham,[3] J. A. Hynek,[4] and K. O. Wright,[5] have measured the equivalent widths of some of the lines in the spectrum of α Persei. The dispersion in all cases, with the exception of Dunham's spectrograms, was lower than that of the present investigation. Struve and Elvey,[2] Dunham,[3] and Wright[5] used their measures to derive curves of growth for α Persei.

Dr. Struve kindly placed at my disposal spectrograms of α Persei taken with the coudé spectrograph of the McDonald Observatory. Two settings of the prisms in the autocollimating prism train of the spectrograph covered the region λλ 3800–6700 with considerable overlap. A one-hour and thirty-five minutes' exposure, taken on January 22, 1941, on Eastman Ia-0 emulsion, provided the material for intensity measures in the region λλ 3800–4727. The plate of the red region taken on January 27, 1941, on 103-F emulsion covered the wave lengths from λ 4440 to λ 6700. The exposure for the red region was two hours and eighteen minutes. On the blue setting the dispersion ranged from 2.5 to 5 A/mm; on the red setting, from 2.5 to 4 A/mm at $H\beta$ and about 15 A/mm at λ 6600.

[1] *M.N.*, **94**, 99, and 538, 1933–1934.

[2] *Ap. J.*, **79**, 409, 1934.

[3] *Mt. W. Ann. Report*, p. 149, 1933–1934.

[4] *Ap. J.*, **82**, 338, 1935.

[5] *Pub. A.A.S.*, **9**, 276, 1939; **10**, 39, 323, and 338, 1940.

SPECTROPHOTOMETRY

A tube photometer equipped with blue, green, and red filters provided the standardizations for the plates. The blue set of standards was used from λ 4000 to λ 4800; the green, from λ 4800 to λ 5900; and the red, from λ 5800 to λ 6700. The development of the spectrograms was simultaneous with that of their standards. Calibrated tracings at a magnification of thirty times were made with the Yerkes microphotometer. The slopes of the red and green characteristic curves differed only slightly from that of the blue curve. The characteristic curves all had stright-line portions extending at least from 30 to 65 per cent deflection.

Dunham's[6] work on the spectrum of α Persei was the basis for the identification of the lines. Consultation of more recent work, including the *M.I.T. Wave Length Tables*, Greenstein's[7] identifications for α Carinae, Menzel's[8] work on the solar chromosphere, and Roach's[9] on γ Cygni provided new identifications and some changes in Dunham's early work.

The first consideration in the selection of lines for measurement was freedom from blends. The measures include most of the well-identified unblended lines in the region λλ 4200–6700. Because solar strengths or relative ϖf values[10] were available or for reasons of interest, other lines, not appreciably blended, supplemented these measures.

The measured lines have weights assigned according to the amount of blending and the line's appearance on the tracing—that is, definiteness of contour, and distinguishableness from the continuous spectrum and neighboring lines. Equivalent widths of weight 3 or 4 are dependable, and those of weight 1 or 2 are uncertain.

The method used to obtain the equivalent widths involved mechanical quadratures. This procedure entails measurement of a line at every millimeter on the tracing and calculation of the equivalent width by summing. In order that the relative accuracy of measurement by mechanical quadratures and with a planimeter might be tested, 25 lines of various intensities and contours were measured by both methods at two different times. The two methods gave results that agreed within the accuracy of measurement. Mechanical quadratures, being considerably faster than the use of a planimeter, was the method adopted.

Systematic errors between the measures from the plates of the red and the blue settings may arise from instrumental and development effects, the characteristic curves, change of dispersion, exposure, grain effect, and the position assumed for the continuum. By comparing the measures in the overlapping region we may determine the size of the errors.

Of the 44 lines measured on both plates, all but 3 lines had considerably larger values from the plate of the blue setting than from that of the red. The average difference between the measures on the two plates was about 21 per cent.

Since the equivalent widths from the two plates differed, it was necessary to correct one or both sets of measures to bring them into agreement. I tried correcting first the measures from the "red" plate to those from the "blue" and then the equivalent widths from the "blue" plate to agree with those from the "red." The "blue" plate was very dense. The continuum, in the region λλ 4160–4660, was of an intensity that fell well above the straight-line portion of the characteristic curve. On the shoulder of the curve a small error in the deflection will give a large error in the intensity. On the "red" plate, however, the continuum and all the lines, with the exception of a small number of the deeper ones, were of intensities that fell on the straight-line portion of the characteristic curve. Three considerations—the existence of photometric difficulties for the "blue"

[6] *Contr. Princeton Obs.*, No. 9, 1929; also, manuscript of unpublished wave lengths in the violet.

[7] *Ap. J.*, **95**, 161, 1942. [8] *Pub. Lick Obs.*, **17**, 1, 1931. [9] *Ap. J.*, **96**, 272, 1942.

[10] To avoid confusion with other uses of g, we shall use the notation ϖ for the statistical weight of the lower level of a line, instead of the g used by R. B. and A. S. King (*Ap. J.*, **87**, 24, 1938).

plate, more homogeneous data, and better agreement with the results of other observers —led to the adoption of the original measures from the "red" plate and the equivalent widths from the "blue" plate, corrected to those from the "red."

Table 1 contains the equivalent widths of 403 lines in the spectrum of α Persei. The measures are listed by elements, and their ions, in the order of increasing atomic weight. Column 1 gives the wave length as listed by Dunham;[6] column 2, the lower excitation potential of the line; column 3, $-\log W/\lambda$;[11] and column 4, the weight of the measure in column 3.

THE CURVE OF GROWTH

Menzel[12] has shown from theory that by plotting $\log W/\lambda$ as a function of $\log X_0$ we may obtain a curve of growth. The optical depth at the center of a line, X_0, is given by

$$X_0 = N_a \frac{\varpi}{b\,(T)}\, 10^{\frac{-5040\chi}{T}} \frac{\pi e^2}{mc} \frac{c}{\sqrt{\pi}\nu_0 v} f\,, \tag{1}$$

where N_a is the total number of atoms of an element in a given state of ionization per centimeter-square column above the photosphere, ϖ is the statistical weight, and χ the excitation potential of the lower level involved.

Prior to an investigation of this kind we do not know X_0. To obtain an observational curve of growth, we are forced to plot $\log W/\lambda$ as a function of factors proportional to $\log X_0$, but not as a function of $\log X_0$ itself. Equation (1) gives X_0 in terms of ϖf values. On the other hand, since

$$\varpi f = \frac{\nu}{3R} \phi \frac{Ss}{\Sigma s}\,, \tag{2}$$

we may express X_0 in terms of multiplet strengths.[12] In equation (2), R is the Rydberg constant; ϕ, the radial quantum integral; S, the strength of a multiplet relative to others in the same transition array; and s, the strength of an individual line relative to Σs, the sum of all the line strengths in the multiplet. To determine an observational curve of growth, we may use ϖf values or theoretical multiplet strengths. We may also derive a curve of growth for one star from $\log X_0$ values for another star. In practice, we use $\log X_0$ values for the sun, since the solar spectrum has been studied in the greatest detail. To plot a curve of growth, we first remove the Boltzmann factor, $5040\chi/T$, from the solar $\log X_0$ values and obtain $\log X_0'$:

$$\log X_0' = \log X_0 + \frac{5040\chi}{T}\,. \tag{3}$$

Menzel and Goldberg derived $\log X_0'$ values from Menzel, Baker, and Goldberg's[13] solar curve of growth based on Allen's[14] equivalent widths. Their $\log X_0'$ values provide the most extensive and homogeneous set of data available for the determination of an observational curve of growth.[15] Menzel and Goldberg's data were used to derive a curve of growth for α Persei.

[11] In the region λλ 4200–4727 the equivalent widths from the "blue" plate have been corrected to agree with those from the "red" plate. For lines measured on both plates the table gives the average of the "red" and the corrected "blue" measures.

[12] *Ap. J.*, **84**, 462, 1936. [13] *Ap. J.*, **87**, 81, 1938.

[14] *Mem. Commonwealth Solar Obs.*, Vol. 1, No. 5, 1934.

[15] Since this investigation was carried out, K. O. Wright has derived solar $\log X_0'$ values from his curve of growth based on laboratory intensities (*Ap. J.*, **99**, 249, 1944). His $\log X_0'$ values should be more reliable, since they are based on laboratory intensities, not on existing theoretical multiplet strengths, as are Menzel and Goldberg's. The theoretical multiplet strengths are based on two assumptions—*LS* coupling and configuration isolation—which do not always hold.

TABLE 1

EQUIVALENT WIDTHS IN THE SPECTRUM OF α PERSEI

λ	Lower E.P.	−log W/λ	Wt.
	H		
4101.75	10.16	2.85	2
4861.35	10.16	2.97	2
	C I		
4770.01	7.45	5.02	4
4775.99	7.46	4.69	2
4826.73	7.46	5.34	3
4931.99	7.65	4.84	3
	Na I		
5682.58	2.093	4.59	3
5688.21	2.095	4.52	3
5890.00	0.000	4.04	3
5895.97	0.000	4.08	3
	Mg I		
4571.09	0.000	4.60	1
4702.97	4.327	4.31	3
5528.40	4.327	4.42	4
	Si I		
5645.71	4.908	5.55	3
5772.24	4.899	4.92	2
5948.69	5.060	4.72	3
	Si II		
5056.03	10.030	4.85	3
6347.19	8.085	4.29	4
6371.36	8.085	4.45	3
	S I		
4694.11	6.50	4.94	1
4695.44	6.50	5.05	2

λ	Lower E.P.	−log W/λ	Wt.
	Ca I		
4226.69	0.000	4.09	1
4283.03	1.878	4.43	3
4302.53	1.891	4.38	1
4318.69	1.891	4.29	3
4425.45	1.871	4.38	3
4585.92	2.515	4.51	3
5581.94	2.512	4.81	3
5588.84	2.515	4.44	3
5590.12	2.510	4.73	2
5601.32	2.515	4.75	3
5857.46	2.920	4.51	4
6122.26	1.878	4.43	4
6162.22	1.891	4.39	2
6439.09	2.515	4.49	4
6449.79	2.510	4.62	3
6471.79	2.515	4.94	3
6499.74	2.512	5.03	3
	Sc II		
4246.83	0.314	4.14	3
4294.79	0.603	4.34	2
4420.63	0.616	4.51	2
4431.37	0.603	4.44	2
4670.34	1.351	4.20	3
5526.80	1.761	4.40	4
5667.09	1.494	4.66	4
5669.04	1.494	4.63	3
5684.32	1.500	4.48	3
6310.07	1.491	4.68	4
6604.54	1.351	4.87	3
	Ti I		
4512.79	0.832	5.06	3
4534.81	0.832	4.82	1
4617.26	1.741	5.01	2
4759.24	2.246	5.39	3
5173.82	0.000	5.11	3
6261.33	1.424	5.50	1
	Ti II		
4287.92	1.075	4.19	2
4301.89	1.156	4.16	2

TABLE 1—*Continued*

λ	Lower E.P.	−log W/λ	Wt.
	Ti II—*Continued*		
4312.86	1.175	4.18	4
4316.81	2.039	4.34	1
4367.66	2.579	4.18	2
4386.82	2.586	4.26	3
4394.07	1.216	4.28	3
4395.05	1.079	4.16	3
4395.84	1.238	4.28	2
4399.76	1.232	4.21	2
4411.11	3.081	4.37	2
4411.94	1.219	4.38	3
4417.71	1.160	4.16	1
4421.95	2.052	4.30	1
4450.49	1.079	4.15	3
4464.50	1.156	4.16	4
4468.49	1.126	4.15	3
4488.30	3.110	4.35	2
4501.29	1.111	4.12	3
4506.75	1.126	4.75	2
4529.49	1.565	4.30	3
4534.02	1.232	4.07	2
4544.02	1.238	4.54	2
4545.14	1.126	4.56	1
4563.78	1.216	4.16	2
4568.30	1.219	4.59	2
4572.00	1.565	4.07	3
4589.96	1.232	4.29	4
4636.35	1.160	4.66	2
4708.73	1.232	4.30	2
4719.48	1.238	4.84	2
4779.97	2.039	4.27	3
4798.49	1.075	4.41	4
4805.14	2.052	4.26	4
4911.22	3.110	4.41	1
5010.20	3.081	4.74	2
5072.31	3.110	4.33	3
5129.17	1.884	4.28	3
5185.88	1.885	4.34	4
5188.71	1.575	4.33	2
5211.55	2.579	4.56	2
5336.84	1.575	4.38	3
5381.05	1.559	4.40	2
5418.76	1.575	4.56	4
6491.58	2.052	4.67	3
	Cr I		
4254.34	0.000	4.21	4
4274.80	0.000	4.25	4
4626.07	0.964	4.65	4
4646.19	1.026	4.45	2
4651.29	0.979	4.87	2
4652.19	0.999	4.70	2
4718.41	3.181	4.91	3
4942.46	0.937	5.03	3
5300.57	0.979	5.31	3

λ	Lower E.P.	−log W/λ	Wt.
	Cr II		
4252.62	3.842	4.37	2
4261.92	3.848	4.29	3
4275.57	3.842	4.36	3
4555.00	4.054	4.39	2
4558.66	4.056	4.18	4
4588.18	4.054	4.27	4
4592.01	4.056	4.34	1
4616.66	4.055	4.61	1
4618.82	4.056	4.32	1
4634.08	4.055	4.34	3
4812.33	3.848	4.51	4
4824.17	3.854	4.29	1
4836.19	3.842	4.43	2
4901.79	.....	5.20	2
5305.89	3.810	4.57	4
5308.43	4.054	4.64	3
5310.74	4.055	4.92	3
5334.90	4.055	4.59	4
5407.60	3.810	4.70	4
5421.02	3.742	4.68	3
5478.46	4.160	4.77	3
5503.22	4.126	4.72	3
5508.53	4.138	4.77	4
5510.64	3.810	4.96	2
	Mn I		
4265.95	2.928	5.40	3
4754.03	2.272	4.61	3
5377.66	3.827	5.50	4
6013.48	3.059	4.83	4
6016.56	3.060	4.92	4
6021.96	3.062	4.98	3
	Mn II		
4738.38	.....	5.45	3
	Fe I		
4216.21	0.000	4.56	1
4227.44	3.318	4.19	1
4238.83	3.382	4.51	1
4241.14	2.819	5.11	3
4246.01	.....	4.70	3
4247.44	3.354	4.37	2
4250.12	2.458	4.24	3
4250.79	1.551	4.30	3
4260.48	2.389	4.27	2
4267.85	.....	4.60	3
4271.78	1.478	4.18	3

TABLE 1—*Continued*

λ	Lower E.P.	−log W/λ	Wt.	λ	Lower E.P.	−log W/λ	Wt.
	Fe I—*Continued*				*Fe* I—*Continued*		
4276.69	3.865	4.89	3	5067.23	4.202	5.08	4
4282.39	2.167	4.25	3	5074.77	4.202	4.55	3
4291.48	0.051	4.64	2	5083.31	0.954	4.59	1
4298.02	3.034	4.52	3	5110.42	0.000	4.56	2
4373.57	{2.548 / 3.005}	4.64	1	5131.48	2.213	4.64	2
				5133.70	4.160	4.43	3
4375.94	0.000	4.33	4	5150.87	0.986	4.56	3
4382.79	.....	4.90	2	5151.97	1.007	4.76	3
4383.56	1.478	4.15	3	5162.30	2.597	4.52	4
4404.77	1.551	4.14	3	5171.57	1.478	4.34	2
4476.05	2.833	4.33	3	5198.82	2.213	4.77	3
4485.69	3.671	4.84	2	5202.34	2.167	4.50	3
4528.62	2.167	4.18	3	5215.16	3.252	4.49	1
4547.89	.....	4.77	3	5216.32	1.601	4.53	1
4550.78	.....	4.77	3	5217.45	3.197	4.61	1
4587.13	.....	4.98	3	5228.41	.....	5.08	2
4601.98	1.601	4.94	1	5229.91	3.269	4.61	4
4602.97	1.478	4.48	3	5232.88	2.927	4.22	3
4607.63	3.252	4.72	1	5250.69	2.188	4.64	1
4611.28	0.911	4.59	4	5263.30	3.252	4.58	1
4625.02	3.227	4.66	3	5266.60	2.985	4.46	2
4630.11	2.269	4.90	2	5281.76	3.025	4.57	3
4643.52	3.638	4.86	3	5288.59	4.353	5.35	4
4647.41	2.936	4.50	1	5294.02	.....	4.99	2
4683.54	2.819	5.22	4	5302.35	3.269	4.47	3
4690.17	3.671	5.13	3	5307.25	1.601	4.67	3
4691.44	2.977	4.59	2	5322.14	2.269	5.43	2
4704.91	.....	5.06	1	5324.21	3.197	4.38	4
4721.13	2.977	4.96	4	5332.82	1.551	4.65	4
4728.50	3.638	4.56	3	5339.98	3.252	4.48	2
4733.58	1.478	4.74	2	5341.04	1.601	4.42	3
4735.84	.....	4.96	3	5343.37	4.353	5.22	3
4745.81	3.638	4.93	4	5367.48	4.426	4.51	4
4772.80	1.551	4.75	4	5369.96	4.396	4.37	3
4787.89	2.985	5.38	3	5371.53	0.954	4.24	4
4788.77	.....	4.97	3	5373.74	4.454	5.16	4
4903.30	2.870	4.54	4	5383.41	4.302	4.44	3
4905.15	.....	5.66	2	5389.51	4.396	4.77	3
4907.80	3.415	4.93	4	5393.18	3.227	4.56	4
4919.01	2.853	4.36	2	5397.18	0.911	4.33	2
4930.33	3.943	5.14	3	5398.25	4.426	4.80	2
4946.39	3.354	4.80	3	5400.52	4.353	4.63	3
4950.20	3.402	5.07	4	5405.79	0.986	4.33	4
4966.09	3.318	4.58	4	5410.96	4.396	4.53	2
4968.67	.....	5.03	2	5415.28	4.353	4.47	2
4973.08	3.943	4.79	3	5417.17	4.396	5.70	3
4978.59	3.967	4.77	2	5424.01	4.302	4.44	3
4994.15	0.911	4.63	1	5429.71	0.954	4.27	3
5001.82	3.865	4.42	1	5432.93	4.426	4.65	4
5002.80	3.382	4.94	3	5434.56	1.007	4.41	4
5012.09	0.855	4.30	3	5445.06	4.368	4.58	3
5014.95	3.926	4.68	1	5446.89	0.986	4.28	2
5022.13	3.967	4.66	1	5466.45	4.353	4.78	4
5039.25	3.354	4.71	1	5497.51	1.007	4.49	4
5044.20	2.839	5.08	3	5506.84	0.986	4.56	2
5049.83	2.269	4.51	3	5554.92	4.529	4.81	4
5060.06	0.000	5.55	4	5563.66	4.173	4.71	3

TABLE 1—*Continued*

λ	Lower E.P.	−log W/λ	Wt.
	Fe I—*Continued*		
5565.60	4.588	4.74	3
5569.56	3.402	4.51	4
5572.91	3.382	4.41	4
5576.09	3.415	4.55	2
5586.80	3.354	4.43	4
5600.26	4.242	5.51	3
5615.64	3.318	4.33	2
5624.66	3.402	4.57	3
5633.94	.....	5.09	4
5638.21	4.202	5.07	3
5686.53	.....	4.95	4
5701.53	2.548	4.79	4
5705.97	4.588	4.65	2
5763.08	4.191	4.76	3
5775.12	4.202	4.93	4
5785.35	.....	4.82	2
5816.38	.....	4.91	2
5852.07	4.529	5.50	4
5859.75	4.529	5.12	3
5862.34	4.529	4.90	4
5883.65	3.943	4.64	4
5905.61	.....	5.49	4
5916.38	2.443	5.66	1
5930.13	4.632	4.68	4
5934.76	3.912	5.16	4
5952.68	3.967	4.86	3
5976.76	3.926	5.03	2
5987.15	4.775	5.12	3
5997.82	4.588	5.08	3
6003.15	3.865	5.05	4
6024.02	4.529	4.72	4
6026.98	.....	5.05	2
6042.07	4.814	4.91	3
6056.08	4.713	4.95	3
6065.52	2.597	4.68	4
6187.86	3.926	5.32	4
6200.51	2.597	5.26	3
6213.44	2.213	4.99	3
6230.77	2.548	4.52	4
6232.83	3.638	4.98	3
6252.67	2.394	4.69	4
6254.19	2.269	4.85	4
6265.09	2.167	5.04	4
6318.08	2.443	4.58	3
6322.71	2.577	4.92	3
6355.15	2.833	5.11	3
6358.61	0.855	5.15	3
6393.67	2.422	4.55	4
6400.00	3.587	4.43	3
6411.47	3.638	4.70	4
6421.43	2.269	4.73	3
6430.87	2.167	4.72	4
6495.08	2.394	4.42	1
6663.44	2.414	4.85	3
6678.02	2.681	4.51	3

λ	Lower E.P.	−log W/λ	Wt.
	Fe II		
4258.18	2.693	4.14	3
4273.35	2.693	4.24	3
4296.60	2.693	4.23	2
4303.20	2.693	4.22	1
4372.25	.....	5.00	3
4385.41	2.766	4.27	2
4416.84	2.766	4.22	3
4472.91	2.832	4.32	3
4508.29	2.843	4.15	3
4515.34	2.832	4.18	3
4520.23	2.795	4.21	3
4522.63	2.832	4.07	2
4541.53	2.843	4.30	3
4555.96	2.816	4.14	2
4576.36	2.832	4.26	3
4620.53	2.816	4.39	3
4629.33	2.795	4.20	3
4635.35	.....	4.68	2
4666.75	2.816	4.25	2
4731.48	2.879	4.28	3
4893.78	.....	4.79	3
5197.54	3.217	4.24	3
5325.54	3.207	4.45	4
5346.61	3.217	4.89	4
5362.86	3.186	4.32	4
5414.03	3.207	4.60	2
5425.29	3.186	4.55	2
5534.91	.....	4.23	2
6147.81	3.872	4.52	3
6149.35	3.872	4.40	3
6369.41	2.879	4.77	2
6416.90	3.875	4.53	3
6432.88	2.879	4.61	4
6456.45	3.887	4.13	4
6516.07	2.879	4.26	3
	Ni I		
4686.13	3.582	5.18	3
4703.81	3.642	5.13	2
4714.41	3.365	4.41	3
4715.81	3.528	4.89	1
4806.98	3.663	5.09	3
4831.16	3.590	4.90	3
4904.42	3.527	4.88	2
4925.64	3.639	5.13	2
4937.37	3.590	4.83	2
4971.41	4.518	5.03	3
4980.15	3.590	4.76	3
4998.24	3.590	5.08	3
5082.38	3.642	5.25	2
5115.42	3.817	4.85	2
5155.82	3.881	4.73	2

TABLE 1—*Continued*

λ	Lower E.P.	−log W/λ	Wt.
Ni I—*Continued*			
5176.65	3.881	5.39	3
5593.74	3.881	4.97	3
5892.79	.....	5.08	3
6175.30	4.072	5.11	3
6176.83	4.071	5.32	3
Ni II			
4362.11	4.012	4.53	2
Cu I			
5105.51	1.383	4.86	4
Zn I			
4722.18	4.012	4.78	4
4810.59	4.060	4.83	3
Sr II			
4077.71	0.000	3.82	1
4215.54	0.000	4.03	1
Y II			
4682.24	0.407	4.45	2
5087.41	1.079	4.45	3
5119.13	0.988	4.94	3
5200.42	0.988	4.51	3
5402.81	1.831	4.89	4
6613.88	.....	4.91	1
Zr II			
4211.89	0.524	4.42	3
4359.69	1.231	4.30	1
4613.92	0.968	5.03	1
5112.28	1.658	4.91	3
Ce II			
4253.47	.....	5.00	3
4270.27	.....	4.89	1
4364.65	.....	4.80	2
4391.75	.....	4.63	2
4460.25	.....	4.66	3
4486.90	.....	5.02	2
4562.38	.....	4.90	3
4606.44	.....	4.91	2
Ba II			
4554.04	0.000	4.16	3
5853.73	0.602	4.40	4
6141.81	0.701	4.19	3
6496.81	0.602	4.30	2
La II			
5114.50	0.234	5.02	2

Let

$$\log X_r = \log X_0' - \frac{5040\chi}{T_1}, \tag{4}$$

where T_1 is the excitation temperature of the star under consideration. In order to determine the excitation temperature, we may assume various values of T_1 and, for a given kind of atom or ion, plot log X_r against log W/λ. The temperature that gives the least relative displacement of the points for lines of low and high excitation potentials—i.e., the points lie most nearly on a curve—is the most probable value.

Plots of the equivalent widths of the neutral iron lines, against log X_r for excitation temperatures of 4400° and 6000°, and then 4000° and 4700°, showed that 4400° is the

most probable value for neutral iron in α Persei. Figure 1 is the 4400° curve for *Fe* I. For most of the other atoms and ions the measured lines did not differ much in excitation potential. The fit of observational curves for excitation temperatures of 4400° and 6000° with the theoretical curve determined the more probable value of the temperature. This procedure indicated temperatures of 4400°, rather than 6000°, for *Fe* II, *Ti* I, *Ti* II, *Cr* II, *Ca* I, *Sc* II, and *Ni* I. For *Cr* I and *Mn* I the position of one or two points of higher excitation potential than the rest suggested 6000° as the more probable excitation temperature. There were too few points to give those higher temperatures any weight, however. Indeed, the range in excitation potential of the measured lines was so small for most of the atoms and ions except neutral iron, and so few lines of any other atom or ion were measured, that no conclusions can be drawn as to the variation of the excitation temperature for different atoms in the atmosphere of α Persei.

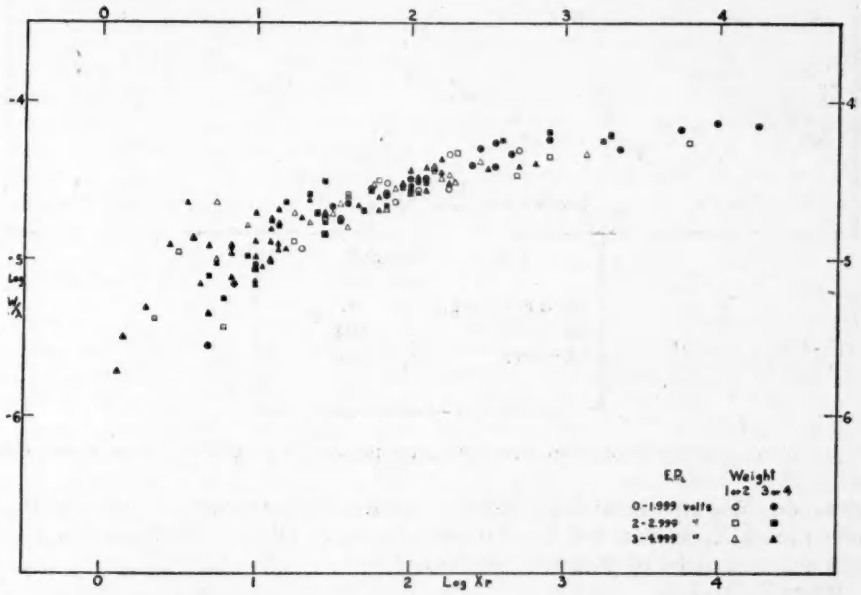

FIG. 1.—Curve of growth from solar log X_0' values for *Fe* I. The excitation temperature is 4400°

Curves of growth from strengths determined in the laboratory should be more reliable than those based on present calculations of multiplet strengths. Then the uncertainties caused by departures from *LS* coupling and isolation of configurations, assumed in the calculation of theoretical multiplet strengths, do not enter.

King and King's[16] relative ϖf values for *Fe* I and *Ti* I were used to plot log W/λ against (log $\varpi f\lambda/5000 - 5040\chi/T$) for temperatures of 4400° and 6000°. The relative positions of points for lines of low excitation potential (0.0–0.2 volts) and for lines of somewhat higher excitation potential (0.85–1.01 volts and 1.4–1.6 volts) corroborated the 4400° excitation temperature determined for *Fe* I from the solar log X_0' curves. Figure 2 is the 4400° curve for *Fe* I. For *Ti* I the 6000° curve was somewhat better than the 4400° curve, contrary to the result obtained from log X_0' values. Because there were only one high-weight and four low-weight points on each curve, the discrepancy for *Ti* I cannot be considered definite.

An excitation temperature of 4400° is somewhat lower than values previously deter-

[16] *Op. cit.*

mined for α Persei. K. O. Wright[17] in his most recent work obtained a value of 4700°. With excitation temperatures derived for other stars, 4400° for α Persei fits in well. For the *F*0 supergiant, α Carinae, Greenstein[7] obtained an excitation temperature of 4900°; for the A0 dwarfs, Sirius and γ Geminorum, Aller[18] found 6000°; and for the sun, Menzel, Baker, and Goldberg[13] derived a value of 4400°. Wright[17] determined an excitation temperature of 4800° for the F5 dwarf, α Canis Minoris; and 4400° for the F8 supergiant, γ Cygni. For each of these stars the effective temperature, as derived from Kuiper's work,[19] exceeds the excitation temperature. It is not surprising that the two temperatures differ, for they may represent different levels in a stellar atmosphere. Effective temperatures of giants are lower than those of dwarfs. Excitation temperatures thus far determined indicate a similar relation for giants and dwarfs.

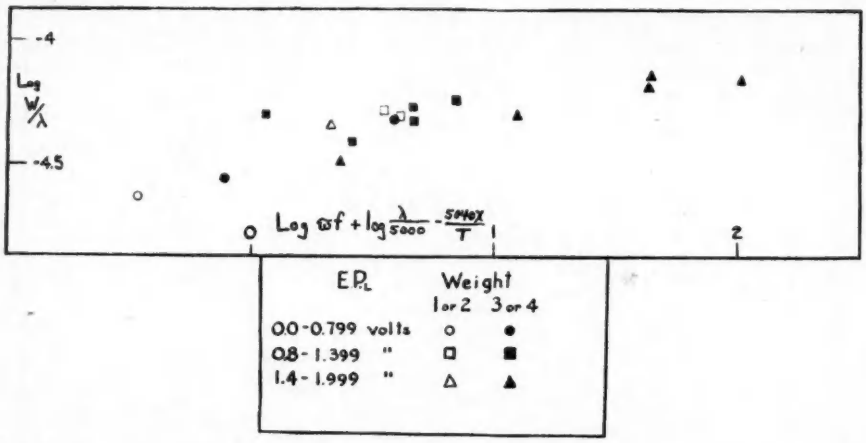

FIG. 2.—Curve of growth from laboratory strengths for *Fe* I. The excitation temperature is 4400°

By superposing an observational curve of growth on the theoretical curve, we may determine the log X_0 scale; v; and the damping constant, (Γ/ν). The theoretical curve of growth was calculated by Menzel's[12] formulae:

1. When $X_0 < 1$,

$$\frac{W}{\lambda}\frac{c}{v} \sim \sqrt{\pi} X_0 . \tag{5}$$

2. When $X_0 > 1$, but not so large that wing damping is appreciable,

$$\frac{W}{\lambda}\frac{c}{v} \sim 2\,(ln X_0)^{1/2} . \tag{6}$$

3. When $X_0 >> 1$ and damping becomes important,

$$\frac{W}{\lambda}\frac{c}{v} = \frac{\pi^{1/4}}{2}(X_0 Z)^{1/2} , \tag{7}$$

where Z is given by

$$Z = \frac{\Gamma}{\nu}\frac{c}{v} . \tag{8}$$

[17] *Pub. A.A.S.*, **10**, 338, 1940.

[18] *Ap. J.*, **96**, 321, 1942.

[19] *Ap. J.*, **88**, 429, 1938.

The three portions of the curve of growth were connected by smooth curves. A horizontal shift of the observational curve, derived from solar log X_0' values, on the theoretical curve corresponds to differences between the solar and stellar values of N_a and v. The vertical shift necessary for the superposition of the two curves determines log (c/v). The Z branch of the theoretical curve which best fits the observational curve gives the value of Z. From equation (8) we may then calculate (Γ/ν). The values of v found for the various atoms and ions, except for the indeterminate case of *Ti* I, range from 3 to 5 km/sec. It is customary to use the average value of log (c/v) to fit a single theoretical curve of growth to the observational curves of all the atoms and ions. I have used a weighted average, since the determination of log (c/v) was of considerably more value for some atoms than for others. Weights were assigned according to the number of points on the curve, the distribution of the points along the curve of growth, especially on the flat portion, and the amount of scatter.

The weighted average value of log (c/v), 4.91, gives a velocity of 3.7 km/sec. If interpreted as thermal motion, this velocity would correspond, for a mean atomic weight of 50, to a kinetic temperature of 35,000°, considerably in excess of Kuiper's[19] value for the effective temperature of α Persei, 6340°. In supergiants Struve and Elvey[2] and others have also found velocities much in excess of the gas-kinetic values. Struve attributes the effect to turbulence in stellar atmospheres.

Goldberg[20] has used the following formula to determine the part of the velocity, v, caused by turbulence, i.e., the contribution of thermal motion to the velocity of the atoms is removed:

$$v_T^2 = v^2 - v_0^2 , \tag{9}$$

where v_T is the turbulent velocity and v_0 is the gas-kinetic velocity. When we determine the gas-kinetic velocity for an effective temperature of 6340° and a mean atomic weight of 50, the turbulent velocity becomes 3.4 km/sec. An atomic weight of 50 is an intermediate value for the elements used in the determination of log (c/v).

A number of observers have derived velocities for α Persei, all the values being larger than that found in the present investigation. Struve and Elvey[2] obtained a velocity of 7 km/sec, and Dunham[3] determined a velocity of 5 km/sec. These velocities correspond to turbulent velocities that are not significantly different from 7 and 5 km/sec, respectively. K. O. Wright[17] obtained a turbulent velocity of 4.2 km/sec. These differences in the velocity result largely from discrepancies in the measures of the different observers and in smaller part from the fitting of a theoretical to an observational curve of growth.

The high dispersion of the spectrograms in the present investigation makes them particularly suitable for the determination of the velocity. The reduction in the amount of blending, with high dispersion, not only provides more unblended lines for measurement but gives a better concept of the position of the continuum. Thus, more accurately defined lines provide equivalent widths for the determination of the velocity. The use of log X_0' values avoids any difficulties that might be encountered when small segments are fitted together to form a curve of growth from theoretical multiplet intensities. We see from Figure 1 that the *Fe* I curve is well defined; the points extend over all three portions of the curve.

For another F-type supergiant, α Carinae, Greenstein[7] obtained a velocity of 3.5 km/sec, close to the velocity determined in this investigation for α Persei. The absolute magnitude of α Carinae is about the same as that of α Persei; Greenstein[7] gives -3.8 ± 0.3 mag. from a Cape trigonometric parallax. The lines of α Carinae are definitely sharper than those of α Persei and lead one to expect a greater difference in the turbulent velocities.

Not enough strong lines have been measured in stellar spectra to permit very accurate

[20] *Ap. J.*, 89, 623, 1939.

determinations of Γ/ν. The values that have been derived for Γ/ν are about ten times the classical value of 1.47×10^{-7} for a mean wave length of 5000 A. For the sun, Miss P. Rubenstein[21] found a Γ/ν of 1.7×10^{-6}. For α Carinae, Greenstein's[7] value of Γ was 1.5×10^{9}; that is, $(\Gamma/\nu) = 2.5 \times 10^{-6}$ at $\lambda = 5000$ A. Using his revised solar strengths, Wright determined a Γ/ν of 5.5×10^{-6} for α Persei. For α Persei, I obtained a value for Γ/ν of 1.2×10^{-6}, smaller than the values determined by other observers and closest to Miss Rubenstein's value for the sun.

Figure 3 gives the observational curve of growth for α Persei. The line is the theoretical curve. We note that there are few points on the dampening portion. Observational errors may be responsible for the scatter along the entire curve of growth, but departures from the current theory of curves of growth may also contribute to the scatter. Approxima-

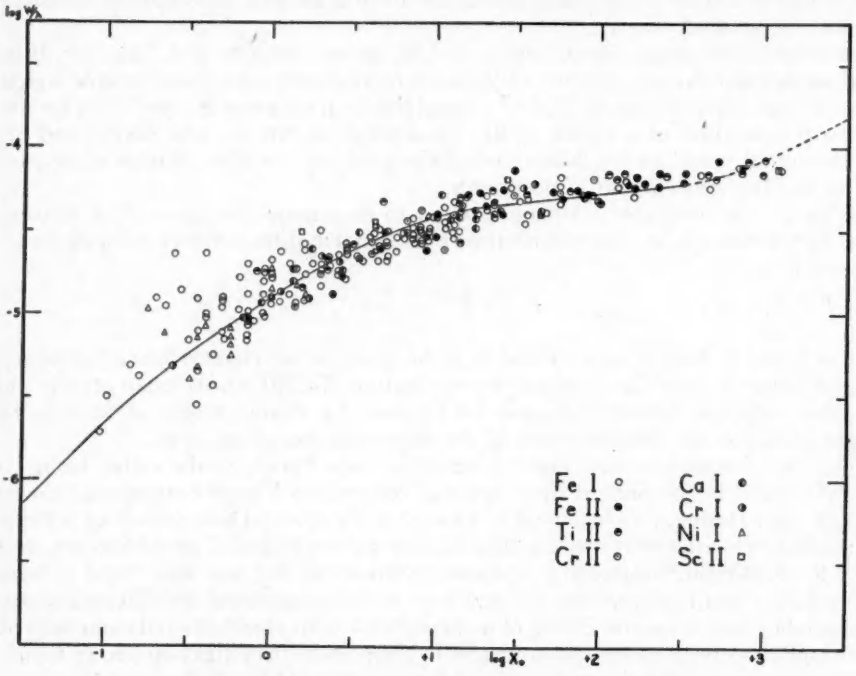

FIG. 3.—Curve of growth for α Persei. The line is the theoretical curve

tions have been made in the derivation of equations (5), (6), and (7). The success that astrophysicists have had in the construction of curves of growth is a point in favor of the current methods. To be sure, departures of an observational curve from the theoretical curve have been found;[22] but it is not clear whether the formulae, the assumption of mean values of v and Γ/ν, or observational errors are responsible.

The assumption of the same value of v for the metallic atoms and ions and the use of a mean damping constant are certainly open to question,[23] but it is not clear how we could make further refinements at present. Since not many of the measured lines lie on the damping portion, uncertainty about that part of the curve is less critical. So far as thermal motion is concerned, the velocities of the different metallic atoms used to form

[21] *Ap. J.*, **92**, 114, 1940.

[22] K. O. Wright, *Ap. J.*, **99**, 249, 1944.

[23] See, e.g., R. Minkowski and R. B. King, *Ap. J.*, **95**, 86, 1942.

the curve of growth (Fig. 3) would differ by only a small amount, probably within the accuracy obtainable from the observational data. For the lighter elements the velocities would differ considerably from those of the metals listed in Figure 3. In practice, we use the curve of growth to obtain log X_0 values for lines of the lighter elements, although those elements were not involved in the determination of the curve. We are, however, considering a turbulent atmosphere, and we do not know whether the turbulent velocities are the same for the different atoms. Unless the data are sufficiently extensive to give a curve of growth for each ion or element, we have no means of studying the effect.

CHEMICAL COMPOSITION

From an observational curve of growth we obtain values of log X_0 which we may use to determine log N_a. Equations (1) and (2) give the fundamental equation as written by Menzel,[24]

$$\log N_a = 17.82 + L - \log \frac{c}{v} + \log b(T) - \log \phi , \tag{10}$$

where

$$L = \log X_0 - \log \frac{Ss}{\Sigma s} + \frac{5040\chi}{T} . \tag{11}$$

Dr. Goldberg has kindly permitted me to use his unpublished formula for ϕ; the formula is based on Slater's[25] approximate wave functions. A value of log N_a was then derived for each kind of atom and ion having measured lines with available theoretical strengths.[26] Only for titanium and silicon could values of log N_a for both the neutral and singly ionized atoms be obtained directly from the observational data. For ionized chromium, iron, and nickel the measured lines in α Persei and even all lines having solar log X_0' values had no theoretical strengths. The measured lines in α Persei and the lines with solar data were of four types—namely, intersystem, interparentage, two-electron-jump transitions, and transitions involving equivalent electrons having terms of unknown parentage. In the first three cases formulae for the calculation of theoretical multiplet strengths have not been derived. In order to compute the strengths for transitions involving terms from equivalent electrons, we must know the parentage.

In order to obtain from the observational data the number of ionized chromium, iron, and nickel atoms in a square-centimeter column above the photosphere, we must know either the ϖf values for the measured lines or the theoretical strengths. No ϖf values have been obtained for these ions; and, for the reasons given above, theoretical strengths have not been calculated. Some of the measured lines for both iron and chromium arise from transitions between terms of different parentage. Assuming the parentage of one of the terms for both, we may use the corresponding theoretical strength as an approximation to the strength of the line resulting from the interparentage transition. The only measured equivalent width for ionized nickel was that of an intercombination line for which no approximation to the strength was attempted.

The large ranges in the values of $(L - \log \phi)$ for *Fe* II and *Cr* II suggested that for some lines the approximate strengths might be closer to the true values than for other lines. We may use the chromospheric strengths to attempt a better approximation.

[24] *Pop. Astr.*, **47**, 133, 1939.

[25] *Phys. Rev.*, **36**, 57, 1930.

[26] Theoretical multiplet strengths, later referred to as "*LS*-coupling strengths" (see n. 15), may be obtained from the following articles: L. Goldberg, *Ap. J.*, **82**, 1, 1935, and **84**, 11, 1936; Menzel and Goldberg, *Ap. J.*, **84**, 1, 1936.

Theoretical line strengths may be obtained from White and Eliason, *Phys. Rev.*, **44**, 753, 1933, and H. N. Russell, *Ap. J.*, **83**, 129, 1936.

William Petrie[27] has determined chromospheric strengths for a number of lines from emission intensities measured on spectrograms of the chromosphere. We may express the emission intensity in terms of ϖf values by the equation

$$I = 8h\nu^3 \frac{\pi^2 e^2}{m c^3} \frac{N_0}{\varpi_0} e^{-\chi_n/kT} \varpi f , \qquad (12)$$

where N_0 is the number of atoms in the ground level for the particular stage of ionization of the element under consideration. By correcting the measured intensities for self-reversal, and removing the factors $e^{-\chi_n/kT}$ and ν^3, he obtained chromospheric strengths for the lines.[28] For use in equation (10) we multiply the strengths by λ and designate them as $\varpi f_E \lambda$. These strengths contain the factor N_0, as well as other constants. Because the values of N_0 are unknown, we cannot use the chromospheric strengths directly to obtain the numbers of singly ionized iron, chromium, and nickel atoms. We can, however, employ the strengths in conjunction with the first approximate strengths.

The difference between the chromospheric strength of a line and log $[(Ss/\Sigma s)\ \phi]$ should, theoretically, be constant for all the lines of a given element in a particular stage of ionization. The observationally determined chromospheric strengths, however, may contain errors. For some lines the approximate strengths may be closer to the true values than for others. By averaging the differences between the two strengths, for all lines having both values, we hope to obtain the correct distribution of errors. The average value, when subtracted from the chromospheric strength of any line of the particular ion, gives an approximation to log $[(Ss/\Sigma s)\ \phi]$. We may then include in the determination of log N_a the observational data for all lines having chromospheric strengths.

The measured lines of *Ti* II provide material for a comparison of the results obtained with the *LS*-coupling strengths and with the approximate strengths used for *Fe* II and *Cr* II. For ten interparentage transitions with strengths derived as in the first approximation for *Fe* II and *Cr* II, we obtain 16.96 for log N_a.

Only 6 lines have both chromospheric and approximate theoretical strengths from which the average difference between the two strengths may be calculated. In the computation of the average $(L - \log \phi)$, however, we include all the lines (16) having chromospheric strengths. The value obtained for log N_a is 17.03.

We should expect the strengths of interparentage transitions to be less than those of the more probable transitions between terms of the same parentage. A reduction in the strengths used to calculate log N_a will give a larger value of N_a. We note that the value of log N_a obtained with chromospheric strengths is larger than that obtained with only the approximate strengths. The difference in log N_a, however, is not significant, since it is less than the mean error in $(L - \log \phi)$ for either determination.

It is possible that for strong lines the approximate strengths are closer to the true values than for the weaker lines. In view of this possibility, we derive the average difference between the chromospheric and approximate strengths from the strengths for the three strongest lines. By subtracting this average difference from the chromospheric strengths of the 16 lines, we obtain a new set of strengths. These new values give 17.41 for log N_a. The difference between this last value of log N_a and the former values is considerably larger than the mean error in each determination. The mean error is 0.27 for 10 lines with approximate strengths and 0.20 for 16 lines with chromospheric strengths. To determine whether the reduction in mean error is merely a result of the use of more lines, we compute log N_a and its mean error by the two methods for 6 lines having both strengths. The mean error is less when chromospheric and approximate strengths are used. Not only is the mean error less, but the value of log N_a is closer to the value of 17.99 obtained from *LS*-coupling strengths.

In the computation of log N_a for *Fe* II from lines having both strengths, we again find

[27] Unpublished.

[28] χ_n is here the excitation potential of the upper level of the line.

that the use of the chromospheric strengths reduces the mean error. For *Cr* II the mean error in log N_a, when chromospheric and approximate strengths are used, is increased. Since only 2 lines are used to determine log N_a, the *Cr* II results do not have so much weight as those for *Ti* II and *Fe* II.

Table 2 contains the values of log N_a derived by the different methods for *Ti* II, *Fe* II, and *Cr* II and the number of lines used in each determination. Because the third method gave a value of log N_a for *Ti* II closest to that from *LS*-coupling strengths and reduced the mean error in log N_a for *Ti* II and *Fe* II, we shall assume that the third method is the best. For log N_a of *Fe* II and *Cr* II we adopt the values in the last line of Table 2.

TABLE 2

VALUES OF LOG N_a FROM APPROXIMATE STRENGTHS

	Ti II		*Fe* II		*Cr* II	
	log N_a	No. of Lines	log N_a	No. of Lines	log N_a	No. of Lines
Approximate	16.96	10	19.19	23	17.94	9
Approximate and chromospheric	17.03	16	19.14	16	18.48	9
Average $\{\log \bar{\omega} f_E \lambda - \log [(Ss/\Sigma s)\phi]\}$ from strong lines only	17.41	16	19.45	16	18.17	9

TABLE 3

CHEMICAL COMPOSITION OF THE ATMOSPHERE OF α PERSEI

Atom	log N_a	Atom	log N_a
C I	21.10	*Cr* II	18.17
Na I	15.90	*Mn* I	16.50
Mg I	19.11	*Fe* I	18.83
Si I	17.73	*Fe* II	19.45
Si II	22.76	*Ni* I	18.51
S I	19.20	*Zn* I	17.98
Ca I	14.85	*Sr* II	15.09
Sc II	15.66	*Y* II	14.73
Ti I	13.96	*Zr* II	14.90
Ti II	17.99	*Ba* II	15.53
Cr I	15.04		

Table 3 gives the values of log N_a computed from the observational data and *LS*-coupling strengths. When theoretical *f*-values are available, their use in the calculation of N_0 and N_1 for each of the elements should give more reliable results. By using a number of lines of each atom or ion in the determination of log N_a, however, we hope to reduce the effect of errors in the *LS*-coupling strengths as well as in the observational data. The approximate values of log N_a for *Fe* II and *Cr* II are included in Table 3. An excitation temperature of 4400° has been used in all the calculations, since only the excitation temperature for *Fe* I is well determined and since there is no conclusive observational evidence of a variation in excitation temperature for different elements. The numbers of the different atoms and ions in a stellar atmosphere are useful in the study of the physical conditions, as the next section will show.

PHYSICAL CONDITIONS

If values of N_a can be determined for a neutral and singly ionized atom, we may derive the electron pressure with the aid of Saha's equation,

$$\log P_e = 2.5 \log T + \log \frac{2\, b_1(T)}{b_0(T)} - \frac{5040\, I}{T} - \log \frac{N_1}{N_0} - 0.48\,, \qquad (13)$$

where P_e is the average electron pressure in dynes /cm^2; T, the temperature; $b_1(T)$ and $b_0(T)$, the partition functions for the singly ionized and neutral atoms, respectively; I, the ionization potential of the neutral atom; and N_0 and N_1, the respective numbers of neutral and singly ionized atoms per centimeter-square column above the photosphere.

The value of the temperature to be used in equation (13) is not certain. It is often argued that the effective temperature should be used. The effective temperature, which is a measure of the total energy passing through a unit surface area of the star, may not be a satisfactory parameter for representing excitation conditions for the atom in question. The energy incident on the atom in the reversing layer, within the particular spectral region that can cause ionization, is far more important. The value of the temperature parameter that may be used to describe the energy will probably vary considerably from wave length to wave length.

One might also consider using the excitation temperature as previously determined. Unfortunately, this parameter applies particularly to atoms in low-energy levels, since lines from atoms in high levels are too far in the violet or too faint to be observed. The excitation temperature thus also varies and is neither characteristic of the whole radiation nor representative of the ionization temperature.

To investigate the dependence of P_e on T, we derive P_e from the values of N_1 and N_0 for silicon, titanium, iron, and chromium for both the effective and excitation temperatures of α Persei. For Kuiper's[19] value of the effective temperature, 6340°, the electron pressure for silicon is 4.1×10^{-3} dynes/cm^2; for titanium, 1.4 dynes/cm^2; for iron, 4.5×10^2 dynes/cm^2; and for chromium, 4.3 dynes/cm^2. For a temperature of 4400°, however, the electron pressures are 2.5×10^{-6} dynes/cm^2 for silicon, 2.5×10^{-3} dynes/cm^2 for titanium, 3.4×10^{-1} dynes/cm^2 for iron, and 8.7×10^{-3} dynes/cm^2 for chromium. The differences in the pressures calculated for the two temperatures show that the electron pressure is very sensitive to the temperature and perhaps also to the ionization potential. We cannot, therefore, obtain a definite result for the electron pressure by this method.

In using in equation (13) one value of T for atoms at different levels, we have assumed an isothermal atmosphere at a mean temperature, T. If we also assume that the atmosphere has a constant composition, of mean atomic weight $\bar{m}$, we may determine the electron pressure by an alternative method.

The electron pressure at the base of the reversing layer, P_{e0}, is given by

$$P_{e0} = n_{e0} kT\,, \qquad (14)$$

where n_{e0} is the number of electrons per cm^3 at the base of the reversing layer. We may express n_{e0} in terms of N_e, the number of electrons per square-centimeter column above the photosphere. We write for N_e,

$$N_e = \int_0^\infty n_e\, dx = \int_0^\infty n_{e0}\, e^{-\bar{m}gx/kT} dx\,, \qquad (15)$$

where n_e is the number of electrons per cm^3, $\bar{m}$ is the average mass of the atoms, and g is the effective gravity. Integrating (15), we obtain

$$N_e = n_{e0} \frac{kT}{\bar{m}\, g}\,. \qquad (16)$$

Solving equation (16) for n_{e0} and substituting the result in equation (14), we find

$$P_{e0} = N_e \bar{m} g \,. \tag{17}$$

The electron pressure at the base of the reversing layer may be expected to depend on the average mass of the atoms, for the electrons are not independent of the atoms. Pannekoek has shown that no appreciable separation is possible[29] because of the high electric charges that would thus be set up.

We do not know the cause of turbulence; but, having postulated its existence, we must allow for its effect on the density distribution and pressure. If we should adopt McCrea's[30] description of turbulence, T in equations (14) and (15) would be given by

$$T = kT_{\text{thermal}} + \tfrac{1}{3} m v_T^2 \,, \tag{18}$$

where T_{thermal} is the temperature representing thermal motion. As the same T is involved in equations (14) and (15), equation (17) would be unchanged. It has been argued that turbulence merely reduces the effective gravity. In that case, also, equation (17) would apply, if we use for g the effective gravity. If our preliminary assumptions of an isothermal and unstratified atmosphere may be made, we may, so far as our present knowledge is concerned, obtain an approximate value of P_{e0} for a supergiant from equation (17).

In a supergiant the tenuous atmosphere, similar to the chromosphere of the sun, may be partially supported by radiation pressure. In order that equation (15) will apply to atmospheres partially supported by radiation pressure, we consider g as the effective gravity. In view of our lack of knowledge about turbulence and, consequently, about the effective gravity, we shall use the surface gravity for g to obtain an approximate value of P_{e0} for α Persei.

The surface gravity is given by

$$\log \frac{g}{g_\odot} = \log \frac{m}{m_\odot} + 4 \log \frac{T}{T_{e\odot}} - 0.4\,(M_\odot - M) \,, \tag{19}$$

where m and $m_\odot$ are the masses of the star and the sun, respectively; T_e and $T_{e\odot}$, the effective temperatures; and M and $M_\odot$, the absolute bolometric magnitudes. Using the mass-luminosity relation derived by Russell and Moore,[31] and Kuiper's[19] values of the effective temperatures and bolometric magnitudes, we obtain for the surface gravity of α Persei 2.6×10^2 cm/sec^2. This value is considerably less than the surface gravity of the sun, 2.74×10^4 cm/sec^2, as is to be expected, and is about the same as Greenstein's[7] value for α Carinae, $\log g = 2.4$.

We are forced to make some assumption as to the source of the electrons and the number from the particular source because the observational data are insufficient. In order to calculate N_e, we make three assumptions: only the metals are ionized; the ratio of abundances of titanium to that of each other metal is the same for α Persei as for the sun; and all the metallic atoms are singly ionized.

The observationally determined numbers of singly ionized titanium, iron, and chromium atoms give the contribution of those metals to the number of electrons. There are too few scandium, strontium, yttrium, zirconium, and barium ions to be appreciable. We base the calculation of the number of other singly ionized metallic atoms on the number of titanium atoms, since that number is the most reliably determined. Assuming the solar ratio of the abundance of titanium to that of any particular metal, we compute the

[29] *B.A.N.*, **1**, 110, 1922; *Handb. d. Ap.*, **3**, 319, 1930. Cf., also, Menzel, *Pub. Lick Obs.*, **17**, 290, 1931.

[30] *M.N.*, **89**, 718, 1929. Cf., also, Menzel, *Pub. Lick Obs.*, **17**, 290, 1931.

[31] *The Masses of the Stars*, p. 75, Chicago: U. of Chicago Press, 1940.

number of those metallic atoms for α Persei. We use the solar abundances derived by Menzel and his collaborators[32] for *Na*, *Mg*, *Al*, *K*, *Ca*, *V*, *Mn*, *Co*, *Ni*, *Cu*, and *Zn*. The number of electrons from these metals is, according to the assumptions above, equal to the number of metallic atoms. For N_e we obtain 6.9×10^{21}.

Unless we know the abundances of the nonmetals as well as the metals, we cannot determine $\bar{m}$. Greenstein[7] has given a method for the determination of the abundance of hydrogen from a consideration of the Stark effect. Unless an excitation temperature considerably different from that for the metals is assumed, the abundances of hydrogen determined by Greenstein for α Carinae and by K. O. Wright for α Persei are excessive. Menzel has found the same difficulty of high excitation temperature or excessive abundance of hydrogen for the sun. In view of these difficulties and the necessity of assuming abundances for three elements having no observed lines—helium, nitrogen, and oxygen—we shall also assume the abundance of hydrogen.

Adopting for α Persei the solar ratio of the number of atoms of hydrogen per square-centimeter column above the photosphere to the number of metallic atoms, we derive N, the number of atoms, for hydrogen. In the same manner as for hydrogen, we estimate the values of N for helium, nitrogen, oxygen, and silicon. We include silicon among the elements with assumed abundances because the values of $\log N_0$ and $\log N_1$ given for silicon in Table 3 are uncertain. The assumption of an excitation temperature of 4400° for silicon is open to question.

The above data give 2.6×10^{-24} for $\bar{m}$. Inserting that value and the previously derived values of N_e and g into equation (17), we obtain 4.7 dynes/cm^2 for P_{e0}.

When P_{e0} is known, the Saha equation provides a relation by which we may determine the temperature. Milne[33] has shown that the electron pressure in the ionization equation (eq. [13]) may be replaced by $P_{e0}/2$. Using the electron pressure of 4.7 dynes/cm^2, we may calculate the temperature which will result for the observational values of N_0 and N_1 for each of the elements silicon, titanium, iron, and chromium. The temperatures obtained are 9900° for silicon, 6600° for titanium, 4800° for iron, and 6100° for chromium.

By assuming an excitation temperature different from 4400°, we can obtain for silicon a temperature from the Saha equation closer to the temperatures of the metals. The value of N_1/N_0 for silicon is sensitive to the excitation temperature because the excitation potentials of the neutral and singly ionized atoms are high and differ by about 5 volts. In order to obtain a value of 6600° for T with an electron pressure of 4.7 dynes/cm^2, we must assume an excitation temperature of 7900° for silicon.

For no reasonable values of the electron pressure and temperature can the temperature obtained for the two elements, silicon and titanium, be reconciled. The temperature for titanium is lower than that for silicon, an element of relatively higher ionization potential and one whose observed lines are of relatively higher excitation potential.

If the sequence of temperatures for silicon, titanium, chromium, and iron is to be considered a function of excitation potential, the temperature for iron is rather low; if a function of ionization potential, the temperature for iron is quite discordant. It may be suggested that the sequence is a function of atomic weight. Even for this relation, the temperature for iron is somewhat low. We recall, however, that the strengths, and therefore N_1, for *Fe* II are uncertain. It would be well to calculate N_1 for iron and for chromium from f-values when theoretical values are available. Then the temperatures derived for those elements would be more reliable.

A sequence with atomic weight would probably indicate stratification, in an atmosphere in which the temperature increased with height above the photosphere. The phys-

[32] Goldberg and Aller, *Atoms, Stars, and Nebulae*, p. 114, Philadelphia: Blakiston Co., 1943.

[33] *M.N.*, **89**, 17, 1928. Milne's equations are based on rather crude assumptions. From a study of more rigorous equations, Menzel (*Pub. Lick Obs.*, **17**, 220, 1931) has found that $P/2_{0e}$ is a good approximation for P in equation (13). In any case, the factor, if not $\frac{1}{2}$, is probably not sufficiently different from $\frac{1}{2}$ to alter the results significantly.

ical explanation for such a temperature gradient is not apparent. It might be suggested that the effective level for a given element depended on its ionization potential. If a pressure gradient existed, we should expect the more easily ionized elements to have lower effective levels. To obtain the computed temperatures for silicon and titanium, however, we should again require an increase of temperature with distance above the photosphere.

The effective level in the atmosphere may depend on the excitation potential of the lower level of the line. If the temperature increases from the top of the atmosphere inward, we should expect that lines of higher excitation potential would be formed nearer the photosphere.

Whether the excitation or the "ionization" temperature, or both, vary is not certain. In the chromosphere Menzel and Cillie[34] have found, for hydrogen and ionized helium, a variation of ionization temperature with ionization potential; for the metals, Menzel[8] and William Petrie[27] have shown a dependence of excitation temperatures on excitation potential. The atmosphere of α Persei is of low density, like the chromosphere. It is probable that, in the atmosphere of α Persei, both the excitation and ionization temperatures vary. The temperature appears to increase with frequency, that is, with excitation potential and with ionization potential.

In a similar manner we calculate P_{e0} for the sun from equation (17). From Menzel, Baker, and Goldberg's[13] data we compute N_0 and N_1 for titanium. We neglect second-stage ionization and take

$$N = N_0 + N_1 . \tag{20}$$

Then we use Menzel and Goldberg's[32] solar abundances to obtain the numbers of the various atoms in a centimeter-square column above the photosphere. We again assume that only the metals are ionized and that all the metallic atoms are singly ionized. For N_e we find 5.6×10^{20}; and for $\bar{m}$, 2.6×10^{-24} grams. The surface gravity of the sun is 2.74×10^4 cm/sec^2. The above values of N_e, $\bar{m}$, and g give 40 dynes/cm^2 for P_{e0}.

Early determinations of P_{e0} by Russell[35] (46 dynes/cm^2) and Menzel[36] (40 dynes/cm^2) also depend on a number of approximations, including that of an isothermal atmosphere. Menzel and Pekeris'[37] theoretical value of P_{e0}, 32 dynes/cm^2, is derived for an atmosphere in which the metals produce the general opacity. In his theoretical calculations of P_e, Strömgren[38] allowed for variation of temperature with optical depth and used neutral hydrogen and the negative hydrogen ion as the sources of continuous absorption. Strömgren's work is based on the Milne-Eddington model of a stellar atmosphere, while the present investigation is based on the Schuster model. Milne[39] has given an approximate expression for the optical depth in the Milne-Eddington model above which the amount of material would equal that above the photosphere in the Schuster model. The optical depth is a function of the intensity ratio in the line; that is, the profiles from the two models are equated at a particular point. For an intensity ratio of one-half, Milne's formula gives $\frac{4}{3}$ for τ. Strömgren's table[38] for $\log A = 3.8$ gives $\log P_e = 1.15$ for $\tau = 0.5$. In view of the assumptions made in the two determinations of the electron pressure and in the formula for their comparison, it is interesting that the order of magnitude of the two values is similar.

We now investigate the validity of the assumptions made in the calculation of P_{e0}. In the case of α Persei, we assumed the solar ratio of abundances of titanium to that of any other metal. The solar ratio of the abundances of titanium to iron is about seven times less than the ratio of the observationally determined numbers of atoms in the atmosphere

[34] *Harvard Circ.*, No. 410, 1935.

[35] *Ap. J.*, **78**, 239, 1933.

[36] *Pub. Lick Obs.*, **17**, 245, 1931. [37] *M.N.*, **96**, 77, 1935.

[38] *Festschrift für Elis Strömgren*, p. 218, Kopenhagen: Einar Munksgaard, 1940.

[39] *Phil. Trans. R. Soc. London*, A, **228**, 421, 1929.

of α Persei. The ratio of titanium to chromium abundances is nearly the same in α Persei and the sun.

For the lighter elements we find similar ratios of carbon to the metals. The ratio of silicon to the metals is thirty times greater in α Persei than in the sun, while the ratio of sulphur to the metals is sixty times less in α Persei than in the sun. We note, however, that the measured lines of carbon, silicon, and sulphur in α Persei are all of high excitation potential and, consequently, sensitive to the excitation temperature assumed.

To test the degree of ionization, we calculate, for the derived value of P_{e0} and possible values of the temperature, the values of N_0, N_1, and N_2 not determined from the observational data. For elements having none or only one of the three values N_0, N_1, and N_2, given by the observational data, we use in the calculations the total number of atoms determined from the solar abundance ratios.

For a temperature of 6600° and a pressure of 4.7 dynes/cm² we find that, among the metals considered, double ionization is appreciable compared with single ionization only for titanium and calcium. For that temperature and pressure the neutral metallic atoms are inappreciable compared with the ionized atoms. The numbers of singly ionized carbon, silicon, and sulphur atoms, at this temperature and pressure, are appreciable compared with the neutral atoms. Including the contribution of the doubly ionized metals and singly ionized nonmetals to N_e, we find 7.4 dynes/cm² for P_{e0}. This new value of the pressure will then give a smaller degree of ionization and a corresponding lower pressure.

The electrons resulting from ionized hydrogen are so great in number that they produce an electron pressure one hundred times larger than 4.7 dynes/cm². Repeating the calculation of degree of ionization with the new pressure and continuing the successive approximations, we find an electron pressure appreciably greater than 4.7 dynes/cm². We do not know, however, that the temperature derived for titanium should be used for hydrogen; nor, indeed, do we know what temperature to use. Therefore, we shall adopt our previous assumption that hydrogen does not contribute to the number of electrons.

At a temperature of 6600° the contribution of oxygen, whose ionization potential is almost the same as that of hydrogen, to the number of electrons is not great enough to alter the pressure of 7.4 dynes/cm².

If we use the value of N_1, 5.8×10^{22}, computed for silicon at an excitation temperature of 4400°, we obtain an electron pressure of about 50 dynes/cm². Evidence against the assumption of the 4400° excitation temperature of the metals has been discussed previously.

Had we assumed a temperature of 4400°, we should have found that an appreciable number of the metallic atoms were neutral and that the nonmetals would not have contributed so greatly to the number of electrons.

The degree of ionization for the sun may be similarly tested. The temperature computed for N_0 and N_1 of titanium and a value of 40 dynes/cm² for P_{e0} is 5000°. We use this temperature and a pressure of 40 dynes/cm² to compute the degree of ionization in the solar atmosphere. We find N_2 inappreciable for the metals; but the number of neutral metallic atoms is appreciable, compared with the singly ionized atoms. For silicon and sulphur, N_1 must be taken into account; but not for hydrogen, oxygen, or carbon. We find 31 dynes/cm² for P_{e0}, close to the value for which the degree of ionization was calculated.

For the sun we find that an electron pressure between 30 and 40 dynes/cm² is substantiated by calculation of the degree of ionization to be expected at that pressure and a temperature of 5000°. For α Persei, at a temperature of 6600°, the limits of 4.7 and 7.4 dynes/cm² have been calculated for the electron pressure. We have seen, however, that, in the case of α Persei, the temperatures derived for different elements are not the same. As the temperatures assumed in the calculation of the above limits for P_{e0} may not hold for each atom and ion, the limits for P_{e0} are uncertain. The value of P_{e0} is especially sensitive to the temperature assumed for the most abundant element, hydrogen. The problem of hydrogen evidently requires further study.

We have mentioned that equations (13) and (17) require the assumption of an isothermal atmosphere at a mean temperature, T. Indeed, this is also true of equation (1). In forming a curve of growth from data for many lines, we have also assumed that N_a is independent of wave length. The conception of "the number of atoms above the photosphere" and, indeed, Menzel's theory of a curve of growth are based on the Schuster model. In this model an atmosphere, transparent except in the lines, is superposed on a distinct radiating surface, the photosphere. In a real star, however, the layers that produce line absorption probably also contribute to the continuous absorption. It would be interesting to attempt to determine the physical conditions in the atmosphere of α Persei for another model. Nevertheless, in any investigation of the conditions in a supergiant atmosphere we are limited by uncertainty in the effective gravity and by the probable existence of appreciable departures from thermodynamic equilibrium, such as this work on α Persei has shown.

I wish to express my appreciation to Lieutenant Commander Donald H. Menzel for his stimulating advice and constant encouragement during this investigation. For the use of the McDonald spectrograms and the Yerkes microphotometer, I wish to thank Dr. O. Struve. I am grateful to Dr. J. L. Greenstein, Dr. S. Chandrasekhar, and Dr. L. H. Aller for helpful consultations. I am indebted to Dr. T. Dunham for the use of his unpublished identifications. Also, I wish to thank Drs. L. Goldberg, K. O. Wright, and W. Petrie for useful information. The latter part of this work was carried out during my tenure as a National Research Fellow.

THE INTERACTION OF A PROTON AND A HELIUM ATOM IN ITS EXCITED STATES. II

MARGARET KIESS KROGDAHL
Columbia, South Carolina
Received March 22, 1945

ABSTRACT

In this paper the calculations of the interaction energy between a proton and an excited helium atom are extended to higher quantum numbers and to some of the singlet levels. As before, the behavior of the interactions for the order of nuclear separations to be expected in early-type stellar atmospheres is studied. The results are used in a more detailed discussion of the shifts of several of the helium lines, special attention being given to the shift predicted on this theory for the forbidden 2p−4f line, λ 4470.

1. *Introduction.*—As was pointed out in an earlier paper,[1] the conditions under which the Stark effect of the helium lines appears in stellar spectra are not necessarily comparable with those under which it is produced in the laboratory. In stellar spectra the Stark effect arises from the influence of near-by charged particles, that is, protons; and the electric fields caused by protons are nonhomogeneous, in contrast to the laboratory fields, which are homogeneous. Accordingly, the problem of calculating the energy of interaction between a proton and an excited helium atom was considered. It was shown that, in accordance with the estimated densities of early-type stellar atmospheres, the nuclear separations which must be considered in such calculations are of the order of 10^3–10^4 atomic units. An application of the results to the prediction of the shifts for some of the triplet lines showed that at such distances the nonhomogeneity of the perturbing field cannot be ignored in comparison to the other terms. In particular, for the forbidden 2p−4f line, λ 4470, it was found that the violet shift predicted on the basis of laboratory data is to some extent compensated at these large distances by a red shift due to the nonhomogeneity term in R^{-3}.

However, in the paper referred to, the necessary calculations and discussions of the line shifts were carried out only for the case $m = 0$; and it is clear that to complete the discussion we should also consider the other values of m. Moreover, the calculations can easily be extended to include some of the levels corresponding to $n = 5$; by doing so we shall be in a position to discuss additional lines of astrophysical interest. Accordingly, in the present paper we shall complete the calculation of the interaction energies through $n = 5$, and for all relevant values of m. Finally, it will be shown how the present discussion may be adapted to the discussion of some of the more interesting singlet lines.

2. *General solution for the fourth-order terms.*—Before proceeding with the explicit calculations of the interaction energies, it is advantageous to obtain a general expression for the coefficient of the R^{-4} term in the perturbation of any level. The first, or R^{-3}, term is, of course, always given by the quantities in Table 1 of paper I. The fourth-order terms can be obtained in a general manner by a procedure analogous to that employed in the case $n = 4$, $m = 0$.

Let us denote, as before, the matrix elements of V, which contain P_1, P_2, and P_3, by ξ, η, and ζ, respectively. Then, for the set of $r = n - |m|$ values of l, which belong to a given n and m, the secular determinant will be of the form

[1] *Ap. J.*, **100**, 333, 1944. This paper will be referred to as "paper I."

$$\begin{vmatrix} \epsilon_1+\frac{\eta_{11}}{R^3}-\lambda & \frac{\xi_{12}}{R^2}+\frac{\zeta_{12}}{R^4} & \frac{\eta_{13}}{R^3} & \frac{\zeta_{14}}{R^4} & 0\ldots. & 0 \\ \frac{\xi_{21}}{R^2}+\frac{\zeta_{21}}{R^4} & \epsilon_2+\frac{\eta_{22}}{R^3}-\lambda & \frac{\xi_{23}}{R^2}-\frac{\zeta_{23}}{R^4} & \frac{\eta_{24}}{R^3} & \frac{\zeta_{25}}{R^4}\ldots. & 0 \\ \frac{\eta_{31}}{R^3} & \frac{\xi_{32}}{R^2}+\frac{\zeta_{32}}{R^4} & \epsilon_3+\frac{\eta_{33}}{R^3}-\lambda & \frac{\xi_{34}}{R^2}-\frac{\zeta_{34}}{R^4} & \frac{\eta_{35}}{R^4}\ldots. & 0 \\ \frac{\zeta_{41}}{R^4} & \frac{\eta_{42}}{R^3} & \frac{\xi_{34}}{R^2}+\frac{\zeta_{34}}{R^4} & \epsilon_4+\frac{\eta_{44}}{R^3}-\lambda & \frac{\xi_{45}}{R^2}+\frac{\zeta_{45}}{R^4}\ldots. & 0 \\ 0 & \frac{\zeta_{52}}{R^4} & \frac{\eta_{35}}{R^3} & \frac{\xi_{45}}{R^2}+\frac{\zeta_{45}}{R^4} & \epsilon_5+\frac{\eta_{55}}{R^3}-\lambda\ldots & 0 \\ \cdot & \cdot & \cdot & \cdot & \cdot & \cdot \\ 0 & 0 & 0 & 0 & 0\ldots.\epsilon_r+\frac{\eta_{rr}}{R^3}-\lambda & \end{vmatrix} = 0, \quad (1)$$

in which the existence of the zero elements is due to the orthogonality of the Legendre polynomials and the fact that we are considering only the terms up to R^{-4}. For the present purposes this determinant can be further simplified in consequence of the following considerations. Now it is clear that, in expanding the determinant correct to the fourth order in $1/R$, the element ζ_{41}/R^4 cannot be multiplied by any term other than a constant. However, when we consider the minor of ζ_{41}/R^4, it is seen that this quantity is always multiplied by higher powers of $1/R$. Hence this element has no effect on our expansion, and we may replace it by zero. In like manner it will be seen that it is not necessary to include any terms of higher order than R^{-2}, except when they occur on the principal diagonal. Hence the secular equation, correct to R^{-4}, reduces to

$$\begin{vmatrix} \epsilon_1+\frac{\eta_{11}}{R^3}-\lambda & \frac{\xi_{12}}{R^2} & 0 & 0 & 0\ldots. & 0 \\ \frac{\xi_{12}}{R^2} & \epsilon_2+\frac{\eta_{22}}{R^3}-\lambda & \frac{\xi_{23}}{R^2} & 0 & 0\ldots. & 0 \\ 0 & \frac{\xi_{23}}{R^2} & \epsilon_3+\frac{\eta_{33}}{R^3}-\lambda & \frac{\xi_{34}}{R^2} & 0\ldots. & 0 \\ 0 & 0 & \frac{\xi_{34}}{R^2} & \epsilon_4+\frac{\eta_{44}}{R^3}-\lambda & \frac{\xi_{45}}{R^2}\ldots. & 0 \\ 0 & 0 & 0 & \frac{\xi_{45}}{R^2} & \epsilon_5+\frac{\eta_{55}}{R^3}-\lambda\ldots. & 0 \\ \cdot & \cdot & \cdot & \cdot & \cdot & \cdot \\ 0 & 0 & 0 & 0 & 0\ldots.\epsilon_r+\frac{\eta_{rr}}{R^3}-\lambda & \end{vmatrix} = 0. \quad (2)$$

Making the substitution

$$q_i = \epsilon_i + \frac{\eta_{ii}}{R^3} \quad (3)$$

and expanding, correct to R^{-4}, we obtain

$$\Pi(q_i-\lambda)-\frac{1}{R^4}\sum_{k=1}^{r-1}\xi^2_{k,\,k+1}\prod_{j\neq k,\,k+1}(\epsilon_j-\lambda)=0 \tag{4}$$

or

$$\Pi(\lambda-q_i)=\frac{1}{R^4}\sum_{k=1}^{r-1}\xi^2_{k,\,k+1}\prod_{j\neq k,\,k+1}(\lambda-\epsilon_j)\,. \tag{5}$$

Thus far the treatment has been "exact." Now, let

$$\lambda_i=q_i+\Delta q_i\,, \tag{6}$$

where Δq_i is a small quantity, of fourth order in $1/R$, to be determined. Then equation (5) becomes

$$\Delta q_i\prod_{j\neq i}(q_i-q_j)\simeq\Delta q_i\prod_{j\neq i}(\epsilon_i-\epsilon_j)=\frac{1}{R^4}\sum_k\xi^2_{k,\,k+1}\prod_{j\neq k,\,k+1}(\epsilon_i-\epsilon_j)\,. \tag{7}$$

Now, unless $i=k$ or $k+1$, one of the quantities $(\epsilon_i-\epsilon_j)$ on the right-hand side vanishes. Hence the sum on the right-hand side always consists of just two terms, those for which $k=i$ and $k=i-1$. Thus,

$$\Delta q_i\prod_{j\neq i}(\epsilon_i-\epsilon_j)=\frac{1}{R^4}\left[\xi^2_{i,\,i-1}\prod_{j\neq i,\,i-1}(\epsilon_i-\epsilon_j)+\xi^2_{i,\,i+1}\prod_{j\neq i,\,i+1}(\epsilon_i-\epsilon_j)\right], \tag{8}$$

or

$$\Delta q_i=\frac{1}{R^4}\left[\frac{\xi^2_{i,\,i-1}}{\epsilon_i-\epsilon_{i-1}}+\frac{\xi^2_{i,\,i+1}}{\epsilon_i-\epsilon_{i+1}}\right]. \tag{9}$$

From equations (6) and (9) we now obtain

$$\lambda_i=\epsilon_i+\frac{\eta_{ii}}{R^3}+\frac{1}{R^4}\left[\frac{\xi^2_{i,\,i-1}}{\epsilon_i-\epsilon_{i-1}}+\frac{\xi^2_{i,\,i+1}}{\epsilon_i-\epsilon_{i+1}}\right]. \tag{10}$$

This formula shows clearly just how the higher-order term in the perturbation of any level depends on the separation of that level from its neighbors; for, since the separation factor occurs in the denominator of the coefficient, the fourth-order term becomes important only when the separation of the levels is quite small. Also it appears in all cases that the energy differences are of much greater importance in determining the perturbations than are the various sets of matrix elements, which are all of the same order of magnitude. Finally, it will be noticed that this is a generalization of the results obtained for the case $n=4$, $m=0$.

Having the general expression for the fourth-order term, we are now in a position to write down the solutions for the remaining energy perturbations. For each of them we shall estimate the relative importance of the R^{-3} and R^{-4} terms in the region of astrophysical interest simply by comparing their coefficients.

3. *The case* n = 3.[2]—To complete the discussion for the ortho-levels belonging to $n=3$, it remains to find the set of perturbations applying when $m=1$. Thus we have to consider the p and d states only, for which the corresponding hydrogen functions are u_{311} and u_{321}. The necessary matrix elements are found to have the values

$$\eta_{22}=+36\,;\qquad \eta_{33}=-18\,;\qquad \xi^2_{23}=+20.25\,. \tag{11}$$

[2] As was noted in paper I, the perturbations for the levels (2,1,1), (3,2,2), etc., are given only by the nonhomogeneity term in R^{-3}. Hence the discussion for $n=2$ is already complete.

The energy difference between the levels is, of course, the same as that found previously for the p and d levels, namely,

$$\epsilon_2 = -0.0024471 . \tag{12}$$

Hence, according to equation (10), the energy changes of the p and d levels are given, respectively, by

$$\Delta E_2 = +\frac{36}{R^3} + \frac{1}{R^4}\frac{20.25}{\epsilon_2} \tag{13}$$

and

$$\Delta E_3 = -\frac{18}{R^3} - \frac{1}{R^4}\frac{20.25}{\epsilon_2} . \tag{14}$$

Now the coefficient of the R^{-4} term is found to have the numerical value -8275. Thus we find that for the d level the R^{-3} and R^{-4} terms are of equal importance for $R = 460$ atomic units. Consequently, in the region of astrophysical significance, namely, $R \simeq 10^3 - 10^4$ atomic units, the R^{-4} terms are negligible.

4. *The case* n = 4.—For this case it remains to discuss the perturbations for $m = 1$ and $m = 2$. When $m = 1$, the secular equation involves the p, d, and f states, for which the η and ξ matrix elements are

$$\left.\begin{aligned} &\eta_{22} = +120 ; \quad \eta_{44} = -72 ; \quad \xi^2_{23} = +86.4 ; \\ &\eta_{33} = -72 ; \quad\quad\quad\quad \xi^2_{34} = +57.6 ; \end{aligned}\right\} \tag{15}$$

and the ϵ's are, as before,

$$\epsilon_2 = -0.0010725 ; \quad \epsilon_3 = -0.0000362 ; \quad \epsilon_4 = 0 . \tag{16}$$

The respective energy perturbations are, therefore,

$$\Delta E_2 = +\frac{120}{R^3} + \frac{1}{R^4}\frac{86.4}{\epsilon_2} = +\frac{120}{R^3} - \frac{83374}{R^4} \text{ (p level)}, \tag{17}$$

$$\Delta E_3 = -\frac{72}{R^3} - \frac{1507786}{R^4} \text{ (d level)}, \tag{18}$$

$$\Delta E_4 = -\frac{72}{R^3} + \frac{1591160}{R^4} \text{ (f level)}. \tag{19}$$

Accordingly, we find that for the f level, for example, the R^{-3} and R^{-4} terms again have opposite signs and are equal for $R = 22{,}100$ atomic units—a result which was to have been expected, since the ϵ's are the same. Hence in this case the R^{-4} term is again not negligible for the values of R with which we shall be concerned.

The energy changes for $m = 2$ are found in the same way. They are given in Table 1.

5. *The case* n = 5.—Corresponding to $n = 5$, there are, in general, 5 sublevels, namely, s, p, d, f, and g. The known[3] energy differences between them can be written

$$\left.\begin{aligned} &\epsilon_1 = -0.0026188 ; \quad \epsilon_3 = -0.0000206 ; \\ &\epsilon_2 = -0.0005511 ; \quad \epsilon_4 = 0 . \end{aligned}\right\} \tag{20}$$

On the basis of the previous calculations, it may be expected that the R^{-4} term will be the dominant one for most of these levels, depending, as it does, on the smallness of the

[3] The energy of the 1s5g level is not given by Bacher and Goudsmit. Accordingly, it is convenient to refer the ϵ's to the f level and let $\epsilon_4 = 0$. This choice, of course, does not affect the final result.

energy differences. Indeed, after calculating the necessary matrix elements and making use of equation (10), we find (for $m = 0$)

$$\Delta E_1 = -\frac{217633}{R^4} \quad \text{(s level)}, \tag{21}$$

$$\Delta E_2 = -\frac{600}{R^3} - \frac{376146}{R^4} \quad \text{(p level)}, \tag{22}$$

$$\Delta E_3 = -\frac{385.7}{R^3} - \frac{10640618}{R^4} \quad \text{(d level)}. \tag{23}$$

Thus, for the d level, the R^{-3} and R^{-4} terms are of equal importance at $R = 27{,}500$ atomic units, which means that the R^{-4} term is undoubtedly the more important one in the range of astrophysical interest.

It is apparent that in the absence of a good value for ϵ_5, equation (10) does not permit us to say much concerning the perturbations of the f and g levels, except that the R^{-3} term is almost certain to be negligible in comparison to the others. It is not impossible that we might even have to consider terms of higher order than the fourth.

The results for the remaining values of m are included in Table 1.

6. *The singlet levels.*—Finally, it remains to show how the entire foregoing discussion, with a few minor changes, applies to the para-levels. It will be recalled that we chose to write as the unperturbed wave function for an excited state of helium the expression

$$\Psi = \frac{1}{\sqrt{2}} [u_1(1)\, u_{n,\,l,\,m}(2) \pm u_1(2)\, u_{n,\,l,\,m}(1)], \tag{24}$$

where the u's denote the normalized hydrogen wave functions and the + and − signs distinguish the para- and ortho-levels, respectively. Thus in calculating the various matrix elements for the singlet case, the only difference is the change in sign just referred to. But the simplification of the matrix elements illustrated in equations (7) and (8) of paper I is independent of the choice of sign. Thus the matrix elements entering into the discussion for any level will be identical with those used for the triplet case.

However, as is well known, the energies of the singlet levels differ somewhat from those of the triplet levels; and the difference between the external perturbations simply represents a difference in the corresponding values of ϵ. Thus, for the sets of singlet levels corresponding to $n = 2$ and $n = 4$ the ϵ's are, respectively,

$$\epsilon_1 = -0.0221357 \tag{25}$$

and

$$\epsilon_1 = -0.0023366\,; \quad \epsilon_2 = +0.0001810\,; \quad \epsilon_3 = -0.0000298\,. \tag{26}$$

For the case $n = 2$ it is simple to verify the fact that, as before, the R^{-3} terms are dominant for the values of R with which we are concerned. This being the case, the perturbations of these levels are effectively the same as those of the ortho-levels.

This is not true, however, for the case $n = 4$. Making use of equation (10), we find (for $m = 0$)

$$\Delta E_1 = -\frac{71496}{R^4} \quad \text{(s level)}, \tag{27}$$

$$\Delta E_2 = -\frac{240}{R^3} + \frac{617986}{R^4} \quad \text{(p level)}, \tag{28}$$

$$\Delta E_3 = -\frac{144}{R^3} - \frac{2720987}{R^4} \quad \text{(d level)}, \tag{29}$$

$$\Delta E_4 = -\frac{96}{R^3} + \frac{2174497}{R^4} \quad \text{(f level)}. \tag{30}$$

Thus it will be noticed that the perturbations for the s, d, and f levels are qualitatively the same as in the triplet case, the coefficients of the R^{-4} terms being somewhat increased according to the decrease in the ϵ's. For the p level the situation is somewhat different, owing, first, to the positive sign of ϵ_2 and, second, to the fact that the magnitude of ϵ_2 is much smaller than in the triplet case. Consequently, not only is the sign of the fourth-order term changed, but its magnitude is about ten times greater than that for the triplet level.

The discussion for the remaining values of m follows along similar lines.

7. *Discussion of the results.*—Table 1 is a collection of all the interactions which have been calculated, giving those terms of the series which are of importance in astrophysical

TABLE 1

		Triplet Levels			Singlet Levels		
		$\lvert m \rvert$					
n..	l	0	1	2	0	1	2
2..	s	0	.....	.....	0	.....	.....
	p	$-\frac{12}{R^3}$	$+\frac{6}{R^3}$	.....	$-\frac{12}{R^3}$	$+\frac{6}{R^3}$	.....
3..	s	$-\frac{4{,}136}{R^4}$	.....	.....	.....	.....	.....
	p	$-\frac{72}{R^3}$	$+\frac{36}{R^3}$	.....	.....	.....	.....
	d	$-\frac{36}{R^3}$	$-\frac{18}{R^3}$	$+\frac{36}{R^3}$	.....	.....	.....
4..	s	$-\frac{42{,}982}{R^4}$	.....	.....	$-\frac{71{,}496}{R^4}$	.....	.....
	p	$-\frac{240}{R^3}-\frac{68{,}183}{R^4}$	$+\frac{120}{R^3}-\frac{83{,}374}{R^4}$	.....	$-\frac{240}{R^3}+\frac{617{,}986}{R^4}$	$+\frac{120}{R^3}+\frac{409{,}867}{R^4}$	.....
	d	$-\frac{144}{R^3}-\frac{1{,}678{,}891}{R^4}$	$-\frac{72}{R^3}-\frac{1{,}507{,}786}{R^4}$	$+\frac{144}{R^3}-\frac{994{,}475}{R^4}$	$-\frac{144}{R^3}-\frac{2{,}720{,}987}{R^4}$	$-\frac{72}{R^3}-\frac{2{,}342{,}753}{R^4}$	$+\frac{144}{R^3}-\frac{1{,}208{,}054}{R^4}$
	f	$-\frac{96}{R^3}+\frac{1{,}790{,}055}{R^4}$	$-\frac{72}{R^3}+\frac{1{,}591{,}160}{R^4}$	$+\frac{994{,}475}{R^4}$	$-\frac{96}{R^3}+\frac{2{,}174{,}497}{R^4}$	$-\frac{72}{R^3}+\frac{1{,}932{,}886}{R^4}$	$+\frac{1{,}208{,}054}{R^4}$
5..	s	$-\frac{217{,}633}{R^4}$	.....	.....	.....	.....	.....
	p	$-\frac{600}{R^3}-\frac{376{,}146}{R^4}$	$+\frac{300}{R^3}-\frac{445{,}335}{R^4}$	.....	.....	.....	.....
	d	$-\frac{385.7}{R^3}-\frac{10{,}640{,}618}{R^4}$	$-\frac{192.9}{R^3}-\frac{9{,}540{,}795}{R^4}$	$+\frac{385.7}{R^3}-\frac{6{,}241{,}331}{R^4}$			
	f						
	g						

problems. This set of quantities permits us to find the shifts of several new lines, in addition to completing the discussion of the ones considered in paper I.

Table 2 contains the calculated line shifts, in atomic units of energy, as a function of the nuclear separation R. The shifts for the various components of the lines are listed separately, the column headed m, m' giving the values of m for the initial and final states, respectively. As before, positive shifts are to the violet, and negative ones are to the red. For the sake of completeness, all the shifts listed in Table 2 of the earlier paper are again given here.

Even a brief inspection of Table 2 serves to confirm the principal conclusion of the earlier paper, namely, that the R^{-3} term is certainly not negligible in the range of R which must be considered. In addition, as before, certain of the lines merit special attention.

Two lines for which the presence of the R^{-3} terms has a pronounced effect in the region of astrophysical interest are λ 4713 and λ 4121, arising from the 2p—4s and 2p—5s tran-

TABLE 2

λ	Notation	m, m'	Shift	Remarks
5876.....	2p−3d	0, 0	$-\frac{24}{R^3}$	All shifts due to nonhomogeneity of field
		1, 0	$-\frac{42}{R^3}$	
		0, 1	$-\frac{6}{R^3}$	
		1, 1	$-\frac{24}{R^3}$	
		1, 2	$+\frac{30}{R^3}$	
4922.....	2P−4D	0, 0	$-\frac{132}{R^3}\left(1+\frac{20,614}{R}\right)$	Nonhomogeneity of field adds to shifts toward red
		1, 0	$-\frac{150}{R^3}\left(1+\frac{18,140}{R}\right)$	
		0, 1	$-\frac{60}{R^3}\left(1+\frac{39,046}{R}\right)$	
		1, 1	$-\frac{78}{R^3}\left(1+\frac{30,035}{R}\right)$	
		1, 2	$+\frac{138}{R^3}\left(1-\frac{8,754}{R}\right)$	
4921.....	2P−4F	0, 0	$-\frac{84}{R^3}\left(1-\frac{25,887}{R}\right)$	Resultant shift is toward red if $R>25,000$; to violet if $R<25,000$
		1, 0	$-\frac{102}{R^3}\left(1-\frac{21,319}{R}\right)$	
		0, 1	$-\frac{60}{R^3}\left(1-\frac{32,215}{R}\right)$	
		1, 1	$-\frac{78}{R^3}\left(1-\frac{24,781}{R}\right)$	
		1, 2	$-\frac{6}{R^3}\left(1-\frac{201,342}{R}\right)$	
4911.....	2P−4P	0, 0	$-\frac{228}{R^3}\left(1-\frac{2,710}{R}\right)$	Nonhomogeneity of field adds significantly to shifts
		1, 0	$-\frac{246}{R^3}\left(1-\frac{2,512}{R}\right)$	
		0, 1	$+\frac{132}{R^3}\left(1+\frac{3,105}{R}\right)$	
		1, 1	$+\frac{114}{R^3}\left(1+\frac{3,595}{R}\right)$	
4713.....	2p−4s	0, 0	$+\frac{12}{R^3}\left(1-\frac{3,582}{R}\right)$	Both components shift to red if $R<3582$; as R increases the nonhomogeneity terms become important
		1, 0	$-\frac{6}{R^3}\left(1+\frac{7,164}{R}\right)$	

TABLE 2—*Continued*

λ	Notation	m, m'	Shift	Remarks
4518.....	2p−4p	0, 0	$-\frac{228}{R^3}\left(1+\frac{299}{R}\right)$	Shifts predominantly due to nonhomogeneity of field
		1, 0	$-\frac{246}{R^3}\left(1+\frac{277}{R}\right)$	
		0, 1	$+\frac{132}{R^3}\left(1-\frac{632}{R}\right)$	
		1, 1	$+\frac{114}{R^3}\left(1-\frac{731}{R}\right)$	
4472.....	2p−4d	0, 0	$-\frac{132}{R^3}\left(1+\frac{12,720}{R}\right)$	Nonhomogeneity of field adds significantly to all shifts
		1, 0	$-\frac{150}{R^3}\left(1+\frac{11,193}{R}\right)$	
		0, 1	$-\frac{60}{R^3}\left(1+\frac{25,130}{R}\right)$	
		1, 1	$-\frac{78}{R^3}\left(1+\frac{19,330}{R}\right)$	
		1, 2	$+\frac{138}{R^3}\left(1-\frac{7,206}{R}\right)$	
4470.....	2p−4f	0, 0	$-\frac{84}{R^3}\left(1-\frac{21,310}{R}\right)$	Resultant shift is toward red if $R>20,000$; to violet if $R<20,000$
		1, 0	$-\frac{102}{R^3}\left(1-\frac{17,550}{R}\right)$	
		0, 1	$-\frac{60}{R^3}\left(1-\frac{26,519}{R}\right)$	
		1, 1	$-\frac{78}{R^3}\left(1-\frac{20,399}{R}\right)$	
		1, 2	$-\frac{6}{R^3}\left(1-\frac{165,746}{R}\right)$	
4121.....	2p−5s	0, 0	$+\frac{12}{R^3}\left(1-\frac{18,136}{R}\right)$	Both components shift to red for $R<18,136$; for large R the nonhomogeneity is important
		1, 0	$-\frac{6}{R^3}\left(1+\frac{36,272}{R}\right)$	
4026.....	2p−5d	0, 0	$-\frac{373.7}{R^3}\left(1+\frac{28,474}{R}\right)$	Shift toward the red principally due to R^{-4} terms
		1, 0	$-\frac{391.7}{R^3}\left(1+\frac{27,165}{R}\right)$	
		0, 1	$-\frac{180.9}{R^3}\left(1+\frac{52,741}{R}\right)$	
		1, 1	$-\frac{198.9}{R^3}\left(1+\frac{47,968}{R}\right)$	
		1, 2	$+\frac{379.7}{R^3}\left(1-\frac{16,438}{R}\right)$	

sitions, respectively. Each has three components, due to the transitions $m = 0 \rightarrow m = 0$ and $m = \pm 1 \rightarrow m = 0$; and the behavior of these components is qualitatively the same for both lines. In the case of the 2p−4s line, it is evident that if R is smaller than 3582 atomic units, both shifts of Table 2 are negative, owing to the dominance of the R^{-4} terms. As R increases, however, the R^{-3} terms gradually become more important, causing the shift for the $m = 0 \rightarrow m = 0$ component to change sign. Finally, if R is larger than 7164 atomic units, both the shifts are dominated by the R^{-3} terms, which are of opposite sign. The same remarks apply to the 2p−5s line, except that for this case the critical values of R are much larger.

Another line having an interesting behavior for the values of R which we are considering is the 2P−4P line, λ 4911. This is a result of the rather large perturbation of the 4P singlet level (see § 6). If R is relatively small, that is, less than 2512 atomic units, the shifts of all the components are governed by the R^{-4} terms, which are all positive. With an increase in R, two of the shifts change sign because of the greater importance of the R^{-3} terms; and if R exceeds 3595 atomic units, the R^{-3} terms are the dominant ones for all the components.

Probably the most interesting, however, are the forbidden lines λ 4470 and λ 4921, arising from the 2p−4f and 2P−4F transitions, respectively. These lines, which are of zero intensity in the absence of a perturbing field, appear in stellar spectra at almost exactly the zero-field position, although, according to laboratory data, they should be displaced to the violet. Now, as was brought out earlier (see § 6 or cf. Table 2) the shifts of these lines differ only slightly, and hence their behavior may be expected to be quite similar. Let us first consider in detail the triplet line.

It was found in the earlier paper that for the $m = 0 \rightarrow m = 0$ and $m = \pm 1 \rightarrow m = 0$ components of this line the R^{-3} terms are negative and therefore tend to compensate the violet shifts given by the R^{-4} terms. In particular, the exact amounts of this compensation by per cent, for the $m = 0 \rightarrow m = 0$ transition, were found to be those given in Table 3 of that paper. Finally, it was seen that, in order to produce a resultant shift of *exactly* zero, the effective value of R would have to be 21,310 atomic units for the $m = 0 \rightarrow m = 0$ component, or 17,550 atomic units for the $m = \pm 1 \rightarrow m = 0$ component. While both of these values of R seem rather high, still it was found that to account for an exactly zero displacement from this point of view alone might not require too great a reduction in the estimated density.

We now have, in Table 2, the shifts for the remaining components of the line. From a brief inspection of these it appears that, on the average, the shifts are to the violet for values of R less than about 20,000 atomic units and toward the red when R is greater, confirming the remarks of the earlier paper. The shift of the $m = 1 \rightarrow m = 2$ component is, however, an exception and is always to the violet for the values of R which must be considered.

It proves instructive, however, to supplement such qualitative considerations with a discussion of more definite estimates of the line shifts. Table 3 contains, for several values of R,[4] the magnitudes of the shifts of the five components of λ 4470, measured in units of 10^{-12} times the atomic unit of energy.[5] The most striking feature of the table is the rapid decrease of the ΔE's with increasing R. This is due in part, of course, to the increasing effect of the R^{-3} terms, which ultimately brings about the change of sign; but a far more noticeable effect is simply that of the decrease of the terms according to at least an R^{-3} law. Because of this, the red shifts for large values of R can never become very large and must possess a maximum for some value of R. We find, for example, that the maximum

[4] We are here simply assigning to R a set of values, leaving until later the question of whether they refer to the mean distance between protons or an "effective" R.

[5] One atomic unit of energy equals 4.307×10^{-11} ergs, or 2.1944×10^{5} cm.$^{-1}$.

red shift of the 1,0 component occurs at $R = 23{,}400$ atomic units and has the value -1.99×10^{-12} atomic units.

The situation is further clarified if we recall that, for the wave length we are considering, 4470×10^{-8} cm., a difference in wave length of 1 A is equivalent to $22{,}810{,}000 \times 10^{-12}$ atomic units of energy. On comparing this with the quantities of Table 3 we find that the red shifts predicted by this theory cannot at all be measured and that the violet shifts are most probably not measurable for values of R much greater than 2000 atomic units. For $R = 1000$ atomic units, the violet shifts are about 0.075 A, while at 900 atomic units they amount to roughly 0.11 A. And under these circumstances the fact that the shift of the 1,2 component is always to the violet is seen to be unimportant.

TABLE 3

m, m'	R					
	900	1,000	2,000	5,000	10,000	22,000
0, 0.....	+2,610,500	+1,706,040	+101,377	+2,192	+95.00	−0.24
1, 0.....	2,590,000	1,688,100	99,131	2,048	77.01	−1.92
0, 1.....	2,425,380	1,531,140	91,950	2,066	99.11	+1.15
1, 1.....	2,425,690	1,513,122	89,700	1,922	81.11	−0.53
1, 2.....	+1,501,900	+ 988,476	+ 61,405	+1,543	+93.45	+3.68

Hence, if we take literally the estimate of $R = 1600$ atomic units for the case of τ Scorpii, we find that the theory predicts a violet shift of only 0.011 A. In addition, since it is possible that the effective value of R to be used in these calculations is somewhat greater than the average distance between protons, it appears that the present theory, taken together with the present estimates of density, can account for the lack of displacement of the 2p−4f line.

It is immediately clear that an exactly similar situation exists in the case of the 2P−4F line. The R^{-3} terms are the same as those for λ 4470, and the only difference in the R^{-4} terms is that their coefficients are a little larger for the reason explained above. Without going into great detail, we find that for $R = 1600$ the shift of the 0,0 component is $311{,}342 \times 10^{-12}$ atomic units, or, at this wave length, 0.017 A. Finally, if the effective R to be used is appreciably larger, the resultant shift of the line is even less.

I am indebted to Dr. S. Chandrasekhar for suggesting this problem and for his constant and friendly encouragement.

SPECTROGRAPHIC OBSERVATIONS OF THIRTEEN ECLIPSING VARIABLES*

OTTO STRUVE
McDonald and Yerkes Observatories
Received May 14, 1945

ABSTRACT

The first part of this paper contains a review of the astrophysical problems encountered in the study of spectroscopic binaries and, more particularly, of eclipsing variables. The second part is a study of the spectroscopic features and radial velocities of 13 eclipsing binaries, based upon measurements of more than 500 spectrograms.

RW Persei.—P = 13.2 days. The H absorption lines outside eclipse are variable in intensity and suggest strong Doppler broadening. During eclipse strong double emission lines of H and weaker ones of *Fe* II and *Ca* II undergo eclipses, as in SX Cassiopeiae. Orbital elements: $\gamma = +6.5$ km/sec; $K_1 = 18.5$ km/sec; $e = 0$. Strong rotational disturbance in partial eclipse shown by H absorption lines.

EY Orionis.—P = 16.8 days. Orbital elements: $\gamma = +28$ km/sec; $K_1 = 55$ km/sec; $e = 0.10$; $\omega = 243°$; T = phase 0.39 P after mid-eclipse

SV Geminorum.—P = 4.01 days. Orbital elements: $\gamma = +24$ km/sec; $K_1 = 44.5$ km/sec; $e = 0.16$; $\omega = 266°$; T = phase 0.56 P after mid-eclipse

RU Monocerotis.—P = 3.58 days. The spectrum shows only broad H lines, probably blended, and interstellar *Ca* II. The spectrum is anomalous because of absence of stellar *Ca* II and *Mg* II. The blended H lines give the elements: $\gamma = +39$ km/sec; $K_{bl} = 44$ km/sec; $e = 0.28$; $\omega = 42°$; T = phase 0.94 P after mid-eclipse. Measures of the widths of the H lines indicate order of magnitude $K_1 = K_2 = 128$ km/sec.

AO Monocerotis.—P = 1.88 days. The spectrum shows double lines of types B3 and B5. Orbital elements: $\gamma = +15$ km/sec; $K_1 = 185$ km/sec; $K_2 = 195$ km/sec; $e = 0$; T (min. vel. of B3 comp.) = phase 0.75 P.

SW Canis Majoris.—P = 10.09 days. The orbit is very eccentric, and there are two components in the spectrum. At the conjunctions the blended lines look stronger than the sums of the components observed at the elongations. Orbital elements: $\gamma = +40$ km/sec; $K_1 = K_2 = 90$ km/sec; $e = 0.50$; $\omega = 180°$; T = phase 0.84 P.

UZ Puppis.—P = 0.79 days. Two components of type A5 or A7 are present in the spectrum. There is a suspicion that the type is somewhat later at the two conjunctions than at the elongations and that the intensities of the blended lines are greater than the sums of the two components when the latter are observed at the elongations. Orbital elements: $\gamma = +25$ km/sec; $K_1 = K_2 = 150$ km/sec; $e = 0$; T (max. vel.) = phase 0.75 P.

VZ Hydrae.—P = 2.90 days. Two spectra of type F5 are present. Orbital elements: $\gamma = +1$ km/sec; $K_1 = 93$ km/sec; $K_2 = 105$ km/sec; $e = 0$; T (min. vel. of br. comp.) = phase 0.25 P.

RU Cancri.—P = 10.17 days. The spectrum has bright lines of *Ca* II which belong to that component which is in front at principal eclipse. Orbital elements: $\gamma = +12$ km/sec; $K_1 = 34$ km/sec; $e = 0$; T (min. vel. of br. comp.) = phase 0.25 P.

Y Leonis.—P = 1.69 days. Orbital elements: $\gamma = +10$ km/sec; $K_1 = 60$ km/sec; $e = 0$; T (min. vel.) = phase 0.25 P.

RW Ursae Majoris.—P = 7.3 days. The spectrum shows bright lines of *Ca* II which belong to that component which is in front at principal eclipse. Orbital elements: $\gamma = -17.5$ km/sec; $K_1 = 72.5$ km/sec; $K_{Ca\,II} = 72$ km/sec; $e = 0$; T (min. vel. of br. comp.) = phase 0.25 P.

SS Bootis.—P = 7.6 days. The spectrum shows strong bright lines of *Ca* II which belong to that component which is in front at principal eclipse. The absorption lines are probably seriously blended; they are fairly well resolved near phase 0.25 P when the brighter component gives a negative velocity, but are almost unresolvable near phase 0.75 P. The orbital elements are based upon the velocity-curve from the emission lines of *Ca* II, and the semiamplitudes K_1 and K_2 have been estimated for the two components: $\gamma = -43$ km/sec; $K_{Ca\,II} = 77$ km/sec; $K_1 = 47$ km/sec; $K_2 = 73$ km/sec; $e = 0$; T (max. vel. of *Ca* II em.) = phase 0.25 P.

AW Pegasi.—P = 10.6 days. The spectrum is F0, peculiar, at mid-eclipse and A2 outside of eclipse. The lines of *Fe* I, *Ti* II, *Ca* I, and *Sr* II give a velocity-curve consistent with the motion of the F0 component: $\gamma = 0$ km/sec; $K_2 = 50$ km/sec; $e = 0$, T (max. vel. of F0 comp.) = phase 0.25 P. The lines of *Fe* II show an unsymmetrical velocity curve with $K_{Fe\,II} = 25$ km/sec and show a minimum at phase 0.45 P and a maximum at phase 0.9 P. The lines of H show no systematic change in velocity with phase. Blending may affect some of these results but probably not all.

* *Contributions from the McDonald Observatory, University of Texas*, No. 110.

INTRODUCTION

The fourth catalogue of spectroscopic binaries by J. H. Moore[1] contained 365 orbits of stars regarded as true binaries. Fifty-five of these were known as eclipsing variables. In the nine years which have elapsed since the publication of Moore's catalogue, several additional orbits of eclipsing variables have been published, so that the number now available from observatories other than McDonald is between 60 and 70. The total number of eclipsing variables listed in Schneller's catalogue for 1941[2] exceeds 1100. The percentage of these stars for which spectrographic orbits have been determined is, therefore, about 6. The spectrographic material, valuable as it has been, is not sufficient for detailed statistical and individual studies of the mechanical properties of close binary systems. There is an even greater lack of information when we consider the astrophysical properties of these stars. Quite naturally, the stellar spectroscopists were primarily interested in deriving accurate velocity-curves. With the exception of a few spectacular systems, like β Lyrae, the spectra as such aroused slight interest; and the great majority of the original papers listed by Moore contain little more than the briefest descriptions of the principal features of the spectra upon which the measurements were based. Twenty years ago stellar spectroscopists were mystified by the existence of a few very unusual spectroscopic binaries among a large number of systems apparently having normal spectra. There was only *one* β Lyr, with its variable emission lines and its normal B9 and abnormal B5 sets of absorption lines; only *one* ϵ Aurigae, with its long period of twenty-seven years and its unsymmetrically broadened lines during eclipse; and only *one* W Ursae Majoris, with a period of a few hours. The unusual binaries were not only rare; they were apparently quite unrelated to one another. The past years have increased the variety of unusual spectroscopic phenomena found in close binaries of all kinds and have led to the discovery of additional systems showing peculiarities previously known in only one or two stars. Thus, we now know from the spectrographic work of Popper and the photometric observations of S. Gaposchkin that RY Scuti shares some of its features with β Lyr. We know that ζ Aurigae and VV Cephei are in many respects similar to ϵ Aur. There has also been some progress in finding the correct physical explanation of these phenomena and in linking together problems which at first had seemed to be unrelated. For example, we attribute the peculiar B5 spectrum of β Lyr to an extended atmosphere or shell, and we make use of the dilution effect to connect this problem with that of the peculiar relative intensities of *He* I triplets and singlets in the spectrum of ϕ Persei. Perhaps even more important is our growing realization that the abnormal spectroscopic features of β Lyr, VV Cep, ϕ Per, etc., must be regarded as extreme examples of phenomena which in a less conspicuous manner exist in many systems previously regarded as normal.

There are, however, several important astrophysical questions which cannot be answered without additional material. What are these new questions? It is, of course, not possible to segregate them entirely from questions of a dynamical nature. Although we shall be able to answer only a few of them, I shall discuss those problems and results which are serving me as a guide in the preparation of my observing programs.

ASTROPHYSICAL QUESTIONS ENCOUNTERED IN THE STUDY OF SPECTROSCOPIC BINARIES

I. PROBLEMS CONNECTED WITH THE AXIAL ROTATION OF BINARY COMPONENTS

a) Observations of numerous systems have shown that in all stars heretofore investigated the direction of rotation is the same as the direction of orbital revolution. Is this *always* the case? If it is, the result must have an important cosmological significance.

b) A few years ago it was considered probable that in all close systems the periods of

[1] *Lick Obs. Bull.*, No. 483, 1936. [2] *Kl. Veröff. Berlin-Babelsberg*, No. 22, 1940.

rotation and revolution are the same. In systems of fairly long period, excessive rotational velocities are frequent. There is one striking case (U Cephei) in which the rotational velocity of one component is much greater than is required by the condition of synchronism, although the orbital period is only 2.49 days.[3] What is the significance of these excessive rotational velocities in close systems?

c) In one system (RZ Scuti) the rotational disturbance determined from *He* I has a range of at least 250 km/sec, while that determined from *H* has a range of about 100 km/sec.[4] This suggests a stratified atmosphere with an extended and slowly rotating *H* shell. Are there other stars with a similar phenomenon?

d) The meager material now available on the spectra of close systems in which the secondary component is a relatively cool subgiant, while the primary is a normal A or B star, suggests that the rotational velocities of the cool components are small (U Cep).[3] But is this always true; and, if it is, has the phenomenon any relation to the well-known avoidance of single stars of the later spectral classes to show rapid rotations?[5]

e) It is probable that the largest rotational velocities on record occur in single stars and not in close binaries. Among different groups of stars the Be's undoubtedly have the largest rotations.[6] As a rule, they are not binaries. The explanation of this phenomenon lies probably in the fact that the majority of binary components are normal stars in size and spectrum. Thus, a B-type binary consisting of two equal components cannot have a period shorter than that which would correspond to $a = r_1 + r_2 = 2r_1$; and this places an upper limit upon the period of rotation of each component. More rapid rotational velocities can occur only in underluminous systems. We do not know enough of them to draw any conclusions from the observations.

II. PERIODIC CHANGES IN THE INTENSITIES OF THE ABSORPTION LINES OF BINARY COMPONENTS

a) One of the most puzzling questions is that of the reported strengthening of the lines of the approaching components. Originally discovered by Bailey[7] in μ^1 Scorpii, this effect was independently described by Miss Cannon[8, 9] and was found by Miss Maury in V Puppis[10] and ζ Centauri.[11] It was independently found by the writer in α Virginis[12] and later in σ Aquilae[13] and β Scorpii.[13] R. M. Petrie[14] made accurate measurements in several spectroscopic binaries and found a small effect of the character found by me, in σ Aql and 2 Lacertae. However, he did not consider the phenomenon as definitely established. On the other hand, fairly reliable measures of equivalent widths in μ^1 Scorpii by Struve and Elvey revealed no change.[15] Popper failed to find a change in V Pup[16] and ζ Cen.[17] My own observations in α Vir, σ Aql, and β Sco were so convincing that I cannot doubt the reality of the phenomenon. Nor is it reasonable to question the extensive Harvard results. Yet my own observations of μ^1 Sco were completely negative. The existence of the effect should be checked, and an attempt should be made to explain it. It is possible that the visual impression of a spectral line and the equivalent width, measured from a tracing, record different things. It is known that such differences exist. For ex-

[3] *Ap. J.*, **99**, 222, 1944. References to specific stars will usually be limited to the last paper in which a complete bibliography may be found.

[4] *Ap. J.*, **101**, 240, 1945.

[5] *Pop. Astr.*, **53**, 214, 1945.

[6] W. W. Morgan, *A.J.*, **51**, 21, 84, 1944.

[7] *Harvard Circ.*, No. 11, 1896.

[8] *Harvard Ann.*, Vol. **28**, Part II, remark 73, 1897.

[9] *Harvard Ann.*, **84**, 169, 1920.

[10] *Ibid.*, p. 178.

[11] *Harvard Circ.*, No. 233, 1922.

[12] *Ap. J.*, **80**, 369, 1934.

[13] *Ap. J.*, **85**, 41, 1937.

[14] Unpublished.

[15] *Pub. A.S.P.*, **54**, 151, 1942.

[16] *Ap. J.*, **97**, 402, 1943.

[17] *Ibid.*, p. 405.

PLATE III

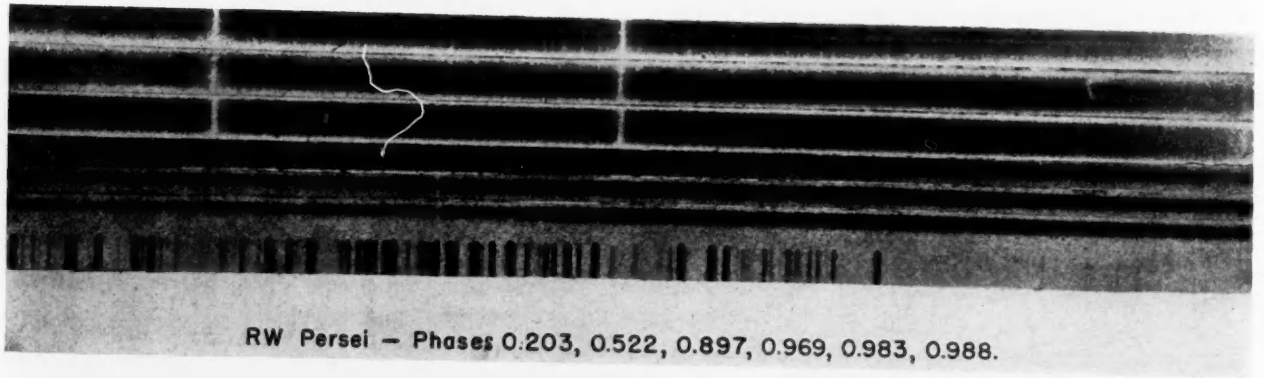

RW Persei — Phases 0.203, 0.522, 0.897, 0.969, 0.983, 0.988.

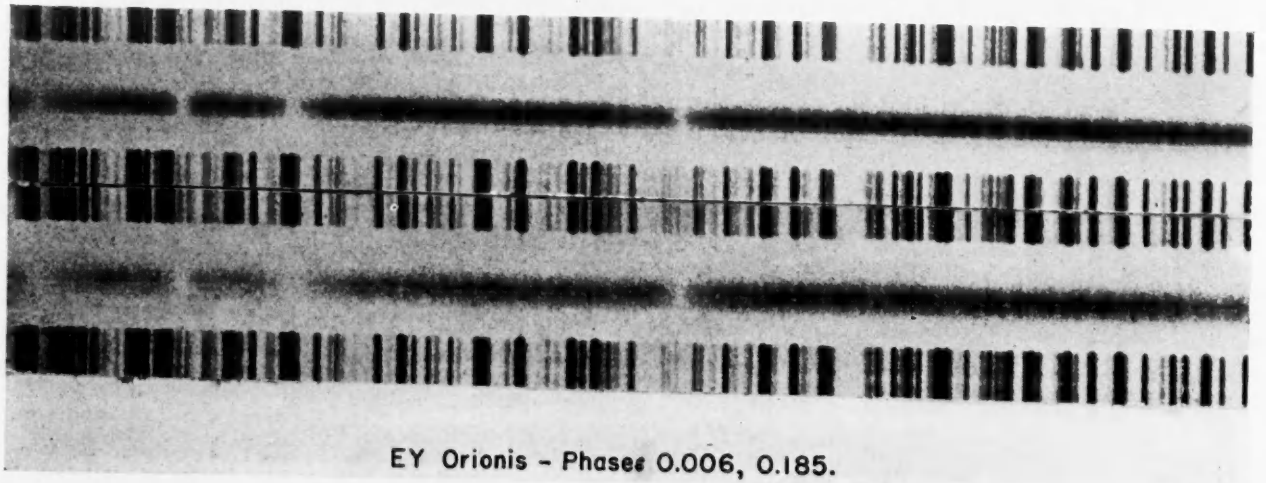

EY Orionis - Phases 0.006, 0.185.

PLATE IV

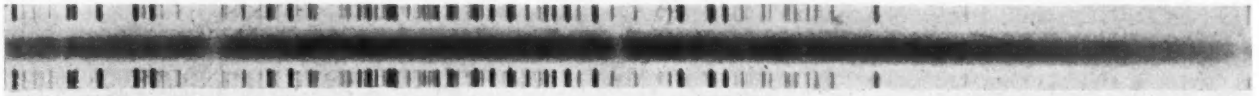

SV Geminorum – Phase 0.707.

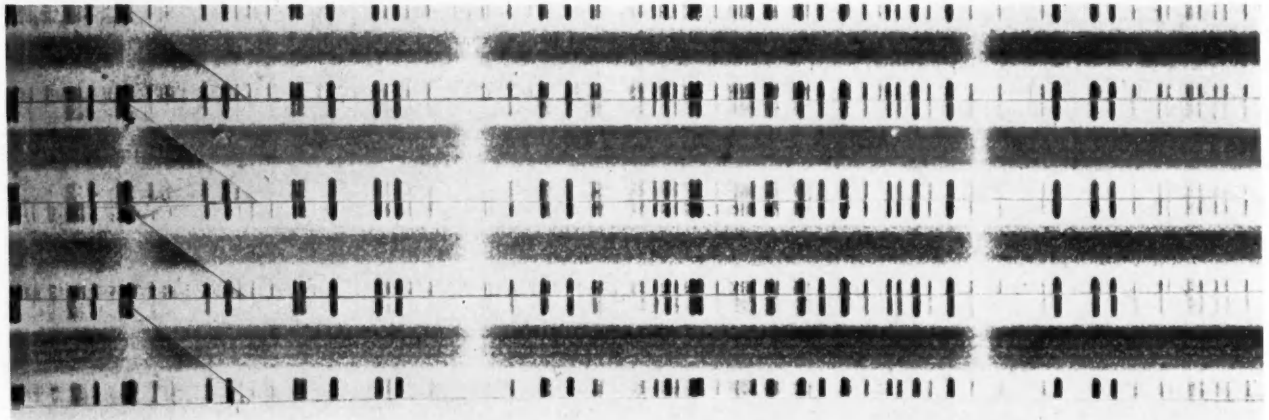

RU Monocerotis – Phases 0.345, 0.684, 0.844, 0.964.

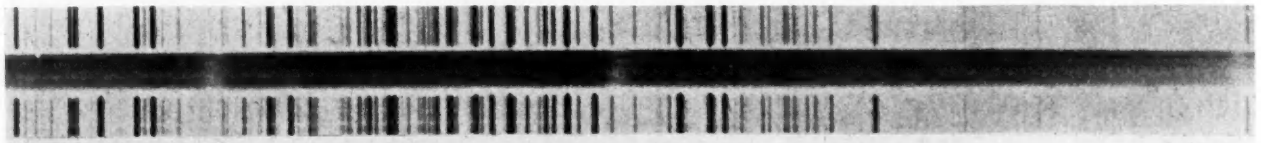

AO Monocerotis – Phase 0.230.

PLATE V

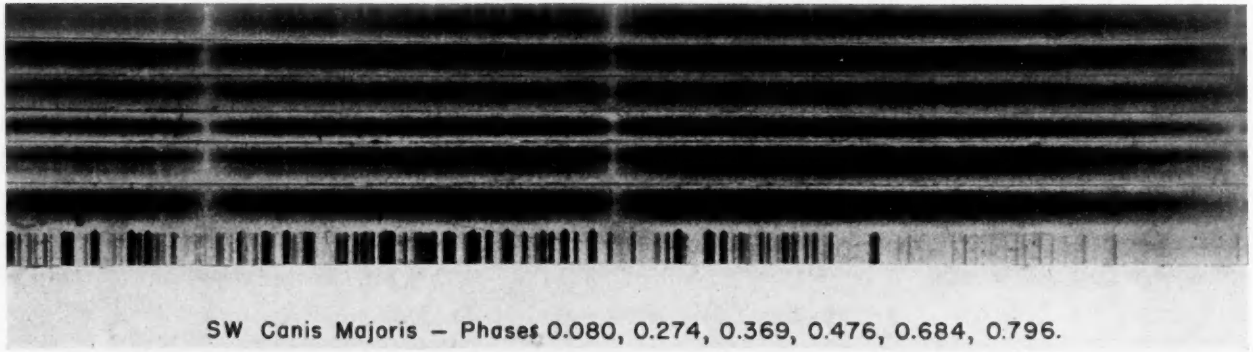

SW Canis Majoris — Phases 0.080, 0.274, 0.369, 0.476, 0.684, 0.796.

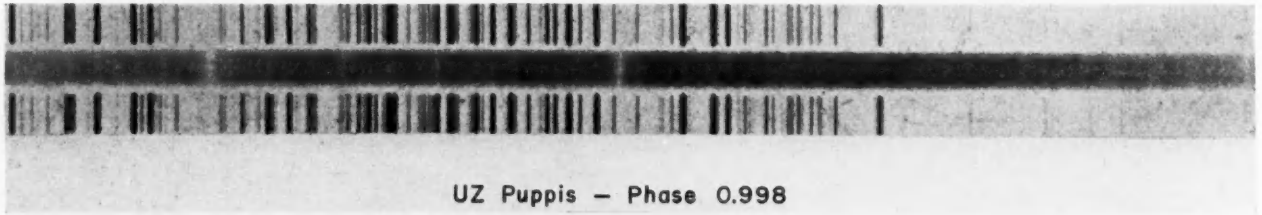

UZ Puppis — Phase 0.998

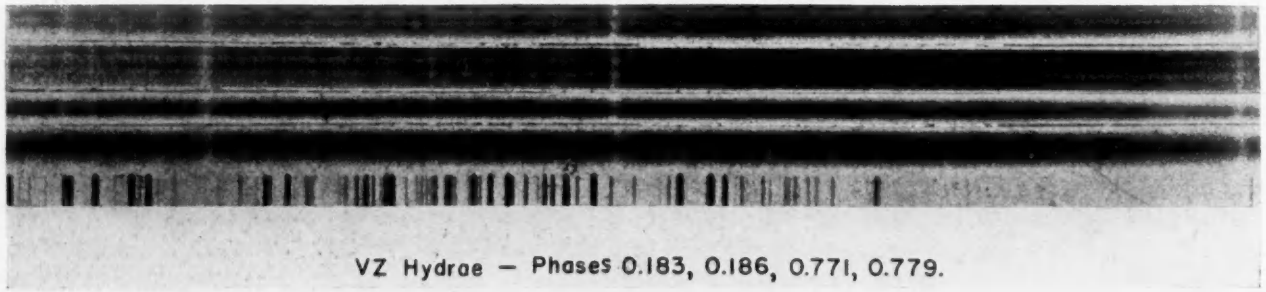

VZ Hydrae — Phases 0.183, 0.186, 0.771, 0.779.

PLATE VI

RU Cancri – Phase 0.590.

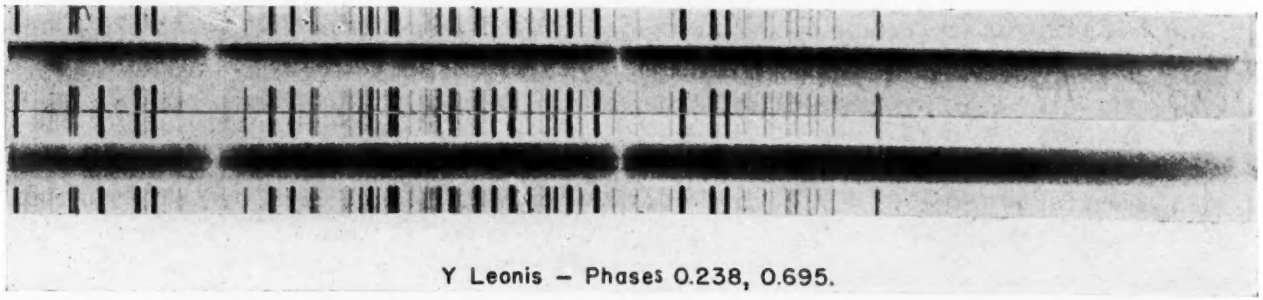

Y Leonis – Phases 0.238, 0.695.

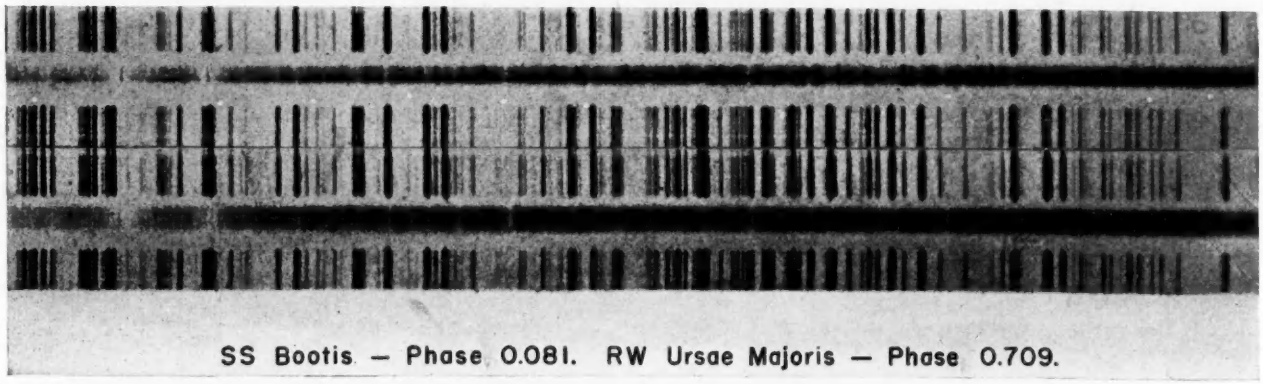

SS Bootis – Phase 0.081. RW Ursae Majoris – Phase 0.709.

PLATE VII

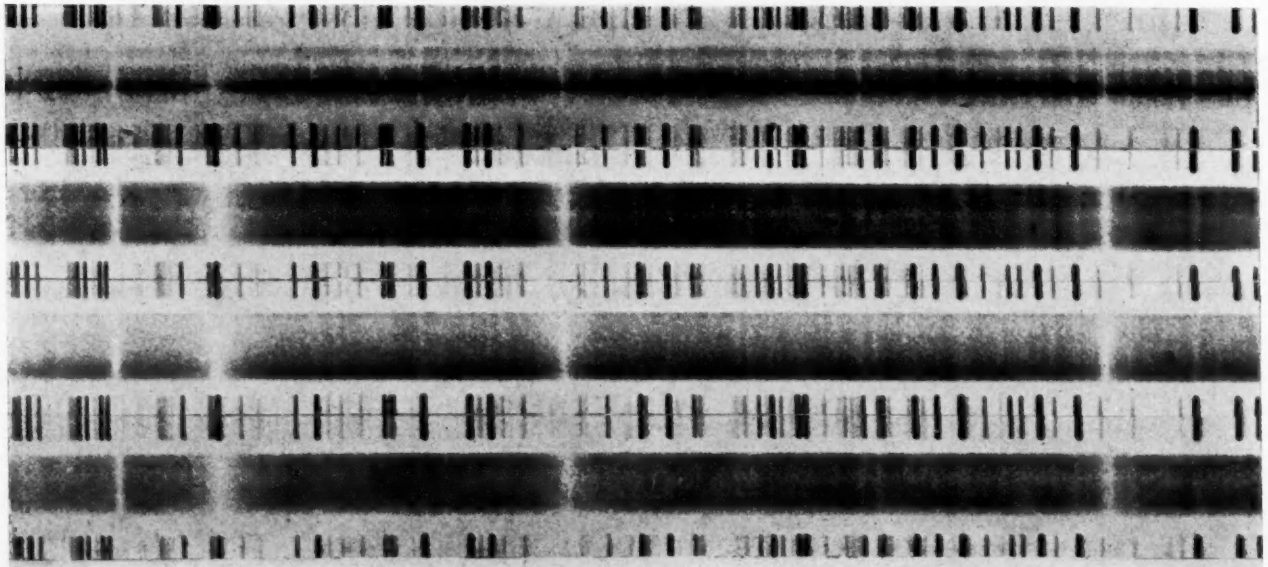

AW Pegasi — Phases 0.001, 0.246, 0.501, 0.739.

ample, a very broad and shallow line may be completely invisible with high dispersion and may have a considerable equivalent width. Such a line can sometimes be easily seen on spectrograms of small dispersion. It is very strange that there are so few cases of this kind of variation recorded in the literature. If we could assume that the observers were focusing their attention upon the relative intensities of the components, and not simply ignoring them, we should certainly have a strong argument against the reality of the phenomenon. But previous experience would hardly justify this assumption. In stars of advanced spectral class, blending causes some very remarkable inconsistencies in the relative intensities of the components, and lack of information is not surprising. A remarkable type of variation is discussed by Sahade and Cesco elsewhere in this issue of the *Journal*.[18] The suspicion was once expressed by Van Arnam[19] that in BD−18°3295 the faint component is observed more often when its velocity is near maximum, and not near minimum, as in α Vir, σ Aql, etc.

b) Some rather strange changes in line intensities, which are strictly periodic but which cannot be attributed to the blending of two component lines, have been found in several close systems (AU Monocerotis[20] and AB Persei[21]). The suspicion exists that absorption lines formed in extended gaseous currents far above the normal reversing layers of the stars give rise to the strengthening of certain lines (*H* in AU Mon) in certain phases (just before principal minimum in AU Mon). The nature of these currents is quite obscure, but they are probably related to the currents in the system of β Lyr, which produce enormous changes in the intensities of the B5 lines.[22] It is important that more stars be found in which this phenomenon can be studied. It is probable that these changes in line intensities are related to the distortions in the velocity-curves of several spectroscopic binaries, to be discussed later.

III. SPECTROSCOPIC PHENOMENA ATTRIBUTED TO THE REFLECTION EFFECT

a) The lines of the second component of α Vir not only vary in equivalent width, as described in Section II (*a*), but they are unusually narrow,[23] especially when observed on the red side. Additional spectrograms have led to the suspicion that these narrow lines are superposed unsymmetrically over very faint, diffuse lines whose rotational broadening may be comparable to that of the broad lines of the principal component.[24] It is theoretically possible that we are here concerned with the reflection effect of the primary on the secondary. There is, as yet, no other observational evidence to confirm this conclusion; nor is there an adequate theory of the formation of a line under the influence of the reflection effect. But it is probable that the influence of reflection upon the absorption lines of a binary component is much greater than upon the total light of the system.[25] The principal function of the diluted radiation of the brighter component is to ionize the outermost layers of the fainter component. This process will be regulated by the temperature of the primary and by the dilution factor. In a close system the latter may be of the order of $\beta = 0.1$ or 0.01. Consider the ionization of *He* in a system whose components have temperatures of $T_1 = 25{,}000°$ and $T_2 = 15{,}000°$ and whose atmospheres are, at their nearest point, $2r_1$ apart, where r_1 is the radius of the brighter component. Then $\beta \sim 0.06$. The ionization produced by the fainter component alone is

$$\log \frac{n_2}{n_1} = -24\,\frac{5{,}040}{15{,}000} + \tfrac{5}{2}\log 15{,}000 - 0.48 + \log \frac{2u_2}{u_1} - \log p_e .$$

[18] *Ap. J.*, **102**, 128, 1945.

[19] *Ap. J.*, **75**, 351, 1932.

[20] Sahade and Cesco, *Ap. J.*, **101**, 235, 1945.

[21] *Ibid.*, p. 232.

[22] *Ap. J.*, **93**, 107, 1941.

[23] *Ap. J.*, **72**, 15, 1930.

[24] *Ap. J.*, **86**, 198, 1937.

[25] Eddington, *Internal Constitution of the Stars*, p. 214, Cambridge, 1926.

The ionization produced by the primary alone, at the nearest point of the atmosphere of the secondary, is

$$\log \frac{n_2'}{n_1'} = -24\,\frac{5{,}040}{25{,}000} + \tfrac{5}{2}\log 25{,}000 - 0.48 + \log\frac{2u_2}{u_1} - \log p_e + \log 0.06\,.$$

The ratio of the two quantities is given by

$$\log \frac{n_2}{n_1} - \log \frac{n_2'}{n_1'} = -2.6\,.$$

The ionization produced by the primary is very much greater than that produced by the secondary. Since all of the continuous radiation of the secondary passes through this ionized region, the corresponding lines must be very strong.

b) There has been much discussion of what appears to be a sound observational result: in many double-lined spectroscopic binaries the types of the two components are more nearly alike than is consistent with the relative surface brightnesses of the stars derived from the two light-minima. This phenomenon has been commented upon by J. S. Plaskett,[26] by Eddington,[27] and, most recently, by S. Gaposchkin.[28] For example, in TV Cassiopeiae[26] the types were found by Plaskett to be A0 and A0, but the depths of the two eclipses are 1.05 and 0.09 mag. There are other striking discrepancies, and some of them were specifically commented upon by Plaskett. A. B. Wyse[29] found that, when the surface brightnesses inferred from the observed spectra at the two minima are compared with the results from the light-curve, satisfactory agreement is obtained for three-fourths of the stars; but "the exceptions are numerous and noteworthy" and cannot be accounted for by reflection, since at principal minimum the spectrum of the secondary is not affected by reflection. It is probably necessary to distinguish between observations made at principal minimum, as were those of Wyse, and observations of double lines at maximum light, as were those of Plaskett. Among the latter type of observations, striking discordances are present for TV Cas, already mentioned, and for RS Vulpeculae, Z Herculis, GO Cygni and U Coronae Borealis. The data pertaining to these stars are as shown in the accompanying table. The spectrographic data for all five stars are based

Star	Spectra	Δm_1	Δm_2	Reference
TV Cas	A0+A0	1.05	0.09	Plaskett, *Dom. Ap. Obs.*, **2**, 141, 1922
RS Vul	B8+B9	0.73	.08	Plaskett, *Dom. Ap. Obs.*, **1**, 141, 1919
Z Her	F2+F2	0.80	.12	Adams and Joy, *Ap. J.*, **49**, 192, 1919
GO Cyg	B9n+A0n	0.54	.23	Pearce, *J.R.A.S. Canada*, **27**, 62, 1933
U CrB	B3+B3	1.02	0.00	Plaskett, *Dom. Ap. Obs.*, **1**, 187, 1920
U CrB	B5+B9	1.02	0.00	Pearce, *Pub. A.A.S.*, **8**, 220, 1936

upon numerous measurements by experienced observers. Pearce comments upon the appreciable difference in spectrum of the two components of GO Cyg. This star is the least abnormal in the list. Plaskett remarks in connection with TV Cas: ". . . . it seems probable that the lines measured as due to the second spectrum, even though they are often only on the border line of visibility, are really present. . . . ." In the case of RS Vul he states: ". . . . the second spectrum . . . . can only be seen and measured with great

[26] *Pub. Dom. Ap. Obs. Victoria*, **1**, 141, 1919; **1**, 187, 1920; **2**, 141, 1922.

[27] *Internal Constitution of the Stars*, p. 214.

[28] *Variable Stars*, p. 36, Cambridge, 1938.

[29] *Lick Obs. Bull.*, No. 464, 1934.

difficulty, and it is estimated to be only one-fourth the intensity of the brighter spectrum. . . . . There can be no doubt of the reality of the second spectrum. . . . ." No doubt of any kind was recorded by Plaskett with regard to U CrB or by Adams and Joy with regard to Z Her.

Among the stars that Wyse observed at principal minimum, the greatest discrepancy occurs in RX Geminorum,[29] with types A2 and A3p and minima of 2.1 and 0.0 mag. Perhaps the peculiarity of the A3 spectrum with weak $H\beta$, sharp $H\gamma$, and strong and broad $H\delta$ and $H\epsilon$ may provide an explanation in terms of shell absorption—a phenomenon which I have observed in SX Cassiopeiae[30] and which probably accounts for the effect described under Section II (*b*).

It is important to observe these stars again in order to ascertain, if possible, whether the spectra of the 5 stars listed above show the same types at principal minimum as were observed for the fainter components at maximum light and whether the spectra are normal. This should permit us to distinguish between the reflection effect and shell absorption.

IV. CHANGES IN SPECTRUM DUE TO DIFFERENCES IN GRAVITY

a) There is no reliable information concerning possible differences in the spectral types of binary components dependent upon their phase angles. The reflection effect may cause differences in the spectra of the two hemispheres directed toward or away from the other component. Differences in gravity may cause the spectrum of the tidal bulges to differ from that of the preceding and following hemispheres. Observation is complicated by the overlapping of lines of two components at phase angles 0° and 180°.

b) It is conceivable that there may also be an appreciable periastron effect in close binaries of high eccentricity.

V. PROBLEMS OF EMISSION LINES

a) There seems to be a growing realization that the formation of emission lines is facilitated in binary systems. Wyse stated in 1934:[29] "The eclipsing binaries on the whole appear to have perfectly normal spectra. This applies to the faint companions as well as to the primaries. Exception is noted in an unexpected tendency of the secondaries to display bright *H* lines." Out of 25 secondaries observed by him, 5 had the characteristic of *H* emission. The types of these secondaries range from A to K. In single stars emission lines are very rare for these types. The number of binaries with *H* emission lines can be considerably augmented by the addition of SX Cas,[30] RX Cas,[31] etc., all of class A or later. There are a few bright-line binaries of types O and B—for example, HD 163181 = V 453 Sco,[32] 29 Canis Majoris = UW CMa,[33] and, of course, β Lyr and RY Sct. But the great majority of B-type binaries show no bright lines. Conversely, we may say that the great majority of Be stars are not binaries. The material indicates that the frequency distribution of bright *H* lines among binaries is entirely different from that observed in single stars.

Binaries of types G and K very often exhibit bright lines of *Ca* II, and the number of these cases is also considerably in excess of what might have been expected from the frequency of occurrence of these lines in single stars.

We know so little about the behavior of the bright lines in binaries that our first task should be the discovery of a greater number of systems having this peculiarity.

b) There is a marked difference in the structure and behavior of the emission lines on the one hand of *H* and of other lines associated with it—namely, *Fe* II, *Ca* II, and occasionally a few others—and on the other hand of *Ca* II when the latter appears alone in systems both components of which have types as late as G or K. In the former group

[30] *Ap. J.*, **99**, 89, 1944.

[31] *Ap. J.*, **99**, 295, 1944.

[32] *Ap. J.*, **99**, 210, 1944.

[33] *Ap. J*, **93**, 84, 1941; **82**, 95, 1935.

the lines are double and are divided by a deep absorption core. In the latter they are single (if observed with moderate dispersion), though sometimes slightly broadened. This difference is probably important, but we need more material to substantiate it.

c) The double components of the *H* emission lines and of other emission lines associated with them undergo eclipses in the stars RW Tauri,[34] SX Cas,[30] and RX Cas[31] but fail to show this effect in W Serpentis.[35] In the three systems with eclipses the emission lines originate in a ring or stream surrounding the early-type component of the binary irrespective of whether that component is the brighter (RW Tau and SX Cas) or the fainter (RX Cas). The direction of the stream motion is the same in all three systems and agrees with the rotation of the component and with the orbital revolution of system. In velocity the stream motion exceeds very greatly that determined from the absorption lines. In RW Tau the displacements of the bright lines are ± 350 km/sec, while the absorption lines are described by Joy as well defined and without any abnormal rotation effect. The periods range from 2.77 days for RW Tau to 36.6 days for SX Cas. The absence of eclipse in the bright lines of W Ser is related to the appearance in this spectrum of forbidden [*Fe* II], while only permitted *Fe* II is seen in SX Cas, RX Cas, and RW Tau. It is possible that the essential difference between W Ser and the other systems is one of size of the emitting nebulosity, but more material is required.

No eclipsing effects have been observed in the *Ca* II emission group. In one star, WW Draconis,[36] the velocity-curve of the *Ca* II emission lines agrees in phase with that of the fainter and less massive K0 component of this system, whose brighter component is of type G2. However, the range of the velocity-curve is smaller than that of the K0 star, and Joy inferred that "the secondary star is surrounded with an envelope of calcium gas which is greatly extended in the direction of the primary by tidal attraction." In AR Monocerotis,[37] where only one component of type K0 is observed, the emission lines follow the velocity-curve of that component with undiminished amplitude. But in both stars the emission lines follow the curve of that component which stands in front at principal eclipse. We need more material to confirm this feature and to explain it.

d) P Cygni type emission and absorption lines are present in several binaries, such as in β Lyr,[22] where the B5 absorption component shows a velocity of expansion; 29 CMa,[33] where such lines appear in certain phases, where there are large periodic changes in the structure and intensity of the emission lines, and where the emission lines exhibit a large "red shift"; and in the Wolf-Rayet spectroscopic binaries, where violet absorption borders are commonly present. The variety of changes in the emission lines is great; and we have, as yet, little material to go by.

e) The frequent occurrence of *Ca* II emission in close binaries is of interest in connection with the suggestion that these lines are also often bright in visual binaries.[38] But it is not quite certain whether this tendency is real.

f) Another phenomenon usually associated with wider pairs is the occurrence of intense [*Fe* II] with relatively weak permitted *Fe* II. Typical examples are Boss 1985 and WY Geminorum, both having composite spectra,[39] and the fainter, B-type component of α Scorpii.[40] It is probable that several other emission-line phenomena are connected with the binary nature of the stars. For example, the complex and variable emission lines of high ionization potential in Z Andromedae, AX Persei, CI Cygni,[41] and stars whose

[34] Joy, *Pub. A.S.P.*, **54**, 35, 1942.

[35] Bauer, *Ap. J.*, **101**, 208, 1945. It should be noted that the light-curve and the velocity-curve of this star are peculiar; and while I am inclined to agree with S. Gaposchkin and with C. A. Bauer that it is a double star, the evidence on this point is not conclusive.

[36] Joy, *Ap. J.*, **94**, 407, 1941.

[37] Sahade and Cesco, *Ap. J.*, **100**, 374, 1944.

[38] Swings and Struve, *Pub. A.S.P.*, **53**, 244, 1941.

[39] *Ap. J.*, **91**, 596, 1940; **93**, 455, 1941.

[40] *Ap. J.*, **92**, 316, 1940.

[41] Merrill, *Ap. J.*, **99**, 15, 1944.

absorption features contain *TiO*, and other low-temperature lines and bands, are best explained by assuming that the star is a binary, whose bright component is cool and whose hot component is so small that it must be regarded as underluminous. There is, however, no direct evidence of the duplicity of these stars (except in α Sco and Mira Ceti).

VI. DEFORMATIONS OF VELOCITY-CURVES

a) This problem has come into the foreground since it was shown, a year ago, that the unsymmetrical velocity-curve of U Cep,[3] first observed by Carpenter in 1930, agrees with the new spectrographic observations. The spectrographic values of e and ω are inconsistent with the photometric value of $e \cos \omega$ determined from the spacings of the minima in the light-curve. A similar asymmetry was found in the velocity-curve of SX Cas[30] and perhaps in that of RX Cas.[31] In SX Cas there is a strong suspicion that the asymmetry arises from absorption in the same stream of gas which gives rise to the disappearing emission components described under Section V (*b*). It is noteworthy that in AU Mon,[20] where the *H* lines show periodic changes in the absorption-line intensities (see Sec. II [*b*]), the velocities derived from these lines give a curve that is unsymmetrical in the same manner as in U Cep. In the latter star, Joy and the writer have found unsymmetrical line contours at and near maximum radial velocity. This is probably the same effect as that observed in AU Mon by Cesco and Sahade. There are some other stars in which discrepancies between photometric and spectrographic values of e have been recorded. One such case, TX Ursae Majoris, is probably not real, according to Hiltner,[42] who finds a small spectrographic value of e which is in good accord with the photometric results. But in u Herculis a new spectrographic investigation by Smith[43] confirms the old value $e = 0.05$ while the light-curve gives $e \leq 0.01$. Another case is MR Cygni, where Pearce[44] found $e = 0.12$, while Miss Swope[45] found, from the light-curve, $e \leq 0.01$. Kopal[46] has suggested that these discrepancies "may quite possibly be a common, rather than an exceptional, feature of close binary systems"; the present evidence favors an explanation in terms of superposed absorption produced in a gaseous stream, as in SX Cas.

b) There is a well-known tendency among spectroscopic binaries to have values of ω in the neighborhood of 90°. The latest information concerning this phenomenon is contained in a paper by S. V. Nekrasova.[47] Her data are reproduced in the accompanying table. The phenomenon is especially pronounced for stars with small eccentricities.

ω	Number of Systems		ω	Number of Systems	
	$e>0.10$	$e<0.10$		$e>0.10$	$e<0.10$
0°– 30°	21	17	180°–210°	11	15
30 – 60	24	19	210 –240	15	7
60 – 90	20	12	240 –270	8	6
90 –120	30	16	270 –300	21	5
120 –150	19	11	300 –330	15	7
150 –180	13	7	330 –360	22	15

Various attempts have been made to explain it. Struve and Pogo[48] suggested the possibility of a systematic tendency in the orientations of the lines of apsides, favoring an

[42] *Ap. J.*, **101**, 108, 1945.

[43] Unpublished.

[44] *J.R.A.S. Canada*, **29**, 413, 1935.

[45] *Harvard Bull.*, No. 914, 1940.

[46] *Ap. J.*, **99**, 239, 1944.

[47] *Bull. Engelhardt Obs. Kazan*, No. 13, p. 10, 1937.

[48] *A.N.*, **234**, 300, 1928.

angle of 90° with the direction toward the galactic center. But the discovery of physically distorted velocity-curves described in Section VI (*a*) indicates that at least a part of the observed frequency distribution may be caused by these distortions.

c) We may tentatively mention here a phenomenon which played an important role in stellar spectroscopy some twenty years ago. In 1908 and 1909 Schlesinger and Curtiss noticed that in Algol and δ Librae the times of spectroscopic conjunction precede mid-eclipse by about 73 minutes and 112 minutes, respectively.[49] These discrepancies were regarded as exceeding the possible errors of the photometric and spectroscopic elements. Later, J. S. Plaskett[50] added new material to the discussion and concluded that in several other eclipsing stars the departures are either negligible or of opposite sense. In 1925 Hellerich[51] summarized the data for 14 stars. He concluded that in most systems the departures are reduced if, in place of elliptical elements, circular elements are computed from the velocity-curves and if all radial velocities obtained during the principal eclipse are omitted. In almost all systems the remaining discrepancies are then within the limits of their probable errors. Martinoff[52] has recently pointed out that the Tikhoff-Nordmann effect undoubtedly contributes to the observed discrepancies. This effect is attributed by Mustel[53] to gravity darkening at the tidal bulge, which is assumed to lag behind, as was suggested by Dugan in the case of U Cep.

VII. SHELL ABSORPTION IN ECLIPSING BINARIES

a) Several eclipsing variables show conspicuous dilution effects in their absorption spectra. The weakness of *Mg* II 4481 in the spectrum of ϵ Aur during principal eclipse[54] and the great strength of the ultimate lines of *Ti* II in VV Cep[55] are good examples. The dilution effect probably explains the weakness of *Mg* II 4481 in SX Cas,[30] and this suggests that the entire observed A-type spectrum may come from the streams rather than from the normal reversing layer of the early-type components. Dilution is prominent in the B5 spectrum of β Lyr.[22]

b) The question arises whether shell absorption may not in some cases vitiate the spectra of the fainter components observed at principal minimum. In SX Cas,[30] whose minima are $A_1 = 0.99$ mag. and $A_2 = 0.32$ mag., the spectrum at principal eclipse is G6, in agreement with prediction. But this G6 spectrum is certainly not normal, because some absorption lines continue to follow the velocity-curve of the A-type component, while those which are strengthened at mid-eclipse show the trend of the G star. I concluded, a year ago, that "the observed spectrum is a blend of a true star of a fairly late spectrum—probably G—and lines of another origin which resemble in character the shell lines of the A star and share with it the descent of the velocity-curve." Yet, the photometric evidence of a total eclipse is complete. In RX Cas[31] the behavior of the *H* absorption lines was even more revealing: they gave no perceptible change in velocity with phase. The K-type component predominates in this star at all phases, but the *H* absorption cores are clearly of shell origin. These cores, incidentally, show remarkable changes in RX Cas, as well as in SX Cas. It is exceedingly tempting to attribute to shell absorption such glaring discrepancies between spectroscopic and photometric classes as that found by Wyse[29] for RX Gem (see Sec. III [*b*]).

c) The importance of the dilution effect in estimating the size of the nebulous shells or streams in binary systems was illustrated in the case of β Lyr.[22] We require informa-

[49] *Pub. Allegheny Obs.*, **1**, 25, 1908; **1**, 129, 1909.

[50] *Pub. Dom. Ap. Obs. Victoria*, **3**, 248, 1926.

[51] *A.N.* **216**, 277, 1922; **223**, 367, 1925.

[52] *Variable Stars*, p. 62, Moscow, 1939.

[53] *Astr. J. Soviet Union*, **11**, 415, 1934.

[54] *Proc. Amer. Phil. Soc.*, **81**, 212, 1939.

[55] *Ap. J.*, **99**, 70, 1944.

tion concerning the behavior of those few lines which are sensitive to dilution: the singlets of *He* I in B stars, the lines of *Mg* II and *Si* II in A stars, and a few selected lines of *Fe* I (λ 4260, etc.)[56] in later-type systems.

VIII. THE ζ AURIGAE EFFECT

a) The line absorption caused by the extended atmosphere of an eclipsing star in the continuous spectrum of the partly eclipsed star has enabled us to study the structure of the atmosphere of the K-type component of ζ Aur.[57] Similar phenomena have been observed in VV Cep[58] and ε Aurigae.[59] All three are peculiar supergiant systems of relatively long period (twenty-seven years in the case of ε Aur). It is exceedingly important to search for other, similar cases. There is a strong indication that the phenomenon may occur even in ordinary systems of short period. In TX UMa,[42] which has a period of 3.06 days, Hiltner found a sharp *Ca* II line before and after mid-eclipse, superposed over a broad line of the F2 eclipsing star. This sharp line is stronger than the normal *Ca* II line of the B8 star, which is the one eclipsed at principal minimum. Hiltner considers it probable that the sharp line in the partial phases is caused by a ζ Aur effect.

b) Distinct satellite lines were found during the partial phases of principal eclipse in β Lyr.[22] These lines appear a short time before mid-eclipse and show large positive velocities; they disappear at mid-eclipse but reappear a few hours later, with large negative velocities. But the contours and the relative intensities of the violet and red satellites are not the same. It has been suggested that they originate in a stream of gas which passes from the B9 component, swings around the following side of the F5 component, and returns along the preceding side of the F5 component. Two related phenomena were observed in U Cep.[3] During the partial phases of eclipse the *H* absorption lines look as though they consist of a sharp line unsymmetrically superposed over a normal, rotationally broadened line. There are also observed distinct satellite lines of *Ca* II, whose velocities do not agree with either of the two components. These phenomena have been tentatively attributed to absorption in a gaseous stream similar to that observed in β Lyr, SX Cas, and RX Cas; but the information at present available is still insufficient. The unsymmetrical superposition of a narrow *H* line upon a broader line results in an apparent reduction of the range of the rotational disturbance, as measured in *H*, if compared to that measured in *He* I, *Ca* II, *Mg* II, and *Si* II. This phenomenon closely resembles that observed in RZ Sct (see Sec. I [*c*]) and attributed there to stratification in an extended atmosphere, because there was no suspicion of superposition. It is impossible to decide whether we have the same phenomenon, produced by one cause; and, if we do, whether we have stratification with diminishing rotational velocities at the greater heights or stream motion which is independent of the atmosphere of either component star. Perhaps there is less distinction between the two pictures than appears at first sight.

IX. LIMB SPECTRA

Redman[60] made the first attempt to measure the equivalent widths of several absorption lines in U Cep and U Sagittae during the partial phases of the eclipse. Both stars have deep total eclipses, and the secondary components are faint and belong to a different spectral class than the primaries. The Balmer lines behave as though they vanish at the limb of U Cep and become distinctly fainter at the limb of U Sge. Redman remarked that this could be due either to the effect of true absorption in the formation of the lines

[56] *Proc. Amer. Phil. Soc.*, **81**, 227, 1939.

[57] Wellmann, *Veröff. Berlin-Babelsberg*, Vol. **12**, No. 4, 1939.

[58] Goedicke, *Pub. U. Michigan Obs.*, Vol. **8**, No. 1, 1939.

[59] Frost, Struve, and Elvey, *Pub. Yerkes Obs.*, Vol. **7**, Part 2, 1932.

[60] *M.N.*, **96**, 488, 1936.

or to the reduction in Stark effect at the higher levels of the reversing layers. Some confirmatory evidence came from my own observations of U Cep.[3] In addition, I found that the lines of *He* I were also weaker at the limb, while *Ca* II and *Si* II did not change appreciably. My conclusion was that in all probability "the lines appear weaker at the limb because the pressures are lower and not because the mechanism of line formation is predominantly one of pure absorption." In RZ Sct[4] the lines of *H*, *He* I, and *Mg* II became much weaker at the limb; and in the case of *H* this is accompanied by a tendency for the lines to become sharper and narrower. The weakening of *Mg* II (which was also suspected in U Cep) may mean that this line is actually formed by the process of pure absorption. Because of the many complicated phenomena occurring during the eclipses, the observations and their interpretation are difficult.

X. SPECTROSCOPIC ASYMMETRY DURING ECLIPSE

Attention has already been drawn to the difference in appearance of the satellite lines in β Lyr before and after mid-eclipse—only a few hours apart. Completely unexplained differences were also noticed in U Cep before and after totality. Thus, "in the first half of the eclipse the lines of *He* I are systematically weaker than in the second half. . . . . There appears to be a real difference in the intensities of lines produced by the receding and approaching limbs of the B8 star, the former having the weaker lines. . . . ." It is possible that this is related to the asymmetry of the light-curve. It may well be that both these phenomena are caused by the streams discussed previously, or to some sort of tidal lag in a rapidly rotating star, as was suggested by Dugan.[61]

XI. UNUSUAL SPECTRA OF BINARY COMPONENTS

a) If the semiamplitudes of the velocity-curves of spectroscopic binaries of a single spectral class are plotted as ordinates against log P as abscissae, the stars fall within an area limited by the x-axis at the bottom, by a curve whose shape is given by[62]

$$K_1 = CP^{-1/3}$$

at the top, and by a vertical straight line at the left. For the B-type stars this straight line occurs approximately at

$$P = 1.3 \text{ days} .$$

The reason for this limitation on the diagram is that in a given spectral class most systems have approximately the same values of

$$r_1 + r_2 = \text{constant} ,$$

$$m_1 + m_2 = \text{constant} ,$$

$$m_2/m_1 = \text{constant} ,$$

$$e = \text{constant} ,$$

so that only the inclination produces a large scatter in the values of K. Stars which fall outside the occupied area are abnormal in some respect. The sharp limitation of the area by the straight line on the left must be caused by the average value of $r_1 + r_2$. Components cannot come closer to one another unless $r_1 + r_2$ is abnormally small. It is important to discover systems which fall outside the occupied area in order to find whether the spectra of these stars are also abnormal. Among the B's the two systems lying above the limiting curve $K_1 = CP^{-1/3}$, namely, β Lyr and BD+6°1309, are both abnormal in spectrum. The question arises whether there are stars which lie to the left of the line $P = 1.3$ days for the B's or $P = 1.0$ day for the A's. Several eclipsing variables are

[61] *Contr. Princeton U. Obs.*, No. 5, 1920.

[62] *M.N.*, **86**, 63, 1925.

known which fall to the left of these lines—for example, S Antliae,[63] with $P = 0.64$ day and two spectra of classes A8 and A8, and UX Ursae Majoris,[64] with $P = 0.197$ day and a spectrum of class A. The masses of these stars are small, compared to those of normal A stars; and the systems behave as typical W UMa stars. It is clear that all A and B stars with $P < 1$ day deserve attention. Such stars must be small, and their spectra should be interesting. Thus, the spectrum of UX UMa suggests underluminous components.

b) Another procedure for picking out abnormally small stars is to select those systems which combine a large value of e with a small value of P. Among such systems RU Monocerotis should be especially interesting, since it has $P = 3.58$ days and $e = 0.38$. The latter value was determined by Krat from the light-curve and was confirmed by Shapley.

c) The results described in Section XI (*a*) have been confirmed by D. J. Martinoff,[65] who plotted the periods of eclipsing variables against their spectral types. The diagram shows that the points are scattered over a wide area, whose edge is sharply limited by a curve running from about $P = 5$ days, Sp. = O5, through $P = 1$ day, Sp. = B0; $P = 0.5$ day, Sp. = A0; $P = 0.3$ day, Sp. = F0; $P = 0.25$ day, Sp. = G0. This curve corresponds to the vertical lines in the diagrams described under Section XI (*a*). If we write Kepler's third law in the form

$$\frac{a^3}{P^2(m_1+m_2)} = 74.5\,,$$

where m_1 and m_2 are in units of $\odot$ and P is in days, and if we assume for contact that $a = r_1 + r_2 = 2r_1$, then the minimum value of P is given by

$$\frac{r_1^3}{P_{\min}^2(m_1+m_2)} = 9.3\,.$$

Martinoff uses typical values for r_1 and $(m_1 + m_2)$ and finds by computation:

Sp.	P_{min}
O8.5	2.56 days
B5	0.80
A0	0.54
F0	0.33
G0	0.30

These values agree sufficiently well with the observed data and with the evidence from spectroscopic binaries. The conclusion arrived at again is that only stars which have abnormally small values of $r_1 + r_2$ can lie beyond the limits of the curve; and these stars, like UX UMa, are very rare. An interesting point in Martinoff's work is the pronounced tendency of eclipsing variables showing ellipticity variation (β Lyr and W UMa types) to crowd near the limiting curve, while ordinary Algol-type stars are located farther from the curve.

XII. RELATIVE INTENSITIES OF DOUBLE LINES IN SPECTROSCOPIC BINARIES

A considerable amount of work has been done by R. M. Petrie[66] on the measurement of equivalent widths of double lines. From these measurements information may be ob-

[63] Joy, *Ap. J.*, **64**, 287, 1926.

[64] Zverev and Kukarkin, *Ver. St. Nishni-Novgorod*, **5**, 125, 1937. A spectrogram taken by me with small dispersion shows only broad H absorption lines. Dr. G. P. Kuiper has informed me that he has obtained additional spectrograms of this variable in order to determine the range in velocity.

[65] *Astr. J. Soviet Union*, **14**, 306, 1937.

[66] *Pub. Dom. Ap. Obs., Victoria*, Vol. **7**, No. 12, 1939; *Pub. A.A.S.*, **10**, 333, 1944.

tained concerning the relative brightnesses of the component stars and their spectral types. It is important to determine whether the data thus determined are in accord with the mass ratio derived from the velocity-curves and with the mass-luminosity relation; also, whether the observed values of Δm agree with the results from the photometric orbits in eclipsing variables.

XIII. THE WOLF-RAYET SPECTROSCOPIC BINARIES

The problems connected with these stars are somewhat different from those encountered in other spectral classes, and they will not be discussed in this paper. Reference is made to recent papers by O. C. Wilson,[67] C. S. Beals,[68] and W. A. Hiltner.[69] There is a suspicion that all typical Wolf-Rayet stars may be binaries and that those which have little or no variation in velocity (of which there seem to be only a few) are binaries with small inclinations.

XIV. SPECIAL SYSTEMS

In addition to the more general problems discussed in the preceding sections, several stars present individual problems. Among these may be listed:

a) The expanding spiraling structure of the nebulosity around β Lyr [70]
b) The interpretation of the eclipse spectrum of ϵ Aur and the nature of the semitransparent infrared component of this system[71]
c) The question of the binary nature of such stars as ϕ Per[72] and ζ Tauri,[73] which have peculiar velocity-curves but whose periods are strictly uniform
d) The interpretation of the sharp absorption lines of VV Cep[58] and of the peculiar structure of the emission lines of this star
e) The suspected duplicity of the lines of Algol near mid-eclipse[74] and the asymmetry of their rotational disturbance
f) The spectroscopic consequences of intrinsic variations in light observed in the components of several binaries—for example, ϵ Aur[75] and RX Cas[76]
g) The reported differences in the spectroscopic phenomena observed in ζ Aur during two eclipses[57]
h) The system of v Sagittarii,[77] which is unique because of its hydrogen-poor spectrum,[78] its stationary[79] emission lines of forbidden[80] and permitted[81] *Ca* II, and its strong *He* I absorption lines.[82] The period is 138 days, and the semiamplitude of the velocity-curve is 48 km/sec
i) The faint companions of several visual binaries, which have already been mentioned as possessing abnormal spectra (bright [*Fe* II] in α Sco, etc.). Among these objects, the companion to Mira Ceti is one of the most remarkable.[83]

[67] *Ap. J.*, **95**, 402, 1942.

[68] *M.N.*, **104**, 205, 1944.

[69] *Ap. J.*, **99**, 273, 1944; **101**, 356, 1945; see also O. Struve, *Ap. J.*, **100**, 384, 1944.

[70] Kuiper, *Ap. J.*, **93**, 133, 1941.

[71] Kuiper, Struve, and Strömgren, *Ap. J.*, **86**, 570, 1937.

[72] Hynek, *Ap. J.*, **100**, 151, 1944.

[73] Hynek and Struve, *Ap. J.*, **96**, 425, 1942.

[74] Morgan, *Ap. J.*, **81**, 348, 1935; Melnikov, *Poulkovo Obs. Circ.*, No. 30, p. 65, 1940.

[75] C. M. Huffer, *Ap. J.*, **76**, 1, 1932.

[76] S. Gaposchkin, *Ap. J.*, **100**, 230, 1944.

[77] R. E. Wilson, *Lick Obs. Bull.*, **8**, 134, 1914.

[78] Greenstein, *Ap. J.*, **91**, 438, 1940.

[79] Merrill, *Pub. A.S.P.*, **56**, 42, 1944.

[80] *Ibid.*, **55**, 242, 1943.

[81] Weaver, *Ap. J.*, **98**, 131, 1943.

[82] J. S. Plaskett, *Pub. Dom. Ap. Obs. Victoria*, **4**, 1, 1927.

[83] See Merrill, *Spectra of Long-Period Variable Stars*, p. 79, Chicago, 1940.

XV. MASS FUNCTIONS

A rather surprising result is the small average value of the mass function derived from our studies of eclipsing variables. Almost without exception, those systems which were chosen because they were known to have deep eclipses have turned out to have relatively small velocity amplitudes. In some cases the mass functions are so small as to impose severe restrictions upon the masses themselves, or upon the mass-ratios, or upon both. In BD .Virginis,[84] for example, we have only one component, of spectral type A5. The mass function is

$$\frac{m_2^3}{(m_1+m_2)^2}\sin^3 i = 0.02\odot .$$

If we designate $m_1/m_2 = a$ and if we require that the mass of the fainter component, whose spectrum from the light-curve should be G, be $m_2 = 1\ \odot$, we find $a = 6$ (since $\sin^3 i \sim 1$); or, more generally,

m_2	a	m_1
2 ⊙	9	18⊙
1	6	6
0.5	4	2

To obtain reasonable masses, a must be at least equal to 4. From the light-curve of this, and of other similar stars we infer that the faint, cool, companions are larger than the hot primary star and may well be considered as subgiants. We now infer that at least in some of these systems the subgiant secondaries have relatively small masses, probably of the order of from 0.5 ⊙ to 1.0 ⊙, and that the mass ratios are somewhere between $a = 4$ and $a = 6$. I am mentioning this here because a star of class G whose mass is less than the solar mass and whose radius is several times larger than that of the sun is not often encountered among the single stars, and its spectrum should be of interest. In several eclipsing variables, though not in BD Vir, these spectra can be observed at principal minimum.

The frequent occurrence of these systems among the eclipsing variables is a result of observational selection. Spectroscopic binaries are discovered as such when the brighter components have large values of K_1. This happens when $a = 1$. Ordinarily, a cannot be less than 1, except in Wolf-Rayet binaries. On the other hand, deep eclipses are discovered if $k = r_1/r_2$ is very small and if, at the same time, J_2/J_1 is also small. This favors systems of the kind of BD Vir.

XVI. THICK ATMOSPHERES

Some of the points discussed in the preceding sections must have a bearing upon the theory of thick atmospheres recently developed by S. Gaposchkin and C. Payne-Gaposchkin.[85] As these authors have stated, the photometric observations of SX Cas and RX Cas and a few other stars show striking differences between light-curves obtained in yellow light and those obtained in blue light. These differences can be formally explained by adopting very different radii for the two effective wave lengths; and this, in turn, leads to the suspicion that the stars have very extensive atmospheres, whose heights are comparable to the radii of the two components. A theoretical discussion of the limb darkening as a function of wave length by the Gaposchkins has given a series of predicted light-curves which strikingly resemble those observed in SX Cas. The spectrographic observations have given reliable evidence of the existence of tenuous gase-

[84] *Ap. J.*, 100, 181, 1944. [85] *Ap. J.*, 101, 56, 1945.

ous streams in SX Cas and a number of other systems. The question arises whether these tenuous streams are identical with the thick atmospheres postulated by the Gaposchkins. The theory of the latter depends upon their strong continuous absorption. The streams produce emission lines and absorption lines. There has been no indication from the spectrograms that they also produce appreciable continuous absorption. On the whole, I had thought that these extra absorption lines are somewhat weaker than the corresponding lines in normal stellar atmospheres. Their contours are suggestive of turbulence, so that moderately strong lines can be produced by relatively small numbers of atoms. Hence I was inclined to disregard the continuous absorption in the streams, except in such peculiar objects as β Lyr. But these arguments are not sufficiently strong to carry any weight against the photometric evidence. In β Lyr and in a few other stars the absorption lines of the component which is supposedly involved in a nebulous ring appear strongly at all phases and are not noticeably cut down by the continuous absorption within the shell. I suppose that this is consistent with the hypothesis of a ring, but it is difficult to see how a distinct line of type B9 could be observed through a "thick atmosphere," surrounding the star completely. In SX Cas the spectrographic evidence is different. It is not possible to separate the absorption lines from the shell and from the star. Hence it is entirely possible that we have a thick atmosphere in the sense required by the theory of the Gaposchkins and that the outer layers of this atmosphere produce the spectroscopic shell phenomena. Such a view might help to reconcile the conflicting pictures of the rotational disturbance in such stars as U Cep and RZ Sct. But there is, as yet, no photometric evidence of a "thick atmosphere" in RZ Sct, while in U Cep it is present but is much less conspicuous than in SX Cas or RZ Ophiuchi. Perhaps all that can be stated with certainty at the present time is that those stars which best show the photometric phenomenon attributed to "thick atmospheres" also show spectroscopic features which have been attributed to absorbing streams of gas located outside the classical boundaries of the two components.

THE OBSERVATIONS

Nearly all eclipsing variables for which there are no spectrographic observations are fainter than magnitude 8 at maximum light, and a useful program should reach stars to magnitude 10 or even 10.5 at maximum. We have seen that the average rate of increase in the number of eclipsing binaries observed with slit spectrographs has been of the order of one or two systems per year. It is clear that in order to secure answers to our questions within a reasonable length of time we must greatly accelerate the observational work. For this reason a fairly comprehensive program of spectrographic work was undertaken at the McDonald Observatory by D. M. Popper, who in 1943 published his results for five spectroscopic binaries, four of which are, at the same time, eclipsing variables.[86] After Dr. Popper's departure on a leave of absence for war research, I revised the program and continued it with the efficient co-operation of Dr. W. A. Hiltner, Dr. Carlos U Cesco, and and Dr. Jorge Sahade. Since the beginning of 1944 we have published the results of our observations of 14 eclipsing stars: SX Cas,[87] RX Cas,[88] U Cep,[89] BM Orionis,[90] BD Vir,[91] AR Mon,[92] TX UMa,[93] SVS 923,[94] W Ser,[95] AB Per,[96] AU Mon,[97] RZ Sct,[98] RZ Eridani,[99] and ER Orionis.[100] Of these 14 stars, 2 had previously determined orbits.

[86] *Ap. J.*, **97**, 394, 1943.
[87] *Ap. J.*, **99**, 89, 1944.
[88] *Ap. J.*, **99**, 295, 1944.
[89] *Ap. J.*, **99**, 222, 1944.
[90] *Ap. J.*, **99**, 87, 1944.
[91] *Ap. J.*, **100**, 181, 1944.
[92] *Ap. J.*, **100**, 374, 1944.
[93] *Ap. J.*, **101**, 108, 1945.
[94] *Ap. J.*, **101**, 114, 1945.
[95] Bauer, *Ap. J.*, **101**, 208, 1945.
[96] *Ap. J.*, **101**, 232, 1945.
[97] *Ap. J.*, **101**, 235, 1945.
[98] *Ap. J.*, **101**, 240, 1945.
[99] *Ap. J.*, **101**, 370, 1945.
[100] *Pub. A.S.P.*, **56**, 34, 1944.

The others were essentially unknown. In addition, W. A. Hiltner published his observations of the Wolf-Rayet star HD 214419,[69] which has since been announced by S. Gaposchkin[101] as an eclipsing variable (HV 11086). The present paper gives the results for 13 additional systems, listed in Table 1. All but one (SW Canis Majoris) are included in Dugan's "Finding List for Observers of Eclipsing Variables."[102] Several stars were suggested by Dr. S. Gaposchkin and Dr. C. Payne-Gaposchkin, notably SW CMa, SV Geminorum, RU Cancri, and AW Pegasi. The observations were made with the Cassegrain spectrograph of the McDonald Observatory; and a large number of the earlier spectrograms of SW CMa, EY Orionis, RU Cnc, and AW Peg were obtained by Drs. Cesco and Sahade. All spectrograms whose numbers are marked "CQ" were taken on glass plates of Eastman 103a-O emulsion with two quartz prisms and a 500-mm camera, giving a dispersion of 55 A/mm at $H\gamma$. Those spectrograms whose numbers are marked Gf/2 were obtained with two glass prisms and a 180-mm Schmidt camera on 103a-O

TABLE 1*

THE OBSERVING PROGRAM

No.	Star	1945		Period (Days)	Char.	Magnitude			D	d	Sp.	Remarks	No. of Plates
		α	δ			M	A_1	A_2					
1....	RW Per	4h16m2	+42° 11′	13.20	A	9.9	2.1	.....	24.	10	A	Short ecl. Long total	55
2....	EY Ori	5 28.6	− 5 44	16.79	A	9.5	0.8	0.1	31.	.....	F8	Long P. Eccentric	41
3....	SV Gem	5 57.6	+24 29	4.01	A	10.0	1.3	.....	15.?	.....	A	Sec? D? Low ρ	21
4....	RU Mon	6 52.0	− 7 31	3.58	A	10.2	0.6	0.6	4.8	0	A	High Ecc. Rev. of apsi.	23
5....	AO Mon	7 4.3	− 4 34	0.94	A	9.4	0.6	0.08?	6.6	0.0	A	$P\times 2$? Ecc?	33
6....	SW CMa	7 6.1	−22 21	10.09	A	9.1	0.5	.....	12.0	0	A0	.....	27
7....	UZ Pup	7 39.3	−13 15	0.79	β	9.7	0.9	0.8	0.5	.....	.....	Two sp?	42
8....	VZ Hya	8 29.0	− 6 8	1.45	A	9.1	0.8	0.0	3.	0.4	F5	Range? d? Sec?	38
9....	RU Cnc	8 34.3	+23 45	10.17	A	9.9	1.5	.....	19.	8.	F9+ G9 Sm K	Long d. Var. P?	33
10....	Y Leo	9 33.8	+26 29	1.69	A	9.8	3.3	.....	7.0	0	A	Total? A and K tp.	34
11....	RW UMa	11 37.8	+52 18	7.33	A	9.9	1.0	0.13	14.6	4.8	F9+ G9 Sm K	Total. Short ecl.	24
12....	SS Boo	15 11.7	+38 45	7.61	A	10.0	0.5	0.1	19.	0	.....	D? d? Sec?	25
13....	AW Peg	21 49.8	+23 45	10.62	A	7.2	0.7	0.12	19.7	10.3	A2	Shal. tot. D? d? Sec?	74

* The data under "Period," "Char.," "M" (maximum light), "A_1," "A_2," "D," "d," and "Sp." are from H. Schneller, *Kat. u. Eph. 1941. Kl. Veröff. Berlin-Babelsberg*, No. 22, except that D and d for RW Per and A_1 and A_2 for UZ Pup are from R. S. Dugan, *Contr. Princeton U. Obs.*, No. 15, 1934. The remarks are all from Dugan.

film. The dispersion on the films was 76 A/mm at $H\gamma$. It must be emphasized that the stars were rather faint (except AW Peg) and that the dispersion used was necessarily quite low, especially with the Gf/2 camera. The scatter of the radial velocities is, therefore, also large. For some stars the dispersion is undoubtedly too small to give complete resolution of double lines. But for many objects the loss in dispersion is more than compensated for by the variety of astrophysical results obtained. A few spectrograms were obtained during the eclipse of Y Leonis, when the star reaches a visual magnitude of 13 and a photographic magnitude of perhaps 14, with glass prisms and a f/1 Schmidt camera giving a linear dispersion of 150 A/mm at $H\gamma$. These films were not used for the measurement of radial velocities. In some of the stars on this program it was important to make the exposures reasonably short, so as not to wipe out significant changes.

RW PERSEI

This star was selected because of its relatively long period, its deep total eclipse, and its inappreciable secondary eclipse. The star should be interesting during the total phase,

[101] *Ap. J.*, **100**, 242, 1944. [102] *Contr. Princeton U. Obs.*, No. 15, 1934.

when the predicted spectral type is G1. A photometric orbit was computed by Shapley[103] from observations by E. C. Pickering. The light-curve was somewhat uncertain, and Shapley assumed that the eclipses are central. The depth of secondary minimum may be 0.02 to 0.05 mag. The principal elements are

$$L_b = 0.87$$
$$a_b = 0.07 = 2\odot \qquad (i = 90°)$$
$$a_f = 0.16 = 5\odot \qquad J_b/J_f = 30$$

The spectrum is of type A5, with very strong lines of *H*, with conspicuous *Ca* I, *Ca* II, *Fe* I, and *Fe* II, and with relatively weak *Mg* II and *Si* II. After the first few spectrograms had been taken, I noticed that the *H* lines had changed in appearance. They had increased in intensity from phase 0.293 to phase 0.522, had then decreased in intensity to phase 0.745, and had again started to increase in intensity. Moreover, $H\beta$ was often present as a very narrow and sharp absorption line, without perceptible wings; $H\gamma$ and $H\delta$ had the appearance of a strong turbulent line-contour superposed over a normal Stark-broadened line; and $H\epsilon$ was very strong and very broad, with the Stark-effect

TABLE 2

INTENSITIES OF H LINES IN RW PERSEI

Phase (in P)	Violet *H* Emission	Red *H* Emission	Phase (in P)	Violet *H* Emission	Red *H* Emission
0.918	0	0	0.975	4	5
.958	0	2	.975	4	5
.961	0	3	.983	9	9
.963	1	3	.988	10	8
.965	1	3	.993	6	2
.969	2	4	.997	3	0
0.972	2	5	0.034	0	0

wings predominating. I therefore suspected that emission might be present in $H\alpha$. A panchromatic film exposed on January 31 at phase 0.899 confirmed the suspicion that $H\alpha$ is strong in emission during full light. A special effort was then made to observe the star completely during two principal eclipses—on February 1 and February 14. These plates showed strong double emission lines at $H\beta$, $H\gamma$, $H\delta$, $H\epsilon$, *Ca* II 3933, and the strongest lines of *Fe* II. The emission components experience eclipses, precisely as in SX Cas, RX Cas, and RW Tau. The intensities of the *H* components are listed in Table 2 as functions of the phase. The phases (in fractions of the period) were computed with the formula

$$\text{Minimum} = \text{JD } 2416032.007 + 13.19890\ \text{E}\ .$$

given by Kordylewski.[104] The data in Table 2 show that the two component lines were equal at phase 0.983 and that maximum total intensity for both lines, taken together occurred at phase 0.985.

Visual observations made with the finder of the 82-inch telescope are given in Table 3. It seems that principal minimum occurred at phase 0.985, or about 4.7 hours earlier than was predicted. It is probably significant that these estimates give a duration of totality of the order of 3 or 4 hours and that this short duration is confirmed by the fact

[103] *Contr. Princeton U. Obs.*, No. 3, 1915.

[104] *Rocznik Astr. Cracovie*, 12, 45, 1934.

that the sum of the emission intensities was still increasing at phase 0.975 and was already decreasing at phase 0.993.

The inference to be made from the eclipses of the bright lines is precisely the same as in SX Cas and RX Cas. The A-type component—the one which is eclipsed at primary eclipse—is flanked by a nebulous stream which flows in the same direction in which the star rotates but whose velocity is much greater. The total separation between the centers of the bright lines at $H\delta$ was measured as 6.0 A. The velocity of each stream corresponds to one-half of this, or 220 km/sec. The normal absorption lines of the A5 star are somewhat diffuse, but I should have been inclined to estimate the corresponding rotational velocity as not more than 100 km/sec.

TABLE 3

ESTIMATED BRIGHTNESS OF RW PERSEI

Phase (in P)	Remarks
0.975	Variable near minimum
.983	Variable at minimum
.988	Variable at minimum
.993	Variable becomes brighter
0.997	Variable still brighter

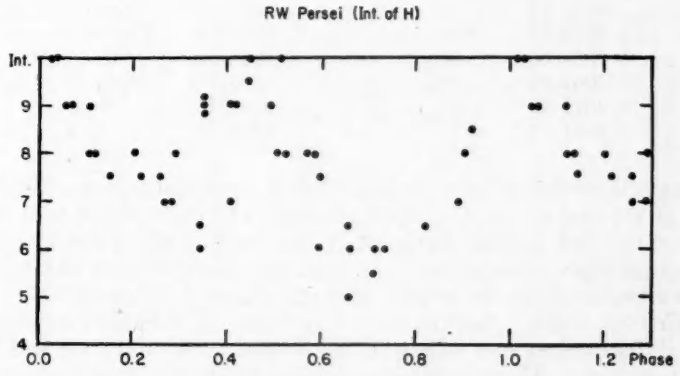

FIG. 1

The variation in the intensities of the H absorption lines is shown in Figure 1, where all plates taken during the eclipse were omitted. There is a pronounced maximum near phase 0 and a minimum near phase 0.7. A secondary maximum occurs at phase 0.5, and a secondary minimum at phase 0.25. This variation is exactly analogous to the variation of the central absorption cores of H in SX Cas,[105] and a somewhat similar variation was also found in RX Cas.[106] But in RW Persei the emission lines are not seen at $H\beta$, γ, δ, and ϵ, except in eclipse, while the other two stars show the emission lines at all phases. It is very important to recognize that the H lines in RW Per are not simply those of a normal reversing layer but are in part produced in an absorbing stream or envelope. When the H lines are weak, they show the usual contours characterized by Stark broadening. It is only when they are strong that we observe the superposed contours characteristic of turbulent motions. It is my impression that during the two cycles of RW Per covered

[105] *Ap. J.*, 99, 101, 1944. [106] *Ap. J.*, 99, 303, 1944.

by my observations the intensities of the *H* lines did not exactly repeat themselves, but the material is not sufficient to establish such a change.

The wave lengths of the star lines used for radial velocity are shown in Table 4, and the velocities are listed in Table 5. Figures 2 and 3 give the velocity-curves for the means of all lines and for the *H* absorption lines alone. If we disregard for the moment the phases 0.95 to 1.0, which fall in the eclipse, we find from Figure 2 a well-marked minimum at phase 0.4, $v = -12$ km/sec, and a less pronounced maximum at phase 0.85, $v = +25$ km/sec. The semiamplitude of the curve $K_1 = 18.5$ km/sec. The curve is symmetrical, suggesting circular motion; but minimum velocity occurs 0.15 P too late and maximum velocity 0.10 P too late, if we accept phase 0 as the time of conjunction. Qualitatively, this is the same discrepancy that I observed in SX Cas, but there is no certainty that the phenomena are physically related. It does not appear to be possible to reconcile the observations with a minimum at phase 0.25, though a maximum at phase 0.75 might perhaps be possible. Under these circumstances we can give only the elements shown in Table 6. The velocity-curve of the *H* lines in Figure 3 is similar to that of all lines, but the scatter is larger. The two cycles are shown by two different symbols. There is no difference. Outside of eclipse all lines give the same curve.

TABLE 4

LIST OF STAR LINES USED FOR RW PERSEI

Element	λ	Element	λ	Element	λ
Ca II	3933.67	*Hδ*	4101.74	*Fe* II	4351.77
Fe II	4024.55	*Fe* II	4173.45	*Ti* II	4395.04
Fe I	4045.82	*Fe* II	4178.85	*Ca* I + *Fe* I	4451.01
Fe I	4063.60	*Sr* II	4215.52	*Ti* II	4443.80
Ni II	4067.05	*Ca* I	4226.73	*Mg* II	4481.23
Fe I	4071.75	*Fe* II	4233.16		
Sr II	4077.71	*Hγ*	4340.47		

During the eclipse the radial velocities show a large disturbance. This is especially pronounced in the case of the *H* absorption lines. The disturbance is of such a nature that the absorption line appears displaced in the direction of the stronger emission line; this precludes an explanation in terms of photographic spreading of the emission. We list in Table 7 the observations secured between phases 0.958 and 0.997.

It is certain from Table 7 that the lines of *H*, *Fe* II, and perhaps *Ca* II and *Mg* II show the rotational disturbance and belong to the A5 star. But *Ca* I, *Fe* I, and *Ti* II take no part in the disturbance. These lines certainly do not belong to that source which experiences partial eclipse. During the total eclipse the entire absorption-line spectrum is changed: *Ca* I, *Fe* I, and *Sr* II are very strong, but the *CH* band is not seen. The type may best be described as gG0; but there remain, even at phases 0.975 and 0.983, fairly strong lines of *H* and *Fe* II, which probably belong to the stream and which I described as "central absorptions" during the measurements. The *Ca* II K line at phase 0.988 is a narrow reversal between emission components. This is probably superposed over a broad, shallow line belonging to the G star. The remarkable persistence of the shell-absorption lines during totality is a phenomenon already encountered in SX Cas, but it is difficult to explain unless we suppose that the streams project in front of the G star, somewhat in the manner of the stream in β Lyr. Otherwise it would be impossible for the stream to produce absorption lines while the A star is completely eclipsed.

It will be noticed from Table 7 that the maximum of the rotational disturbance in *H* occurs at phase 0.965, the minimum at phase 0.975, while from the intensities of the bright lines and the estimates of the star's brightness we had concluded that mid-eclipse took place at phase 0.985. This discrepancy is probably real. The interval between the two critical phases of the rotational disturbance, namely, 0.01 $P = 3.2$ hours, is prob-

TABLE 5*

RADIAL VELOCITIES OF RW PERSEI

PLATE G f/2	DATE 1945	U.T.	PHASE		VELOCITIES (KM/SEC)		
			In Days	In Period	All Lines	*H*	*Ca* II
4889	Jan. 23	2:06	3.868	0.293	+ 6.7	+25.7	+ 15.8
4892	24	3:15	4.915	.372	− 4.0	− 0.9	− 7.5
4900	25	1:28	5.841	.443	+ 7.2	+20.0	− 3.9
4917	26	2:37	6.889	.522	−14.3	−12.1	− 22.6
4928	27	1:22	7.837	.594	− 0.8	+15.3	+ 3.3
4929	27	2:29	7.883	.597	+ 9.1	+ 4.1	+ 29.1
4946	28	1:24	8.838	.670	+10.5	+22.0	+ 6.7
4956	29	1:18	9.834	.745	+10.4	+24.4	+ 51.3
4975	30	1:22	10.837	.821	+12.4	+23.2	+ 54.9
4987	31	1:27	11.840	.897	+18.2	+56.1	+ 65.4
4999	31	8:13	12.122	.918	+35.5	+45.5	+102.3
5007	Feb. 1	2:18	12.876	.975	− 3.2	− 9.3	.....
5008	1	4:44	12.977	.983	+22.5	+18.1	+ 27.6
5009	1	6:16	13.041	.988	+14.5	+23.2	+ 68.6
5010	1	7:45	13.103	.993	+10.0	+23.2	+ 46.5
5011p	1	9:06	13.159	.997	+27.4	+34.8	.....
5018	2	1:32	0.645	.049	+28.7	+31.7	+ 13.1
5019	2	2:03	0.666	.050	+14.3	+25.4	+ 16.8
5036	3	1:24	1.639	.124	+19.4	+20.9	+ 19.7
5037	3	1:58	1.663	.126	+12.0	+25.0	+ 23.5
5053	4	2:25	2.682	.203	+15.0	+25.8	+ 23.3
5054	4	3:20	2.720	.206	+12.5	+21.9	+ 27.0
5061	5	5:02	3.791	.287	− 6.0	+19.4	.....
5071	6	1:28	4.642	.352	−22.1	−20.4	− 18.3
5072	6	2:20	4.678	.354	−21.0	−10.9	− 44.2
5092	7	1:32	5.645	.428	−18.4	−26.0	− 48.2
5093	7	2:07	5.669	.429	−18.8	−11.7	− 18.5
5110	8	1:31	6.644	.503	− 4.5	−22.2	− 7.3
5111	8	2:04	6.667	.505	− 6.4	−11.3	− 25.6
5130	9	1:34	7.646	.579	− 9.8	−18.0	+ 0.2
5131	9	2:04	7.667	.581	− 6.8	−18.8	− 21.9
5151	10	1:31	8.644	.655	+10.0	+21.4	+ 22.1
5152	10	1:57	8.662	.656	+27.4	+35.0	+ 25.9
5162	11	1:32	9.645	.731	+21.5	+40.7	+ 25.8
5163	11	2:06	9.669	.733	+16.6	+35.2	+ 37.2
5182	13	1:29	11.643	.882	+ 5.2	+50.0	+ 70.5
5204	14	1:40	12.650	.958	+56.4	+75.7	+ 66.5
5205	14	2:26	12.682	.961	+64.4	+71.5	+ 66.4
5206	14	3:07	12.711	.963	+42.3	+77.2	+ 62.6
5207p	14	3:55	12.744	.965	+32.9	+84.7	+ 32.9
5208	14	4:56	12.787	.969	+24.4	+48.8	+ 25.2
5209	14	5:58	12.830	.972	+56.0	+22.1	.....
5210p	14	7:01	12.873	.975	.....	+11.8	.....
5219	15	1:30	0.444	.034	+11.2	+22.0	+ 29.1
5220	15	1:57	0.463	.035	+14.9	+23.2	+ 10.8
5246	16	1:44	1.454	.110	+15.4	+32.0	+ 28.9
5247	16	2:32	1.488	.113	+ 1.9	+17.5	+ 6.7
5249p	17	3:58	2.547	.193	+22.4	+23.4	+ 10.4
5263	18	1:41	3.452	.262	−17.2	0.0	− 42.1
5264	18	2:17	3.477	.263	− 6.2	−18.7	− 1.0
5268	19	1:56	4.463	.338	−16.9	− 6.7	− 23.1
5269	19	2:32	4.488	.340	−11.3	− 8.4	− 23.2
5284	20	1:40	5.451	.413	−15.0	− 0.7	− 23.1
5285	20	2:23	5.481	.415	−12.4	− 4.0	− 30.9
5303	21	1:53	6.460	0.489	−17.4	−14.4	− 23.2

* The letter "p" following the plate number designates a poor plate; "vp," very poor.

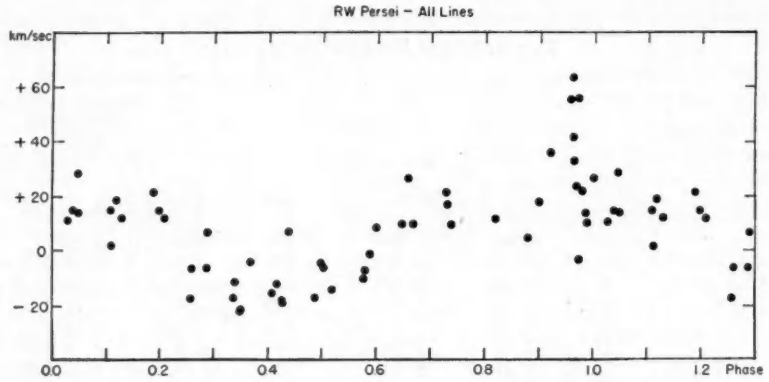

FIG. 2

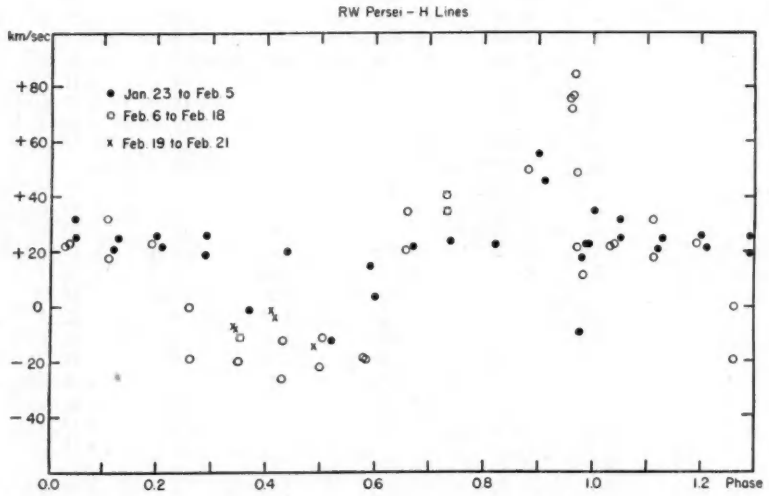

FIG. 3

TABLE 6

ORBITAL ELEMENTS OF RW PERSEI

$P = 13.20$ days (assumed)
$\gamma = +6.5$ km/sec
$\kappa_1 = 18.5$ km/sec
$e = 0$
T = (min. vel.) = phase 0.4 day P after principal eclipse

$$\frac{m_2^3}{(m_1 + m_2)^2} \sin^3 i = 0.009 \odot$$

$$a_1 \sin i = 3.4 \times 10^6 \text{ km}$$

ably consistent with the duration of totality. But it is certain from the data in Table 2 that mid-eclipse could not have occurred as early as phase 0.970 and that it probably occurred after phase 0.983. On the other hand, the possible uncertainty of the *H* velocities is not sufficient to place the minimum of the rotational disturbance much later than phase 0.975. I believe that we must conclude that the rotational disturbance of *H* is

TABLE 7

RADIAL VELOCITIES OF RW PERSEI

Phase	*H*	*Ca* II	*Fe* II	*Mg* II	*Ca* I	*Fe* I	*Ti* II
0.958	+76(2)	+67(1)	+97(2)	+88(1)	− 3(1)	+ 7(1)	+ 6(1)
.961	+72(2)	+67(1)	+47(2)	.....	.....	.....	.....
.963	+77(2)	+63(1)	+63(2)	.....	−13(1)	+37(1)	−24(1)
.965	+85(1)	+33(1)	.....	.....	.....	.....	.....
.969	+48(2)	+25(1)	+34(1)	+ 58(1)	+15(1)	+ 5(3)	− 6(2)
.972	+22(2)	.....	+63(1)	+116(1)	.....	+22(1)	.....
.975	+12(2)	.....	.....	.....	.....	.....	.....
.975	− 9(2)	.....	+ 6(1)	+ 4(1)	− 6(1)	.....	.....
.983	+18(2)	+28(1)	+ 7(3)	+ 33(1)	+23(1)	+17(2)	−16(1)
.988	+23( )	+69(1)	+ 7(3)	+ 39(1)	+23(1)	− 3(3)	+ 1(2)
.993	+23(2)	+47(1)	0(3)	+ 27(1)	+42(1)	+13(1)	− 2(1)
0.997	+35(1)	.....	+30(3)	− 2(1)	+37(1)	.....	+36(1)

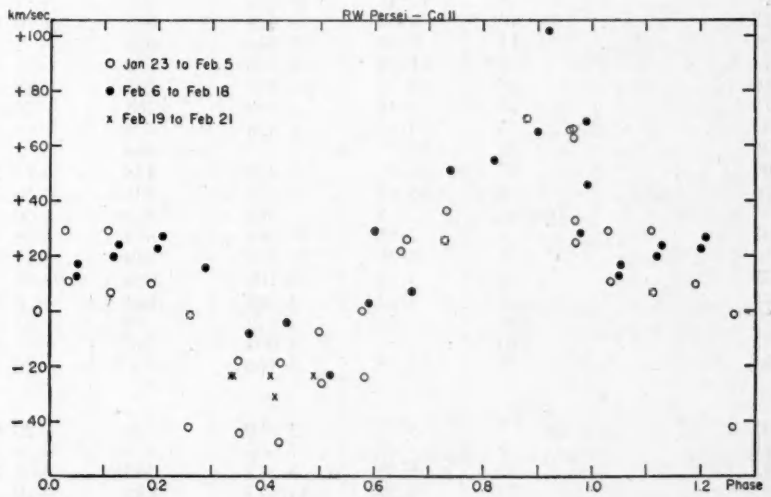

FIG. 4

largely a phenomenon of the shell and not so much one of the partial eclipse of the A-type star. It may be likened to the phenomenon of the satellite lines in β Lyr rather than to that of the rotational effect in B9 lines of β Lyr. If the satellites were unresolved from the B5 lines, they would also produce something like a rotational disturbance in the shell lines.

The *Ca* II line λ 3933 is sharp and strong and should give fairly reliable velocities. These are plotted in Figure 4. The amplitude of the curve is much larger than for *H* or

TABLE 8

LIST OF STAR LINES USED FOR EY ORIONIS

Element	λ	Element	λ	Element	λ
Ca II	3933.67	*Sr* II	4077.71	*Fe* II	4351.77
Fe I	4045.82	*Hδ*	4101.74	*Ti* II	4395.04
Fe I	4063.60	*Ca* I	4226.73	*Ti* II	4443.80
Ni II	4067.05	*Fe* II	4233.16	*Mg* II	4481.23
Fe I	4071.75	*Hγ*	4340.47		

TABLE 9

RADIAL VELOCITIES OF EY ORIONIS

Plate	Date	U.T.	Phase		Velocities (Km/Sec)
			In Days	In Period	
CQ	1944				
3783	Sept. 21	11:31	15.086	0.899	+45.9
3798p	27	11:42	4.304	.256	−22.0
3817	30	10:25	7.251	.432	+25.7
3829	Oct. 1	10:28	8.253	.492	+44.6
3848	4	10:27	11.252	.670	+68.5
3863	5	9:57	12.232	.728	+93.6
3879p	6	8:39	13.219	.787	+63.8
3896	7	9:45	14.223	.847	+65.4
3909	9	10:17	16.246	.968	+26.1
3910	9	11:41	16.304	.971	+39.1
3921	10	9:30	0.424	.025	+10.1
3936	11	9:59	1.444	.086	− 2.2
3942	12	11:49	2.520	.150	−11.3
3956	13	10:33	3.468	.207	−25.8
3970	14	11:18	4.499	.268	−36.6
3985	15	9:51	5.438	.324	−15.2
3996	16	10:12	6.453	.384	+ 2.6
4009	17	10:10	7.452	.438	+25.2
4026	18	10:44	8.475	.505	+46.5
4094	Dec. 13	7:13	13.962	.832	+60.2
4107	14	7:55	14.991	.893	+55.3
4116	15	6:26	15.929	.949	+41.0
4128	16	5:41	0.109	.006	+15.3
4141	17	4:32	1.061	.063	+ 6.0
4179	19	5:48	3.112	.185	−22.3
4193	20	4:37	4.064	.242	−43.8
4208	21	6:55	5.160	.307	−26.5
	1945				
4305	Jan. 7	5:27	5.310	.316	−20.6
4311p	9	5:19	7.305	.435	+28.2
4323	11	5:31	9.313	.555	+61.9
4334p	13	9:22	11.473	.683	+69.5
G *f*/2					
4893	24	4:23	5.477	.326	−22.7
4902	25	3:05	6.422	.382	+18.5
4949	28	4:18	9.473	.564	+60.2
4959	29	3:31	10.441	.622	+75.7
4977	30	2:40	11.405	.679	+75.4
4990	31	3:28	12.438	.741	+79.8
5021	Feb. 2	3:47	14.452	.861	+66.0
5038	3	2:52	15.413	.918	+40.1
5055	4	4:01	16.461	.980	+ 7.2
5222	15	3:11	10.638	0.634	+84.0

for the mean of all lines—from −20 km/sec to +70 km/sec—but there is a strange break in the slope at phase 0, and I believe that the high and broad maximum at phase 0.9 must be due to the absorption in the stream. Such a maximum is also observed in SX Cas. There is no conclusive evidence of a change from one cycle of the variable to the next.

EY ORIONIS

The spectrum of this star is more nearly dA7 than F8 (as listed in Table 1). The metallic lines are fairly sharp, and the *H* lines are strong and have broad wings; *Ca* II K is strong and deep but is not strong enough for class F. The spectrum does not change appreciably during the eclipse. At phase 0.006 P the spectral class is dA7, though the metallic lines may be slightly narrower and deeper than on other plates. Since the eclipses are very different in depth, we infer that they are probably not total. The star lines are given in Table 8, and the radial velocities in Table 9. Only one component can be seen in

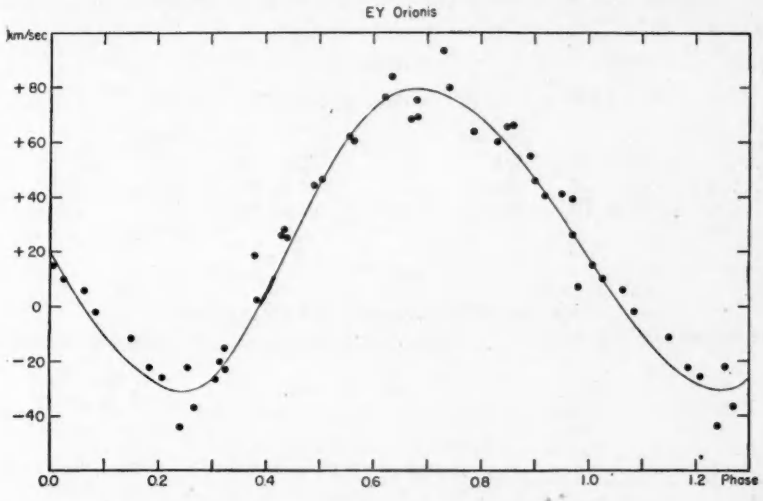

FIG. 5

the spectrum. The velocity-curve, in Figure 5, is unsymmetrical, and the orbit is eccentric. The approximate elements are in Table 10. The phases were computed with the

TABLE 10

ORBITAL ELEMENTS OF EY ORIONIS

$P = 16.789$ days (assumed)
$\gamma = +28.0$ km/sec
$K_1 = 55$ km/sec
$e = 0.10$
$\omega = 243°$
$T =$ phase 0.39 P
$\dfrac{m_2^3}{(m_1 + m_2)^2} \sin^3 i = 0.29 \odot$
$a_1 \sin i = 12.6 \times 10^6$ km

elements by Morgenroth:[107]

$$\text{Minimum} = \text{JD } 2425866.68 + 16.789\ E\ .$$

[107] *A.N.*, **247**, 183, 1932.

The observations by Morgenroth show no secondary minimum; those by Lause[108] show a weak suggestion of one at phase 8.1 days = 0.48 P. Using this value, we obtain from Lause's light-curve

$$e \cos \omega = \frac{\pi\left(t_2 - t_1 - \frac{P}{2}\right)}{P\,(1 + \operatorname{cosec}^2 i)} \approx -0.03 .$$

The spectroscopic elements give

$$e \cos \omega = -0.045 .$$

The agreement is probably better than can be expected from the observations, but the probability is great that we have in the case of EY Ori a binary of well-established eccentricity.

TABLE 11

LIST OF STAR LINES USED FOR SV GEMINORUM

Element	λ	Element	λ	Element	λ
Ca II	3933.67	*Hδ*	4101.74	*Hγ*	4340.48
He I	4009.27	*He* I	4120.81	*He* I	4387.93
He I	4026.19	*He* I	4143.77	*He* I	4471.48

TABLE 12

RADIAL VELOCITIES OF SV GEMINORUM

Plate G*f*/2	Date 1945	U.T.	Phase		Velocities (Km/Sec)	
			In Days	In Period	Abs.	*Ca* II
4930	Jan. 27	3:45	0.868	0.217	−25.6	.....
4948	28	3:23	1.853	.463	−28.8	.....
4958	29	2:53	2.832	.707	+76.1	+11.7
4976	30	2:03	3.797	.948	+37.1	+15.2
4989	31	2:50	0.824	.206	−12.7	+14.7
5030	Feb. 2	8:56	3.078	.768	+65.0	.....
5045	3	6:55	3.994	.997	+45.3	+20.7
5046	3	7:44	0.022	.005	+40.6	+13.0
5082	6	8:27	3.052	.762	+60.5	+30.2
5101p	7	7:58	0.026	.006	+51.2	.....
5119	8	7:02	0.987	.246	− 1.9	.....
5132	9	2:47	1.810	.452	+ 3.0	+29.6
5153	10	2:33	2.800	.699	+74.4	+11.1
5164p	11	2:54	3.815	.952	+44.5	.....
5165	11	3:51	3.854	.962	+57.1	+ 6.8
5183	13	2:14	1.781	.445	−32.9	− 1.3
5184	13	3:00	1.813	.453	+ 5.7	+10.0
5221	15	2:34	3.795	.947	+70.5	+ 5.7
5248	16	4:07	0.854	.213	+15.8	+ 9.0
5265	18	2:59	2.806	.700	+84.3	.....
5266	18	3:51	2.842	0.709	+66.4	+26.8

[108] *A.N.*, **250**, 13, 1933.

SV GEMINORUM

This star was placed upon the program at the suggestion of Mrs. C. Payne-Gaposchkin, who had found certain complications in her discussion of the light-curve. The spectral type is B3 or perhaps B2. The lines are broad and ill-defined, and the measurements are very uncertain. Only one component can be seen in the spectrum. Because the period is almost exactly 4 days, the observations occur in compact groups; and it is possible that the exact time of primary minimum has been missed. The spectrum at phases 0.997 and 0.005 P is precisely the same as at other phases, but the lines may be somewhat

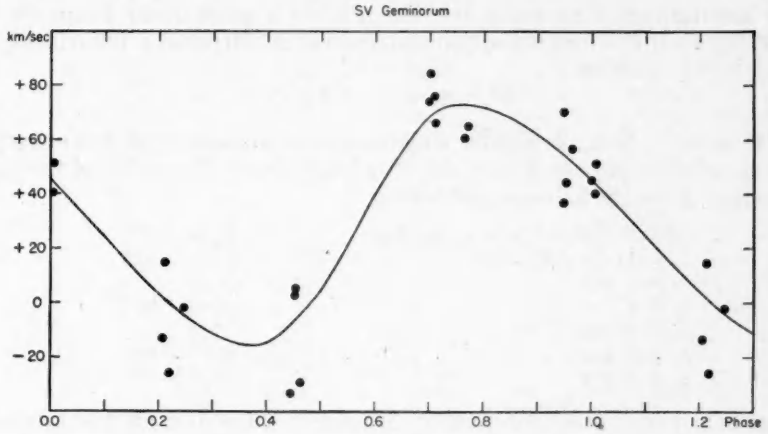

FIG. 6

TABLE 13

ORBITAL ELEMENTS OF SV GEMINORUM

$P = 4.006$ days (assumed)
$\gamma = +29$ km/sec
$K_1 = 44.5$ km/sec
$e = 0.16$
$\omega = 266°$
$T =$ phase 0.56 P

$$\frac{m_2^3}{(m_1 + m_2)^2} \sin^3 i = 0.035 \odot$$

$$a_1 \sin i = 2.4 \times 10^6 \text{ km}$$

narrower. The star lines are listed in Table 11, and the velocities in Table 12. The *Ca* II lines are of interstellar origin and give a mean velocity of

$$V_{Ca\,II} = +14.5 \pm 1.7 \text{ km/sec}.$$

The phases were computed from the elements by Enebo:[109]

$$\text{Principal minimum} = \text{JD } 2418662.46 + 4.00604\ E.$$

The velocity-curve in Figure 6 suggests an appreciable asymmetry; but because of the poor distribution in the observations and their large scatter, the eccentricity remains under suspicion. The approximate elements are given in Table 13.

[109] See Dugan, *Contr. Princeton U. Obs.*, No. 15, p. 14, 1934.

RU MONOCEROTIS

The spectrum of this famous star is very disappointing. It shows strong and very broad lines of *H* and a sharp interstellar line of *Ca* II K. The spectral type is about B9, but the absence of any other lines is peculiar. On a few plates I have suspected exceedingly faint lines of *He* I and *Mg* II, but they are not strong enough for accurate measurement. The absence of a stellar line of *Ca* II is perhaps not surprising for class B9. But in that case the lines of *H* are abnormally strong. On the other hand, if the type is A0, then the absence of stellar *Ca* II is abnormal. I believe the star has an abnormal spectrum, in the sense that the *H* lines are excessively broad and strong. This presumably indicates that the luminosity is abnormally low. But it is not a white dwarf. From the intensity of interstellar *Ca* II K we estimate that the distance is 500 parsecs. Introducing this and $m = 10.2$ in the equation

$$M = m + 5 - 5 \log D ,$$

we find $M = +1.7$, which is slightly underluminous, considering that the star probably consists of two stars of only slightly differing brightnesses. A solution of the light curve by Dubiago[110] gives the following elements:

$P = 3.5847363$ for even minima	$L_1 = .577$
$t_0 =$ JD 2416901.180	$L_2 = .423$
$e = 0.383$	$\frac{J_1}{J_2} = .942$
$\omega = 4°$	
$i = 87°36'$	$\rho_1 = .222$
$r_1 = 0.133$	$\rho_2 = 0.385$
$r_2 = 0.111$	

The large eccentricity was confirmed by Shapley.[111] There is a marked rotation of the line of apsides, with a period estimated by Dubiago and Martinoff[112] to be several centuries and by Shapley to be of the order of 1000 years. Luyten[113] has pointed out that

TABLE 14

LIST OF STAR LINES USED FOR RU MONOCEROTIS

Element	λ	Element	λ
Ca II	3933.67	*He* I	4471.48
Hδ	4101.74	*Mg* II	4481.26
Hγ	4340.48		

the values of $(t_2 - t_1)/P$ change linearly with the time over the interval 1901–1928. He believes that the time when ω was 0° may have been long before 1900, and consequently e may be much in excess of 0.4. He suggested that "spectroscopic observations on a few nights could settle the matter." In reality the spectrum is almost worthless, because it is probably badly blended. Nevertheless, all spectrograms were measured. The star lines are given in Table 14 and the velocities in Table 15. The velocity-curve in Figure 7, in which three poor spectrograms were omitted, is distinctly unsymmetrical. The approximate orbital elements are given in Table 16.

All phases were computed from the elements

$$\text{Principal minimum} = \text{JD } 2416901.180 + 3.5847363\ \text{E} .$$

The asymmetry of the velocity-curve is of a nature to be expected from the photometric data; but the values e and ω are probably uncertain, and K may be quite wrong if the

[110] *Ver. St. Nishni-Novgorod*, No. 8, 1929.

[111] *Proc. Amer. Acad.*, **66**, 469, 1931 (*Harv. Reprints*, No. 72).

[112] *A.N.*, **235**, 225, 1929.

[113] *Pub. U. Minnesota*, **2**, 47, 1935.

TABLE 15

RADIAL VELOCITIES OF RU MONOCEROTIS

PLATE G*f*/2	DATE 1945	U.T.	PHASE		VELOCITIES (KM/SEC)	
			In Days	In Period	Abs.	*Ca* II
4894	Jan. 24	5:47	3.023	0.844	+110.3	+10.6
4895	24	7:29	3.094	.863	+ 78.9	+29.5
4903	25	4:00	0.365	.102	+ 14.2	+36.3
4904	25	4:58	0.405	.113	+ 14.6	+17.9
4918	26	3:46	1.355	.378	+ 6.4	+28.9
4933	27	6:05	2.451	.684	+ 57.8	+35.2
4934	27	6:50	2.483	.693	+ 15.8	+50.4
4952	28	7:07	3.494	.975	+ 57.2	+38.7
4964p	29	7:30	0.925	.258	+ 56.5	.....
5027	Feb. 2	7:00	1.320	.368	+ 28.1	+44.1
5080	6	6:41	1.721	.480	+ 36.7	+24.3
5100	7	6:55	2.773	.774	+ 78.0	.....
5118	8	6:00	0.109	.030	+ 7.3	+ 8.5
5137	9	5:36	1.092	.305	+ 9.8	+23.4
5169	11	6:21	3.124	.871	+ 74.5	+29.2
5185	13	3:50	1.434	.400	+ 25.8	+25.7
5223	15	3:47	3.432	.957	+ 71.5	+35.7
5224	15	4:24	3.457	.964	+ 80.8	+35.7
5254p	17	7:08	1.986	.554	+ 31.0	+27.2
5270	19	3:10	0.236	.066	+ 20.0	+19.9
5271p	19	4:09	0.277	.077	+ 22.9	+ 8.5
5286	20	3:13	1.238	.345	+ 6.2	+30.5
5287	20	3:59	1.270	0.354	+ 9.9	+15.9

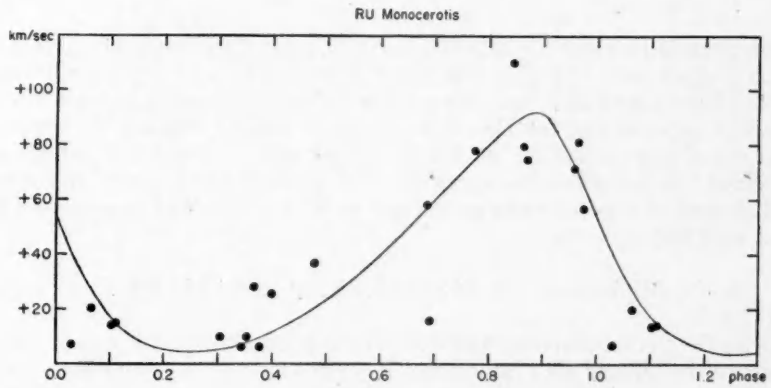

FIG. 7

TABLE 16

ORBITAL ELEMENTS OF RU MONOCEROTIS

P = 3.5847 days (assumed)
γ = +39 km/sec
K = 44 km/sec (blended)
e = 0.28
ω = 42°
T = phase 0.94 P

blending is really serious. We can, however, conclude from the widths of the *H* lines that the relative velocities of the components cannot be very great. We have approximately:

At phase 0.68, width of $H\gamma$ is 9.3 A ;

At phase 0.84, width of $H\gamma$ is 13.0 A .

Thus, the total broadening of the line at maximum separation of the components corresponds to about 3.7 A or 255 km/sec. If the two components were of similar mass, the semiamplitudes would then be

$$K_1 = K_2 = 128 \text{ km/sec} .$$

It is not unreasonable that the blended line should give $K = 44$ km/sec. This would mean that one component is a little more luminous than the other. It is possible that plates of higher contrast would show other measurable lines. Although the apparent

TABLE 17

LIST OF STAR LINES USED FOR AO MONOCEROTIS

Element	λ	Element	λ
Ca II	3933.67	*Hγ*	4340.47
He I	4026.22	*He* I	4471.51
Hδ	4101.74		

magnitude is about 10, the star is quite blue and therefore relatively easy to photograph. The mean velocity from the interstellar lines is

$$V_{Ca\,II} = +27.4 \pm 1.7 \text{ km/sec} .$$

AO MONOCEROTIS

The spectrum of this star is really B3, and not A, as was given in the previous literature. With a short period of only 0.94 day this should be an exceptionally interesting system. The lines are double, and the spectra of the components are not alike. When the stronger component of the *He* I lines is shifted toward the red, the stronger component of the *H* lines is shifted toward the violet, and vice versa. The lines are faint and ill-defined. Nevertheless, the measurements are fairly consistent. But a plot with $P = 0.94$ showed at once that the period had to be doubled. The phases were therefore computed with the elements

$$\text{Minimum} = \text{JD } 2426735.333 + 1.8847454 \text{ E} .$$

This is twice the period given by Lause.[114] The star is not unusual, except, perhaps for the reversal of the *H* and *He* I intensities. If we attribute this to differences in spectral type, we should designate the *He* I star as B3 and the other component as B5. The B5 component is the one which is eclipsed at the minimum at phase 0. Since the two minima are of equal depth, we cannot call this the principal minimum. Table 17 gives the star lines, Table 18 the velocities, and Table 19 the orbital elements. The mean velocity from the interstellar line *Ca* II K is

$$V_{Ca\,II} = +35.4 \pm 1.4 \text{ km/sec} .$$

[114] *A.N.*, **260**, 292, 1936.

TABLE 18

RADIAL VELOCITIES OF AO MONOCEROTIS

Plate G//2	Date 1945	U.T.	Phase		Velocities (Km/Sec)				
			In Days	In Period	Ca II	He I		H	
						I	II	I	II
5039	Feb. 3	3:30	0.985	0.523	+48.7	+ 10.0	.....	+ 61.1	.....
5040	3	4:00	1.006	.534	+41.1	+ 6.3	.....	+ 32.5	.....
5041	3	4:33	1.029	.546	+37.2	− 22.2	.....	+ 61.0	.....
5056	4	4:45	0.152	.081	+30.0	+107.6	.....	+ 48.7	.....
5073	6	2:48	0.187	.099	+40.1	+ 51.6	.....	+ 56.1	.....
5074	6	3:22	0.210	.111	+59.0	+187.3	.....	+ 53.7	.....
5075	6	3:54	0.232	.123	+36.2	+136.4	.....	− 6.3	.....
5094	7	3:18	1.207	.640	+54.7	− 98.6	.....	− 46.0	+187.9
5095	7	3:49	1.229	.652	+31.8	−120.4	+190.0	− 75.4	+180.4
5112	8	2:47	0.301	.160	+ 1.9	+167.3	−137.0	−109.3	+160.6
5113	8	3:17	0.322	.171	+28.5	+177.7	.....	−115.9	+188.0
5133	9	3:30	1.331	.706	+24.2	−156.4	.....	+168.7	− 93.0
5134	9	3:53	1.347	.715	+31.0	−168.7	+193.0	+150.9	.....
5154	10	3:12	0.433	.230	+42.1	+233.5	−167.0	−105.6	+225.5
5155	10	3:36	0.450	.239	+34.6	+159.5	.....	− 6.8	.....
5166	11	4:39	1.494	.793	+34.1	−163.8	.....	+209.5	− 63.8
5167	11	5:03	1.510	.801	+49.3	−167.5	+249.4	+239.8	−126.0
5186	13	4:27	1.600	.849	+22.7	−146.4	.....	− 55.0	+227.4
5187	13	4:50	1.616	.857	+29.5	−112.9	+197.8	+147.6	− 91.7
5188	13	5:21	1.638	.869	+22.5	− 89.0	+171.1	+199.8	− 38.4
5225	15	4:52	1.734	.920	+44.0	− 54.0	.....	+102.8	.....
5226	15	5:15	1.750	.929	+32.5	+ 8.3	.....	+ 95.6	.....
5227	15	5:38	1.766	.937	+32.5	− 49.6	.....	+ 53.3	.....
5252	17	6:08	0.017	.009	.....	+ 5.5	.....	− 7.9	.....
5253	17	6:32	0.033	.018	+31.6	+ 55.7	.....	+ 71.2	.....
5267	18	4:44	0.958	.508	+35.2	+ 41.3	.....	+ 63.4	.....
5272	19	4:42	0.072	.038	.....	+ 21.7	.....	+ 30.3	.....
5273	19	5:12	0.093	.049	+27.1	+105.0	.....	+ 22.0	.....
5274	19	5:57	0.124	.066	+50.0	+ 95.5	.....	+ 34.9	.....
5288	20	4:46	1.075	.570	+42.2	−106.0	.....	+ 84.9	.....
5289	20	4:57	1.082	.574	+30.7	− 26.7	.....	+ 72.8	.....
5290	20	5:26	1.102	.585	+45.9	− 36.2	.....	+ 65.5	.....
5304	21	4:53	0.195	0.103	+26.4	+106.4	.....	+ 3.1	.....

TABLE 19

ORBITAL ELEMENT OF AO MONOCEROTIS

P = 1.8847 days (assumed)
γ = +15 km/sec
K_1 = 185 km/sec
K_2 = 195 km/sec
e = 0 (assumed)
T (min. vel. of B3 comp.) = phase 0.75 P
$m_1 \sin^3 i = 5.5 \odot$
$m_2 \sin^3 i = 5.2 \odot$
$a_2 \sin i = 4.8 \times 10^6$ km
$a_2 \sin i = 5.1 \times 10^6$ km

The velocity-curves in Figures 8 and 9 are plotted separately for *He* I and *H*. The elements were obtained using the *He* I lines alone, since the *H* lines are somewhat affected by blending. It will be noticed that in measuring the *H* lines I could not always correctly

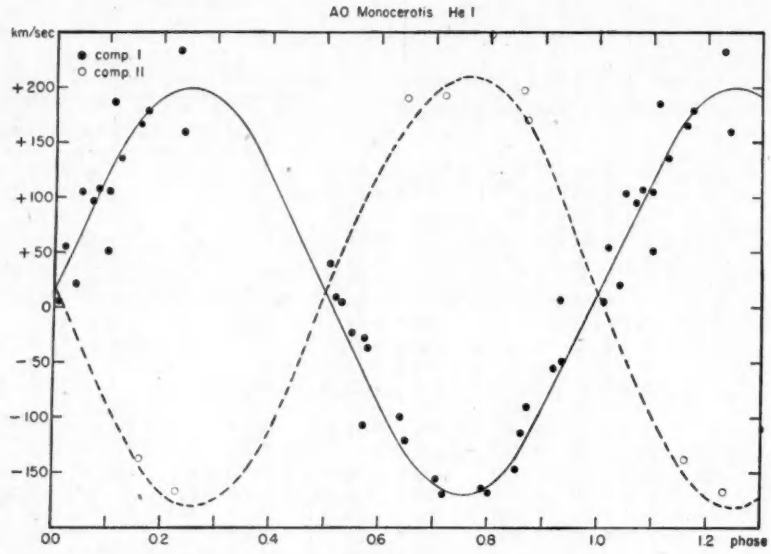

FIG. 8

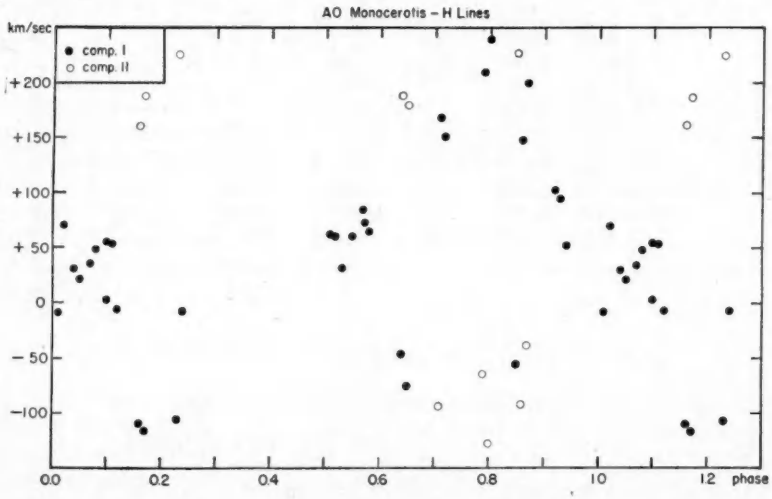

FIG. 9

identify the stronger component, while in the case of *He* I the identification was always certain.

Attention is called to the fact that the star which I have observed is BD−4°1822. This is in accordance with the original identification by the discoverer, C. Hoffmeister,[115]

[115] *A.N.*, **242**, 129, 1931.

and is contrary to the later identification by Florja[116] with BD−4°1826 = HD 54003. This later misidentification is quoted by Prager.[117] The star BD−4°1826 has a good A2 spectrum, and its velocity seems to be approximately constant.

SW CANIS MAJORIS

This star was placed upon the observing program at the suggestion of Dr. S. Gaposchkin and Dr. C. Payne-Gaposchkin. The published data concerning the light-curve show only one minimum with $A_1 = 0.5$ mag., and there appears to have been some uncertainty on the part of Florja[118] as to whether the period is really 10 days or 20 days. Florja also states that one minimum by the discoverer, C. Hoffmeister, is not represented by his period. The spectrographic observations leave little doubt that the orbit is very eccentric. The phases were computed from the elements

$$\text{Minimum} = \text{JD } 2426709.324 + 10.092\ E\ .$$

The star lines are given in Table 20. The most outstanding feature of the radial velocities in Table 21 is the occurrence of widely spaced double lines between the narrow limits of

TABLE 20

LIST OF STAR LINES USED FOR SW CANIS MAJORIS

Element	λ	Element	λ	Element	λ
Ca II	3933.67	*Sr* II	4077.71	*Hγ*	4340.48
Fe I	4005.25	*Hδ*	4101.74	*Fe* II	4351.77
Fe I	4045.82	*Sr* II	4215.52	*Fe* I	4383.55
Fe I	4063.60	*Ca* I	4226.73	*Ca* I + *Fe* I	4435.01
Ni II	4067.04	*Fe* II	4233.16	*Ti* II + *Fe* I	4443.09
Fe I	4071.75	*Fe* I + *Sc* II	4325.53	*Mg* II	4481.26

phase of 0.79 and 0.89 P. On five spectrograms within these limits the *Ca* II line is clearly double, with the violet component about twice as strong as the red. These spectrograms were obtained on the following dates:

Plate	Date	JD	Difference in Days
4132	1944, Dec. 16	2431440.911	.....
4907	1945, Jan. 25	480.782	40
4920	26	481.773	41
5228	Feb. 15	501.751	61
5229	15	501.763	61

Accidentally, these observations are all spaced by multiples of about 20 or 21 days, and they provide no test of the period. A plot of the radial velocities with $P = 20$ days gives an even greater scatter than that in Figure 10, where $P = 10$ days. Moreover, the eccentricity would become very much greater for the longer period; and, while we cannot definitely exclude this longer period, I suppose we are entitled to accept the opinion of the photometric observers, who, after weighing the evidence, concluded that the shorter period must be correct.

The velocity-curve in Figure 10 gives only the stronger component. One poor spectro-

[116] *Pub. Sternberg Astr. Inst. Moscow*, Vol. 8, No. 2, 1937.

[117] *Harvard Ann.*, 111, 186, 1941. The mean radial velocity of BD − 4°1826 from 9 spectrograms taken between January 26 and 30, 1945, is +28.9 ± 1.4 km/sec.

[118] *Ver. St. Nishni-Novgorod*, Vol. 4, No. 38, 1932; 5, 106, 1937; *Pub. Sternberg Astr. Inst. Moscow*, Vol. 8, No. 2, 1937.

TABLE 21

RADIAL VELOCITIES OF SW CANIS MAJORIS

PLATE	DATE	U.T.	PHASE		VELOCITIES (KM/SEC)	
			In Days	In Period	I	II
CQ	1944					
4119	Dec. 15	9:32	7.517	0.745	+ 11.3	.....
4132	16	9:52	8.531	.845	−100.8	+154.5
4149	17	10:55	9.575	.949	+ 10.7	.....
	1945					
4294	Jan. 4	7:18	7.240	.717	+ 53.0	.....
4313	9	7:22	2.151	.213	+ 51.3	.....
G*f*/2						
4907	25	6:46	8.034	.796	− 43.8	+161.2
4920	26	6:33	9.025	.894	− 27.4	+114.4
4935	27	7:27	10.062	.997	+ 32.8	.....
4953	28	8:02	0.995	.099	+ 48.8	.....
4963	29	6:53	1.947	.193	+ 43.3	.....
4992	31	4:30	3.848	.381	+ 98.2	− 18.8
5026	Feb. 2	6:18	5.922	.587	+ 52.7	.....
5043	3	5:42	6.898	.684	+ 71.2	.....
5058p	4	5:39	7.895	.782	+ 40.4	.....
5081	6	7:27	9.970	.988	+ 31.4	.....
5098	7	5:38	0.803	.080	+ 63.1	.....
5099	7	6:10	0.825	.082	+ 58.6	.....
5116	8	5:02	1.778	.176	+ 47.7	.....
5117	8	5:16	1.787	.177	+ 53.4	.....
5136	9	4:50	2.769	.274	+ 91.3	− 18.5
5157	10	4:47	3.767	.373	+ 88.7	.....
5168	11	5:34	4.800	.476	+ 43.8	.....
5189	13	5:54	6.814	.675	+ 48.6	.....
5190	13	6:16	6.829	.677	+ 61.2	.....
5228	15	6:01	8.819	.874	− 60.5	+149.5
5229	15	6:19	8.831	.875	− 32.4	+150.2
5291	20	6:00	3.726	0.369	+ 39.8	.....

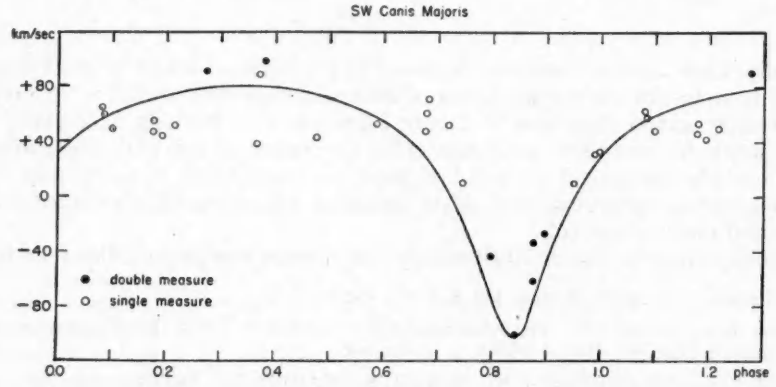

FIG. 10

gram was omitted. We see that this is the eclipsing star at principal minimum. The elements in Table 22 do not represent the observations very satisfactorily, but it would be futile to attempt further refinement with the present set of observations.

The spectral type of SW CMa, when the lines are single, is about A8. The *H* lines and *Ca* II are strong, and the Stark wings of *H* are pronounced. The metallic lines of *Fe* I, etc. (see Table 20), are fairly strong and very narrow. The spectrum is full of many narrow and fairly strong lines, resembling ordinary late A or early F stars without appreciable rotation. This character of spectrum is observed at phases near 0.10 and 0.68. Between these phases, from about 0.20 to 0.50, the lines are diffuse and weak. On a few plates near phase 0.3 I was able to see double lines, but on most of the spectrograms the components are not resolved. However, the combined intensities of these unresolved lines appear to me to be distinctly weaker between phases 0.20 and 0.50 than the intensities of the single lines at phases 0.10 and 0.68. I have the impression that this is not due to the doubling of the lines but that there is a real change in the integrated intensi-

TABLE 22

ORBITAL ELEMENTS OF SW CANIS MAJORIS

$P = 10.092$ days (assumed)	$T =$ phase 0.84 P
$\gamma = +40$ km/sec	$m_1 \sin^3 i = 2.0 \odot$
$K_1 = 90$ km/sec	$m_2 \sin^3 i = 2.0 \odot$
$K_2 = 90$ km/sec	$a_1 \sin i = 10.8 \times 10^6$ km
$e = 0.50$	$a_2 \sin i = 10.8 \times 10^6$ km
$\omega = 180°$	

ties. Take the line *Sr* II 4077 at phases 0.684 and 0.796. The components at the latter phase are very weak, while at the former the line is very strong. Normally (as, for example, in VZ Hydrae), the stronger of the two components of a double line is reduced in equivalent width by less than 50 per cent; and to the eye this decrease in intensity, though easily perceptible, does not render invisible lines of moderate intensity.

At phases between 0.8 and 0.9 the lines of SW CMa are again double and very faint; *Ca* II, *H*, and *Sr* II all have the stronger component on the violet side (*Fe* I 4045 is an apparent exception, but this is probably caused by the overlapping of the red component of *Fe* I 4045 with the violet component of another line). With this disparity in the brightnesses of the two components, the almost complete absence of the violet components of *Fe* I 4045, 4063, and 4071 is distinctly unexpected. This phenomenon should be verified by means of spectrophotometric measures. It may indicate that the spectral lines tend to be stronger at the tidal bulges, though it may also be related to the peculiar and as yet unexplained variations in the line intensities which have been observed in other systems.

UZ PUPPIS

The phases of this remarkable β Lyr type variable, discovered by C. Hoffmeister, were computed with the elements by Florja:[119]

$$\text{Principal minimum} = \text{JD } 2426033.251 + 0.794853\,E\,.$$

An improved light-curve was obtained by Tschernov in 1940,[120] and an improved set of photometric elements was given by Soloviev[121] in 1943:

$$\text{Principal minimum} = \text{JD } 2426033.251 + 0.7948495\,E\,.$$

[119] *Pub. Sternberg Astr. Inst. Moscow*, Vol. 8, No. 2, 1937.

[120] *Circ. Tadjik Obs.*, No 47, 1940.

[121] *Astr. Circ. Acad. Sci. Soviet Union*, No. 19, 1943.

TABLE 23

LIST OF STAR LINES USED FOR UZ PUPPIS

Element	λ	Element	λ	Element	λ
Ca II	3933.67	*Fe* I	4071.75	*Ca* I	4226.73
Fe I	4045.82	*Sr* II	4077.71	*Hγ*	4340.47
Fe I	4063.60	*Hδ*	4101.74	*Mg* II	4481.23

TABLE 24

RADIAL VELOCITIES OF UZ PUPPIS

Plate Gf/2	Date 1945	U.T.	Phase		Velocities (Km/Sec)	
			In Days	In Period	I	II
4908	Jan. 25	7:31	0.434	0.546	+ 50.0	.....
4909	25	8:29	.474	.596	+105.1	−147.2
4921	26	7:06	.623	.784	+172.9	−195.9
4932	27	5:30	.761	.957	+ 68.2	.....
4938	27	8:47	.103	.130	− 76.9	+161.7
4951	28	6:07	.197	.248	−107.9	+217.9
4961p	29	4:43	.344	.433	+ 9.0	.....
4962	29	6:23	.413	.520	+ 24.2	.....
4984	30	8:15	.696	.876	+ 62.3	.....
4993	31	5:03	.767	.965	+ 43.6	.....
4994	31	5:40	.793	.998	+ 21.4	.....
4995	31	6:14	.023	.029	+ 10.1	.....
5024	Feb. 2	5:19	.395	.497	+ 45.0	.....
5025	2	5:48	.415	.522	+ 64.4	− 88.0
5042	3	5:10	.583	.746	+184.6	−223.7
5057	4	5:21	.011	.014	+ 10.6	.....
5062	5	7:57	.324	.408	− 30.8	.....
5076	6	4:24	.382	.481	+ 34.8	.....
5077	6	4:55	.404	.508	+ 25.7	.....
5078	6	5:28	.427	.537	+ 25.5	.....
5079	6	6:04	.452	.569	+ 40.8	.....
5096	7	4:30	.592	.745	+162.9	.....
5097	7	5:03	.614	.772	+183.8	−117.2
5114	8	3:47	.767	.965	+ 30.9	.....
5115	8	4:16	.787	.990	+ 38.9	.....
5135	9	4:22	.201	.253	−118.7	+185.2
5156p	10	4:11	.398	.501	+ 20.0	.....
5170	11	7:06	.725	.912	+ 89.6	.....
5171	11	7:40	.748	.941	+ 48.1	.....
5191	13	6:45	.326	.410	− 37.1	.....
5192	13	7:17	.348	.438	+ 0.4	.....
5193	13	7:49	.371	.467	+ 8.2	.....
5211	14	7:54	.579	.728	+176.3	−149.3
5230	15	6:44	.736	.926	+ 74.6	.....
5231	15	7:12	.755	.950	+ 73.9	.....
5232	15	7:39	.774	.974	+ 19.4	.....
5255p	17	7:48	.396	.498	+ 1.2	.....
5275p	19	6:52	.767	.965	+ 75.4	.....
5292	20	6:30	.162	.204	−135.2	+123.3
5293	20	7:00	.183	.230	−127.8	+138.1
5294	20	7:31	.204	.257	−129.3	+129.3
5305	21	5:47	0.337	0.424	+ 2.8	.....

Soloviev also gives the magnitude at maximum and the two amplitudes:

$$M = 9.44 \text{ mag.} ; \qquad A_1 = 1.48 \text{ mag.} ; \qquad A_2 = 1.06 \text{ mag.}$$

The minima are sufficiently different to make it certain that the period cannot be twice the observed value. The spectrum is of type A5 or A7 with strong *Ca* II and with rotationally broadened metallic lines. The *H* lines have strong Stark-effect wings, and the star is of moderate luminosity. The spectrum shows two components of very different intensities but of approximately the same spectral type. The star lines are given in Table 23, the radial velocities in Table 24, and the orbital elements in Table 25. Only the velocities of the stronger component are plotted in Figure 11.

TABLE 25

ORBITAL ELEMENTS OF UZ PUPPIS

$P = 0.795$ day (assumed)	T (max. vel.) = phase 0.75 P
$\gamma = +25$ km/sec	$m_1 \sin^3 i = 1.1 \odot$
$K_1 = 150$ km/sec	$m_2 \sin^3 i = 1.1 \odot$
$K_2 = 150$ km/sec	$a_1 \sin i = 1.6 \times 10^6$ km
$e = 0$ (assumed)	$a_2 \sin i = 1.6 \times 10^6$ km

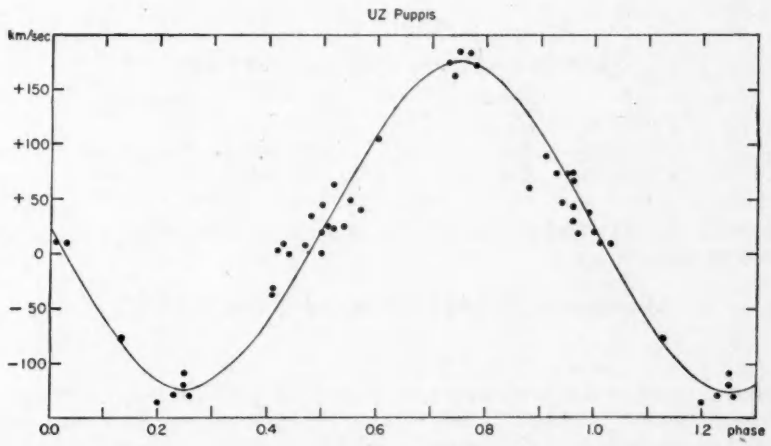

FIG. 11

The distribution of the observations is quite unfavorable. Nevertheless, there is a strong suspicion that the intensities of the lines and even the spectral type vary with the phase. These changes are summarized in Table 26.

The character of the variation resembles that in SW CMa; but there seems to be, in addition, some tendency for *Ca* I 4226 to be relatively stronger when the lines are single. I believe that the spectral class is later at phases 0.0 and 0.50 than at phases 0.25 and 0.75. In this star the duplicities are even less consequential than in SW CMa because of the great difference in the intensities of the components.

VZ HYDRAE

The period as given in Table 1 was derived by the discoverer, D. J. K. O'Connell,[122] who found only one minimum present. In recent years this variable has been observed

[122] *Harvard Bull.*, No. 889, 1932.

extensively by B. Wood at Princeton and by B. Wood and F. E. Roach at the University of Arizona,[123] but the results of this work are not yet available. Table 27 gives the star lines, Table 28 the radial velocities, and Table 29 the orbital elements. The velocity-curve is given in Figure 12. The spectral class is F5; and the lines are double, with components of approximately the same spectral type but of different brightnesses. There seems to be no such anomaly in the intensities of the lines as was observed in UZ Pup and SW Canis Majoris. A plot of the observations with the published period of 1.45 days

TABLE 26

INTENSITIES OF SPECTRAL LINES IN UZ PUPPIS

Feature	Phase			
	0.00	0.25	0.50	0.75
Ca II	Strong, broad	Strong, narrow	Strong, broad	Strong, narrow
Ca I	Strong	Weak	Strong	Weak
Fe I	Moderate	Moderate	Moderate	Moderate

TABLE 27

LIST OF STAR LINES USED FOR VZ HYDRAE

Element	λ	Element	λ	Element	λ
Fe I	4045.82	*Fe* I	4071.75	*Ca* I	4226.73
Fe I	4063.60	*Sr* II	4077.71	*Hγ*	4340.47
Ni II	4067.04	*Hδ*	4101.74		

showed at once that the real period is twice this value. Accordingly, the phases were computed with the elements

$$\text{Minimum} = \text{JD } 2421925.825 + 2.9042998\ E\ .$$

RU CANCRI

The spectral types of the components are given by Wyse (Table 1) as F9 and G9, but the fainter component is observed only during primary eclipse. The most interesting features of this spectrum are fairly narrow and faint emission lines of *Ca* II. These lines belong to the secondary and appear a little strengthened on a well-exposed plate taken during totality. The scatter of the bright-line velocities is too large to allow us to determine even the amplitude of the velocity-curve, but indications are that $K_{Ca\,II}$ is somewhat larger than K_1. Table 30 gives the star lines, Table 31 the radial velocities, and Table 32 the orbital elements. Seven poor spectrograms were omitted from the plot in Figure 13. The photometric orbit was computed by Shapley and, more recently, by Fetlaar. The latter's results are:[124]

$A_1 = 1.53$ mag.	$a_0 = 1.00$	$r_1 = 0.173$
$A_2 = 0.04$ mag.	$L_2 = 0.756$	$r_2 = 0.064$
$D = 0.386$ day	$L_1 = 0.244$	$\cos i = 0.009$
$d = 0.176$ day	$k = 0.37$	$\gamma = 23$

[123] See recent annual reports of the Princeton and Steward observatories in *Publications of the American Astronomical Society*.

[124] *Bull. Astr. Inst. Netherlands*, **6**, 29, 1930.

TABLE 28

RADIAL VELOCITIES OF VZ HYDRAE

Plate G*f*/2	Date 1945	U.T.	Phase		Velocities (Km/Sec)	
			In Days	In Period	I	II
4897	Jan. 24	10:04	1.852	0.638	+ 66.3	− 62.0
4910	25	9:21	2.823	.972	− 1.0	.....
4911	25	10:08	2.855	.983	+ 5.8	.....
4923	26	9:42	0.933	.321	− 82.3	+ 79.8
4936	27	7:51	1.856	.639	+ 72.3	− 90.7
4939p	27	9:11	1.912	.658	+ 71.4	−137.9
4954	28	8:36	2.887	.994	− 1.9	.....
4965	29	8:02	0.959	.330	− 71.3	+ 93.5
4996	31	6:45	0.001	.000	+ 12.6	.....
4997	31	7:12	0.020	.007	+ 4.3	.....
4998	31	7:36	0.037	.013	− 1.7	.....
5012	Feb. 1	9:55	1.133	.390	− 41.8	+ 64.7
5028	2	7:42	2.041	.703	+ 97.4	− 93.9
5029	2	8:07	2.058	.709	+100.3	−125.8
5044	3	6:11	0.074	.025	+ 8.1	.....
5063	5	8:50	2.184	.752	+ 88.4	−109.4
5064	5	9:25	2.208	.760	+ 98.7	−105.1
5083	6	9:08	0.292	.101	− 44.3	.....
5084	6	9:30	0.307	.106	− 55.3	+ 54.7
5102	7	8:47	1.277	.440	− 15.9	.....
5103	7	9:21	1.301	.448	− 11.5	.....
5120	8	7:54	2.240	.771	+ 88.0	−107.1
5121	8	8:26	2.262	.779	+101.6	− 92.3
5138	9	6:12	0.265	.091	− 28.8	.....
5172	11	8:11	2.348	.808	+ 82.9	− 79.3
5173	11	8:38	2.367	.815	+ 68.7	− 82.0
5194	13	8:18	1.449	.499	+ 0.8	.....
5195	13	8:42	1.465	.504	+ 0.7	.....
5212	14	8:21	2.451	.844	+ 71.2	− 63.1
5213	14	8:47	2.469	.850	+ 64.0	− 44.9
5233	15	8:00	0.532	.183	− 78.7	+109.9
5234	15	8:13	0.541	.186	− 78.4	+130.9
5235	15	8:26	0.550	.189	− 76.0	+119.2
5256p	17	8:18	2.545	.876	+ 19.4	.....
5295	20	7:57	2.625	.904	+ 10.3	.....
5296	20	8:16	2.638	.908	+ 20.5	.....
5297	20	8:39	2.654	.914	− 3.8	.....
5306	21	6:29	0.660	0.227	−103.7	+101.5

TABLE 29

ORBITAL ELEMENTS OF VZ HYDRAE

P = 2.9043 days (assumed)
γ = +1 km/sec
K_1 = 93 km/sec
K_2 = 105 km/sec
e = 0 (assumed)
T (min. vel. of br. comp.) = phase 0.25 P
$m_1 \sin^3 i = 1.2 \odot$
$m_2 \sin^3 i = 1.1 \odot$
$a_1 \sin i = 3.7 \times 10^6$ km
$a_2 \sin i = 4.2 \times 10^6$ km

The phases were computed with Nijland's elements

Principal minimum = JD 2422650.720 + 10.172988 E .

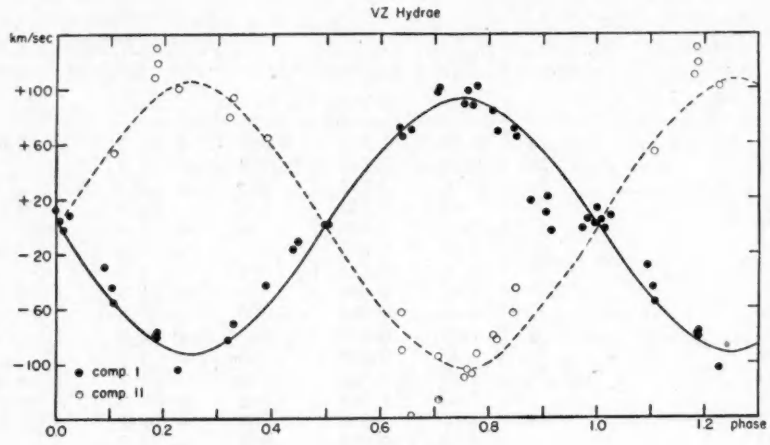

FIG. 12

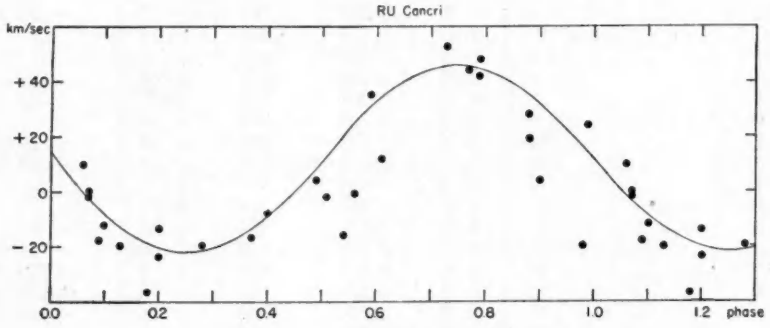

FIG. 13

TABLE 30

LIST OF STAR LINES USED FOR RU CANCRI

Element	λ	Element	λ	Element	λ
Ca II	3933.67	*Hδ*	4101.74	*Fe* I	4383.55
Ca II	3968.47	*Sr* II	4215.52	*Ti* II	4395.04
Fe I	4045.82	*Ca* I	4226.73	*Ti* II	4404.75
Fe I	4063.60	*Fe* I	4260.49	*Ti* II	4415.16
Ni II	4067.04	*Fe* I + *Sc* II	4325.53	*Ca* I + *Fe* I	4435.01
Fe I	4071.75	*Hγ*	4340.47	*Ti* II + *Fe* I	4443.09
Sr II	4077.71	*Fe* II	4351.77	*Mg* II	4481.26

Y LEONIS

The short period and the very deep primary minimum render this star exceptionally interesting. The phases were computed with the elements

Principal minimum = JD 2427164.357 + 1.686076 E

TABLE 31

RADIAL VELOCITIES OF RU CANCRI

PLATE	DATE	U.T.	PHASE		VELOCITIES (KM/SEC)	
			In Days	In Period	Abs.	Ca II Em.
CQ	1944					
3818	Sept. 30	11:50	5.195	0.511	− 2.4	.....
3830	Oct. 1	11:50	6.195	.609	+12.3	.....
3849	4	11:54	9.198	.904	+ 4.5	.....
3864vp	5	11:17	10.172	.000	−40.9	.....
3880p	6	11:02	0.989	.097	−11.8	.....
3898	7	11:51	2.023	.199	−24.3	+ 96.8
3957	13	11:57	8.027	.789	+42.3	− 40.3
3986	15	11:36	10.012	.984	−20.3	.....
3997	16	11:44	0.845	.083	−17.5	.....
4010vp	17	11:31	1.836	.180	−40.4	.....
4027	18	12:00	2.856	.281	−20.3	.....
4096	Dec. 13	9:04	7.869	.774	+44.0	− 76.1
4109	14	11:12	8.958	.881	+28.5	− 48.5
4131	16	8:26	0.669	.066	− 1.5	+ 47.7
4156	17	12:15	1.828	.180	−37.3	+117.9
4186	19	10:51	3.770	.371	−16.9	.....
	1945					
4302	Jan. 6	8:56	1.344	.132	−19.6	+ 47.3
4309vp	8	9:00	3.347	.329	−16.9	.....
4316vp	9	12:20	4.486	.441	−53.8	.....
4320	10	11:59	5.471	.538	−15.8	.....
4331	12	11:52	7.466	.734	+53.3	− 78.2
4337vp	13	12:00	8.472	.833	+43.4	.....
G*f*/2						
4940	27	9:46	2.033	.200	−14.4	.....
4969	29	10:10	4.050	.398	− 8.3	.....
4985	30	9:39	5.028	.494	+ 4.4	+ 28.6
5000	31	8:56	5.998	.590	+34.7	− 33.1
5031	Feb. 2	9:55	8.039	.790	+47.5	− 44.6
5047	3	8:36	8.984	.883	+18.8	.....
5059	4	10:42	10.072	.990	+24.0	+ 38.3
5214vp	14	9:29	9.848	.968	+10.6	+ 16.3
5236	15	8:51	0.649	.064	+10.4	+ 68.5
5237	15	9:23	0.671	.066	− 0.1	+ 12.6
5298	20	9:16	5.666	0.557	− 1.4	.....

TABLE 32

ORBITAL ELEMENTS OF RU CANCRI

$P = 10.173$ days (assumed)

$\gamma = +12$ km/sec

$K_1 = 34$ km/sec

$e = 0$ (assumed)

T (min. vel. of br. comp.) = phase 0.25 P

$$\frac{m_2^3}{(m_1+m_2)^2}\sin^3 i = 0.042 \odot$$

$$a_1 \sin i = 4.8 \times 10^6 \text{ km}$$

without applying heliocentric corrections. These elements were found, by Piotrovski[125] in 1936 and by Zessewitsch[126] in 1943, to give an excellent representation of their observations. My own estimates at the periscopic finder of the 82-inch telescope gave a well-observed minimum on

JD 2431495.863 geocentric = JD 2431495.868 heliocentric .

The corresponding phase is 1.663 days. This places the minimum about half an hour earlier than was predicted from the ephemeris. The photometric orbit has been computed by Mrs. M. B. Shapley and, more recently, by Fetlaar.[127] S. Gaposchkin has adopted the following elements:[128]

$A_1 = 2.97$ mag.	$L_b = 0.93$	$r_2 = 0.25$
$A_2 = 0.05$ mag.	$L_f = 0.07$	$i = 88°.1$
$\alpha_0 = 1.00$	$k = 0.85$	$\gamma = 20.0$

Gaposchkin has predicted a spectral type of G6 for the fainter component. The star lines are given in Table 33, the radial velocities in Table 34, and the orbital element in Table 35. The spectrum is of type A3, with broad *H* lines and with reasonably nar-

TABLE 33

LIST OF STAR LINES USED FOR Y LEONIS

Element	λ	Element	λ	Element	λ
Ca II	3933.67	*Fe* I	4071.75	*Fe* I + *Sc* II	4325.53
Fe I	4045.82	*Sr* II	4077.71	*Hγ*	4340.47
Fe I	4057.44	*Hδ*	4101.74	*Fe* II	4351.77
Fe I	4063.60	*Sr* II	4215.52	*Mg* II	4481.26
Ni II	4067.04	*Ca* I	4226.73		

row metallic lines. Despite the short period, the rotational broadening is not excessive. An effort was made to photograph the spectrum of the secondary with short exposures, using the glass prisms and an *f*/1 Schmidt camera, whose dispersion is one-half of that of the regular *f*/2 camera. The most critical exposure was taken at phase 0.987 P with an expose of 20 minutes. The observed mid-eclipse occurred at phase 0.986 P. Hence, the entire exposure was presumably obtained during totality. The spectrum is underexposed, but there is at least some indication that the *H* lines are weak. There may also be present a few low-temperature lines, such as *Ca* I. But it is impossible to classify the spectrum. My impression is that even on this short exposure there is still some light from the A star or that the spectrum of the secondary is earlier than might have been expected.

The velocity-curve in Figure 14 shows what appears to be a pronounced rotational disturbance between phases 0.95 and 1.05. This is in accord with the total duration of the eclipse, which is given as 6 hours by Dugan.

RW URSAE MAJORIS

The spectral types of the components are dF9 and dG9, according to Wyse,[129] but the fainter component is observed only at principal minimum. Photometric orbits have

[125] *Acta Astr. Cracovie*, **3**, 36, 1936.

[126] *Astr. Circ. Acad. Sci. Soviet Union*, No. 18, 1943.

[127] *Bull. Astr. Inst. Netherlands*, **6**, 29, 1930.

[128] *Variable Stars* ("Harvard Mono.," No. 5), p. 73, Cambridge, 1938.

[129] *Lick Obs. Bull.*, **17**, 39, 1934.

been derived by Shapley and, more recently, by Fetlaar.[130] S. Gaposchkin[128] has adopted the following mean elements:

$A_1 = 1.00$ mag. $\quad L_b = 0.60 \quad r_2 = 0.07$
$A_2 = 0.06$ mag. $\quad L_f = 0.40 \quad i = 84°.2$
$a_0 = 1.00 \quad k = 0.35 \quad \gamma = 12.0$

TABLE 34

RADIAL VELOCITIES OF Y LEONIS

Plate G*f*/2	Date 1945	U.T.	Phase		Velocities (Km/Sec)
			In Days	In Period	
4912	Jan. 25	11:09	0.253	0.150	−36.8
4913	25	11:50	0.281	.167	−26.2
4924	26	10:59	1.246	.739	+68.3
4925	26	11:39	1.273	.755	+72.7
4941	27	10:25	0.536	.318	−43.7
4942	27	10:55	0.557	.330	−59.2
4970	29	10:46	0.865	.513	+16.9
4971	29	11:09	0.881	.523	+20.7
4979	30	4:11	1.590	.943	+32.5
4980	30	4:46	1.615	.958	+51.1
4981	30	5:27	1.643	.974	+53.0
4982p	30	6:23	1.682	.998	−21.6
4983	30	7:17	0.033	.020	−27.8
5001	31	9:36	1.130	.670	+66.4
5002	31	10:05	1.150	.682	+67.2
5003	31	10:36	1.172	.695	+73.4
5032	Feb. 2	10:39	1.488	.883	+44.7
5048	3	9:16	0.744	.441	−13.7
5049	3	10:44	0.805	.477	−18.8
5065	5	10:16	1.100	.652	+63.4
5085	6	9:59	0.402	.238	−50.1
5104	7	10:13	1.412	.837	+51.8
5122	8	9:12	0.683	.405	+ 1.2
5123	8	9:57	0.715	.424	−10.4
5140	9	7:39	1.619	.960	+45.2
5144	9	9:45	0.020	.012	−30.2
5145	9	10:26	0.049	.029	−18.2
5174	11	9:12	0.311	.184	−47.0
5196	13	9:15	0.627	.372	−29.4
5238	15	9:52	0.967	.574	+29.1
5239	15	10:19	0.986	.585	+56.3
5257	17	8:54	1.240	.735	+75.1
5299	20	9:54	0.909	.539	+20.7
5300	20	10:29	0.934	0.554	+29.7

TABLE 35

ORBITAL ELEMENTS OF Y LEONIS

$P = 1.686$ days (assumed)
$\gamma = +10$ km/sec
$K_1 = 60$ km/sec
$e = 0$ (assumed)
T (min. vel.) = phase 0.25 P

$$\frac{m_2^3}{(m_1 + m_2)^2} \sin^3 i = 0.038 \odot$$

$$a_1 \sin i = 1.4 \times 10^6 \text{ km}$$

[130] *Bull. Astr. Inst. Netherlands*, **3**, 195, 1926.

The phases were computed with the elements by Nijland:

$$\text{Principal minimum} = \text{JD } 2418987.405 + 7.328269\ E\ .$$

The spectrum shows two fairly well-marked and narrow emission lines of *Ca* II K and H. These lines belong to the eclipsing star at primary eclipse and have about the same

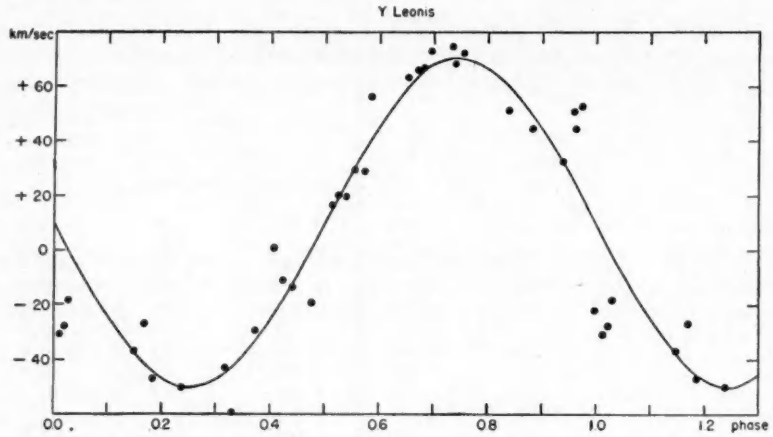

FIG. 14

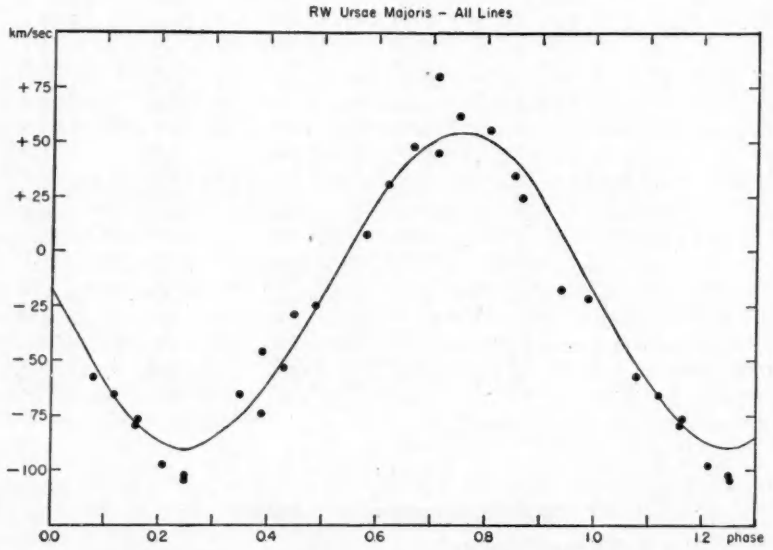

FIG. 15

amplitude as the absorption lines of the brighter component. The star lines are given in Table 36, the radial velocities in Table 37, and the orbital elements in Table 38. The velocity-curve is in Figure 15.

TABLE 36

LIST OF STAR LINES USED FOR RW URSAE MAJORIS

Element	λ	Element	λ	Element	λ
Ca II	3933.67	*Fe* I	4071.75	*Fe* I + *Sc* II	4325.53
Fe I	4045.82	*Sr* II	4077.71	*Hγ*	4340.47
Fe I	4063.60	*Hδ*	4101.74	*Fe* I	4383.55
Ni II	4067.04	*Ca* I	4226.73	*Fe* I	4415.16

TABLE 37

RADIAL VELOCITIES OF RW URSAE MAJORIS

Plate G *f*/2	Date 1945	U.T.	Phase		Velocities (Km/Sec)	
			In Days	In Period	Abs.	Em.
4914	Jan. 25	12:38	6.251	0.853	+ 35.2	.....
4926p	26	12:36	7.250	.989	− 21.0	.....
4943	27	11:38	0.881	.120	− 65.9	.....
4972	29	11:46	2.886	.394	− 45.8	.....
5004	31	11:18	4.867	.664	+ 47.7	.....
5014	Feb. 1	11:54	5.892	.804	+ 56.3	−109.0
5033	2	11:33	6.877	.938	− 17.0	− 71.9
5050	3	11:50	0.561	.077	− 56.8	.....
5060	4	11:54	1.564	.213	− 97.6	.....
5066	5	11:19	2.540	.347	− 65.7	− 54.7
5088	6	12:37	3.594	.490	− 24.8	− 25.2
5105	7	11:19	4.540	.620	+ 31.5	.....
5124	8	10:50	5.519	.753	+ 62.0	.....
5139	9	6:51	6.353	.867	+ 24.4	− 40.6
5175	11	10:01	1.157	.158	− 78.6	.....
5176	11	10:55	1.195	.163	− 76.7	.....
5197	13	10:01	3.157	.431	− 53.1	.....
5198	13	12:49	3.274	.447	− 27.9	.....
5216	14	11:39	4.225	.577	+ 8.1	.....
5240	15	10:59	5.198	.709	+ 45.1	−110.3
5241p	15	11:33	5.221	.712	+ 80.1	−129.3
5277	19	9:33	1.810	.247	−102.2	+ 44.6
5278	19	10:27	1.847	.252	−104.7	+ 41.5
5301	20	11:13	2.879	0.393	− 73.8	+ 55.6

TABLE 38

ORBITAL ELEMENTS OF RW URSAE MAJORIS

$P = 7.328$ days (assumed)

$\gamma = -17.5$ km/sec

$K_1 = 72.5$ km/sec

$K_{Ca\ II\ em} = 72$ km/sec

$e = 0$ (assumed)

T (min. vel. of br. comp.) = phase 0.25 P

$$\frac{m_2^3}{(m_1 + m_2)^2} \sin^3 i = 0.29 \odot$$

$$a_1 \sin i = 7.3 \times 10^6 \text{ km}$$

SS BOOTIS

The spectral type of this star is about dG5 at maximum light and perhaps a little later at principal minimum. The most interesting feature is a pair of very narrow, but strong, emission lines of *Ca* II. These lines belong to the star which is in front at principal minimum. In this respect all four stars whose bright *Ca* II lines have been measured agree perfectly. But in one of them, AR Mon, the eclipsing star is the brighter, while in

TABLE 39

LIST OF STAR LINES USED FOR SS BOOTIS

Element	λ	Element	λ	Element	λ
Ca II em.	3933.67	*Sr* II	4077.71	*Fe* I	4404.75
Ca II em.	3968.47	*Hδ*	4101.74	*Fe* I	4415.16
Fe I	4045.82	*Sr* II	4215.52	*Ca* I + *Fe* I	4435.01
Fe I	4063.60	*Ca* I	4226.73	*Ti* II + *Fe* I	4443.09
Ni II	4067.04	*Fe* I + *Sc* II	4325.53	*Ca* I + *Ca* I	4455.82
Fe I	4071.75	*Fe* I	4383.55	*Mg* II	4481.26

TABLE 40

RADIAL VELOCITIES OF SS BOOTIS

Plate G *f*/2	Date 1945	U.T.	Phase		Velocities (Km/Sec)			
			In Days	In Period	All Lines	λ 4045 I	λ 4045 II	*Ca* II Em.
4944	Jan. 27	12:31	5.435	0.715	−40.8	− 50.2	.....	.....
4973	29	12:39	7.440	.978	−45.2	− 58.7	.....	− 48.4
5005p	31	12:05	1.810	.238	−50.0	− 79.2	+ 7.2	+ 29.7
5006	31	12:43	1.837	.242	−41.4	.....	.....	+ 25.3
5015	Feb. 1	12:45	2.838	.373	−40.4	− 83.4	+40.0	+ 28.9
5034	2	12:36	3.832	.504	−40.7	− 25.9	.....	− 32.8
5067	5	12:29	6.827	.898	−40.2	− 26.2	.....	− 63.7
5086	6	10:51	0.153	.020	−36.0	− 26.2	.....	− 48.9
5087	6	11:45	0.191	.025	−51.0	− 50.9	.....	.....
5106	7	12:29	1.221	.161	− 4.9	− 42.9	.....	.....
5125	8	11:47	2.192	.288	−36.9	− 96.5	+47.5	+ 41.6
5126	8	12:38	2.227	.293	−30.9	− 76.0	.....	.....
5146	9	11:28	3.179	.418	−44.5	− 76.0	.....	− 19.8
5147	9	12:32	3.223	.424	−50.2	− 84.3	+47.3	+ 1.9
5177	11	11:52	5.195	.683	−34.1	− 51.5	.....	−109.9
5178p	11	12:38	5.227	.687	− 7.2	+ 1.9	.....	.....
5199	13	11:42	7.189	.945	−48.3	− 47.6	.....	− 31.6
5200	13	12:34	7.225	.950	−38.0	− 55.9	.....	− 62.7
5217	14	12:34	0.619	.081	−35.5	− 14.9	.....	− 6.2
5242	15	12:10	1.602	.211	−37.1	− 97.4	.....	.....
5243	15	12:44	1.626	.214	−43.7	−101.5	+13.7	+ 25.5
5259	17	12:07	3.600	.473	−37.7	− 60.8	.....	− 24.8
5279	19	11:36	5.578	.733	−68.8	.....	.....	.....
5280	19	12:38	5.621	.739	−23.2	+ 21.2	−94.0	−118.8
5302	20	12:16	6.606	0.868	−57.9	− 36.6	.....	−107.6

the other four—WW Dra, RU Cnc, RW UMa and SS Bootis—it is the fainter component. The absorption lines are strong and sharp. Hence it was a surprise to find that they did not give reliable radial velocities. The lines are probably badly blended. In fact, λ 4045 is clearly double on several plates. Hence, I have remeasured this line alone, with the results given in Table 40. The star lines used for the velocities listed under the heading "All Lines" are given in Table 39. The velocities of λ 4045 show a well-pro-

nounced minimum at phase 0.25 P when $V = -90$ km/sec. But the maximum at phase 0.75 P is indicated by only one velocity at $V = +20$ km/sec. There is no doubt that the lines appear quite differently at these two phases: near 0.25 P they are either clearly double, with a weak component on their red sides, or they are shaded toward the red. Near phase 0.75 P they are almost always single and symmetrical. A priori, it would be possible to explain this in two ways:

a) The orbit is eccentric with ω near 180°, so that the separation is large at phase 0.25 P and small at 0.75 P; or

b) The intensities of the components vary in such a manner that the violet component

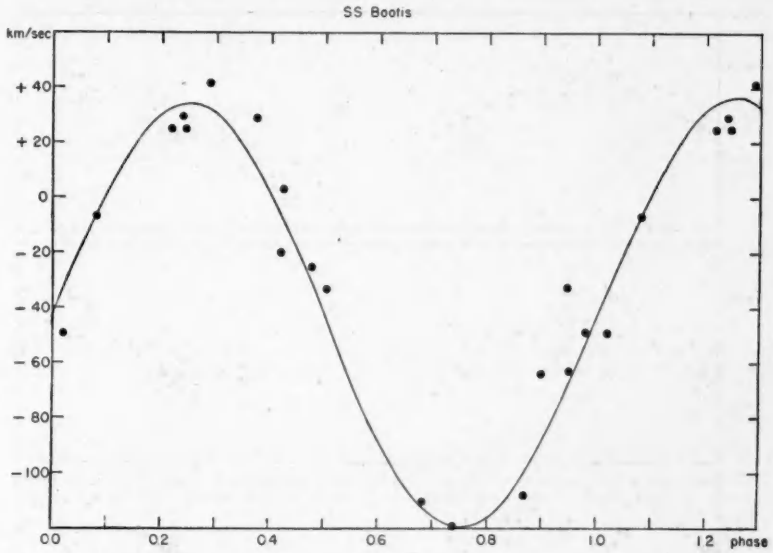

FIG. 16

TABLE 41

ORBITAL ELEMENTS OF SS BOOTIS

P	= 7.606 days (assumed)
γ	= −43 km/sec
$K_{Ca\ II\ em}$	= 77 km/sec
K_1 abs.	= 47 km/sec
K_2 abs.	= 73 km/sec
e	= 0 (assumed)
T (max. vel. of *Ca* II em.)	= phase 0.25 P
$m_1 \sin^3 i$	= 0.83 ⊙
$m_2 \sin^3 i$	= 0.55 ⊙
$a_1 \sin i$	= 4.9×10^6 km
$a_2 \sin i$	= 7.6×10^6 km

is strongest when its velocity is negative; such a strong component would blend with the other component, and we should measure mostly single lines.

Because of the beautifully symmetrical velocity-curve given by the *Ca* II emission lines (Fig. 16), the second hypothesis is probably the correct one. The orbital elements in Table 41 refer to the emission lines. I have added a rough estimate of K_1 and K_2 for the absorption lines.

The phases were computed with the elements by Hoffmeister:

$$\text{Principal minimum} = \text{JD } 2420707.420 + 7.60605\,E\,.$$

Several limiting solutions of the light-curve have been made by Sitterly.[131] These vary greatly among themselves, and Sitterly showed that the problem is almost indeterminate without photometric observations of exceptional accuracy. The spectrographic results suggest that the total luminosities of the components differ by a relatively small amount.

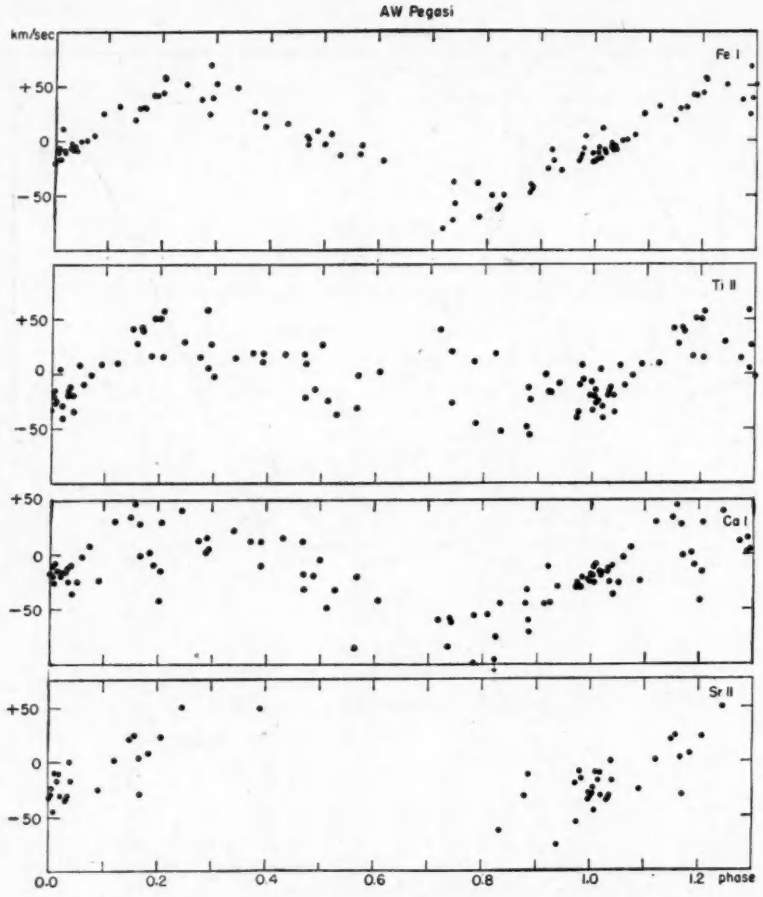

FIG. 17

AW PEGASI

The variability of this star was discovered by Plaut. The light-curve was determined by Jacchia and later by Rügemer,[132] who found a range of 1.26 mag. at principal eclipse. The eclipses are very different in depth, and the spectral type of the secondary should differ appreciably from that of the primary. This is strikingly confirmed by the observations at primary mid-eclipse. They show a spectrum of type approximately F0, with

[131] *Pop. Astr.*, **30**, 231, 1922. [132] *Beob. Zirk.*, **14**, 74, 1932.

sharp lines; but the *Ca* II line is too narrow and weak and is more nearly consistent with a type not later than A5, while the *H* lines are also too weak, resembling the lines in the late F stars; *Sr* II is not especially strong, and the spectrum does not resemble that of a supergiant. This spectrum lasts between phases 0.996 P and 0.020 P. On both sides of these phases it is gradually transformed into a spectrum of class A2 with many, rather broad lines suggestive of large rotation or considerable turbulence. The *H* lines and *Ca* II K are especially strong. There are 19 members of the Balmer series, which places the star in the main sequence. The phases at which the spectrum is completely transformed may best be estimated from Figure 17, in which the velocity of the *Sr* II

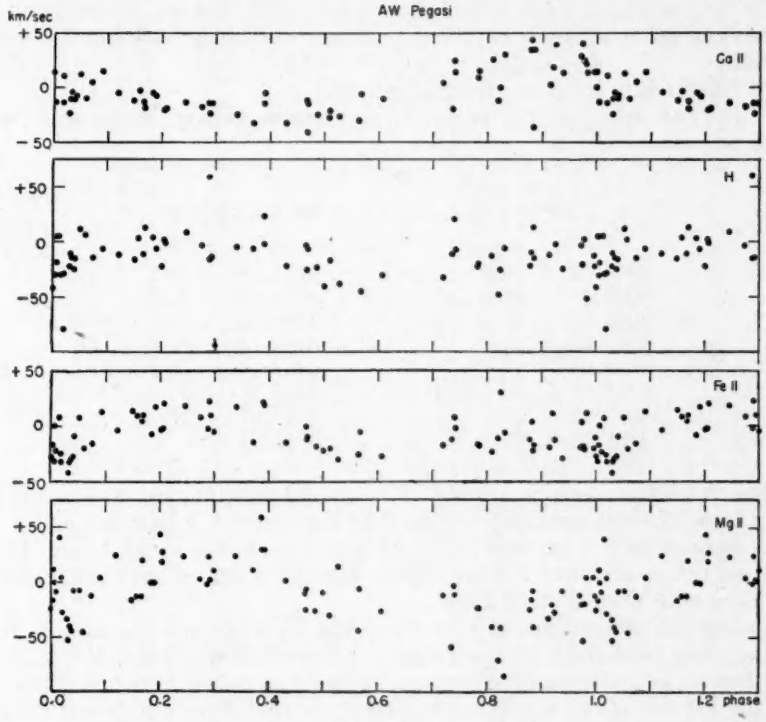

FIG. 18

lines are plotted. These lines were measured fairly regularly between phases 0.83 P and 0.24 P. These values should be approximately correct. The spectroscopic data then give:

Duration of pure F0 spectrum	6 hours
Duration of mixed F0 + A2 spectrum	99 hours
Middle of F0 spectrum	phase 0.08 P
Middle of mixed spectrum	phase 0.07 P

The phases were computed with the elements by Rügemer:

$$\text{Principal minimum} = \text{JD } 2426543.480 + 10.62228\ E\ .$$

We see at once that the duration of the pure F0 spectrum may well be identified with the duration of total eclipse, but the duration of the blended spectrum extends way beyond the limits of partial eclipse. The systematic displacement of the middles of the two intervals may be due to a small error in the photometric elements.

Table 42 lists the star lines of AW Peg, and Table 43 the radial velocities. It was evident from the beginning of this work that different lines gave different velocity-curves. The difference between *Fe* I and *Ca* II is especially striking. The line λ 3933 of *Ca* II is very strong and sharp and should give reliable results. Yet the velocity-curve is quite different from that of the *Fe* I lines. The latter came from that component of the binary which is in front during the principal eclipse. Curves similar to that of *Fe* I are given by *Ca* I, *Ti* II, and *Sr* II. They have a pronounced maximum at phase 0.25 P and a minimum at phase 0.75 P. The systematic difference between *Ca* I and *Fe* I is due to blending of *Ca* I. The range is about 100 km/sec. The line of *Ca* II shows a range of only about 50 km/sec, with a minimum at or near phase 0.45 P and a maximum at about 0.9 P. The lines of *Mg* II, *Fe* II, and *H* show intermediate curves. It is difficult to interpret these differences satisfactorily. The principal results derived from this study are the following:

1. The F0 star is in front at principal eclipse.

2. All lines corresponding to low excitation energies belong, in the main, to the F0 star in all phases.

TABLE 42

LIST OF STAR LINES USED FOR AW PEGASI

Element	λ	Element	λ	Element	λ
Ca II	3933.67	*Fe* II	4173.45	*Fe* I	4383.55
Fe I	4005.25	*Fe* II	4178.34	*Ti* II	4395.04
Fe I	4045.82	*Sr* II	4215.52	*Fe* I + *Ti* II	4404.75
Fe I	4063.60	*Ca* I	4226.73	*Fe* I + *Ti* II	4415.16
Ni II	4067.04	*Fe* II	4233.16	*Ca* I + *Fe* I	4435.01
Fe I	4071.75	*Fe* I + *Sc* II	4325.53	*Ti* II + *Fe* I	4443.09
Sr II	4077.71	*Hγ*	4340.47	*Mg* II	4481.26
Hδ	4101.74	*Fe* II	4351.77		

3. Those A2 features which are absent in the F0 star, namely, the broad *H* wings, disappear completely at principal eclipse, showing that this eclipse is total.

4. The lines of *Fe* I, *Ca* I, and *Ti* II which belong, in the main, to the F0 star are sharp during the total eclipse but are diffuse during the rest of the cycle; this may suggest blending with lines of the A2 star.

5. At phase 0.5 P the lines of *Fe* I, *Ca* I, and *Ti* II are not appreciably weakened, though they may be slightly narrower than at phases 0.25 P and 0.75 P. The persistence of these lines at secondary eclipse may mean that this eclipse is not total and that the light of the F0 star is not appreciably reduced, or that these lines originate in the A2 star with an intensity comparable to that observed in the blended spectrum.

6. The lines of *Fe* II are probably mostly produced in the A2 star; they are relatively weak during totality and are quite strong outside of eclipse. But the velocity-curve given by *Fe* II has an abnormally small range and is, besides, somewhat unsymmetrical. Since the curves of *Fe* I, *Ca* I, and *Ti* II are completely symmetrical (though opposite in phase), I believe it is preferable to suppose that the orbit is circular and that the asymmetry of the curve from *Fe* II is due to a distortion of these lines.

7. It would be tempting to suppose that the distortion is due to blending with lines of the F0 star. But this is not possible, since the *Fe* II lines of the F0 star are relatively much fainter than the lines of *Fe* I, *Ca* I, and *Ti* II. Hence, the blending effect should influence the latter lines much more than *Fe* II, but we have already seen that they belong in the main to the F0 star.

8. The *H* lines are strong and have well-defined cores. Measurements of these lines should be quite reliable. The velocity-curve shows little, if any, change in velocity with phase. This could conceivably be due to blending, because the *H* lines of the F0 star, though weak, are narrow and deep and might be able to influence the measurements.

TABLE 43

RADIAL VELOCITIES OF AW PEGASI

Plate CQ	Date 1944	U.T.	Phase in Period	*Ca* II	*Fe* I	*Sr* II	*H*	*Fe* II	*Ca* I	*Ti* II	*Mg* II	*Ni* II
3720...	Sept. 11	6:14	0.001	+15	−19	−32	−41	−27	− 18	−33	−24	.....
3948...	Oct. 13	3:44	.004	−13	−17	−29	−29	−32	− 20	−21	−16	.....
3721...	Sept. 11	6:58	.004	.....	−11	−23	+ 5	−17	− 11	−15	+12	.....
3722...	11	7:52	.007	.....	− 6	−44	−18	+ 1	− 26	−27	0	.....
3723...	11	8:56	.011	.....	−16	− 9	+ 5	−23	− 8	−25	− 8	.....
3724...	11	9:50	.015	.....	+12	−17	−29	+ 8	− 15	+ 4	+41	.....
3784...	22	1:45	.019	+11	− 8	−10	−79	−26	− 19	−29	+ 4	.....
3630...	Aug. 21	5:10	.020	−13	−11	−31	−28	−32	− 17	−40	−28	.....
3785...	Sept. 22	4:54	.031	−23	− 7	−34	−22	−42	− 16	−20	−33	.....
3632...	Aug. 21	8:14	.032	−10	− 2	−33	−10	−32	− 13	−16	−52	.....
3633...	21	9:07	.035	− 4	− 8	−31	−14	−29	− 25	−12	−40	.....
3634...	21	10:00	.039	−10	− 5	0	−24	−27	− 10	−20	−44	.....
3635...	21	10:52	.042	− 7	− 8	−17	−16	− 8	− 36	−34	− 7	.....
3678...	Sept. 1	4:18	.052	+13	0	.....	+12	+ 8	− 25	+ 8	− 7	.....
3833...	Oct. 3	2:50	.059	− 9	+ 1	.....	+ 7	−20	− 2	−10	−45	.....
3684...	Sept. 1	10:02	.074	+ 5	+ 6	.....	−14	−15	+ 7	− 1	−12	.....
3963...	Oct. 14	2:16	.092	+15	+25	−25	− 6	+13	− 24	+ 9	+ 5	.....
3639...	Aug. 22	7:18	.122	− 4	+32	+ 2	−11	− 3	+ 30	+10	+25	.....
3842...	Oct. 4	2:17	.151	−12	+19	+21	−15	+14	+ 34	+42	−16	.....
3691...	Sept. 2	7:16	.158	− 3	+30	+24	+ 4	+ 9	+ 46	+28	−12	.....
3694...	2	9:36	.167	−12	+31	+ 4	−11	+ 5	+ 28	+42	−12	.....
3695...	2	10:06	.169	−18	+30	−29	+13	+11	− 1	+39	+21	.....
3977...	Oct. 15	2:06	.185	− 4	+42	+ 8	+ 4	− 7	+ 2	+16	0	.....
3726...	Sept. 13	6:52	.192	− 7	+42	.....	− 6	+18	− 9	+51	0	.....
3727p..	13	9:36	.202	.....	+44	.....	−22	− 3	− 42	+51	+44	.....
3728p..	13	10:10	.205	−20	+58	.....	+ 2	− 2	− 16	+15	+20	.....
3793...	24	1:36	.207	−19	+57	+23	− 1	+21	+ 29	+57	+28	.....
3853...	Oct. 5	2:41	.246	−13	+52	+51	+ 9	+19	+ 40	+29	+24	.....
3734...	Sept. 14	4:14	.275	−17	+38	.....	− 3	+ 9	+ 13	+15	+ 4	.....
3737...	14	7:28	.288	−14	+24	.....	+60	− 2	+ 2	+58	− 1	.....
3989...	Oct. 16	4:50	.290	−23	+69	.....	−16	+23	+ 15	+ 6	+24	.....
3739...	Sept. 14	8:56	.294	−14	+39	.....	−13	+10	+ 5	+27	+ 3	.....
3741p..	14	10:29	.300	.....	+52	.....	−95	− 4	.....	− 2	+12	.....
3869...	Oct. 6	2:26	.339	−25	+49	.....	− 4	+18	+ 22	+14	+24	.....
4003...	17	1:37	.372	−32	+27	.....	− 6	−14	+ 12	+19	+12	.....
3749vp.	Sept. 15	8:36	.387	.....	.....	.....	.....	.....	.....	.....	+60	.....
3750...	15	9:10	.389	−14	+25	.....	+24	+22	+ 12	+11	+31	.....
3751...	15	9:40	.391	− 5	+13	+49	− 2	+19	− 10	+19	+31	.....
3886...	Oct. 7	2:09	.432	−32	+16	.....	−22	−13	+ 15	+18	+ 2	.....
3758...	Sept. 16	4:58	.467	−11	+ 3	.....	− 3	0	+ 12	+18	− 9	.....
4015...	Oct. 18	2:19	.469	−41	− 3	.....	−25	−12	− 18	−22	−25	.....
3759...	Sept. 16	5:38	.469	−14	+ 2	.....	− 6	− 9	− 32	+10	− 5	.....
3647...	Aug. 26	4:14	.487	−24	+ 9	.....	−23	−18	− 19	−14	−26	.....
3651...	26	8:00	.501	−27	− 3	.....	−40	−22	− 5	+27	− 9	+24
3653...	26	10:44	.512	−21	+ 6	.....	−16	−20	− 48	−24	−30	.....
3902...	Oct. 8	2:31	.527	−26	−13	.....	−38	−29	− 32	−37	+15	+ 7
3760...	Sept. 17	5:44	.564	−30	−12	.....	.....	−25	− 85	−31	−43	.....
3761...	17	6:27	.567	− 6	− 4	.....	−45	− 5	− 21	− 1	− 5	.....
3657...	Aug. 27	10:52	.607	−10	−18	.....	−30	−27	− 42	+ 2	−26	.....
3914...	Oct. 10	3:11	.719	+ 4	−80	.....	−32	−17	− 59	+41	−11	.....
3266...	June 15	11:10	.736	−19	−72	.....	−11	−12	− 84	.....	−58	.....
3765...	Sept. 19	2:19	.739	+24	−37	.....	+21	+ 8	− 58	+21	− 2	.....
3766...	19	3:04	.742	+15	−57	.....	− 7	− 2	− 61	−26	−11	.....
3810...	30	4:39	.783	+10	−38	.....	−22	−16	− 98	+12	−23	.....
3811...	30	5:07	.785	+16	−69	.....	−20	−18	− 55	−44	−23	.....
3927...	Oct. 11	1:56	.808	+25	−50	.....	−12	−23	− 55	.....	−40	.....
3274...	June 16	8:57	0.821	−12	−62	.....	−48	−11	−148	+19	−70	.....

TABLE 43—*Continued*

Plate CQ	Date 1944	U.T.	Phase in Period	*Ca* II	*Fe* I	*Sr* II	*H*	*Fe* II	*Ca* I	*Ti* II	*Mg* II	*Ni* II
3701p..	Sept. 9	9:12	0.824	0	−59	.....	−25	+31	− 75	.....	−40	.....
3773...	20	2:04	.832	+30	−49	−62	− 6	− 6	− 44	−52	−84	.....
3822...	Oct. 1	4:52	.878	+35	−48	−31	−22	−12	− 45	−48	−24	− 1
3661...	Aug. 30	9:00	.882	+44	−39	.....	−10	+ 4	− 32	−12	−15	.....
3662...	30	9:33	.884	−35	−44	.....	+13	−22	− 60	−55	− 7	.....
3825...	Oct. 1	6:55	.886	+35	−42	−11	−15	−17	− 70	−23	−40	.....
3709...	Sept. 10	7:44	.913	+ 3	−26	.....	−11	−19	− 44	0	−32	.....
3711p..	10	9:25	.920	+18	− 8	.....	.....	+12	− 11	−16	−20	.....
3777...	21	1:36	.924	+39	−18	.....	− 2	−12	− 44	−17	−27	.....
3625...	Aug. 20	8:24	.938	+14	−27	−76	−24	−29	− 28	− 8	− 7	.....
3670...	31	7:52	.972	+29	−18	−19	− 3	−19	− 29	−40	−11	.....
3671...	31	8:32	.974	+41	−16	−54	−20	+ 4	− 25	−34	−19	.....
3672...	31	9:14	.977	+25	−12	.....	+ 2	−18	− 29	−10	−52	.....
3673...	31	9:58	.980	+22	− 7	− 8	+ 2	−21	− 29	+ 8	−19	.....
3674...	31	10:44	.983	+13	+ 5	−16	−51	+12	− 21	− 5	+ 5	.....
3718...	Sept. 11	4:59	.996	+15	−12	−34	−13	−20	− 22	−20	+ 5	.....
3719...	11	5:33	0.998	0	−19	−28	−22	−10	− 25	− 7	−12	.....

9. Perhaps the most confusing feature of the spectrum outside of eclipse consists of the fact that the lines of *Fe* I, *Fe* II, *Ti* II, *Ca* I, *Mg* II, etc., all look exactly alike in contour, so that it is tempting to attribute them all to the same source.

10. Since it is not possible with the present material to reconcile these inconsistencies, I believe we can only rely, with some degree of probability, upon the lines of *Fe* I, *Ca* I, and *Ti* II for giving us the velocity-curve of the F0 star. The corresponding elements are given in Table 44.

TABLE 44

ORBITAL ELEMENTS OF AW PEGASI FROM Fe I LINES

$$P = 10.622 \text{ days (assumed)}$$
$$\gamma = 0 \text{ km/sec}$$
$$K_2 = 50 \text{ km/sec}$$
$$e = 0 \text{ (assumed)}$$
$$T \text{ (max. vel. of F0 star)} = \text{phase } 0.25\ P$$
$$\frac{m_1^3}{(m_1 + m_2)^2} \sin^3 i = 0.14\ \odot$$
$$a_2 \sin i = 7.3 \times 10^6 \text{ km}$$

SYSTEMATIC ERRORS

Because the dispersion used in this work was smaller than that employed in most radial-velocity measurements, I have measured a number of spectrograms of two standard stars—α Persei and β Geminorum—obtained with the same instrumental settings and at the same time as the spectrograms of eclipsing variables. The velocities adopted by J. H. Moore for these stars are:

α Per: $V = -2.4 \pm 0.1$ km/sec
β Gem: $V = +3.3 \pm 0.0$

The results of my measurements are given in Table 45, and the lines used in these stars in Table 46. The lines do not all give consistent results. For example, λ 4005 in α Per gives too large a positive velocity. But it did not seem advisable to adjust the wave lengths. Blends undoubtedly cause serious errors in the wave lengths. Since the values used in Table 46 are essentially the same as those used for the eclipsing variables, the

systematic errors derived here are probably characteristic of the entire work. These errors are:

α Per, G *f*/2 series: McDonald-Moore = +3.3 ± 0.6 km/sec
α Per, CQ series: McDonald-Moore = −0.7 ± 0.4
β Gem, CQ series: McDonald-Moore = +0.3 ± 0.5

TABLE 45

RADIAL VELOCITIES OF α PERSEI

Plate G*f*/2	Date 1945	U.T.	Velocities (Km/Sec)	Plate G*f*/2	Date 1945	U.T.	Velocities (Km/Sec)
5017	Feb. 2	1:14	+12.8	5244	Feb. 16	1:09	− 2.1
5035	3	1:02	+ 3.4	5245	16	1:12	+ 2.0
5051	4	0:55	−13.6	5260	18	1:05	− 4.9
5052	4	0:58	− 1.3	5261	18	1:06	− 6.0
5068	6	1:02	+ 3.7	5262	18	1:07	+ 1.2
5069	6	1:04	+ 2.2	5281	20	1:09	− 0.8
5070	6	1:06	+ 6.9	5282	20	1:12	− 4.9
5089	7	1:02	+ 4.3	5283	20	1:14	+ 3.7
5090	7	1:04	+ 4.0				
5091	7	1:06	+ 4.8	Mean	.....	.....	+ 0.9±0.55
5107	8	1:02	− 1.7				
5108	8	1:04	− 1.7	Plate CQ	Date 1944	U.T.	Velocities (Km/Sec)
5109	8	1:06	− 1.2				
5127	9	1:04	− 2.2	3892	Oct. 7	7:32	− 4.9
5128	9	1:05	− 1.3	3893	7	7:43	− 4.2
5148	10	1:03	+ 0.3	3918	10	6:55	+ 0.5
5149p	10	1:06	+ 8.3	3932	11	6:05	− 4.2
5150	10	1:08	− 1.9	3940	12	10:16	− 4.4
5159	11	1:01	+ 2.7	3953	13	8:39	− 2.3
5160	11	1:03	+ 2.3	3981	15	7:49	− 2.4
5161	11	1:05	+12.3	3982	15	7:51	− 0.1
5179	13	1:00	− 1.3	3992	16	8:08	− 3.7
5180	13	1:02	+ 2.0	3993	16	8:10	− 3.3
5181	13	1:04	− 0.8	4020	18	5:51	− 4.8
5201	14	1:04	− 0.1	4021	18	5:53	− 3.0
5202	14	1:06	+ 2.0				
5203	14	1:08	− 3.1	Mean	.....	.....	− 3.1±0.34
5218	15	1:08	+ 4.0				

RADIAL VELOCITIES OF β GEMINORUM

Plate CQ	Date 1944	U.T.	Velocities (Km/Sec)	Plate CQ	Date 1944	U.T.	Velocities (Km/Sec)
3899	Oct. 7	12:32	+ 4.3	3988	Oct. 15	12:38	+ 7.9
3943	12	12:39	+ 3.2	3999	16	12:30	+ 3.3
3958	13	12:34	+ 1.3	4028	18	12:35	+ 2.5
3959	13	12:36	+ 0.3	4029	18	12:37	+ 2.9
3972	14	12:38	+ 8.0				
3987	15	12:36	+ 2.3	Mean	.....	.....	+ 3.6±0.54

The corresponding corrections have not been applied to the measurements. It should be remembered that the lines of most eclipsing binaries are much broader than those of α Per and that the blends may be somewhat different.

As a measure of the precision of each series we find: a probable error of one plate of

α Per in G *f*/2 series = ± 3.3 km/sec ;

a probable error of one plate of

$$\alpha \text{ Per in CQ series} = \pm 1.2 \text{ km/sec} ;$$

and a probable error of one plate of

$$\beta \text{ Gem in CQ series} = \pm 1.8 \text{ km/sec} .$$

TABLE 46

LIST OF STAR LINES USED FOR α PERSEI

Element	λ	Element	λ	Element	λ
Fe I	4005.25	*Sr* II	4077.71	*Fe* I + *Sc* II	4325.41
Fe I	4045.82	*Hδ*	4101.74	*Hγ*	4340.48
Fe I	4063.60	*Sr* II	4215.52	*Fe* II	4351.77
bl	4067.11	*Ca* I	4226.73		
Fe I	4071.75	*Fe* II	4233.16		

LIST OF STAR LINES FOR β GEMINORUM

Element	λ	Element	λ	Element	λ
Fe I	4005.25	*Fe* I	4143.88	*Fe* I + *Sc* II	4325.41
Fe I	4045.82	*Sr* II	4215.52	*Fe* I	4383.55
Fe I	4063.60	*Ca* I	4226.73	*Fe* I + *Ti* II	4404.75
Fe I	4071.75	*Fe* I	4271.78	*Fe* I + *Ti* II	4415.16

CONCLUSIONS

Out of the profusion of observational results secured in the past few years on the spectra of eclipsing variables there emerge several phenomena which appear to me to be of major importance. Most of the questions which I discussed in the beginning of this paper can be related to one of these major phenomena. It is possible that the first and the second may later be found to be produced by the same cause, but there is no such evidence available now.

1. The occurrence of rapidly moving streams of gas in close binary systems is not a rare phenomenon; it manifests itself in the form of emission lines, of absorption lines which are seen to be superposed over the normal stellar absorption lines, or of distortions in the velocity-curves produced by lines which cannot be seen as distinct features on top of the stellar lines. These streams show certain regularities in respect to direction of motion, intensity of lines, etc. There are few, if any, criteria to predict which stars are most likely to show these effects. Among eclipsing variables chosen at random, we may expect, perhaps, one star out of eight or ten to show some easily observable manifestation of these streams.

2. Periodic variations in the line intensities of binary components may be related to such effects as reflection and gravity, and there is a strong suspicion that the spectral type may be slightly different at different phases. This type of variation is most easily observed in double-lined binaries, but this is perhaps due only to the greater ease with which comparisons can be made in these objects. It is difficult to estimate the frequency of such variable-line binaries.

3. Stars chosen either because they fall outside the area defined by the relation between K and P and by $P_{\min}$ = constant or because they have a large eccentricity with a short period are likely to have unusual spectra. For values of P which are smaller than the limiting value established for normal stars and for binaries of abnormally large eccentricity the spectra must correspond to the characteristics of underluminous stars.

4. There is some indication that the bright lines of *Ca* II do not originate in streams which are detached from the two stellar bodies but are produced in the atmosphere of

one of the components. The fact that these components are sometimes seen with great intensity at principal mid-eclipse certainly[99] suggests that they are produced even in that hemisphere of the eclipsing component which is turned away from the eclipsed component. Lack of appreciable broadening or doubling precludes their coming from a nebulous layer of dimensions comparable to the radius of the star. It is more probable that we are here concerned with a reversal whose origin may not be very different from the origin of the reversals in the *Ca* II lines observed on the disk of the sun.

5. The origin of the bright lines of *H* must be entirely different from that of *Ca* II lines and must be related to the small optical depth for continuous absorption in the gaseous streams. It is instructive to find that in many systems the streams produce only absorption lines, while in others (RW Per) the emission lines make their appearance only during the eclipse.

6. The principal result which we have obtained is the recognition of the complexity of the absorption lines in several binaries. Theories of line formation must be applied with great caution to these peculiar spectra, and it is important that we should realize that it is often impossible to conclude from the appearance of a line that it represents the superposition of a normal stellar absorption line and of a line produced in a gaseous stream high above the reversing layer. In RW Per the emission lines appear only during the eclipse (except *Ha*). There must be other binaries in which the emission lines are never observed because the inclination may not be sufficient to produce a deep eclipse. It is possible that if we should apply to the lines of such a star the usual formulae of radiative transfer in a reversing layer the conclusions would be erroneous. It is tempting to try to speculate on the relative equivalent widths of the *H* absorption and emission lines. If we disregard cyclic processes and consider only a two-state problem, within a "thin" shell, then the absorption line will predominate so long as the radius of the shell is comparable to the radius of the star. But in large shells the two equivalent widths should be approximately the same: were it not for the rotation of the shell, the emission line would exactly fill in the absorption line, and no trace of the shell would appear in the spectrum. It is only because of the Doppler effect that we observe the emission lines. These considerations might suggest that our spectrograms would give us no indication of any *extended stationary atmospheres* whose projected diameters were smaller than the slit of the spectrograph and in which the assumptions we have made were realized.

7. It should be pointed out that the various spectroscopic anomalies which have been discussed in this paper are not the usual thing among spectroscopic binaries. Although these anomalies are not infrequent, the great majority of close systems have probably normal spectra.

I am indebted to Dr. Carlos U. Cesco and Dr. Jorge Sahade for many of the spectrograms in the CQ series used in this work, especially those of AW Peg. Mr. Armin J. Deutsch has taken several spectrograms of RU Cnc and SW CMa. The members of the Yerkes Observatory computing bureau have assisted with the reductions and with the diagrams. To Dr. S. Gaposchkin and Dr. C. Payne-Gaposchkin I am grateful for valuable information concerning the light-curves of several stars. Professor R. Prager of Harvard Observatory has very kindly furnished numerous references to the literature on eclipsing variables.

SPECTROSCOPIC OBSERVATIONS OF THE ECLIPSING VARIABLE WX CEPHEI*

JORGE SAHADE AND CARLOS U. CESCO
Yerkes and McDonald Observatories
Received May 2, 1945

ABSTRACT

The system of WX Cephei is formed by two stars of about equal dimensions, one of them of type A2 and the other of perhaps a slightly later A type. The range in velocity is about 180 km/sec for both stars, and $\gamma \sim 0$ km/sec. It was assumed that $e = 0$ and $P = 3.37843$ days. This system is extremely interesting because its spectrum shows double lines which change in intensity through the different phases.

WX Cephei = BD+62° 2091 (8.6 mag.) = AG Hels 13234 (9.0 mag.) = HD 213631 (Sp. A0; $\alpha = 22^h27^m8$, $\delta = +63°0'$ [1900.0]) was known to be a short-period variable since the announcement by Schneller[1] in May, 1928. The discovery was made on Babelsberg plates, and the provisional designation was 242.1928. Forty observations by Zessewitsch[2] in August, 1928, did not show a change in light but left the possibility open that the star belongs to the Algol-type group. This assumption was completely confirmed by a light-curve published three years later by Schneller,[3] who gave the following elements:

Period[4]	3.3777 days	k (ratio of the radii of the stars)	1.0
Time of minimum	JD 2425088.524	$r_{1,2}$ (radius of the components)	0.24
Duration of eclipse	12.4 hours	i (inclination of the orbit)	90°
Duration of totality	0 hour	J_f/J_b	1/1.176
Magnitude at maximum	8.80 mag.	L_f	0.46
Principal range	0.89 mag.	L_b	0.54
Secondary range	0.70 mag.	$\bar{\rho}_{1,2}$ (density of the components)	0.043 ⊙
α_0 (fraction of area of the primary star eclipsed at principal mid-eclipse)	1.0	m_f	9.69 mag.
		m_b	9.50 mag.

New photometric observations by Himpel[5] indicated that the primary range is 0.48 mag. and that the secondary is 0.38 mag.

In 1934 the determination of a photographic and a photovisual light-curve of WX Cephei was undertaken at Harvard by S. Gaposchkin.[6] The observations led him to the conclusion that Schneller's period should be increased, and he gave for the time of primary minimum the value

$$\text{JD } 2427743.969 + 3.37843\,E.$$
$$\pm 0.085 \quad \pm 0.00015$$

Gaposchkin's observations indicate that the secondary minimum has a depth of 0.38 mag. photographically and 0.33 mag. photovisually, but they were not well enough distributed to give a good indication of the depth of the principal minimum. Nevertheless, in his paper Gaposchkin assumed that the depths of both minima are the same. He also

* *Contributions from the McDonald Observatory, University of Texas*, No. 111.

[1] *A.N.*, **233**, 42, 1928; Schneller's first light-elements were published in *Beob. Zirk.*, **10**, 92, 1928, and *A.M.*, **234**, 377, 1929.

[2] *Veränderliche Sterne*, Vol. 1, No. 5, Nishni-Novgorod, U.S.S.R., 1928.

[3] *Veröff. Berlin-Babelsberg*, **8**, Part VI, 31, 1931.

[4] The first published period was 1.6895 days.

[5] *A.N.*, **252**, 63, 1934.

[6] *Harvard Bull.*, No. 898, 1935.

PLATE VIII

SPECTRUM OF THE PRIMARY STAR OF THE SYSTEM WX CEPHEI (TYPE A2) AT PHASE 1.736 DAYS

PLATE IX

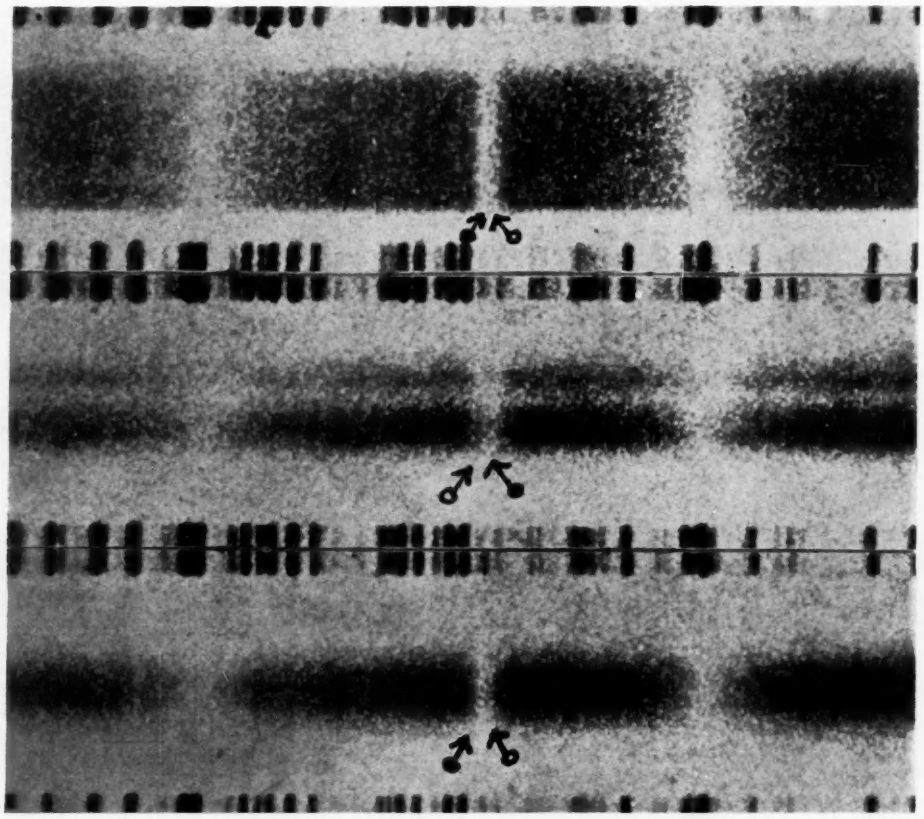

SPECTRA OF WX CEPHEI TAKEN AT PHASES 0.408, 0.906, AND 1.368 DAYS, RESPECTIVELY

This reproduction shows the region of λ 3930 taken in the interval between primary and secondary minimum of light; the violet component of *Ca* II K belongs to the primary star (type A2) and the red component to the secondary star.

The plate illustrates the changes in line intensities which are presented in a schematic form in Fig. 2. The symbol ♂ indicates the strong component; ♂, the weak component.

found that the magnitude at maximum is 9.09 mag. photographically and 9.18 mag. photovisually and that "the color index is sensibly constant, with a value of −0.05 mag."

All the photometric observations, then, indicate that WX Cephei is a system of two stars having almost the same dimensions and surface brightnesses.

THE OBSERVATIONS

For the purpose of determing the spectroscopic orbit of WX Cephei (which is included in Dugan's *Finding List*[7] with the indication "important for radial velocity observation") the star was observed during the months of August, September, and October, 1944, with the 82-inch reflecting telescope of the McDonald Observatory. Sixty spectrograms were obtained during this period, and they cover eighteen consecutive cycles of the variable. All the exposures were made on Eastman 103a-O emulsion, using the quartz Cassegrain spectrograph and the 500-mm camera—a combination which gives a linear dispersion of 55 A/mm at $H\gamma$. The slit width was always 0.075 mm; and the exposure time at maximum light of the order of 45 minutes, in fair seeing.

THE SPECTRUM

At maximum light the spectra of WX Cephei show both components of the system, the primary being of about type A2 and the secondary perhaps of a slightly later A type. The latter is in front at primary minimum.

The classification of the primary component was made by examining the plate CQ 3774 (Pl. VIII) taken at phase 1.736 days, that is, about one hour after secondary minimum of light; and the criterion used was the relation $(H + H\epsilon)/K$. The spectral type of the secondary component seems to be later than the type of the primary star, because on the spectrograms on which the K lines belonging to both stars are separated, the line for the A2 star is sharper. Unfortunately, we have not been able to obtain a spectrogram showing the pure spectrum of the secondary star.

Besides the fact that the spectrum of WX Cephei shows double lines, there is a remarkable phenomenon connected with the intensities of the *Ca* II K line of both components, which has not, thus far, been observed in an eclipsing system. The spectroscopic material available to the writers shows quite definitely that these intensities undergo periodic changes (Pl. IX). No attempt has been made to give numerical estimates of the intensities, because the spectrograms are quite different in quality. Despite this and despite the fact that on the plates taken in the intervals of phases 1.590–1.930 and 3.122–3.347 days, it is impossible to distinguish the two components; the spectrograms undoubtedly show that the phenomenon is symmetrical, an increase in the intensity of one of them corresponding to a decrease in the intensity of the other and the maximum intensity of one corresponding to the minimum intensity of the other.

It seems safe to summarize the changes as follows:

a) The components of the *Ca* II K line belonging to both stars are equal in intensity at about phases 0.6, 1.3, 2.0, and 3.0 days;

b) The K line of the A2 star is relatively the stronger in the intervals 3.0–0.6 and 1.3–2.0 days, while the K line belonging to the secondary star is the stronger in the intervals 0.6–1.3 and 2.0–3.0 days;

c) The K line of the A2 star reaches maximum intensity at both minima of the light-curve (on the plate CQ 3774, taken almost at secondary minimum, which shows only the spectrum of the A2 star, the K line is much stronger than on any other spectrogram);

d) The K line of the secondary star reaches maximum intensity at about the phases of maximum and minimum velocity.

The *H* lines, which also appear double, seem to indicate that they follow the variations observed in the *Ca* II K line.

[7] *Contr. Princeton U. Obs.*, No. 15, p. 28, 1934.

THE RADIAL VELOCITIES

On our spectrograms the only line suitable for radial velocity measurements is the K line of *Ca* II. The *H* lines do not always show the doubling as distinctly as does the *Ca* II K line, and the metallic lines are too faint and on most of the plates they are practically invisible. Of the 60 plates secured, only 41 were measured, because on the rest the region of λ 3930 is not well shown.

TABLE 1

RADIAL VELOCITIES OF WX CEPHEI

Plate	Date 1944	U.T.	Phase (in Days)	Radial Velocities from Ca II K Line (in Km/Sec)	
				Primary Component	Secondary Component
CQ 3621	Aug. 19	8:42	0.136	− 36.6	+150.1
3831	Oct. 2	7:19	0.159	− 15.6	.....
3649	Aug. 26	6:26	0.286	− 21.7	+128.0
3652	Aug. 26	9:21	0.408	− 49.7	+ 88.3
3990	Oct. 16	5:56	0.588	− 60.0	+ 85.1
3768	Sept. 19	6:04	0.621	− 68.4	+106.9
3693	Sept. 2	8:52	0.631	− 86.1	+ 91.5
3871	Oct. 6	3:48	0.634	− 95.8	+ 52.1
3876	Oct. 6	7:21	0.783	.....	+ 75.7
3949	Oct. 13	4:30	0.906	− 83.5	+ 90.3
3837	Oct. 3	4:35	1.045	− 93.6	+ 68.9
3663	Aug. 30	10:22	1.072	−100.6	+ 89.2
3626	Aug. 20	9:34	1.173	−102.3	+ 55.1
3627	Aug. 20	10:56	1.230	.....	+ 41.0
3915	Oct. 10	3:48	1.256	− 95.0	+ 42.2
3655	Aug. 27	8:24	1.368	− 39.2	+ 82.1
3656	Aug. 27	10:00	1.435	− 50.2	.....
3812	Sept. 30	5:54	1.478	− 32.8	+119.3
3813	Sept. 30	6:41	1.511	− 62.4	+ 52.3
3729	Sept. 13	11:07	1.590	+ 4.9	.....
3888	Oct. 7	3:21	1.615	− 6.0	.....
3890	Oct. 7	5:49	1.718	− 1.5	.....
3774	Sept. 20	8:50	1.736	− 11.4	.....
3964	Oct. 14	2:52	1.838	+ 3.1	.....
3668	Aug. 31	6:22	1.905	+ 17.5	.....
3762	Sept. 17	7:26	2.058	+ 93.5	− 59.7
3844	Oct. 4	5:24	2.079	+ 90.0	− 35.8
3929	Oct. 11	3:12	2.231	+ 73.2	− 89.2
3930	Oct. 11	4:10	2.271	+ 79.2	− 67.9
3736	Sept. 14	6:44	2.408	.....	− 98.6
3823	Oct. 1	5:32	2.463	+134.9	− 80.8
4016	Oct. 18	3:06	2.470	+ 66.6	−144.4
3779	Sept. 21	4:49	2.569	+ 95.9	− 98.6
3978	Oct. 15	2:47	2.835	+ 83.8	− 99.4
3800	Sept. 28	6:08	2.867	+ 66.9	− 98.5
3801	Sep. 28	7:28	2.921	+ 51.7	− 80.2
3857	Oct. 5	6:21	3.119	+ 2.0	.....
3640	Aug. 22	8:21	3.122	+ 4.6	.....
3641	Aug. 22	9:23	3.165	− 6.2	.....
3642	Aug. 22	10:13	3.200	− 4.9	.....
3643	Aug. 22	10:58	3.231	− 1.8	.....

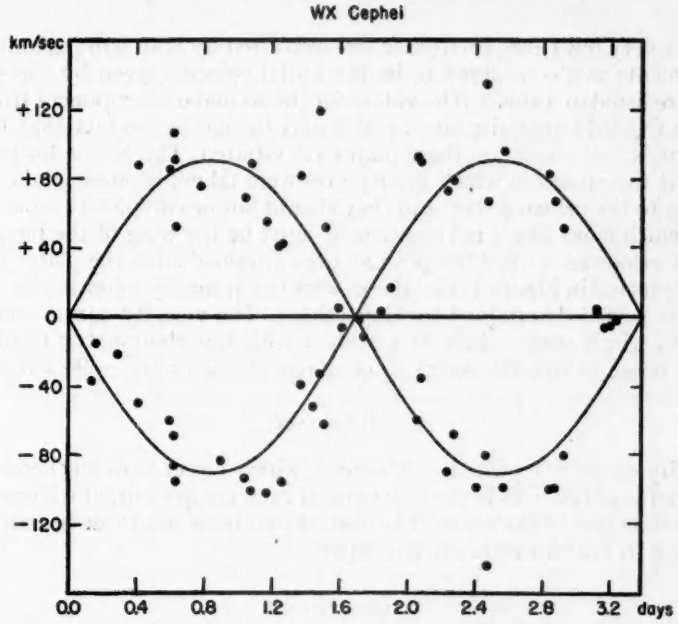

FIG. 1.—Velocity-curve of WX Cephei

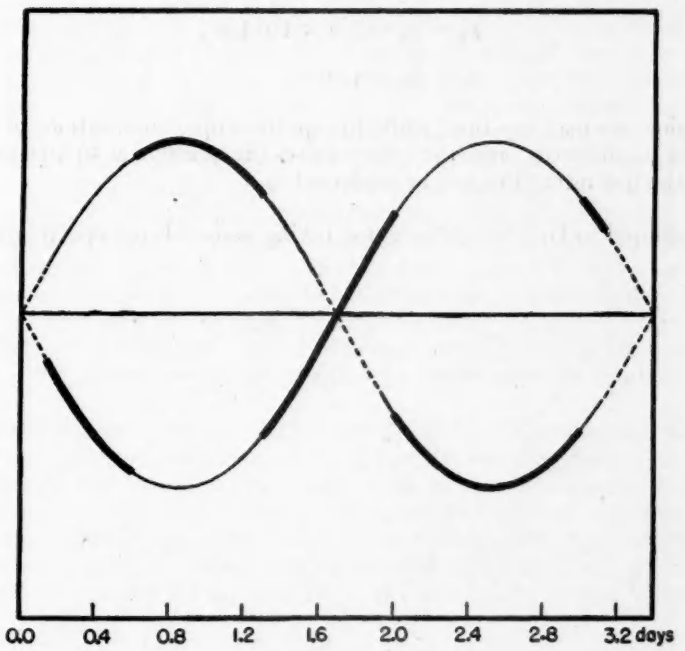

FIG. 2.—The heavy lines show where each component of the *Ca* II K line is strong

Except in a very few cases, each plate was measured by both writers, and the mean of the measurements was considered to be the radial velocity given by the spectrogram. The results are listed in Table 1. The values for the secondary component from the plates CQ 3621 and CQ 3649 are quite large, which may be due to the fact that the red components of the K line shown on these plates are vitiated. The K line for the secondary component, at the phases in which these plates were taken, is much weaker than the K line belonging to the primary star; and they should not be completely separated, so that the feature which looks like a red component must be the wing of the line.

The radial velocities, except the positive ones obtained from the plates CQ 3621 and CQ 3649, are plotted in Figure 1; the phases were computed by adopting the time of minimum and the period determined by Gaposchkin. The velocity-curves were drawn assuming $e = 0$, which seems likely in a system with the photometric elements of WX Cephei. The range in velocity seems to be about the same ($K \sim 90$ km/sec) for both stars, and

$$\gamma \sim 0 \text{ km/sec} .$$

The velocity-curve is repeated in Figure 2, which presents in a schematic form the relative strengths of the lines in the spectrum of each component, at different phases, by means of the thickness of the curve. The dashed part indicates those phases at which the lines belonging to the two stars are not separated.

CONCLUSIONS

Assuming Schneller's values for i and $r_{1,2}$, the spectroscopic observations suggest that a, r, and m are of the following order of magnitude:

$$a_1 \sim a_2 \sim 4.2 \times 10^6 \text{ km} ,$$

$$r_1 \sim r_2 \sim 2.0 \times 10^6 \text{ km} ,$$

$$m_1 \sim m_2 \sim 1.0 \odot .$$

In conclusion, we may say that, while the spectroscopic observations of WX Cephei agree with the photometric ones, the system raises the question as to how the variations observed in the line intensities can be explained.

We are indebted to Dr. Otto Struve for taking some of the spectrograms and for discussion.

THE APPARENT DISTRIBUTION OF PRECEDING AND FOLLOWING SUNSPOTS

W. GLEISSBERG
Istanbul University Observatory, Turkey
Received May 5, 1945

ABSTRACT

Spot counts from the Mount Wilson maps of sunspots yield the result that preceding spots show a western excess while following spots show an eastern excess. This result is in agreement with Bjerknes' theory of sunspots, provided that it is accepted that the excesses arise from systematic inclinations of the spot axes.

From a statistical study of the areas of sunspots during the period 1889–1901 Mrs. Maunder[1] found that the total area of sunspots was greater on the eastern half of the sun's visible hemisphere than on its western half. Using Mrs. Maunder's statistical data, I have shown[2] that an average inclination of the spot axes of about 0.6° would be sufficient to explain the observed eastern excess of the areas of sunspots. Taking into consideration that possibly a connection exists between preceding and following spots (especially if spots of different polarities are parts of one vortex, as suggested by Bjkernes),[3] one might expect a systematic difference in the direction of the axes of preceding and following spots. In this case preceding and following spots would not show the same eastern excess.

To investigate whether there is such a different behavior of the two classes of spots, it would be best to compare, for each class of spots, the total areas on the eastern and the western half of the sun's disk. Observational results from which the areas of preceding and following spots could be taken are, however, not available at Instanbul. I was obliged, therefore, to use the *number* of the observed spots instead of their *areas*. The number of preceding and following spots can be taken from the magnetic observations of sunspots published by Hale and Nicholson.[4] This publication contains the results of observations made during the years 1917–1924. During the last years of this period only few sunspots have been observed, since a minimum of spot activity occurred in 1923. Moreover, the well-known change of the polarities that is connected with the beginning of a new spot cycle happened at that time. I have preferred, therefore, not to use the observations of the years 1922–1924, in order to have a definite relation between the polarity of a spot and its character as preceding or following the spot. Since the number of spots observed in 1917–1921 was much greater than that of the spots observed in 1922–1924, the omission of the latter ones cannot exercise any influence on the result of the present investigation.

On the Mount Wilson drawings from January 4, 1917, to December 16, 1921, a total of 22,798 spots were counted; only those drawings which were incomplete because of bad weather conditions were not used. The classification of the spots as preceding or following spots was made not according to their location within the group but merely according to their polarities. During the years 1917–1921 preceding spots on the northern hemisphere were connected with positive fields (in the Mount Wilson drawings designated by *R*) and on the southern hemisphere with negative fields (in the Mount Wilson drawings

[1] *M.N.*, **67**, 451, 1907.

[2] *Pub. Istanbul U. Obs.*, No. 12, 1940.

[3] *Ap. J.*, **64**, 93, 1926.

[4] *Papers Mt. W. Obs.*, Vol. **5**, 1938 (Carnegie Inst. Pub. No. 498).

designated by V). The numbers of R and V spots counted in the four quadrants of the sun's visible hemisphere are given in Table 1.

Taking into consideration that during the years for which the spot counts have been made, R spots were leaders and V spots were followers on the northern hemisphere and that the polarities were opposite on the southern hemisphere, we find from Table 1 the numbers of preceding and following spots, which are given in Table 2 for the western and the eastern half of the sun's disk.

TABLE 1

NUMBER OF R SPOTS AND V SPOTS IN THE FOUR QUADRANTS OF THE SUN'S DISK

Spots	N.W.	S.W.	N.E.	S.E.
R	3676	2039	3467	2310
V	2355	3277	2434	3240

TABLE 2

NUMBER OF PRECEDING (P) AND FOLLOWING (F) SPOTS ON THE WESTERN AND THE EASTERN HALF OF THE SUN'S DISK

Spots	West	East
P	6,953	6,707
F	4,394	4,744
Total	11,347	11,451

The data in Table 2 show that in 1917-1921 there was a western excess of preceding spots and an eastern excess of following spots and that the well-known eastern excess of all spots results from the fact that the eastern excess of following spots surpasses the western excess of preceding spots. If these excesses are produced by an inclination of the spot axes, the above result leads to the conclusion that the axes of preceding spots are sloped downward from east to west while the axes of following spots are sloped downward from west to east. This conclusion would agree with Bjerknes' theory of sunspots.

PHOTOGRAPHS OF THE CORONA TAKEN DURING THE TOTAL ECLIPSE OF THE SUN ON JULY 9, 1945, AT PINE RIVER, MANITOBA, CANADA

W. A. HILTNER AND S. CHANDRASEKHAR
Yerkes Observatory
Received July 18, 1945

ABSTRACT

An expedition which went to Pine River, Manitoba, Canada, to observe the total eclipse of the sun on July 9, 1945, is described, and coronal photographs secured during the eclipse are presented.

At a conference held at the Yerkes Observatory in May, 1945, it was decided to send an expedition to Canada to observe the total eclipse of the sun on July 9, 1945, and secure photographs of the corona. The authors of this report undertook to organize the expedition.

In view of the very short duration of the totality of this eclipse (it was 37 seconds at Pine River), it appeared to us that, for the sake of the completeness of the record, attempts should be made to secure both small-scale and large-scale photographs of the corona in order that both the outermost extensions of the corona and the structure of the inner parts could be studied. It was further thought that the 6-inch UV telescope of the Yerkes Observatory with an appropriate reduction in the aperture would prove suitable for obtaining a small-scale photograph, while a long-focus camera in combination with a coelostat would be adequate for obtaining the large-scale photographs. Accordingly, the 6-inch UV telescope was dismounted for transporting to the site of observation to be selected. As for the long-focus camera, it appeared that a 2-inch doublet, which was available, would be inadequate to insure sufficient intensity of light during the short period of totality. Drs. L. G. Henyey and J. L. Greenstein therefore designed a 4-inch doublet, corrected for the green and the blue, and 20 feet in focal length. The lens was made in the optical shop of the Observatory by Mr. Fred Pearson on very short notice. This lens was used to obtain the large-scale photographs. A wooden framework for the camera was contructed at the Observatory. Further, a common drive was devised for both the 6-inch UV telescope and the coelostat.

After some consideration it was decided to observe the eclipse in the general neighborhood of Pine River, Manitoba, as this region appeared to be a fair compromise between accessibility and duration of totality. From the point of view of weather conditions, there did not seem much room for choice.

The expedition, consisting of the two writers of this report (later joined by Dr. Burke Smith), left Williams Bay on June 28 and arrived at Pine River on June 30. After some exploration, the site was chosen on July 1 on a slight ridge commanding a clear view of the eastern sky and some five miles from Pine River. This was 0.7 mile south of the central line of totality, and the altitude of the place was estimated at 1100 feet.

A concrete foundation was laid for mounting the 6-inch telescope, the coelostat, and the common driving mechanism. Two further piers were also erected for supporting the wooden framework of the 20-foot camera. The adjustments of the instruments were made during the following days, though the cloudy sky prevailing during a large part of the time made this a matter of some difficulty.

The eastern sky was clouded at sunrise on July 9, but the drifting clouds produced a clear region some twenty-five minutes before totality. During totality there were clouds only very near the horizon in the eastern sky; however, there was a thick bank of clouds

in the western sky extending to an altitude of about 40°. The entire sky clouded over again half an hour later.

The program which was carried through was the following:

Dr. Burke Smith, who had in the meantime joined the expedition, acted as a counter, and counted backward from 60, starting at exactly one minute before the computed instant of the second contact ($7^h17^m45^s$ central war time),[1] the zero to be announced when the Baily's beads disappeared. (Actually, as it turned out, the second contact occurred at the predicted moment within a fraction of a second.)

The 6-inch telescope, the aperture of which had been reduced to 3 inches, was operated by Chandrasekhar. One exposure of 14 seconds was given on a backed Eastman 33 plate. The 20-foot camera was operated by Hiltner, who took two exposures of 20 seconds and 5 seconds, respectively, on (unbacked) Eastman spectroscopic plate II-H. Positive contact prints from the 3 photographs secured are shown in Plates X and XI.

It will be noticed that in the small-scale photograph (Pl. X, *a*) the disk of the moon appears somewhat oval. This must be due to an accidental disturbance of the telescope during the operation having caused a slight backlash in the driving mechanism. However, this does not affect the quality of the photograph in the regions where the structure of the corona becomes distinguishable. It will be seen that the coronal extensions can be traced fully to over 2 solar diameters. The large-scale photographs (Pls. X, *b*, and XI), particularly the one with the longer exposure (Pl. XI), show an extraordinary amount of detailed structure. While these photographs resemble in many ways the earlier photographs taken during the minimum phase of solar activity and reveal, as could have been anticipated, an equatorial type of corona, it would appear that the streamers in the equatorial plane are perhaps more fully developed than in the earlier photographs. It should perhaps be recorded in this connection that there was exceptional auroral activity during the days immediately preceding and following the date of the eclipse.

The original plates have been calibrated, and we hope to present the results of a quantitative study of the intensity distribution in the corona in a later paper.

Even so modest an expedition as ours could not have been successfully completed without the co-operation of many individuals. To the names already mentioned we would like to add: Dr. O. Struve who first suggested the organizing of the expedition and later supported it; Dr. W. W. Morgan, who advised and assisted us with the development and the printing of the photographs; Messrs. E. Krebs and J. Vosatka, who assisted in various ways with the preparations of the expedition; Mr. D. M. Stephens, deputy minister of the Department of Mines and Natural Resources, Winnipeg, who gave us valuable information concerning the regions where the track of totality crossed Saskatchewan and Manitoba; Constables Wannamaker and Dempsey of the Royal Canadian Mounted Police, in charge of the region of Pine River, who co-operated with the objectives of the expedition in numerous ways; and, finally, Mr. Harry J. Marko, proprietor of the Pine River Hotel, Pine River, for exceptional consideration and hospitality during our stay in Pine River.

[1] The time signals from the Bureau of Standards, Washington, D.C., were available on a Hallicrafter Sky Champion radio installed on the site.

PLATE X

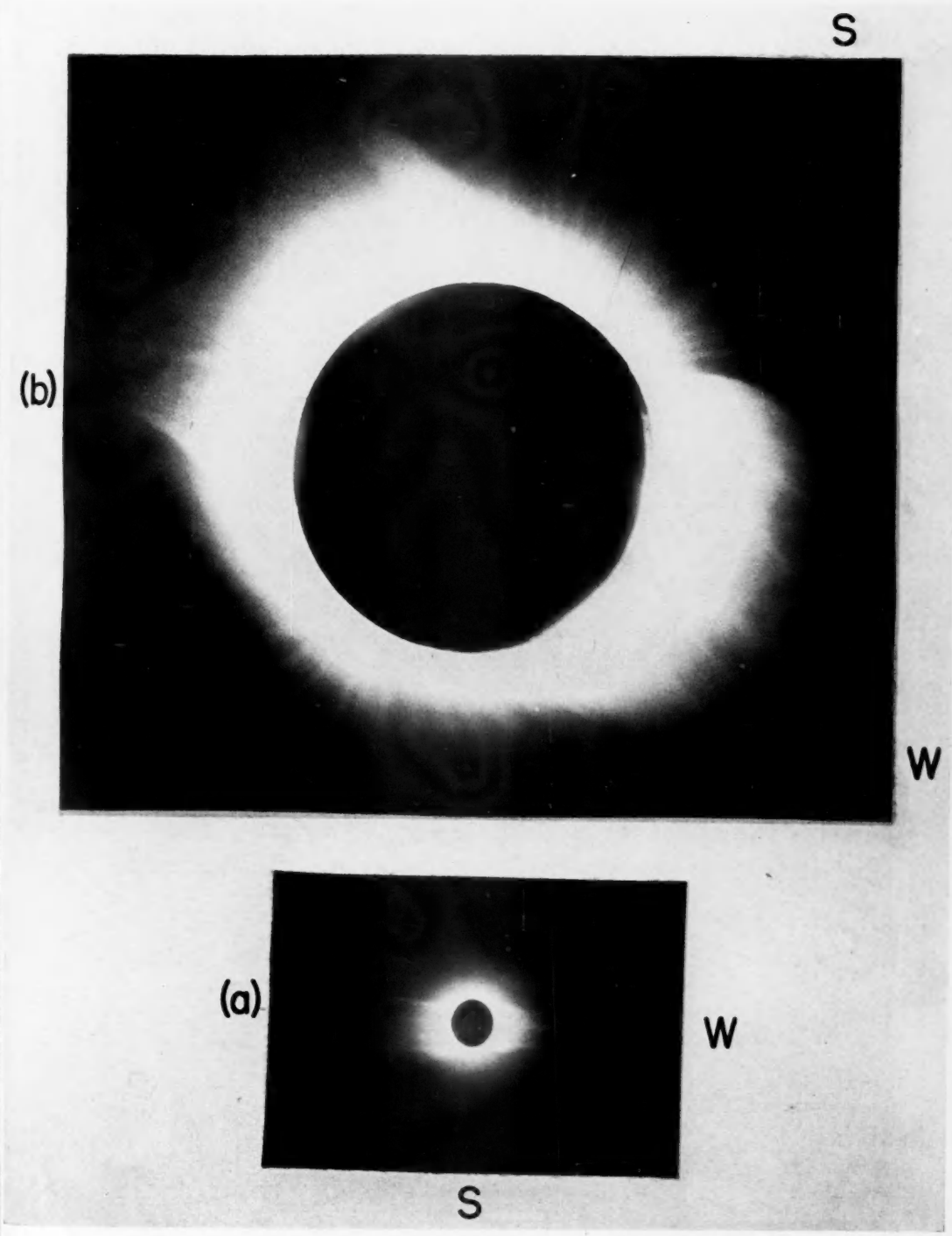

PHOTOGRAPHS OF SOLAR CORONA TAKEN JULY 9, 1945

a) 14-second exposure with 6-inch UV telescope (aperture reduced to 3 inches)
b) 5-second exposure with 20-foot camera

PLATE XI

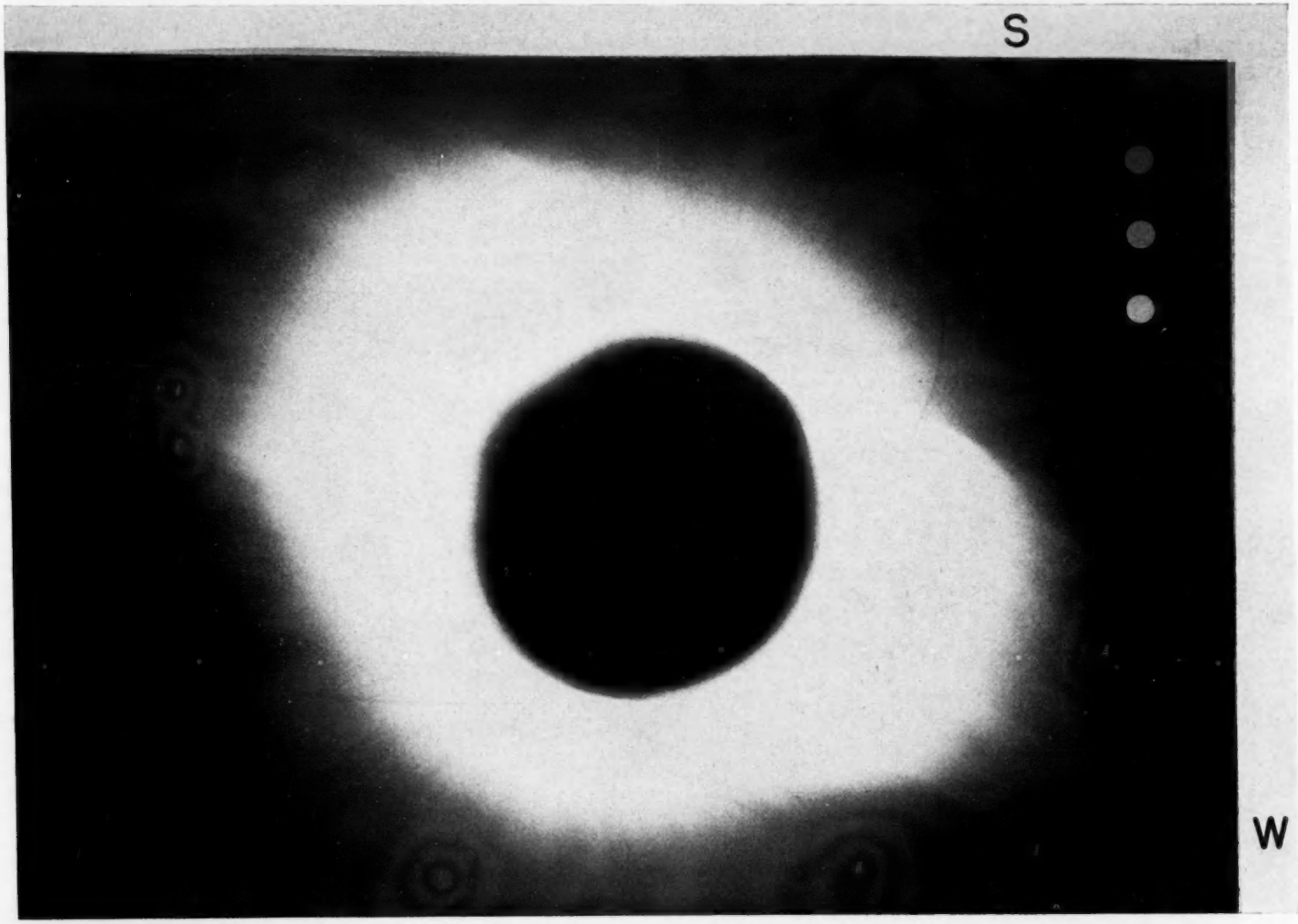

PHOTOGRAPH OF SOLAR CORONA TAKEN JULY 9, 1945

NOTES

NOTE ON THE SUSPECTED GRAVITATIONAL RED SHIFT OF THE ORION STARS

Professor E. Finlay Freundlich, of St. Andrews University, has called my attention to a paper published by him in Volume **20**, page 561, 1919, of the *Physikalische Zeitschrift*, in which he has discussed the difference between the radial velocities of a group of stars in Orion and the velocity of the nebula. The result obtained by him was +6.0 km/sec, while the result obtained by Titus and me was +15.0 km/sec.[1] The more recent result is based upon the four stars of the Trapezium and the spectroscopic binary HD 37041, which is also imbedded in the brighter parts of the Orion nebula. Freundlich's results are based upon a group of stars within the limits of $5^h12^m.8$ to $5^h35^m.8$ in right ascension, and $-7°20'$ to $+3°13'$ in declination.

It is possible that because of the use of stars located only in the main parts of the Orion nebula and also because of our determination of the orbital elements of two spectroscopic binaries the systematic effect of the stellar velocities was somewhat increased. The fact that our independent observations not only have failed to remove this discrepancy but have materially increased it serves to show that the phenomenon is real. But, of course, the interpretation of this phenomenon as a gravitational red shift is only one of several possible explanations.

O. Struve

Yerkes Observatory
April 27, 1945

ERRATA

On page 324, Volume **101**, the values tabulated in Table 1 are not L_a's as defined in equation (9), page 323, but $\mathcal{L}_a = \lambda L_a$ as defined in *Ap. J.*, **100**, 357, 1944 (eq. [18]).

In line 2 of Table 1, "Radial Velocities of SX Hydrae," *Ap. J.*, **101**, 377, 1945, the residual O−C for plate CQ 3136 should read −2 instead of −18.

[1] *Ap. J.*, **99**, 88, 1944.

REVIEWS

Annales de géophysique, Vol. 1, No. 1. Edited by the *Revue d'optique théorique et instrumentale*. Paris, 1944.

The first issue of this new French scientific periodical, devoted to geophysics, appeared in Paris in August, 1944, at the time of the liberation of the French capital. If there were need for any further proof of the earnest endeavor of our French colleagues to promote a rapid and profound renaissance of scientific research in their country after the war, the appearance of this new periodical, planned and started during the German occupation, would provide it. The board of editors contains the names of half-a-dozen well-known French astronomers. Since the magazine covers fields closely related to astronomy, such as the spectra of the night sky, the aurora borealis, and the twilight, it will doubtless find its place on the library shelves of most astronomical institutions, even if the latter do not include a section devoted to geophysical research.

The first issue contains a long paper on the blue-violet region of the night-sky spectrum by J. Cabannes and J. Dufay and one on the sodium emission in the twilight and night-sky spectrum by J. Bricard and A. Kastler. There are also papers on the indirect gravimetric measurement of the density of rocks; on instruments for the measurement of the ionic conductivity of air; on the geomagnetic properties of certain outflows of lava; on cloud formations; on clockwork-driven recorders for seismographs; and on the diurnal variation of the air ionization. Bibliographic reviews are also included.

The paper by Cabannes and Dufay will be welcomed by those who have devoted attention to the difficult observation and interpretation of the emission bands appearing in the night-sky spectrum. Because of the weakness of the night-sky emission, only very low dispersion and resolving-power have been used thus far. The reviewer is of the opinion that it would be better to get one good spectrogram with higher resolving-power—even if it should require a whole new-moon period of observing, or longer—than to collect many spectrograms and take averages. What we really need now is precise information on the structures of the observed emission bands. Skeptics may, with good reason, go so far as to state that no identification of night-sky features is satisfactory, or even possible, with the available observational material, except that of [*O* I], *Na*, N_2^+ (occasionally), and possibly the Vegard-Kaplan system of N_2. The French astronomers have realized this need for a higher resolving-power as well as, if not better than, most others, since they have been pioneers in the interpretation of the optical properties of the earth's atmosphere (ozone layer, night sky, sodium emission, etc.). We understand that a serious effort is being made in France to improve the observational data.

Be this as it may, Cabannes and Dufay have felt that it would be worth while to rediscuss systematically their numerous low-dispersion observations in the blue-violet region. There will be unanimous agreement that they were right in doing so; there was, indeed, a real need for a unified treatment of their entire observational material, which, up to the present, had given rise only to numerous scattered short publications, mostly in the *Comptes rendus*. Their glass spectrograph, constructed in 1933, involves a very interesting type of $F/0.7$ camera of 80-mm focal length, designed by Cojan. Most likely, at present, such a four-lens system would rather be replaced by a camera of the Schmidt type, although the definition of the Cojan objective appears to be quite good. The prism of extra-dense flint has a base of 205 mm and a height of 115 mm. The dispersion at $H\gamma$ is 150 A/mm. On fast plates a good night-sky spectrum, covering the blue-violet region, may be obtained in from five to seven hours.

The authors obtained more than 100 spectrograms in the region from 3830 to 5160 A during the period 1933–1935. The best plates were measured under a comparator, independently by Cabannes and by Dufay; the measured wave lengths agree, on the whole, quite satisfactorily. In addition, a number of plates were recorded with a microphotometer. While the microphotometer probably reveals, and enables one to measure, structural features in a complex emission more accurately than the eye, the reviewer has always, on the whole, been skeptical as to the reality of faint lines "discovered" on one or even several tracings and not seen with a magnifier. Yet, it must be recognized that the discussion of the microphotometric tracings by Cabannes and

Dufay gives rather convincing results. All in all, 82 radiations have been measured in the region λλ 3830–5160 A (75 under the microscope and 77 on tracings) and are listed. In general, the wave lengths obtained by direct measurement do not differ by more than 3 A from those obtained from tracings. Moreover, the tracings reveal for nine bands the direction of degradation: six are degraded toward the red, and three toward the violet.

While, as stated by the authors, the reality of some of the lines listed may still be doubted, the list of wave lengths constitutes a progress over the tables previously available. One of the latter, prepared very conservatively and cautiously by Elvey, Swings, and Linke, on the basis of material obtained at McDonald Observatory, contains only 21 lines in the same region; these agree fairly well in wave length with the corresponding features listed by Cabannes and Dufay.

The paper by Bricard and Kastler on the sodium emission in the twilight and night sky is a preliminary quantitative study of the absorption of the D lines by sodium vapor. While few accurate, decisive results are obtained, the paper is of great interest because of the new observational and theoretical suggestions included. The problem consists essentially in the study of the absorption of the atmospheric D-line emission by layers of sodium vapor at given temperatures and densities. Such a study, which had been suggested by various authors, should reveal the width of the sodium emission and hence help in deciding as to the mechanism of excitation of the emission. If we have to deal with optical resonance of sodium atoms, the D lines should be extremely sharp, and their width should reveal the average temperature in the region of emission. On the other hand, a sodium emission resulting from the photodissociation of sodium compounds, such as sodium chloride, by ultraviolet solar radiation, should give broader lines. However, a definite statement as to the actual line width thus produced by photodissociation is not possible at present because the distribution of solar radiation in the ultraviolet near λ 1700 is not known and because no laboratory information is available on the photodissociation of sodium chloride. Another way of attacking the problem of the excitation mechanism is by determining the average height at which the sodium emission takes place, since the far ultraviolet solar radiation required for the photodissociation of sodium compounds may be found only in very high layers (higher than 100 km) of the earth's atmosphere. This is also considered by Bricard and Kastler. Eventually the problem should also be discussed by polarization methods.

The glass-prism spectrograph used is similar (or identical?) to that of Cabannes and Dufay, and the observations were made at the Pic du Midi Observatory from 1940 to 1944. The contrast between the D emission and the twilight background is considerably enhanced by placing in front of the slit a polarizer that absorbs the vibration normal to the solar rays: such absorption weakens the background much more strongly than the D emission.

The experimental conditions (absorption tubes, microphotometry, etc.) and the sources of error have been discussed very thoroughly. Two series of observations related in the paper itself lead to very unsatisfactory results, which the authors try to explain by deficiencies of the experimental procedure. In an addendum, more elaborate, recent observations are discussed, leading to more consistent results. The width of the twilight D emission found in the latest experiments corresponds to a temperature of approximately 240° K, hence pointing rather toward a pure resonance excitation. The night-sky sodium emission is not absorbed so easily, and its excitation mechanism remains obscure; the authors suggest that two mechanisms are indeed operative, but this remains doubtful.

There seems to be a seasonal intensity variation of the twilight sodium emission which, according to the authors, may be related to the seasonal variations in the height of the "D" layer[1] of the ionosphere. The sodium emission is even affected by meteorological conditions, possibly on account of absorption by water vapor, which may also play a role in the seasonal variation. Meteors have also been suggested as an explanation for a seasonal variation. Accurate measurement of the maximum intensity of the sodium emission at the most favorable time of the year gives a number of the order of 1 to 2×10^{14} transitions $^2P \rightarrow {}^2S$ per square meter per second. From their discussion the authors conclude that the D emission should be observable in the day-sky radiation with a spectrograph of high resolving-power. The intensity variation of the sodium emission at twilight indicates a height of approximately 74 km.

The number of sodium atoms per unit area of the luminescent layer is of the order of 10^{10} atoms/cm^2. The presence of a rather large number of free sodium atoms at a height of the order of 74 km is considered by the authors as rather puzzling, since double collisions are still very frequent (10^6 per second). The authors quote the mechanisms of regeneration of free sodium atoms

[1] This ionospheric designation "D" has nothing to do with sodium emission.

from sodium chloride and from sodium oxide (*NaO*) as suggested by Bernard and by Chapman. The reviewer suggests that the three-body collisions be considered carefully: once formed in some way, a free sodium atom may, after all, not recombine so easily.

The essential result of the authors, a height of 74 km for the sodium-luminescent layer, agrees well with the figure obtained independently by Elvey and Farnsworth.[2]

Among scientists who are not quite familiar with the French language, some misunderstanding may arise due to the use by Bricard and Kastler of the expression "auroral" in "auroral sky," "auroral radiation," "auroral spectrum," etc., meaning that the dawn (in French: *aurore*) is concerned. Among astronomers, the adjective "auroral" is already used in connection with a certain type of forbidden transitions and in connection with the aurora borealis. It might be desirable to reach some kind of agreement on this matter of terminology.

The magazine is well printed. Many will regret that the pages of the articles are not indicated on the cover page. Some will not like the large size adopted. But these are minor matters. Let us congratulate our French colleagues on their initiative and wish them good luck.

P. SWINGS

PASADENA, CALIFORNIA

Telescopes and Accessories. By GEORGE Z. DIMITROFF and JAMES G. BAKER. ("Harvard Books on Astronomy.") Philadelphia: Blakiston Co., 1945. Pp. v+309. $2.50.

This volume in the "Harvard Books on Astronomy" series should prove interesting and valuable to a wide audience. Written nonmathematically throughout, it is very fully illustrated, and many of the 146 figures and plates are new. Photographs are included, showing most of the large modern telescopes, as well as the leading types of auxiliary apparatus. The discussion of the principles of astronomical photography, photometry, and spectroscopy should be of particular interest to amateur astronomers who wish to extend their activities into new fields of observational astronomy. A nonastronomical reader may find some unevenness in the level of previous scientific information required for intelligent reading, but this is an inevitable consequence of the wide range of topics covered.

Chapters i and ii describe the nature of light and the elementary concepts of waves, quanta, color, polarization, refraction, and reflection, as well as the structure and properties of the human eye. Visual astronomical telescopes and their accessories form the main subject of chapter ii. In Table 1 optical descriptions are given for four common types of f/15 doublet objectives; domestic optical glass is used, and when glass is generally available the data should encourage construction of such objectives by amateurs. The optical principles of reflectors are next discussed. The authors recommend the doublet objective lens for amateur telescope-makers. They point out that the precision of optical finish required is lower in a lens than in a mirror surface. Parabolization has always been a difficulty. The mounting and use of the mirror is relatively inconvenient. If the amateurs can successfully construct lenses and prisms, most types of auxiliary apparatus could fall within their range; even spectroscopes or spectrographs are possible. Chapter iii, on the photographic process, summarizes the essential features of scientific photographic technique and defines the general concepts of quantitative astronomical photography. The nature of the emulsion, the theory of image-formation, and the chemical processes of development are followed by an outline of photometry.

For the varied aims of astronomical photography, different kinds of telescopes have been developed. The relative merits and uses of the leading types are outlined in chpater iv. The optical aberrations are briefly defined and illustrated with some quantitative data for the parabolic reflector. (The insert to Fig. 47 is rather confusing.) The optical properties of the more complex types of reflecting systems are next discussed. Table 10 is a summary of the aberrations, useful field, and focal ratio of the standard telescopes and of the newer types designed by Couder, Schmidt, Maksutov, Baker, and others. There now exists a considerable variety of complex reflectors involving aspheric surfaces; it would be of interest to have tests of the type with a flat field designed by Baker. Among those using only spherical surfaces I would particularly like to mention the recent Maksutov design. A spherical mirror is used, with a weak meniscus achromatic single lens to correct the spherical aberration of the mirror. By proper choice of the sepa-

[2] *Ap. J.*, 96, 451, 1942.

ration of lens and mirror the coma can be eliminated. The field is large, but the focal surface has a radius of curvature equal to the focal length. The two spherical surfaces of the meniscus can be figured with any desired accuracy. For moderate speeds—f/2.5 or f/3—and apertures up to 2 or 3 feet, I believe there may be reason to prefer the Maksutov to the Schmidt type. It is probable that the figure of even the best Schmidt correcting plate has sufficient small-scale irregularity to produce considerable extra-focal halo and loss of resolving-power in low-contrast images. The chapter continues with a discussion of standard fast photographic lenses; its value is greatly enhanced by a set of illustrations and tables of data for such commercial lenses as the Cooke, Ross, Petzval, and Biotar. While the aberrations of these lenses are briefly discussed, there still exists a need for a general description of the merits of the commercial-lens types, with data on the speed, field, and resolution to be expected. The question must often arise as to how complex a lens system is needed for a given astronomical problem. An answer cannot usually be obtained from professional opticians and manufacturers, who seldom provide any quantitative data.

The chapter on spectroscopy is rich in information; it covers the standard types of slit, slitless, and nebular spectrographs. The spectra reproduced suffer somewhat from the high contrast of the printing process. The authors describe the factors that influence the design of an instrument for a given dispersion and determine the choice of the most efficient collimator, camera, and dispersing unit. An interesting modification of the slitless spectrograph is described on page 133, and it is worth an investigation. Exposures with modern fast telescopes are severely limited by the light of the night sky. The sky directly fogs the plate in a slitless spectrograph or an objective-prism telescope. If moderate dispersions and widened spectra are required for accurate classification, it is quite common to find that spectra can be obtained only for stars 5–7 mag. brighter than the limiting magnitude for direct photography. The new device proposed is essentially a mask placed at the focal plane of the telescope, so that transparent apertures exist only where stars are found. The mask can be prepared from a direct photograph of the field, by the use either of a positive photograph or of a punched metal sheet. The slitless spectrograph becomes essentially a multiple-slit spectrograph. The direct fogging of the plate is eliminated. A collimator with considerable field must follow the mask, together with a suitable dispersing unit and camera. In the ideal case where the mask apertures are as small as the tremor disk of the telescope, one may obtain, by prolonged exposure, spectra of stars whose tremor disk has a surface brightness only slightly greater than that of the sky. In any case, one may hope to approach more nearly the limiting magnitude attained in slit spectrographs, if not quite to that given by direct photography. Mechanical and optical difficulties may be considerable, but experiments with such a device would be valuable.

Chapter vi reviews the elementary principles of photometry and the use of visual or photoelectric photometers. The use of the microphotometer is briefly described and illustrated. Chapter vii contains much new material on modern instrumental advances in solar research. Special attention is paid to the instruments at the McMath-Hulbert Observatory, and mechanical and optical descriptions are given for the tower telescopes and the radial-velocity spectroheliograph. The developments in the field of the coronagraph and the quartz monochromator are discussed; more of the excellent photographs might have been included. "Building a Telescope" (chap. viii) covers the optical and mechanical details of the large instruments, and in 40 photographs shows most of the newer telescopes and their mountings, drives, and auxiliary instruments. Appendix I includes a description of the use of nonreflecting coats. Appendixes III–VI give lists of the larger telescopes and observatories, with apertures, focal ratios, and brief historical notes.

JESSE L. GREENSTEIN*

Yerkes Observatory

* On leave of absence for war research.